A PDF CLOSURE MODEL FOR COMPRESSIBLE TURBULENT CHEMICALLY REACTING FLOWS

Final Report 1992

NASA Grant No. NAG 3-836

W. Kollmann, MAME Dept. University of California, Davis

Davis, CA 95616

Table of contents.

1.0	Introduction	1
2.0	Objectives	2
3.0	Research work	2
3.1	Foundations of pdf methods	2
3.2	Interaction of turbulence and chemical kinetics	3
3.3	Mapping methods for pdf equations	4
3.4	Prediction of supersonic turbulent flames	4
4.0	References	6
	Appendix I.	
	Appendix II.	
	Appendix III.	
	Appendix IV.	

1.0 Introduction.

Prediction methods based on probability density functions (pdfs) have played an important role in turbulent combustion for some time. The interaction of mixing and chemical reactions is an important factor in determining the performance of practical combustion devices. In the special application of the SSME pre-burner, this interaction can affect the internal fluid mixing and as a result significantly alter the exit temperature profile. To fully anticipate the effect of the interaction of mixing and combustion reactions in a design process requires extensive research in turbulent combustion in a range of Mach numbers relevant for the applications. The aim of this effort is to develop accurate prediction methods.

Prediction methods for turbulent reacting flows developed in analogy to nonreacting flows were based on statistical moments of first and second order. The mean value of density (and other thermodynamic variables) were determined using an assumed form for the pdf of the scalar variables describing the local thermodynamic state. This approach is acceptable for reacting flows if only the expectations of the stable species and temperature and density are of interest and where the reactions are so fast that equilibrium is achieved. It is well known that assumed forms of the pdf are not flexible enough to represent truly the variation of the pdf occurring in a turbulent nonhomogeneous flow with finite rate chemistry (Kollmann and Chen, 1992). Hence, methods employing the pdf directly have been developed for turbulent reacting flows (Pope, 1985, Kollmann, 1990). They have several significant advantages, notably the ability to deal with the highly nonlinear source terms arising in combustion rigorously in closed form. The aim of the present project were the analysis of pdf methods and the development of closures for mixing and turbulent transport of single point pdfs in compressible and incompressible flows.

The main parts of the project were the analysis of the foundations of pdf methods

including the recent development of mapping closures (Chen et al. 1989). The closure models for turbulent mixing were analyzed in detail and pdf methods were extended to compressible turbulent flows. The application of a particular pdf method to supersonic turbulent jet flames burning hydrogen with air was used as a test case to evaluate the closure model.

2.0 Objectives.

The objective of the proposed research project was the analysis of single point closures based on pdfs and characteristic functions and the development of a prediction method for the joint velocity-scalar pdf in turbulent reacting flows. Turbulent flows of boundary layer type and stagnation point flows with and without chemical reactions were be calculated as principal applications. Pdf methods for compressible reacting flows were developed and tested in comparison with available experimental data.

3.0 Research work.

The research work carried in this project was concentrated on the closure of pdf equations for incompressible and compressible turbulent flows with and without chemical reactions.

3.1 Foundations of pdf methods.

The single point pdf equations, which are the central part of the prediction methods for turbulent reacting flows, can be deduced from the exact and closed transport equation for the characteristic functional containing all the statistical information on the complete flow field. The result of this derivation is the equation for the characteristic function, corresponding via Fourier transformation to the single point pdf. It follows that two equivalent formulations of single and multi-point pdf equations emerge as a consequence of the functional equation at special argument functions composed of Dirac-pseudofunctions. All nonclosed terms can

be given in terms of the characteristic function or pdfs and closure models can be set up in either formulation. This fact can be exploited to obtain equivalent expressions for a closure model. For instance, it turns out that the exact mixing term and, therefore, the pair-exchange model for it in the single point pdf equation, has the property to increase the width of the characteristic function (analogous to a random process with positive diffusivity for the pdf) as turbulence decays, since the limit of zero fluctuations is given by unity as Fourier transform of the Dirac spike for the pdf. The detailed discussion of these results can be found in appendix I.

3.2 Interaction of Turbulence and Chemical Kinetics.

The objective of this part of the project is to provide a fundamental understanding of the physics inherent in various processes causing turbulence to interact with chemical kinetics. In view of the importance of various practical combustion processes that occur in turbulent flows, the emphasis is put on the influence of turbulence on chemical kinetics.

The interaction of turbulence and chemical reactions occurs in turbulent reacting flows over a wide range of flow conditions. Various degrees of interaction between turbulence and chemical reactions can lead to different phenomena. Weak interactions between turbulence and chemical reactions may simply modify the flame slightly causing wrinkles of flame surface (Williams, 1989). Strong interactions could cause a significant modification in both the chemical reactions and the turbulence. If chemical reactions cause small density changes in the flow, then the turbulence is weakly affected by the chemical process, but the turbulence may still have strong influence on the chemical reactions. However, the purpose of combustion is generating heat; therefore, one expects large density changes (i.e., an order of magnitude) which can alter the fluid dynamics significantly.

The research work was aimed at the investigation of mean reaction rates in nonprem ixed systems. Rigorous bounds were established for the mean reaction rates in binary and

multi-component mixtures for given fluctuation levels of composition and temperature. The combustion of methane with air was used as an application of the prediction model incorporating finite rate chemistry. Mixedness parameters were evaluated and the bounds on the reaction rates were verified. The main conclusion was that the quasi-laminar calculation of mean reaction rates is unacceptable if unconditional mean values are used. The details can be found in appendix II.

3.3 Mapping methods for pdf equations.

A new approach for the closure of pdf equations was suggested by Kraichnan (Chen et al., 1989) during the grant period and an investigation of the applicability of mapping closures to turbulent combustion problems was undertaken. Kraichnan's idea to apply mappings as tool in constructing closures for pdf equations (Chen et al. 1989, Kraichnan 1990, Feng 1991, Pope 1991, Valiño et al. 1991) proved very successful for the case of a single scalar variable in homogeneous turbulence. It was not clear how powerful this approach is for the case of more than one variable (Pope, 1991). Pope's (1991) method relies on the cumulative distribution function and the representation of the pdf of $n > 1$ random variables as the product of n conditional pdfs. The resulting closure is, therefore, dependent on the ordering of the n variables appearing in the conditions. The investigation of mapping methods in the context of the present project lead to the important result, that the use of the cumulative distribution function can be avoided altogether and that the mapping equations can be established directly using the pdf equation. No particular ordering of the variables is required. The detailed results are presented in appendix III.

3.4 Prediction of supersonic turbulent flames.

The prediction of turbulent supersonic nonpremixed flames was the central part of the

present project. The effects of compressibility, the interaction with random shocks created in the turbulent zone and shocks created outside the turbulent zone are crucial to the successful prediction of compressible turbulent flows. Pdf methods can be adapted to deal with these phenomena and a detailed investigation into pdf formulations for compressible reacting flows was carried out. It was found that even for equilibrium chemistry at least three scalar variables are necessary to fix the local thermodynamic state. In fact, it is advantageous to consider a fourth scalar to obtain a pdf equation with the familiar structure. Compressibility effects are dealt with using the generalized Langevin approach. A pdf closure including mixture fraction, the logarithm of the (dimensionless) density, the internal energy per unit mass and the relative rate of volume expansion was established. The supersonic flames of Evans et al. (1978) were used as test cases and several successful runs were carried out. The results are presnted in detail in appendix IV.

4.0 References.

Chen, H., Chen, S. and Kraichnan, R.H. (1989). *Probability distribution of a stochastically advected scalar field*. Phys. Rev. Lett., **62**, 2657.

Evans, J.S., Schexnayder, C.J. and Beach, H.L. (1978). *Application of a Two - Dimensional Parabolic Computer Program to Prediction of Turbulent Reacting Flows*. NASA Technical Paper no. 1169.

Feng, G. (1991). *Mapping closure and non-Gaussianity of the scalar probability density functions in isotropic turbulence*. Phys. of Fluids A. **3**, 2438.

Kollmann, W. (1990). *The pdf approach to turbulent flow*. Theoret. Comput. Fluid Dynamics **1**, 249.

Kollmann, W. and Chen, J.-Y. (1992). *The interaction of turbulence and chemical kinetics*. in "Major Research Topics in Combustion" (M.Y. Hussaini et al. eds), Springer V., New York, 359.

Kraichnan, R.H. (1990). *Models for Intermittency in Hydrodynamic Turbulence*. Phys. Rev. Lett. **65**, 575.

Pope, S.B. (1985). *Pdf Methods for Turbulent Reacting Flows*. Progr. Energy Comb. Sci. **11**. 119.

Pope, S.B. (1991). *Mapping closures for turbulent mixing and reaction*. Theoret. and Computat. Fluid Dynamics **2**, 255.

Valiño, L., Ros, J. and Dopazo, C. (1991). *Monte-Carlo implementation and analytic solution*

of an inert-scalar turbulent-mixing test problem using a mapping closure, Phys Fluids A. **3**, 2191.

Williams, F. A. (1989). *Structure of flamelets in turbulent reacting flow and influence of combustion on turbulence fields*, Lecture Notes in Engineering, vol.40, Springer V., 195.

Appendix I.

Theoret. Comput. Fluid Dynamics (1990) 1: 249–285

Theoretical and Computational Fluid Dynamics

Review Paper

The pdf Approach to Turbulent Flow[1]

W. Kollmann

Department of Mechanical Engineering, University of California at Davis, Davis, CA 95616, U.S.A.

Communicated by M.Y. Hussaini

Abstract. Probability density function (pdf) methods provide a complete statistical description of turbulent flow fields at a single point or a finite number of points. Turbulent convection and finite-rate chemistry can be treated in closed and exact form with pdfs in contrast to methods based on statistical moments. The equations for pdfs at a finite number of points are indeterminate due to molecular transport and pressure-gradient terms which require pdfs of higher order. The theoretical foundation of pdfs methods are developed in this paper starting from the exact and linear equations on the functional level. The closure problem for single-point pdf equations is treated in detail and several closure models are analyzed. Turbulent combustion at low Mach numbers constitutes an important area of application and selected results for a turbulent methane flame are presented as an example. The extension of pdf methods to supersonic turbulent flows with and without chemical reactions are outlined. Progress in the numerical solution of pdf equations is reviewed briefly. In the concluding remarks, both the advantages and disadvantages of pdf methods are evaluated.

1. Introduction

Significant progress has been achieved over the last 10 years in the theory and application of evolution equations for probability density functions (pdfs) to turbulent flows at low Mach numbers. Pope (1985) reviewed the development up to 1985 and provided a detailed introduction to this subject. The present paper is concerned with the theoretical foundation and recent development of pdf methods. Pdf methods derive their justification from the basic fact that turbulent convection and chemical reactions can be dealt with in exact and closed form. This is in stark contrast to the approach based on statistical moments, which requires closure models for nonlinear processes such as convection or chemical reactions. Pdf methods succeed here because they transform certain nonlinear processes into linear terms with variable coefficients by converting the associated dependent variables in the basic laws into independent variables of the pdf. Hence, two of the most important closure problems encountered in moment equations are overcome by pdf methods. Furthermore, pdfs provide a complete statistical description of the fluctuations at a single point or a finite number of points in the flow field. However, the equation governing the evolution of the pdf at n points is indeterminate, because the terms accounting for molecular transport and the fluctuating pressure gradient require the pdf at $n+1$ points. The closure problem for these two terms must be overcome to arrive at a determinate equation. The numerical solution of pdf equations was for some time considered next to

[1] This research was supported by NASA–Lewis Grants NAG 3-667 (T. Van Overbeke project monitor) and NAG 3-836 (R. Claus project monitor) and by a grant from the Spanish Ministry of Education (CAICYT) during the authors stay at the University of Zaragoza in 1985–1986).

impossible, rendering the interest in pdfs academic. However, stochastic simulation techniques pioneered by Pope (1985) proved very successful for homogeneous and nonhomogeneous flows (in particular the parabolic type). The reason for the difficulty in the numerical solution of pdf equations is the large number of independent variables of the pdf in contrast to moment methods, which may consist of a large number of equations governing functions of a few independent variables. The reason for the success of stochastic simulation techniques is the fact that the numerical effort grows only linearily with the number of independent variables. As a consequence, a variety of turbulent flows ranging from incompressible turbulent shear layers (see Pope, 1985; Kollmann and Wu, 1987; Haworth and Pope, 1987) to turbulent reacting flows with strong density fluctuations and finite-rate chemistry (Pope and Correa, 1986; Jones and Kollmann, 1987; Chen *et al.*, 1989) can now be computed with pdf methods.

The aim of this paper is to provide a detailed discussion of the theory and application of pdf methods. In Section 2 the basic laws governing the flow of Newtonian fluids are set up first in the Eulerian and the Lagrangean frame for later reference. Then the exact and linear equations for the characteristic functionals in Eulerian and Lagrangean frames are discussed. They form the theoretical basis for pdf and moment methods. Pdf equations in both the Eulerian and the Lagrangean frames are then derived as Fourier transforms of the equations for the characteristic functions, which follow from the exact equations on the functional level. The case of the single-point pdf equation is the primary focus of the subsequent sections. In Section 3 the possible formulations for the nonclosed terms in the pdf equation are discussed first. Their properties are assessed and the closure models for the molecular-transport and the fluctuating pressure-gradient terms are reviewed. Single-point pdf equations do not provide information on turbulent length or time scales. Hence, methods of incorporating scale information are introduced in order to complete the prediction method. Section 4 is devoted to the application of pdf methods and their extension to new areas. The most important applications are turbulent combustion flows. The example of a turbulent nonpremixed methane flame is presented in some detail to verify the power of pdf methods. Then the extension to supersonic flows and the interaction of turbulence with shock waves are discussed along with directions for future research. The numberical-solution method was presented in detail in Pope's (1985) review article. Hence, only the most recent developments are discussed briefly in Section 5. Finally, in Section 6 conclusions are drawn for the theory and application of pdf methods.

2. Theoretical Background

The analysis of turbulent flows is restricted to Newtonian fluids in the gaseous phase for which the thermodynamic relations for ideal gases are assumed to hold. The basic laws of physics are assembled first in an appropriate form for later use. Then it is shown that pdf methods are part of a general framework for the treatment of turbulent flows on the functional level. This functional formulation is discussed briefly and the pdf-transport equation is derived from it.

2.1. Basic Laws

The thermodynamic state of a flowing mixture of ideal gases is locally specified if the composition and two independent (intensive) thermodynamic variables and velocity are known. The values for this set of variables are governed by the balance laws for mass, momentum, and energy and the thermodynamic state relations for ideal gases. The balances can be set up in several frames: we consider their form in the Eulerian frame, where the flow is observed at an arbitrary location in the flow field, and the Lagrangean frame, where the flow is observed following an arbitrary material point of the fluid. The independent variables for the Eulerian frame are thus the observer position $\mathbf{x}$ and time t, whereas for the Lagrangean frame the label variable $\mathbf{a}$ and time t are used. The usual choice for the label $\mathbf{a}$ is the position of the material point identified by $\mathbf{a}$ at the reference time zero. The position of a material point in the Lagrangean frame is denoted by $\mathbf{X}(\mathbf{a}, t)$ and serves as transformation between the frames

$$\mathbf{x} = \mathbf{X}(\mathbf{a}, t), \qquad \mathbf{a} = \mathbf{X}^{-1}(\mathbf{x}, t),$$

where $\mathbf{X}^{-1}$ denotes the position at time zero of the material point, that is at position $\mathbf{x}$ at time t

(uppercase letters indicate dependent variables in the Lagrangean frame and lowercase letters are used for the Eulerian frame). If the mapping $\mathbf{X}$ and its inverse $\mathbf{X}^{-1}$ are twice continuously differentiable, then the partial derivatives in the Eulerian frame can be transformed into the Lagrangean frame and vice versa. The gradient, for instance, transforms according to (Euler relations (Truesdell, 1954))

$$\frac{\partial}{\partial x_\alpha} = \frac{1}{2J}\varepsilon_{\alpha\beta\gamma}\varepsilon_{\delta\eta\omega}\frac{\partial X_\beta}{\partial a_\eta}\frac{\partial X_\gamma}{\partial a_\omega}\frac{\partial}{\partial a_\delta} \tag{1}$$

and

$$\frac{\partial}{\partial a_\alpha} = \frac{J}{2}\varepsilon_{\alpha\beta\gamma}\varepsilon_{\delta\eta\omega}\frac{\partial X_\beta^{-1}}{\partial x_\eta}\frac{\partial X_\gamma^{-1}}{\partial x_\omega}\frac{\partial}{\partial x_\delta}, \tag{2}$$

where J denotes the Jacobian determinant

$$J = \tfrac{1}{6}\varepsilon_{\alpha\beta\gamma}\varepsilon_{\delta\eta\omega}\frac{\partial X_\delta}{\partial a_\alpha}\frac{\partial X_\eta}{\partial a_\beta}\frac{\partial X_\omega}{\partial a_\gamma}. \tag{3}$$

(Note that repeated subscripts imply summation and that $\varepsilon_{\alpha\beta\gamma}$ is the permutation tensor.) Repeated application of (1) or (2) leads to transformation formulae for second and higher derivatives. We will need in particular the relation for the Laplacian, which is given by

$$\Delta_x = \frac{1}{2J}\varepsilon_{\alpha\beta\gamma}\varepsilon_{\delta\eta\omega}\frac{\partial X_\zeta}{\partial a_\eta}\frac{\partial X_\varphi}{\partial a_\omega}\frac{\partial}{\partial a_\delta}\left(\frac{1}{J}\frac{\partial X_\zeta}{\partial a_\beta}\frac{\partial X_\varphi}{\partial a_\gamma}\frac{\partial}{\partial a_\alpha}\right). \tag{4}$$

The time derivative in the Lagrangean frame plays a fundamental role, because velocity and acceleration are by definition given as

$$V_\alpha(\mathbf{a}, t) \equiv \left(\frac{\partial X_\alpha}{\partial t}\right)_{\mathbf{a}}, \qquad A_\alpha(\mathbf{a}, t) \equiv \left(\frac{\partial V_\alpha}{\partial t}\right)_{\mathbf{a}}.$$

It transforms to the Eulerian frame according to

$$\left(\frac{\partial}{\partial t}\right)_{\mathbf{a}} = \left(\frac{\partial}{\partial t}\right)_{\mathbf{x}} + v_\alpha(\mathbf{x}, t)\frac{\partial}{x_\alpha} \equiv \frac{D}{Dt} \tag{5}$$

which is called the substantial or Stokes derivative. The transformation rules (1)–(5) enable us now to set up the basic laws in both frames.

Mass Balance. Mass is conserved and this statement translates into

$$\frac{\partial \rho}{\partial t} + \frac{\partial}{\partial x_\alpha}(\rho v_\alpha) = 0 \tag{6}$$

for the Eulerian frame, where $\rho(\mathbf{x}, t)$ denotes the density. Transformation to the Lagrangean frame leads to an integral of (6) given by

$$\frac{R(\mathbf{a}, 0)}{R(\mathbf{a}, t)} = J, \tag{7}$$

where $R(\mathbf{a}, t) = \rho(\mathbf{x}, t)$ for $\mathbf{x} = \mathbf{X}(\mathbf{a}, t)$. Equation (7) is therefore the mass balance in the Lagrangean frame.

Species Balance. A mixture of n ideal gases is considered and its composition is described in terms of mass fractions $Y_i(\mathbf{a}, t) = y_i(\mathbf{x}, t)$, $\mathbf{x} = \mathbf{X}(\mathbf{a}, t)$ $i = 1, \ldots, n$. Chemical reactions may occur and the Y_i are therefore not conserved, but may be consumed or produced according to a reaction mechanism consisting of many steps. At this point we only need to know that the rate Q_i of production due to chemistry is a local function of the thermodynamic variables (no derivatives or integrals with respect to time or space/label appear in the Q_i). The balance for the mass fraction y_i in the Eulerian frame is then given by

$$\rho\frac{Dy_i}{Dt} = \frac{\partial}{\partial x_\alpha}\left(\rho\Gamma_i\frac{\partial y_i}{\partial x_\alpha}\right) + \rho q_i, \qquad i = 1, \ldots, n, \tag{8}$$

where Γ_i denotes the Fickian mass diffusivity. Transformation to the Lagrangean frame is carried out using (1), (5), and (7) and results in

$$\frac{\partial Y_i}{\partial t} = \frac{1}{2R_0}\varepsilon_{\alpha\beta\gamma}\varepsilon_{\delta\eta\omega}\frac{\partial X_\zeta}{\partial a_\eta}\frac{\partial X_\varphi}{\partial a_\omega}\frac{\partial}{\partial a_\delta}\left(\frac{R^2\Gamma_i}{R_0}\frac{\partial X_\zeta}{\partial a_\beta}\frac{\partial X_\varphi}{\partial a_\gamma}\frac{\partial Y_i}{\partial a_\alpha}\right) + Q_i, \qquad i = 1, \ldots, n, \tag{9}$$

where $R_0 \equiv R(\mathbf{a}, 0)$.

Momentum Balance. Newton's second law leads to the balance equation for momentum. In the Eulerian frame it appears as

$$\rho\frac{Dv_\alpha}{Dt} = -\frac{\partial p}{\partial x_\alpha} + \frac{\partial \tau_{\alpha\beta}}{\partial x_\beta} + \rho f_\alpha, \tag{10}$$

where $\tau_{\alpha\beta}$ is the stress tensor and f_α is the external force per unit mass. Transformation to the Lagrangean frame is straightforward and results in

$$\frac{\partial V_\alpha}{\partial t} = -\frac{1}{2R_0}\varepsilon_{\alpha\beta\gamma}\varepsilon_{\delta\eta\omega}\frac{\partial X_\beta}{\partial a_\eta}\frac{\partial X_\gamma}{\partial a_\omega}\frac{\partial P}{\partial a_\delta} + \frac{1}{2R_0}\varepsilon_{\beta\gamma\zeta}\varepsilon_{\delta\eta\omega}\frac{\partial X_\gamma}{\partial a_\eta}\frac{\partial X_\zeta}{\partial a_\omega}\frac{\partial T_{\alpha\beta}}{\partial a_\delta} + F_\alpha, \tag{11}$$

where $P(\mathbf{a}, t) = p(\mathbf{x}, t)$ is the pressure and $T_{\alpha\beta}(\mathbf{a}, t) = \tau_{\alpha\beta}(\mathbf{x}, t)$ is the stress tensor in the Lagrangean frame. Newtonian fluids satisfy the linear constitutive relation

$$\tau_{\alpha\beta} = \mu\left(\frac{\partial v_\alpha}{\partial x_\beta} + \frac{\partial v_\beta}{\partial x_\alpha} - \frac{2}{3}\delta_{\alpha\beta}\frac{\partial v_\gamma}{\partial x_\gamma}\right) \tag{12}$$

between stress and rate of strain where μ is the dynamic viscosity.

Energy Balance and State Relations. The first law of thermodynamics applied to a differential control volume leads to the energy balance in the Eulerian frame. This balance can be set up in several equivalent forms depending on the choice of the thermodynamic variables. For enthalpy $h(\mathbf{x}, t)$ it is given by

$$\rho\frac{Dh}{Dt} = \frac{Dp}{Dt} + \Phi - \frac{\partial q_\alpha}{\partial x_\alpha}. \tag{13}$$

The specific enthalpy for a mixture of ideal gases is composed of the enthalpies of the components

$$h = \sum_{i=1}^{n}\frac{\bar{h}_i}{M_i}y_i, \tag{14}$$

where $\bar{h}_i$ is the molal enthalpy and M_i is the molecular mass of the ith component. The molal enthalpy $\bar{h}_i$ in turn consists of the formation enthalpy $\bar{h}_i^0$ and the sensible enthalpy

$$\bar{h}_i = \bar{h}_i^0 + \int_{T_0}^{T} dT'\,\bar{c}_p(T'), \tag{15}$$

where $\bar{c}_p(T)$ denotes the molal specific heat at constant pressure. The dissipation function Φ is defined by

$$\Phi \equiv \tau_{\alpha\beta}\frac{\partial v_\alpha}{\partial x_\beta} \tag{16}$$

and the energy flux q_α consists of conductive, diffusive, and radiative fluxes

$$q_\alpha = -k\frac{\partial T}{\partial x_\alpha} - \rho\sum_{i=1}^{n}\frac{\bar{h}_i}{M_i}\Gamma_i\frac{\partial y_i}{\partial x_\alpha} + q_\alpha^R. \tag{17}$$

The system of equations is closed if the ideal gas equation

$$p = \rho RT \tag{18}$$

is included and the chemical sources Q_i are specified. The energy balance in the Lagrangean frame can be deduced from the first law of thermodynamics for a differential system or by transformation of the

Eulerian form (13). The result is given by

$$\frac{\partial H}{\partial t} = \frac{1}{R}\frac{\partial P}{\partial t} + \frac{1}{R}\Phi - \frac{1}{2R_0}\varepsilon_{\alpha\beta\gamma}\varepsilon_{\delta\eta\omega}\frac{\partial X_\beta}{\partial a_\eta}\frac{\partial X_\gamma}{\partial a_\omega}\frac{\partial Q_\alpha}{\partial a_\delta}, \tag{19}$$

where

$$\frac{1}{R}\Phi = \frac{1}{2R_0}\varepsilon_{\alpha\zeta\gamma}\varepsilon_{\delta\eta\omega}T_{\alpha\beta}\frac{\partial X_\zeta}{\partial a_\eta}\frac{\partial X_\gamma}{\partial a_\omega}\frac{\partial V_\beta}{\partial a_\delta} \tag{20}$$

is the dissipation function per unit mass in the Lagrangean frame. The basic laws were presented in terms of composition y_i, enthalpy h, density ρ, and velocity $\mathbf{v}$. This set of variables is not always the most convenient one and linear or nonlinear combinations of these variables are used later for the treatment of turbulent flows with chemical reactions. For low Mach numbers it can be shown (Pope, 1985), by Taylor series expansion of the state relations, that chemical sources are, to the lowest order, independent of pressure fluctuations and that the substantial derivative of the pressure in the energy equation can be neglected unless strong pressure variations are imposed by unsteady boundary conditions. Hence a set of thermochemical variables $\Psi_i(\mathbf{x}, t)$ emerges for low Mach number flows, that determines the state of the fluid mixture locally and these variables are governed by transport equations (Eulerian frame)

$$\rho\frac{D\psi_i}{Dt} = \frac{\partial}{\partial x_\alpha}\left(\rho\Gamma_i\frac{\partial\psi_i}{\partial x_\alpha}\right) + \rho q_i, \qquad i = 1, \ldots, l, \tag{21}$$

or (Lagrangean frame)

$$\frac{\partial\Psi_i}{\partial t} = \frac{1}{2R_0}\varepsilon_{\alpha\beta\gamma}\varepsilon_{\delta\eta\omega}\frac{\partial X_\zeta}{\partial a_\eta}\frac{\partial X_\varphi}{\partial a_\omega}\frac{\partial}{\partial a_\delta}\left(\frac{R^2\Gamma_i}{R_0}\frac{\partial X_\zeta}{\partial a_\beta}\frac{\partial X_\varphi}{\partial a_\gamma}\frac{\partial\Psi_i}{\partial a_\alpha}\right) + Q_i, \qquad i = 1, \ldots, l. \tag{22}$$

The source terms $q_i(\mathbf{x}, t) = Q_i(\mathbf{a}, t)$, $\mathbf{x} = \mathbf{X}(\mathbf{a}, t)$ are not identical with the sources in (8) and (9). Their structure depends on the particular thermochemical formulation or model employed for the local description of the reacting mixture. The complete system of equations determining the local mechanical and thermodynamic state consists now of mass balance, momentum balance, and scalar balances (21) or (22) together with the relations between the ψ_i and the thermodynamic variables. It can be expected that l is less than $n + 1$ for certain classes of flows. Non-premixed turbulent flames at low Mach- numbers for instance can be modeled using a single conserved scalar ($l = 1$ and $Q_1 = 0$). This is discussed in more detail in a subsequent section. The case of supersonic turbulent flows is dealt with in a slightly different fashion.

2.2. Characteristic Functionals

A complete statistical description of a turbulent flow can be achieved if the characteristic functional (see Hopf, 1952; Hopf and Titt, 1953; Lewis and Kraichnan, 1962; Foias, 1974; Vishik *et al.*, 1979; Constantin *et al.*, 1985)

$$m[d, \mathbf{v}, \varphi_1, \ldots, \varphi_l] \equiv \left\langle \exp\left\{ i\int_0^T d\tau\left[(\rho, d) + (\mathbf{v}, \mathbf{v}) + \sum_{i=1}^{l}(\psi_i, \varphi_i)\right]\right\}\right\rangle \tag{23}$$

for variables in the Eulerian frame or

$$M[d, \mathbf{x}, \varphi_1, \ldots, \varphi_l] \equiv \left\langle \exp\left\{ i\int_0^T d\tau\left[(R, d) + (\mathbf{X}, \mathbf{x}) + \sum_{i=1}^{l}(\Psi_i, \varphi_i)\right]\right\}\right\rangle \tag{24}$$

for variables in the Lagrangean frame is specified. The arguments of the functionals m and M are the functions $d(\mathbf{x}, t)$, $\mathbf{v}(\mathbf{x}, t)$, $\varphi_i(\mathbf{x}, t)$ and $d(\mathbf{a}, t)$, $\mathbf{x}(\mathbf{a}, t)$, $\varphi_i(\mathbf{a}, t)$, respectively, which are square integrable in the flow domain $\mathfrak{R} \times [0, T]$. The expressions (ρ, d), etc., indicate the scalar product

$$(v_\alpha, v_\alpha) \equiv \int_{\mathfrak{R}(t)} d\mathbf{x} v_\alpha(\mathbf{x}, t)v_\alpha(\mathbf{x}, t) \tag{25}$$

in the Eulerian frame and

$$(X_\alpha, x_\alpha) \equiv \int_{\mathfrak{R}(0)} d\mathbf{a} X_\alpha(\mathbf{a}, t)x_\alpha(\mathbf{a}, t) \tag{26}$$

in the Lagrangean frame, where $\mathfrak{R}(t)$ is the flow domain at time t and $[0, T]$ is the time interval of interest. The angular brackets represent the mathematical expectation, which is defined as a functional integral over the space of all realizations of the turbulent flow field (see Vishik *et al.* (1979) for the definitions of the appropriate function spaces). This functional integration requires the existence of the probability measure (see Daletskii (1962) and Skorohod (1974) for functional integration). For incompressible flows and homogeneous boundary conditions, the existence of the probability measure has been established (see Hopf and Titt, 1953; Foias, 1974; Vishik *et al.*, 1979), but not its uniqueness. For compressible and reacting flows this is still an open question. We assume in the following that the probability measure for compressible and reacting flows exists. With this assumption we can proceed to set up the transport equations for characteristic functionals following the method put forward by Vishik *et al.* (1979). Noting that the characteristic functionals are independent of time t and location $\mathbf{x}$ and label $\mathbf{a}$, we have to form functional derivatives (see Averbukh and Smolyanov, 1962) in order to establish the dynamical change at a given time and location or label. The transport equations for the derivatives of the Eulerian functional m can be obtained without difficulty (see Lewis and Kraichnan, 1962; Dopazo and O'Brien, 1974; Kollmann, 1987). The mass balance (6) leads to

$$\frac{\partial}{\partial t}\frac{\delta m}{\delta d(\mathbf{x}, t)} = i\frac{\partial}{\partial x_\alpha}\frac{\delta^2 m}{\delta d(\mathbf{x}, t)\delta v_\alpha(\mathbf{x}, t)}, \tag{27}$$

where $\delta/\delta d(\mathbf{x}, t)$ denotes the functional derivative (Averbukh and Smolyanov, 1962) defined by

$$\int_{\mathfrak{R}} d\mathbf{x}\int_0^T dt\frac{\delta m}{\delta d(\mathbf{x}, t)}h(\mathbf{x}, t) \equiv \frac{d}{d\varepsilon}m[d + \varepsilon h]|_{\varepsilon=0}. \tag{28}$$

Momentum balance (10) leads to

$$\frac{\partial}{\partial t}\frac{\delta^2 m}{\delta d(\mathbf{x}, t)\delta v_\alpha(\mathbf{x}, t)} = i\frac{\partial}{\partial x_\beta}\frac{\delta^3 m}{\delta d(\mathbf{x}, t)\delta v_\alpha(\mathbf{x}, t)\delta v_\beta(\mathbf{x}, t)} + \frac{\partial \Pi}{\partial x_\alpha} - \frac{\partial T_{\alpha\beta}}{\partial x_\beta} + if_\alpha\frac{\partial m}{\delta d(\mathbf{x}, t)}, \tag{29}$$

where the external force per unit mass f_α was assumed to be nonrandom and Π denotes the pressure functional

$$\Pi[d, v, \varphi_1, \ldots, \varphi_l] \equiv \left\langle p(\mathbf{x}, t)\exp\left\{i\int_0^T d\tau[(\rho, d) + \cdots]\right\}\right\rangle \tag{30}$$

and $T_{\alpha\beta}$ denotes the stress functional

$$T_{\alpha\beta}[d, v, \varphi_1, \ldots, \varphi_l] \equiv \left\langle \tau_{\alpha\beta}(\mathbf{x}, t)\exp\left\{i\int_0^T d\tau[(\rho, d) + \cdots]\right\}\right\rangle. \tag{31}$$

The stress functional for Newtonian fluids can be given explicitly in terms of m:

$$T_{\alpha\beta} = -iu\left(\frac{\partial}{\partial x_\beta}\frac{\delta m}{\delta v_\alpha(\mathbf{x}, t)} + \frac{\partial}{\partial x_\alpha}\frac{\delta m}{\delta v_\beta(\mathbf{x}, t)} - \tfrac{2}{3}\delta_{\alpha\beta}\frac{\partial}{\partial x_\gamma}\frac{\delta m}{\delta v_\gamma(\mathbf{x}, t)}\right). \tag{32}$$

The viscosity μ was assumed to be constant. The thermochemical variables ψ_i governed by (21) lead to (Kollmann, 1987)

$$\begin{aligned}\frac{\partial}{\partial t}\frac{\delta^2 m}{\delta d(\mathbf{x}, t)\delta\varphi_j(\mathbf{x}, t)} &= i\frac{\partial}{\partial x_\beta}\frac{\delta^3 m}{\delta d(\mathbf{x}, t)\delta v_\beta(\mathbf{x}, t)\delta\varphi_j(\mathbf{x}, t)} + i\frac{\partial}{\partial x_\beta}\left(\rho\Gamma_j\frac{\partial}{\partial x_\beta}\frac{\delta m}{\delta\varphi_j(\mathbf{x}, t)}\right)\\ &\quad + iq_j\left(\frac{\delta}{i\delta\varphi_1(\mathbf{x}, t)}, \ldots, \frac{\delta}{i\delta\varphi_l(\mathbf{x}, t)}\right)\frac{\delta m}{\delta d(\mathbf{x}, t)}, \qquad j = 1, \ldots, l,\end{aligned} \tag{33}$$

where the transport coefficient $\rho\Gamma_j$ was assumed constant. The sources $q_j(\varphi_1, \ldots, \varphi_m)$ appearing in (21) become operators acting on m. If q_j is not a polynomial in the φ_j, then it may turn out to be a pseudodifferential operator (see, for instance, Taylor, 1974) on the functional level in (33). The functional equations for the Lagrangean functional M are obtained in similar fashion as shown by Monin (1962) for the case of incompressible turbulence. Mass balance (7) leads to the equation

$$\frac{\delta M}{\delta d(\mathbf{a}, 0)} = \frac{i}{6}\varepsilon_{\alpha\beta\gamma}\varepsilon_{\delta\eta\omega}\lim\frac{\partial}{\partial a'_\alpha}\frac{\delta}{\delta x_\delta(\mathbf{a}', t)}\frac{\partial}{\partial a''_\beta}\frac{\delta}{\delta x_\eta(\mathbf{a}'', t)}\frac{\partial}{\partial a^*_\gamma}\frac{\delta}{\delta x_\omega(\mathbf{a}^*, t)}\frac{\delta M}{\delta d(\mathbf{a}, t)}, \tag{34}$$

where the limit is carried out for $\mathbf{a}'$, $\mathbf{a}''$, $\mathbf{a}^*$ approaching $\mathbf{a}$. The mass balance (7) is not an evolution equation and thus (34) is not of evolution type. The balance of momentum (11) leads to

$$\frac{\partial^2}{\partial t^2}\frac{\delta^2 M}{\delta d(\mathbf{a},0)\delta \mathbf{x}_\alpha(\mathbf{a},t)} = -\tfrac{1}{2}\varepsilon_{\alpha\beta\gamma}\varepsilon_{\delta\eta\omega}\lim\frac{\partial}{\partial a'_\eta}\frac{\delta}{\delta x_\beta(\mathbf{a}',t)}\frac{\partial}{\partial a''_\omega}\frac{\delta}{\delta x_\gamma(\mathbf{a}'',t)}\frac{\partial \Pi}{\partial a_\delta}$$
$$+\tfrac{1}{2}\varepsilon_{\beta\gamma\zeta}\varepsilon_{\delta\eta\omega}\lim\frac{\partial}{\partial a'_\eta}\frac{\delta}{\delta x_\gamma(\mathbf{a}',t)}\frac{\partial}{\partial a''_\omega}\frac{\delta}{\delta x_\zeta(\mathbf{a}'',t)}\frac{\partial T_{\alpha\beta}}{\partial a_\delta} + iF_\alpha\frac{\delta M}{\delta d(\mathbf{a},0)} \tag{35}$$

and the thermochemical balances (22) imply that

$$\frac{\partial}{\partial t}\frac{\delta^2 M}{\delta d(\mathbf{a},0)\delta\varphi_j(\mathbf{a},t)} = \frac{i}{2}\varepsilon_{\alpha\beta\gamma}\varepsilon_{\delta\eta\omega}\lim\frac{\partial}{\partial a'_\eta}\frac{\delta}{\delta x_\zeta(\mathbf{a}',t)}\frac{\partial}{\partial a''_\delta}\frac{\delta}{\delta x_\phi(\mathbf{a}'',t)}$$
$$\times\frac{\partial}{\partial a_\delta}\left(D_j\lim\frac{\partial}{\partial a^*_\beta}\frac{\delta}{\delta x_\zeta(\mathbf{a}^*,t)}\frac{\partial}{\partial a^{**}_\gamma}\frac{\delta}{\delta x_\phi(\mathbf{a}^{**},t)}\frac{\partial}{\partial a_\alpha}\frac{\delta M}{\delta\varphi_j(\mathbf{a},t)}\right)$$
$$+iQ_j\left(\frac{\delta}{i\delta\varphi_1(\mathbf{a},t)},\ldots,\frac{\delta}{i\delta\varphi_l(\mathbf{a},t)}\right)\frac{\delta M}{\delta d(\mathbf{a},0)},\qquad j=1,\ldots,l. \tag{36}$$

The transport coefficients $D_j \equiv R^2\Gamma_j/R_0$ are again assumed constant in order to avoid unnecessary complications. Variable transport coefficients can be dealt with, but the resulting equations become rather unwieldy.

The transport equations for the Eulerian and the Lagrangean functionals exhibit several properties of fundamental importance. First we note that the equations are linear in contrast to the physical balances, which are highly nonlinear. Furthermore, the system of functional equations is closed in both Eulerian and Lagrangean frames if we consider the first functional derivatives of m or M as unknowns. This follows from the fact that both the stress functional $T_{\alpha\beta}$ according to (32) and the pressure functional Π can be expressed in terms of m or M. No explicit form for the pressure functional can be given, but the thermochemical relations imply that the pressure can be expressed in terms of ρ and $\psi_1, \ldots, \psi_l$ and thus there exists a relation between Π and m or M. Finally, we outline a procedure to establish the characteristic functional m or M from the solutions of the functional equations, which provide the first derivatives of m or M. We note that functional differentiation and appropriate combination of the solutions of the system of functional equations (27)–(33) or (34)–(36) lead to a Poisson–Levy equation (see Feller, 1986) for m or M. The Dirichlet problem for this Poisson–Levy equation can be solved analytically and the result shows that m and M can be represented as functional integrals with respect to a Wiener measure (see Theorem 3.5 in Feller (1986)).

2.3. Finite-Dimensional Characteristic Functions and pdfs: Eulerian Frame

The functional equations contain all the statistical information on the turbulent reacting or nonreacting flow. In particular, the transport equations for finite-dimensional characteristic functions follow from them. The governing equations for finite-dimensional pdfs are thus determined also, because pdfs are the Fourier transforms of characteristic functions. The derivation of the equations for finite-dimensional characteristic functions are outlined for the single-point case. We note first that the generalized argument functions

$$d^* = \hat{d}\delta(\mathbf{x}-\mathbf{x}^0)\delta(t-t^0),\qquad v^*_\alpha = \hat{v}_\alpha\delta(\mathbf{x}-\mathbf{x}^0)\delta(t-t^0),\qquad \varphi^*_j = \hat{\varphi}_j\delta(\mathbf{x}-\mathbf{x}^0)\delta(t-t^0), \tag{37}$$

where $\hat{d}$, $\hat{v}_\alpha$, $\hat{\varphi}_j$ are parameters independent of $\mathbf{x}$ and t, produce the single-point characteristic function m_1 when applied to m,

$$m[d^*, v^*, \varphi_1^*, \ldots, \varphi_l^*] = m_1(\hat{d}, \hat{v}, \hat{\varphi}_1, \ldots, \hat{\varphi}_l; \mathbf{x}^0, t^0), \tag{38}$$

and m_1 is, according to (23), defined by

$$m_1(\hat{d}, \hat{v}, \hat{\varphi}_1, \ldots, \hat{\varphi}_l; \mathbf{x}^0, t^0) = \left\langle \exp\left\{ i\left[\hat{d}\rho(\mathbf{x}^0,t^0) + \hat{v}\cdot\mathbf{v}(\mathbf{x}^0,t^0) + \sum_{j=1}^{l}\hat{\varphi}_j\psi_j(\mathbf{x}^0,t^0)\right]\right\}\right\rangle. \tag{39}$$

Variational derivatives reduce to partial derivatives with respect to the parameters $\hat{d}$, $\hat{v}$, $\hat{\varphi}_j$, as for

instance in

$$\frac{\delta m}{\delta d(\mathbf{x}^0, t^0)}[d^*, v^*, \varphi_1^*, \ldots, \varphi_l^*] = \frac{\partial}{\partial \hat{d}} m_1(\hat{d}, \hat{\sigma}, \hat{\varphi}_1, \ldots, \hat{\varphi}_l; \mathbf{x}^0, t^0). \tag{40}$$

Derivatives with respect to $\mathbf{x}$ and t appear differently for m and m_1. From the definition of the functional derivative (28) it follows that

$$\frac{\partial}{\partial t}\frac{\delta m}{\delta d(\mathbf{x}, t)} = i\left\langle \frac{\partial \rho}{\partial t}(\mathbf{x}, t) \exp\left\{ i \int_0^T d\tau \left[(\rho, d) + (\mathbf{v}, v) + \sum_{j=1}^{l} (\psi_j, \varphi_j) \right] \right\} \right\rangle, \tag{41}$$

whereas it follows from (38) that

$$\begin{aligned} \frac{\partial m_1}{\partial t^0} = {} & i\hat{d}\left\langle \frac{\partial \rho}{\partial t^0}(\mathbf{x}^0, t^0) \exp\{i[\cdots]\} \right\rangle + i\hat{v}_\alpha \left\langle \frac{\partial v_\alpha}{\partial t^0}(\mathbf{x}^0, t^0) \exp\{i[\cdots]\} \right\rangle \\ & + i \sum_{j=1}^{l} \hat{\varphi}_j \left\langle \frac{\partial \psi_j}{\partial t^0}(\mathbf{x}^0, t^0) \exp\{i[\cdots]\} \right\rangle, \end{aligned} \tag{42}$$

where

$$[\cdots] \equiv \hat{d}\rho(\mathbf{x}^0, t^0) + \hat{\mathbf{v}} \cdot \mathbf{v}(\mathbf{x}^0, t^0) + \sum_{j=1}^{l} \hat{\varphi}_j \psi_j(\mathbf{x}^0, t^0)$$

holds. Using (40)–(42) it is easy to show that the following relation holds for time derivatives:

$$\frac{\partial m_1}{\partial t^0} = \hat{d}\frac{\partial}{\partial t^0}\frac{\delta m}{\delta d(\mathbf{x}^0, t^0)}[*] + \hat{v}_\alpha \frac{\partial}{\partial t^0}\frac{\delta m}{\delta v_\alpha(\mathbf{x}^0, t^0)}[*] + \sum_{j=1}^{l} \hat{\varphi}_j \frac{\partial}{\partial t^0}\frac{\delta m}{\delta \varphi_j(\mathbf{x}^0, t^0)}[*], \tag{43}$$

where $[*] \equiv [d^*, \mathbf{v}^*, \varphi_1^*, \ldots, \varphi_l^*]$. Note that differentiation has to be carried out first and then the arguments $[*]$ are applied. Furthermore, note that standard and functional differentiation do not commute. Similarly it follows for the substantial derivative that

$$\begin{aligned} \frac{\partial}{\partial t^0}\frac{\partial m_1}{i\partial \hat{d}} + \frac{\partial}{\partial x_\alpha^0}\frac{\partial^2 m_1}{i\partial \hat{d} i\partial \hat{v}_\alpha} = {} & -i\hat{d}\frac{\delta^2}{(i\delta d(\mathbf{x}^0, t^0))^2}\frac{\partial}{\partial x_\alpha^0}\frac{\delta m}{i\delta v_\alpha(\mathbf{x}^0, t^0)}[*] \\ & + i\hat{v}_\beta\left\{ \frac{\partial}{\partial t^0}\frac{\delta^2 m}{i\delta d(\mathbf{x}^0, t^0) i\delta v_\beta(\mathbf{x}^0, t^0)} + \frac{\partial}{\partial x_\alpha^0}\frac{\delta^3 m}{i\delta d(\mathbf{x}^0, t^0) i\delta v_\alpha(\mathbf{x}^0, t^0) i\delta v_\beta(\mathbf{x}^0, t^0)} \right\}[*] \\ & + i\sum_{j=1}^{l} \hat{\varphi}_j \left\{ \frac{\partial}{\partial t^0}\frac{\delta^2 m}{i\delta d(\mathbf{x}^0, t^0) i\delta \varphi_j(\mathbf{x}^0, t^0)} + \frac{\partial}{\partial x_\alpha^0}\frac{\delta^3 m}{i\delta d(\mathbf{x}^0, t^0) i\delta v_\alpha(\mathbf{x}^0, t^0) i\delta \varphi_j(\mathbf{x}^0, t^0)} \right\}[*] \end{aligned} \tag{44}$$

holds. The transport equation for m_1 can now be deduced from this equation by evaluating the terms on the right-hand side of (44) with the aid of (29) and (33). The result can be stated in the form (superscripts of $\mathbf{x}^0$, t^0, and hats are omitted from now on)

$$\begin{aligned} & \frac{\partial}{\partial t}\frac{\partial m_1}{i\partial d} + \frac{\partial}{\partial x_\alpha}\frac{\partial^2 m_1}{i\partial d i\partial v_\alpha} - i\sum_{j=1}^{l} \varphi_j q_j \left(\frac{\partial}{i\partial \varphi_1}, \ldots, \frac{\partial}{i\partial \varphi_l} \right)\frac{\partial m_1}{i\partial d} \\ & \quad = -id\left\langle \rho^2 \frac{\partial v_\alpha}{\partial x_\alpha}\hat{m}_1 \right\rangle + iv_\alpha \left\langle \left(-\frac{\partial p}{\partial x_\alpha} + \frac{\partial \tau_{\alpha\beta}}{\partial x_\beta} + \rho f_\alpha \right)\hat{m}_1 \right\rangle + i\sum_{j=1}^{l} \varphi_j \left\langle \frac{\partial}{\partial x_\alpha}\left(\rho \Gamma_j \frac{\partial \psi_j}{\partial x_\alpha} \right)\hat{m}_1 \right\rangle, \end{aligned} \tag{45}$$

where

$$\hat{m}_1 \equiv \exp\left\{ i\left[d\rho(\mathbf{x}, t) + \mathbf{v} \cdot \mathbf{v}(\mathbf{x}, t) + \sum_{j=1}^{l} \varphi_j \psi(\mathbf{x}, t) \right] \right\}.$$

The transport equation for the pdf

$$\begin{aligned} & f_1(d, \mathbf{v}, \varphi_1, \ldots, \varphi_l; \mathbf{x}, t) dd \cdot d\mathbf{v} \cdot d\varphi_1 \ldots d\varphi_1 \\ & \quad = \text{Prob}\{ d \le \rho(\mathbf{x}, t) \le d + dd,\ v_\alpha \le v_\alpha(\mathbf{x}, t) \le v_\alpha + dv_\alpha,\ \varphi_j \le \psi_j(\mathbf{x}, t) \le \varphi_j + d\varphi_j,\ \alpha = 1, \ldots, 3,\ j = 1, \ldots, l \} \end{aligned} \tag{46}$$

can be obtained by Fourier transformation of (45) or it can be derived directly from the basic laws (see Lundgren, 1967; Pope, 1985; Kollmann, 1987). It can be given in the following form:

$$d\frac{\partial f_1}{\partial t} + dv_\beta \frac{\partial f_1}{\partial x_\beta} + \sum_{j=1}^{m} \frac{\partial}{\partial \varphi_j}(dq_j(\varphi_1, \ldots, \varphi_l) f_1)$$
$$= \frac{\partial}{\partial d}\left\langle \rho^2 \frac{\partial v_\alpha}{\partial x_\alpha} \hat{f} \right\rangle + \frac{\partial}{\partial v_\alpha}\left\langle \left(\frac{\partial p}{\partial x_\alpha} - \frac{\partial \tau_{\alpha\beta}}{\partial x_\beta} - \rho f_\alpha \right) \hat{f} \right\rangle - \sum_{j=1}^{l} \frac{\partial}{\partial \varphi_j}\left\langle \frac{\partial}{\partial x_\beta}\left(\rho \Gamma_j \frac{\partial \psi_j}{\partial x_\beta} \right) \hat{f} \right\rangle, \tag{47}$$

where

$$\hat{f} \equiv \delta(\rho(\mathbf{x}, t) - d)\,\delta(\mathbf{v}(\mathbf{x}, t) - \mathbf{v}) \prod_{j=1}^{l} \delta(\psi_j(\mathbf{x}, t) - \varphi_j) \tag{48}$$

is the Fourier transform of $\hat{m}_1$. The equations for higher-dimensional (multipoint) characteristic functions and pdfs can be obtained in the same manner (see Lundgren, 1967).

The equations for the characteristic function m_1 and the pdf f_1 share several important properties. They were deduced from the closed and linear equations for derivatives of the characteristic functional, but they themselves are not closed at any finite-dimensional level. Viscous and diffusive terms as well as the pressure-gradient introduce the two-point characteristic functions or pdfs into the single-point equations and this property carries over to higher-dimensional equations. Hence, the equations for finite-dimensional characteristic functions and pdfs are always indeterminate.

2.4. Finite-Dimensional Characteristic Functions and pdfs: Lagrangean Frame

The transport equations for finite-dimensional characteristic functions and pdfs in the Lagrangean frame can be derived using the same ideas as for the Eulerian frame. There is, however, sufficient difference in detail to warrant a brief discussion. We consider again the single-point case. The generalized argument functions analogous to the Eulerian case would be

$$d^* = \hat{d}\delta(\mathbf{a} - \mathbf{a}^0)\delta(t), \qquad \mathbf{x}_\alpha^* = \hat{\mathbf{x}}_\alpha \delta(\mathbf{a} - \mathbf{a}^0)\delta(t - t^0), \qquad \varphi_j^* = \hat{\varphi}_j \delta(\mathbf{a} - \mathbf{a}^0)\delta(t - t^0), \tag{49}$$

where the parameters $\hat{d}$, $\hat{\mathbf{x}}$, $\hat{\varphi}_j$ are independent of the label $\mathbf{a}$ and time t. We note, however, that d^* is taken at the reference time zero, because the actual density can be expressed in terms of the initial density via the integrated mass balance (7). The characteristic functional M taken at the generalized arguments (49) turns out to be the single-point characteristic function $M_1(\hat{d}, \hat{\mathbf{x}}, \hat{\varphi}_1, \ldots, \hat{\varphi}_l)$. It is important to notice at this point that M_1 does not contain the information on the statistics of the velocity fluctuations, whereas the characteristic functional $M[d, \mathbf{x}, \varphi_1, \ldots, \varphi_l]$ incorporates all statistical properties of velocity. Since the velocity is a quantity of primary interest, we modify the argument functions $\mathbf{x}^*$ as follows,

$$x_\alpha^{**} = \hat{x}_\alpha \delta(\mathbf{a} - \mathbf{a}^0)\delta(t - t^0) + \frac{\partial \hat{x}_\alpha}{\partial t^0}\delta(\mathbf{a} - \mathbf{a}^0)\frac{\partial}{\partial t^0}\delta(t - t^0), \tag{50}$$

and regard $\partial \hat{x}_\alpha / \partial t \equiv \hat{v}_\alpha$ as a parameter like $\hat{d}$. Note that choosing the argument function $x_\alpha(\mathbf{a}, t)$ for the characteristic functional M implies the choice of the derivative $\partial x_\alpha / \partial t$. The derivative $\partial x_\alpha / \partial t$ would be a redundant argument on the functional level. However, if we choose $x_\alpha(\mathbf{a}, t)$ only at a single point as in x_α^*, then the derivative $\partial x_\alpha / \partial t$ is not determined and derivatives become unknown variables. Taking the characteristic functional of the modified arguments now leads to

$$M[d^*, \mathbf{x}^{**}, \varphi_1^*, \ldots, \varphi_l^*] = \left\langle \exp\left\{ i \left[\hat{d}R(\mathbf{a}^0, t^0) + \hat{x}_\alpha X_\alpha(\mathbf{a}^0, t^0) + \hat{v}_\alpha \frac{\partial X_\alpha}{\partial t}(\mathbf{a}^0, t^0) + \sum_{j=1}^{l} \hat{\varphi}_j \Psi_j(\mathbf{a}^0, t^0) \right] \right\} \right\rangle \tag{51}$$

which is indeed the desired characteristic function $M_1(\hat{d}, \hat{\mathbf{x}}, \hat{\mathbf{v}}, \hat{\varphi}_1, \ldots, \hat{\varphi}_l)$ of density, position, velocity, and thermochemical scalars in the Lagrangean frame. The characteristic functional M_1 involves, strictly speaking, two time levels, namely zero and t^0, but for $t^0 \gg 0$ all correlations with quantities at the initial time zero will have died out and, therefore, M_1 is considered a single-point characteristic function. We note a fundamental difference between M_1 and its Eulerian counterpart m_1. The Eulerian function m_1 depends on the probabilistic variables $(\hat{d}, \hat{\mathbf{v}}, \hat{\varphi}_1, \ldots, \hat{\varphi}_l)$ and parametrically on $(\mathbf{x}, t)$,

whereas the Lagrangean function M_1 depends on the augmented probabilistic set $(\hat{d}, \hat{\mathbf{x}}, \hat{\mathbf{v}}, \hat{\varphi}_1, \ldots, \hat{\varphi}_l)$ and parametrically on $(\mathbf{a}, t)$. The time rate of change of the characteristic function M_1 can be expressed in terms of the functional derivatives of $M[d, \mathbf{x}, \varphi_1, \ldots, \varphi_l]$

$$\frac{\partial}{\partial t^0}\frac{\partial M_1}{i\partial \hat{d}} - i\hat{x}_\alpha \frac{\partial^2 M_1}{i\partial \hat{d} i\partial \hat{v}_\alpha} = i\hat{v}_\alpha \frac{\partial^2}{\partial t^{02}} \frac{\delta^2 M}{i\delta d(\mathbf{a}^0, 0) i\delta x_\alpha(\mathbf{a}^0, t^0)}[*] + i\sum_{j=1}^{l} \hat{\varphi}_j \frac{\partial}{\partial t^0} \frac{\delta^2 M}{i\delta d(\mathbf{a}^0, 0) i\delta \varphi_j(\mathbf{a}^0, t^0)}[*], \quad (52)$$

where $[*]$ denotes the arguments given by (51). The dynamic equations (35) and (36) for the functional derivatives of M can now be used to eliminate the time derivatives on the right-hand side of (52). The result can be given in the form (superscripts and hats are omitted from now on)

$$\begin{aligned}
&\frac{\partial}{\partial t}\frac{\partial M_1}{i\partial d} - ix_\alpha \frac{\partial^2 M_1}{i\partial d i\partial v_\alpha} - i\sum_{j=1}^{l} \varphi_j Q_j\left(\frac{\partial}{i\partial \varphi_1}, \ldots, \frac{\partial}{i\partial \varphi_l}\right)\frac{\partial M_1}{i\partial d} \\
&\quad = iv_\alpha\left\{-\tfrac{1}{2}\varepsilon_{\alpha\beta\gamma}\varepsilon_{\delta\eta\omega} \lim \frac{\partial}{\partial a'_\eta}\frac{\delta}{\delta x_\beta(\mathbf{a}', t)}\frac{\partial}{\partial a''_\omega}\frac{\delta}{\delta x_\gamma(\mathbf{a}'', t)}\frac{\partial \Pi}{\partial a_\delta}[*]\right. \\
&\qquad \left. + \tfrac{1}{2}\varepsilon_{\beta\gamma\zeta}\varepsilon_{\delta\eta\omega} \lim \frac{\partial}{\partial a'_\eta}\frac{\delta}{\delta x_\gamma(\mathbf{a}', t)}\frac{\partial}{\partial a''_\omega}\frac{\delta}{\delta x_\zeta(\mathbf{a}'', t)}\frac{\partial T_{\alpha\beta}}{\partial a_\delta}[*]\right\} - iv_\alpha F_\alpha \frac{\partial M_1}{i\partial d} \\
&\qquad - \sum_{j=1}^{l} \varphi_j \varepsilon_{\alpha\beta\gamma}\varepsilon_{\delta\eta\omega} \lim \frac{\partial}{\partial a'_\eta}\frac{\delta}{\delta x_\zeta(\mathbf{a}', t)}\frac{\partial}{\partial a''_\delta}\frac{\delta}{\delta x_\phi(\mathbf{a}'', t)}\frac{\partial}{\partial a_\delta} \\
&\qquad \times\left(D_j \lim \frac{\partial}{\partial a^*_\beta}\frac{\delta}{\delta x_\zeta(\mathbf{a}^*, t)}\frac{\partial}{\partial a^{**}_\gamma}\frac{\delta}{\delta x_\phi(\mathbf{a}^{**}, t)}\frac{\partial}{\partial a_\alpha}\frac{\delta M}{\delta \varphi_j(\mathbf{a}, t)}\right)[*],
\end{aligned} \quad (53)$$

where the limits are carried out for the labels $\mathbf{a}'$, $\mathbf{a}''$, $\mathbf{a}^*$, $\mathbf{a}^{**}$ approaching $\mathbf{a}$. The right-hand side of (53) contains the nonclosed terms generated by pressure gradient and viscous transport. The transport equation for M_1 can be considerably shortened (but not simplified) if a mixed Eulerian/Lagrangean form of the basic laws is employed, which is given by

$$R_0 \frac{\partial V_\alpha}{\partial t} = -J\frac{\partial P}{\partial X_\alpha} + J\frac{\partial T_{\alpha\beta}}{\partial X_\beta} + R_0 F_\alpha$$

and

$$R_0 \frac{\partial \Psi_j}{\partial t} = R_0 Q_j + J\frac{\partial}{\partial X_\alpha}\left(R\Gamma_j \frac{\partial \Psi_j}{\partial X_\alpha}\right).$$

It follows that (53) can be recast as

$$\begin{aligned}
&\frac{\partial}{\partial t}\frac{\partial M_1}{i\partial d} - ix_\alpha \frac{\partial^2 M_1}{i\partial d i\partial v_\alpha} - i\sum_{j=1}^{1} \varphi_j Q_j\left(\frac{\partial}{i\partial \varphi_1}, \ldots, \frac{\partial}{i\partial \varphi_l}\right)\frac{\partial M_1}{i\partial d} \\
&\quad = iv_\alpha\left\langle\left(-J\frac{\partial P}{\partial X_\alpha} + J\frac{\partial T_{\alpha\beta}}{\partial X_\beta}\right)\hat{M}\right\rangle - iv_\alpha F_\alpha \frac{\partial M_1}{i\partial d} + i\sum_{j=1}^{l} \varphi_j\left\langle J\frac{\partial}{\partial X_\alpha}\left(R\Gamma_j\frac{\partial \Psi_j}{\partial X_\alpha}\right)\hat{M}\right\rangle,
\end{aligned} \quad (54)$$

where

$$\hat{M} = \exp i\left\{R(\mathbf{a}, 0)d + X_\alpha(\mathbf{a}, t)x_\alpha + V_\alpha(\mathbf{a}, t)v_\alpha + \sum_{j=1}^{l} \Psi_j(\mathbf{a}, t)\varphi_j\right\}$$

and therefore

$$M_1 = \langle \hat{M} \rangle$$

holds. The transport equation for the Lagrangean pdf F_1 can be deduced from (54) using a Fourier transform. The result can be given in the form

$$\begin{aligned}
&d\frac{\partial F_1}{\partial t} + dv_\alpha \frac{\partial F_1}{\partial x_\alpha} + \sum_{j=1}^{l}\frac{\partial}{\partial \varphi_j}[dQ_j(\varphi_1, \ldots, \varphi_l)F_1] \\
&\quad = -\frac{\partial}{\partial v_\alpha}\left\langle\left(-J\frac{\partial P}{\partial X_\alpha} + J\frac{\partial T_{\alpha\beta}}{\partial X_\beta}\right)\hat{F}\right\rangle - dF_\alpha \frac{\partial F_1}{\partial v_\alpha} - \sum_{j=1}^{l}\frac{\partial}{\partial \varphi_j}\left\langle J\frac{\partial}{\partial X_\alpha}\left(R\Gamma_j\frac{\partial \Psi_j}{\partial X_\alpha}\right)\hat{F}\right\rangle,
\end{aligned} \quad (55)$$

where $\hat{F}$ is the Fourier transform of $\hat{M}$ and J denotes the Jacobian defined in (3). It is instructive to compare the transport equations for the Eulerian pdf (47) and the Lagrangean pdf (55). We know already that f_1 and F_1 are not equal due to different sets of independent variables. The left-hand sides of (47) and (55) have the same structure, but the right-hand sides show two subtle differences. The volume-expansion term is absent from (55) and the Jacobian appears as a factor of the pressure-gradient and the viscous-diffusive terms. Both differences can be traced back to the definition of the generalized argument functions (51) of the characteristic functional, where $d(\mathbf{a}, 0)$ is taken as the density at the reference time zero. If we define

$$d^* \equiv \hat{d}\delta(\mathbf{a} - \mathbf{a}_0)\delta(t - t^0)$$

instead, we obtain the pdf $F_1^*(d, \mathbf{x}, \mathbf{v}, \varphi_1, \ldots, \varphi_l; \mathbf{a}, t)$ governed by

$$d\frac{\partial F_1}{\partial t} + dv_\alpha \frac{\partial F_1}{\partial x_\alpha} + \sum_{j=1}^{l} \frac{\partial}{\partial \varphi_j}[dQ_j(\varphi_1, \ldots, \varphi_l)F_1]$$
$$= \frac{\partial}{\partial d}\left\langle R^2 \frac{\partial V_\alpha}{\partial X_\alpha}\hat{F}\right\rangle - \frac{\partial}{\partial v_\alpha}\left\langle\left(-\frac{\partial P}{\partial X_\alpha} + \frac{\partial T_{\alpha\beta}}{\partial X_\beta}\right)\hat{F}\right\rangle - dF_\alpha \frac{\partial F_1}{\partial v_\alpha} - \sum_{j=1}^{l} \frac{\partial}{\partial \varphi_j}\left\langle \frac{\partial}{\partial X_\alpha}\left(R\Gamma_j \frac{\partial \Psi_j}{\partial X_\alpha}\right)\hat{F}\right\rangle, \quad (56)$$

which has exactly the same structure as in the Eulerian case (47). The relation between the Eulerian solution $f_1(d, \mathbf{v}, \varphi_1, \ldots, \varphi_l; \mathbf{x}, t)$ of (47) and the Lagrangean solution $F_1(d, \mathbf{x}, \mathbf{v}, \varphi_1, \ldots, \varphi_l; \mathbf{a}, t)$ of (56) is discussed in detail by Pope (1985) and Kollmann and Wu (1987). It is shown by Kollmann and Wu (1987) that F_1 and f_1 differ only by a factor independent of the arguments of F_1 and f_1. This concludes the discussion of the exact pdf transport equations and the following sections are now devoted to the construction of closed pdf equations.

3. Pdf Methods

In the previous section if was shown that the transport equation for the pdf (which describes the mechanical and thermodynamic state of Newtonian fluids in turbulent motion at a finite number of points in space and time) follows from the determinate and linear equation for the characteristic functional. The equations for finite-dimensional pdfs and characteristic functions are, however, indeterminate and the closure problem must be overcome in order to obtain a solvable set of equations. In this section the properties of the closed and nonclosed terms in pdf equations, as well as methods of closure, are discussed.

3.1. Properties of the Single-Point pdf Equation

The pdf $f_1(d, \mathbf{v}, \varphi_1, \ldots, \varphi_l; \mathbf{x}, t)$ is governed by the transport equation (47), which has the form of a conservation law

$$\frac{\partial}{\partial t}(df_1) + \frac{\partial}{\partial x_\alpha}(dv_\alpha f_1) + \sum_{k=1}^{l+4} \frac{\partial}{\partial y_k}(F_k) = 0, \quad (57)$$

where $y_k \equiv \{d, \mathbf{v}, \varphi_1, \ldots, \varphi_l\}$ represents the set of probabilistic and independent variables while F_k represents the corresponding fluxes. The solution f_1 of this equation must satisfy two fundamental conditions,

$$f_1 \geq 0 \quad (58)$$

and

$$\int d\mathbf{y}\, f_1(\mathbf{y}; \mathbf{x}, t) = 1, \quad (59)$$

in order to qualify as a pdf. Dividing (47) by d and integrating over the probabilistic variables $\mathbf{y}$ leads to

$$\frac{\partial}{\partial t}\int d\mathbf{y}\, f_1 = 0.$$

Hence, (59) is preserved provided that initial and boundary conditions conform with (58) and (59).

Multiplication of (47) with expressions of the form

$$\prod_{k=1}^{l+4} (y_k - \langle y_k \rangle)^{\alpha_k}$$

($\alpha_k \geq 0$ is an integer) and integration over the range of the y_k, $k = 1, \ldots, (l + 4)$, leads to the transport equations for the statistical moments.

The left-hand side of the pdf transport equation (47) contains the convective transport of f_1 in physical space and the convection in the space spanned by the thermochemical variables $\varphi_1, \ldots, \varphi_l$. The latter group

$$\sum_{j=1}^{l} \frac{\partial}{\partial \varphi_j} (dq_j(\varphi_1, \ldots, \varphi_m) f_1)$$

is closed as long as the source terms q_j of the scalar transport equations (21) are local functions of the scalars $\psi_1, \ldots, \psi_l$. These sources may be highly nonlinear (as in the case of combusting flows) and can be dealt with rigorously in the pdf and characteristic function equations in contrast to moment equations. Their basic property is apparent from the way q_j appears in the terms: $dq_j(\varphi_1, \ldots, \varphi_l)$ has the role of a convection velocity in scalar space analogous to the velocity v_α in physical (Euclidean) space. If $q_j \leq 0$, then the pdf is moved to higher values of φ_j in accordance with the properties of a source term in (21). If q_j is furthermore constant, the shape of the pdf remains unchanged during this convection along the φ_j-axis in the absence of other effects.

The right-hand side of (47) contains the three nonclosed terms. The term

$$\frac{\partial}{\partial d} \left\langle \rho^2 \frac{\partial v_\alpha}{\partial x_\alpha} \hat{f} \right\rangle = \frac{\partial}{\partial d} \left\{ \left\langle \rho^2 \frac{\partial v_\alpha}{\partial x_\alpha} \middle| \rho = d, \mathbf{v} = \mathbf{v}, \psi_j = \varphi_j, j = 1, \ldots, l \right\rangle f \right\} \tag{60}$$

represents the effect of volume expansion on the pdf. This term is zero if density is constant for material points, because

$$\frac{D\rho}{Dt} = -\rho \frac{\partial v_\alpha}{\partial x_\alpha}.$$

This case includes stratified flows (where ρ may change with label **a** but not with time t) and incompressible flows (where ρ is constant in space and time). The relative rate of volume expansion is nonzero in turbulent reacting flows and in turbulent flows at transonic and supersonic speeds. The conditional moment in (60) can then be viewed as a convection velocity along the density axis. Positive rate of volume expansion leads to negative convection speed and the pdf is moved toward lower density in accordance with the mass balance. The second group of terms on the right-hand side of (47) represents the motion of the pdf in velocity space. The effect of the pressure gradient on the pdf can be elucidated in some detail for the special case of incompressible flow and for points **x** far away from boundaries. Pressure is then determined by a Poisson equation

$$\Delta p = -\rho \frac{\partial v_\alpha}{x_\beta} \frac{\partial v_\beta}{\partial x_\alpha}$$

whose solution

$$p(\mathbf{x}, t) = -\frac{\rho}{4\pi} \int \frac{d\mathbf{y}}{|\mathbf{x} - \mathbf{y}|} \frac{\partial v_\alpha}{\partial y_\beta} \frac{\partial v_\beta}{\partial y_\alpha} \tag{61}$$

allows us to express $\langle (\partial p / \partial x_\alpha) \hat{f} \rangle$ as follows (see Hanjalic and Launder, 1972; Lumley, 1978; Pope, 1985):

$$\left\langle \frac{\partial p}{\partial x_\alpha} \hat{f} \right\rangle = -\frac{\rho}{4\pi} \int d\mathbf{y} \frac{\partial}{\partial x_\alpha} |\mathbf{x} - \mathbf{y}|^{-1} \frac{\partial^2}{\partial y_\beta \partial y_\gamma} \langle v_\beta(\mathbf{y}) v_\gamma(\mathbf{y}) \hat{f} \rangle. \tag{62}$$

The expectation in the integrand involves the two-point pdf $f_2(\ldots; \mathbf{x}, \mathbf{y}, t)$, since

$$\langle v_\beta(\mathbf{y}, t) v_\gamma(\mathbf{y}, t) \hat{f} \rangle = \int d\mathbf{v}^{(2)} v_\beta^{(2)} v_\gamma^{(2)} f_2(d, \mathbf{v}, \varphi_1, \ldots, \varphi_l, \mathbf{v}^{(2)}; \mathbf{x}, \mathbf{y}, t),$$

where the values of $\mathbf{v}(\mathbf{y}, t)$ are denoted by $\mathbf{v}^{(2)}$. From the fact that pressure is related via a differential

equation to velocity, it follows that the pdf flux due to the pressure gradient cannot be expressed in terms of f_1. It involves necessarily the two-point pdf f_2.

The external force f_α per unit mass is considered for two cases: first, the nonfluctuating case where

$$\frac{\partial}{\partial v_\alpha}\langle \rho f_\alpha \hat{f}\rangle = f_\alpha(\mathbf{x}, t)\frac{\partial}{\partial v_\alpha}(df_1)$$

appears in closed form, and, second, the fluctuating case where the statistical properties of f_α must be specified in order to arrive at the proper form for this term. If the external force corresponds, for instance, to a Wiener process, then f_α is not defined and the momentum balance must be written as a system of stochastic differential equations containing

$$f_\alpha\, dt = g_{\alpha\beta}\, dW_\beta(t),$$

where $g_{\alpha\beta}\, dW_\beta(t)$ denotes the velocity increment and $dW_\beta(t)$ denotes the increment of a vector Wiener process (see Keizer, 1987) with zero mean and unit variance. The pdf equation then contains

$$-\frac{\partial}{\partial v_\alpha}\langle \rho f_\alpha \hat{f}\rangle = \frac{1}{2}\frac{\partial^2}{\partial v_\alpha \partial v_\beta}(g_{\alpha\gamma}g_{\gamma\beta}f_1),$$

where $\frac{1}{2}g_{\alpha\gamma}g_{\gamma\beta}$ is the tensorial diffusivity in the velocity space. This aspect of the pdf equation is discussed in more detailed in Section 3.2. The remaining terms on the right-hand side of (47) represent molecular transport in velocity and scalar space. They can be rearranged in such a way that their effect on the pdf becomes more transparent. For the sake of simplicity we assume, for the moment, that $\alpha\Gamma_j = \rho\Gamma = \mu =$ constant are valid. Simple manipulations lead to

$$\begin{aligned}
-\frac{\partial}{\partial v_\alpha}\left\langle \frac{\partial \tau_{\alpha\beta}}{\partial x_\beta}\hat{f}\right\rangle - \sum_{j=1}^{I}\frac{\partial}{\partial \varphi_j}\left\langle \frac{\partial}{\partial x_\beta}\left(\rho\Gamma_j\frac{\partial \Psi_j}{\partial x_\beta}\hat{f}\right)\right\rangle &= \underline{\frac{\partial}{\partial x_\beta}\left(\rho\Gamma_j\frac{\partial f_1}{\partial x_\beta}\right)} + \frac{\partial}{\partial x_\beta}\left\langle\left(\mu\frac{\partial v_\alpha}{\partial x_\beta} - \tau_{\alpha\beta}\right)\frac{\partial \hat{f}}{\partial v_\alpha}\right\rangle \\
&\quad + \frac{\partial}{\partial x_\beta}\left\langle \rho\Gamma\frac{\partial \rho}{\partial x_\beta}\frac{\partial \hat{f}}{\partial d}\right\rangle - \underline{\frac{\partial^2}{\partial v_\alpha \partial v_\gamma}\langle \Phi_{\alpha\gamma}\hat{f}\rangle} - \frac{\partial^2}{\partial v_\alpha \partial d}\left\langle \tau_{\alpha\beta}\frac{\partial \rho}{\partial x_\beta}\hat{f}\right\rangle \\
&\quad - \sum_{j=1}^{I}\frac{\partial^2}{\partial v_\alpha \partial \varphi_j}\left\langle \tau_{\alpha\beta}\frac{\partial \Psi_j}{\partial x_\beta}\hat{f}\right\rangle - \underline{\sum_{j=1}^{I}\sum_{k=1}^{I}\frac{\partial^2}{\partial \varphi_j \partial \varphi_k}\langle \Phi_{jk}\hat{f}\rangle} \\
&\quad - \sum_{j=1}^{I}\frac{\partial^2}{\partial \varphi_j \partial d}\left\langle \rho\Gamma\frac{\partial \Psi_j}{\partial x_\beta}\frac{\partial \rho}{\partial x_\beta}\hat{f}\right\rangle - \sum_{j=1}^{I}\frac{\partial^2}{\partial \varphi_j \partial v_\alpha}\left\langle \rho\Gamma\frac{\partial \Psi_j}{\partial x_\beta}\frac{\partial v_\alpha}{\partial x_\beta}\hat{f}\right\rangle,
\end{aligned} \tag{63}$$

where

$$\Phi_{\alpha\gamma} = \mu\frac{\partial v_\alpha}{\partial x_\beta}\frac{\partial v_\gamma}{\partial x_\beta}$$

and

$$\Phi_{jk} = \rho\Gamma\frac{\partial \Psi_j}{\partial x_\beta}\frac{\partial \Psi_k}{\partial x_\beta}$$

denote the rates of dissipation. The essential properties of the molecular transport terms are contained in the underlined expressions. An inspection of those terms shows that molecular transport affects the pdf f_1 differently in physical and velocity–scalar spaces. The distribution of the pdf in physical space is smoothed exactly the same way as velocity and scalars are smoothed by viscous and diffusive transport. This contribution is, however, negligible for turbulent flows at high Reynolds and Peclet numbers. The underlined terms representing transport in velocity-scalar space are of the leading order in high Re/Pe-numbers flows and affect the pdf analogously to the time-inverse heat conduction equation (i.e., heat conduction with negative diffusivity) given by

$$\frac{\partial f_1}{\partial t} = -\frac{\partial^2}{\partial v_\alpha \partial v_\beta}(D_{\alpha\beta}f_1),$$

where

$$D_{\alpha\beta} \equiv \langle \Phi_{\alpha\beta} | \rho = d, \mathbf{v} = \mathbf{v}, \Psi_j = \varphi_j\rangle$$

is positive definite (note that the trace of $\Phi_{\alpha\beta}$ is the dissipation function). The initial-value problem for this equation is not well-posed and it follows that closure models for the molecular transport terms cannot be based on this type of differential equation. The effect of the molecular transport terms in velocity–scalar space is in essence to reduce variances and convariances while leaving normalization and mean values unchanged. The pdf in freely decaying turbulent flows will approach a Dirac-pseudofunction due to the molecular transport terms acting in velocity–scalar space.

3.2. Formulations

The presence of nonclosed terms in the transport equations for finite-dimensional pdfs requires additional information in order to arrive at a finite and determinate system of equations. This closure problem can be tackled in several different but not necessarily equivalent formulations. Three approaches are outlined, two of which have been the basis for successful modeling efforts.

Formulation I: Pdf. The nonclosed terms are analyzed as fluxes of the pdf in the multidimensional space spanned by velocity and scalar variables. The exact form of the nonclosed terms is given directly by the transport equation (47). The essential step in the analysis is the determination of the structure of the set formed by all realizable states in velocity and scalar spaces. The velocity space is usually a three-dimensional Euclidean space, but the scalar space can possess intricate boundaries. In particular, chemically reacting flows lead to a description of the local state that requires many scalar variables. The range $\mathfrak{R}$ of these variables is bounded and the boundary $\partial\mathfrak{R}$ of this range is determined by complex relationships (see, for instance, the case of CH_4 combustion (Chen *et al.*, 1989)). However, the following fundamental restrictions are imposed on the possible forms of the boundary $\partial\mathfrak{R}$ of the scalar range: The boundary $\partial\mathfrak{R}$ is an orientable, singly connected, and piecewise smooth hypersurface (dimension $l-1$) that encloses a convex body of nonzero l-dimensional volume. The enclosed volume does not have to be bounded. The condition of convexity is relevant for the mixing models to be discussed later. The existence of boundaries in velocity or scalar space imposes a condition on model expressions for nonclosed fluxes: the flux component normal to the boundary $\partial\mathfrak{R}$ (where the normal exists) must be negative or zero if the normal is defined as positive outward (which is only possible for orientable surfaces). Then

$$\sum_{k=1}^{l} n_k F_k(\mathbf{y}) \le 0, \qquad y_1, \ldots, y_l \quad \text{on } \partial\mathfrak{R}. \tag{64}$$

If this condition is violated, unphysical states becomes accessible.

Formulation II: Characteristic Function. Characteristic functions are the Fourier transforms of pdfs and therefore an equivalent formulation under mild conditions. They have been used rarely in the treatment of turbulent flows (see Kollmann, 1987). Characteristic functions possess several interesting properties which can be exploited for the construction of closure models. For the sake of simplicity, the case of a single probabilistic variable is considered. The distribution function $F_1(y)$ and characteristic function $m_1(\zeta)$ can be decomposed uniquely into the sum of three distinct contributions (Jordan and Lebesgue theorems (Lukacs, 1970))

$$F_1(y) = aF_d(y) + bF_{ac}(y) + cF_s(y), \qquad a, b, c \ge 0, \quad a + b + c = 1,$$

and

$$m_1(\zeta) = am_d(\zeta) + bm_{ac}(\zeta) + cm_s(\zeta),$$

where F_d is a step function, F_{ac} is absolutely continuous and has a derivative everywhere, and F_s is continuous but singular in the sense that its derivative is zero nearly everywhere. The decomposition of the characteristic function is completely analogous to the distribution function; m_d is the characteristic function of the discrete distribution, hence it is almost periodic (see Lukacs, 1970)

$$\limsup_{|\zeta|\to\infty} |m_d| = 1,$$

m_{ac} is the characteristic function of the absolutely continuous distribution, hence

$$\lim_{|\zeta|\to\infty} m_{ac}(\zeta) = 0,$$

and m_s is the characteristic function of the singular distribution, where the limit of $m_s(\zeta)$ as $|\zeta| \to \infty$ can be any number between zero and unity. The singular part of distribution and characteristic functions is tacitly omitted for flows at finite Reynolds numbers. The pdf is then given as a generalized derivative of the distribution function and the pdf and characteristic function are indeed equivalent. However, the analysis of turbulent flows in the limit of infinite Reynolds number leads to the investigation of subsets of the flow field, which have zero measure and fractal dimension (see Mandelbrot, 1974; Levich *et al.*, 1984). This analysis is based on the fundamental but unproven assumption proposed by Kolmogorov (see Chapter 8 of Monin and Yaglom (1975)), that the rate of dissipation

$$\langle \varepsilon \rangle = \left\langle \frac{1}{\mathrm{Re}} \frac{\partial v_\beta}{\partial x_\alpha} \frac{\partial v_\alpha}{\partial x_\beta} \right\rangle$$

becomes independent of the Reynolds number for $\mathrm{Re} \gg 1$ and approaches a nonzero and finite limit value as $\mathrm{Re} \to \infty$. The rate of dissipation is dominated by the enstrophy $\Omega^2 \equiv \omega_\alpha \omega_\alpha$ (density is taken here as constant)

$$\langle \varepsilon \rangle = \langle \mathrm{Re}^{-1}\, \Omega^2 \rangle + \frac{\partial^2}{\partial x_\alpha \partial x_\beta} \langle \mathrm{Re}^{-1}\, v_\alpha v_\beta \rangle$$

because the difference with $\langle \varepsilon \rangle$ is only a transport term. Hence, the instantaneous rate of dissipation is concentrated on subsets of the flow field, where enstrophy becomes unbounded as $\mathrm{Re} \to \infty$. The values of ε are (for this limit) restricted to zero nearly everywhere and to infinity on a set of measure zero, such that a finite and nonzero mean value exists. It is easy to construct a simple example for such a random variable. For instance, the discrete pdf

$$f_1(\varepsilon; \mathrm{Re}) \equiv \left(1 - \frac{1}{\mathrm{Re}}\right) \delta(\varepsilon) + \frac{1}{\mathrm{Re}} \delta(\varepsilon - \mathrm{Re}\langle \varepsilon \rangle), \qquad 0 < \langle \varepsilon \rangle < \infty,$$

or the discrete characteristic function

$$m_1(\zeta; \mathrm{Re}) \equiv 1 - \frac{1}{\mathrm{Re}} (1 - \exp\{i\zeta \langle \varepsilon \rangle \mathrm{Re}\})$$

has the mean value $\langle \varepsilon \rangle$, which is independent of Re, and the variance $\langle \varepsilon'^2 \rangle = \langle \varepsilon \rangle^2 (\mathrm{Re} - 1)$, which is proportional to Re. Letting $\mathrm{Re} \to \infty$ a random variable is produced that assumes the value zero with probability one, but has nonzero mean $\langle \varepsilon \rangle$ and unbounded variance. Pdfs, such as the one constructed in this example, are, however, rather awkward to handle and are, therefore, not suitable for the analysis of variables defined on fractal sets in the limit of infinite Reynolds number. Characteristic functions are then the superior tool because they allow the explicit treatment of singular contributions which cannot be ruled out *a priori* for the limit of infinite Reynolds number. Further properties of characteristic functions can be deduced from its definition. Characteristic functions are always bounded and continuous in contrast to pdfs which may be unbounded or pseudofunctions. Since characteristic functions and pdfs are related by Fourier transformation, results obtained in one formulation can be translated into the other if both satisfy the conditions for Fourier transformation.

Formulation III: Langevin Equation. Single-point pdf equations can be simulated under certain conditions by an ensemble of notional particles, whose dynamics are governed by stochastic differential equations. This approach was developed by Pope (1985) and is essentially based on Markovian stochastic processes. We outline the basic ideas and derive the pdf equation for this approach. The Lagrangean point of view is adopted and the basic laws for a material point **a** are set up in mixed Eulerian/Lagrangean formulation:

$$\frac{\partial X_\alpha}{\partial t} = V_\alpha, \tag{65}$$

$$\frac{\partial R}{\partial t} = -R \frac{\partial V_\alpha}{\partial X_\alpha}, \tag{66}$$

$$\frac{\partial V_\alpha}{\partial t} = -\frac{1}{R} \frac{\partial P}{\partial X_\alpha} + \frac{1}{R} \frac{\partial T_{\alpha\beta}}{\partial X_\beta} + F_\alpha, \tag{67}$$

$$\frac{\partial \Psi_j}{\partial t} = \frac{1}{R}\frac{\partial}{\partial X_\alpha}\left(D_j \frac{\partial \Psi_j}{\partial X_\alpha}\right) + Q_j, \qquad j = 1, \ldots, l. \tag{68}$$

The right-hand sides of the basic laws (66)–(68) are split into expectations and fluctuations as follows:

$$\frac{\partial R}{\partial t} = A(R, \langle V_\alpha \rangle) + B\left(R, \frac{\partial V'_\alpha}{\partial X_\alpha}\right),$$

$$\frac{\partial V_\alpha}{\partial t} = A_\alpha(R, \langle P \rangle, \langle T_{\beta\gamma} \rangle, \langle F_\alpha \rangle) + B_\alpha\left(R, \frac{\partial P'}{\partial X_\alpha}, \frac{\partial T'_{\beta\gamma}}{\partial X_\gamma}, F'_\alpha\right),$$

$$\frac{\partial \Psi_j}{\partial t} = A_j(R, \langle \Psi_k \rangle) + B_j\left(R, \frac{\partial}{\partial X_\alpha}\left(D_j \frac{\partial \Psi'_j}{\partial X_\alpha}\right)\right), \qquad j = 1, \ldots, l.$$

The terms denoted with A, A_α, A_j represent the deterministic part and may depend on expectations and the dependent variables R, V_α, Ψ_j. The B, B_α, B_j represent the random parts, which depend on fluctuations such as $\partial V'/\partial X_\alpha$ (which cannot be expressed in terms of the dependent variables at a single label **a** or observer position **x**) in addition to expectations and the dependent variables R, V_α, Ψ_j. Hence, the deterministic parts are given by

$$A \equiv -R\frac{\partial \langle V_\alpha \rangle}{\partial X_\alpha},$$

$$A_\alpha \equiv -\frac{1}{R}\frac{\partial \langle P \rangle}{\partial X_\alpha} + \frac{1}{R}\frac{\partial \langle T_{\alpha\beta} \rangle}{\partial X_\beta} + \langle F_\alpha \rangle,$$

$$A_j \equiv \frac{1}{R}\frac{\partial}{\partial X_\alpha}\left(D_j \frac{\partial \langle \Psi_j \rangle}{\partial X_\alpha}\right) + Q_j(\Psi_1, \ldots, \Psi_l, R),$$

where $D_j \equiv R\Gamma_j$ = constant and the sources Q_j were assumed to be local functions of R, $\Psi_1, \ldots, \Psi_l$. The random contributions contain all the fluctuations that cannot be expressed as functions of the dependent variables; hence

$$B \equiv -R\frac{\partial V'_\alpha}{\partial X_\alpha},$$

$$B_\alpha \equiv -\frac{1}{R}\frac{\partial P'}{\partial X_\alpha} + \frac{1}{R}\frac{\partial T'_{\alpha\beta}}{\partial X_\beta} + F'_\alpha,$$

$$B_j \equiv \frac{1}{R}\frac{\partial}{\partial X_\alpha}\left(D_j \frac{\partial \Psi'_j}{\partial X_\alpha}\right).$$

Note that the random parts have the structure of additive (such as F'_α) and multiplicative (such as $\partial P'/\partial X_\alpha$) coloured noise (see Soong, 1973; Lindenberg *et al.*, 1983). It follows that the system (65)–(68) can be written in the form

$$\frac{\partial Y_j}{\partial t} = A_j(\mathbf{Y}, \langle \mathbf{Y} \rangle) + B_{jk}(\mathbf{Y}, \langle \mathbf{Y} \rangle)\frac{\partial W_k}{\partial t}, \tag{69}$$

where $\mathbf{Y} \equiv (R, \mathbf{X}, \mathbf{V}, \Psi_1, \ldots, \psi_l)$ is the vector of the dependent variables and W_k is a random differentiable vector representing all the additional unknowns contained in B, B_α, B_j. We now relax the conditions on the random processes W_k and only require that the increments of W_k are bounded. The relations (69) must now be regarded as a system of stochastic differential equations (see Pope, 1985) and appears as

$$dY_j = A_j\, dt + B_{jk}\, dW_k, \qquad j = 1, \ldots, (l + 7). \tag{70}$$

This system is solvable if the initial conditions and the processes W_k are specified. For turbulent flows these processes are, however, not known unless the characteristic functional has been determined. Hence we investigate, in later sections, random processes that are capable of simulating some (but not all) of the properties of the fluctuations occurring in a turbulent flow. It is shown that specifying such processes is equivalent to constructing closure models for the pdf equation (56). In order to establish

this equivalence and possible restrictions on the pdf equation for this case, it is derived for the solution process of the system (70) of stochastic differential equations. This derivation cannot be based on a straightforward time differentiation because dW_k/dt does not necessarily exist. We proceed therefore in a different manner following Soong (1973) for the case where W_k is at least continuous. The single-point pdf $F_1(d, \mathbf{x}, \mathbf{v}, \varphi_1, \ldots, \varphi_l; \mathbf{a}, t) \equiv F_1(y_1, \ldots, y_{l+7}; \mathbf{a}, t)$ satisfies the fundamental relation

$$F_1(\mathbf{y}; \mathbf{a}, t) = \int d\mathbf{y}' F_1^c(\mathbf{y}'; \mathbf{a}, t|\mathbf{y}; \mathbf{a}, t + \Delta t) F_1(\mathbf{y}'; \mathbf{a}, t), \tag{71}$$

where F_1^c denotes the pdf of $\mathbf{Y}$ at $(\mathbf{a}, t + \Delta t)$ conditioned upon $\mathbf{Y} = \mathbf{y}'$ at $(\mathbf{a}, t)$. The conditional pdf F_1^c can be expressed in terms of the conditional characteristic function M_1^c

$$F_1^c(\mathbf{y}; \mathbf{a}, t + \Delta t) = \frac{1}{2\pi} \int d\mathbf{y}' \exp(-iy'_\alpha y_\alpha) M_1^c(\mathbf{y}; \mathbf{a}, t|\mathbf{y}'; \mathbf{a}, t + \Delta t).$$

If all moments of finite order exist for the conditional pdf, then M_1^c is differentiable at the origin and can be expanded in a Taylor series at the origin. Using the well-known relation between moments and the derivatives of the characteristic function at the origin, we obtain ($L \equiv l + 7$)

$$F_1(\mathbf{y}; \mathbf{a}, t + \Delta t) = \sum_{n_1=0}^{\infty} \cdots \sum_{n_L=0}^{\infty} \prod_{j=1}^{L} \frac{(-1)^{n_j}}{n_j!} \frac{\partial^{n_j}}{\partial y_j^{n_j}} \{h_{n_1 \cdots n_L} F_1(\mathbf{y}; \mathbf{a}, t)\}.$$

Moving the first term of the series to the left-hand side, dividing by Δt, and letting $\Delta t \to 0$ leads finally to the pdf equation

$$\frac{\partial F_1}{\partial t} = \sum_{n_1=0}^{\infty} \cdots \sum_{n_L=0}^{\infty} \prod_{j=1}^{L} \frac{(-1)^{n_j}}{n_j!} \frac{\partial^{n_j}}{\partial y_j^{n_j}} \{H_{n_1 \cdots n_L}(\mathbf{y}; \mathbf{a}, t) F_1(\mathbf{y}; \mathbf{a}, t)\}, \tag{72}$$

where

$$h_{n_1 \cdots n_L} \equiv \left\langle \prod_{j=1}^{L} (Y_j(\mathbf{a}, t + \Delta t) - Y_j(\mathbf{a}, t))^{n_j} | \mathbf{Y}(\mathbf{a}, t) = \mathbf{y} \right\rangle \tag{73}$$

and

$$H_{n_1 \cdots n_L} \equiv \lim_{\Delta t \to 0} \frac{h_{n_1 \cdots n_L}}{\Delta t} \tag{74}$$

are called the derivate moments of F_j^c. The validity of the pdf equation (72) hinges on the existence of the moments $H_{n_1 \cdots n_L}$. We restrict ourselves to random processes in (70) such that all derivate moments exist. Then there are only two possibilities for the order of the pdf equation (72) (see Theorem 7.2.1 Soong (1973)): it is two or infinity. Only the first case, corresponding to all $A_{n_1, \ldots, n_L}$ with $\sum_{j=1}^{L} n_j \geq 3$ being zero, is of interest. The pdf equation for this case follows from (72) as

$$\frac{\partial F_1}{\partial t} + \frac{\partial}{\partial y_j} \{H_j(\mathbf{y}; \mathbf{a}, t) F_1(\mathbf{y}; \mathbf{a}, t)\} = \frac{\partial^2}{\partial y_j \partial y_k} \{H_{jk}(\mathbf{y}; \mathbf{a}, t) F_1(\mathbf{y}; \mathbf{a}, t)\}, \tag{75}$$

which has the same structure as the classical convection–diffusion equation. An important example for the random processes W_k is noted. If the W_k are Wiener processes, then the system (70) is of the Ito type. The increments of W_k satisfy (see Pope, 1985; Keizer, 1987)

$$\langle \Delta W_k(\mathbf{a}, t) \rangle = 0$$

and

$$\langle \Delta W_k(\mathbf{a}, t) \Delta W_l(\mathbf{a}, t) \rangle = 2D_{kl}(\mathbf{a})t.$$

The system (70) now allows for the explicit calculation of the derivate moments $H_{n_1, \ldots, n_L}$ in terms of the coefficients of (70) and the properties of the Wiener process (whose increments are independent of $\mathbf{Y}$). It follows (see, for instance, Chapter 7.3 in Soong (1973)) that

$$H_k(\mathbf{y}; \mathbf{a}, t) = A_k(\mathbf{y}; \mathbf{a}, t) \tag{76}$$

and

$$H_{kl}(\mathbf{y}; \mathbf{a}, t) = B_{km}(\mathbf{y}; \mathbf{a}, t) D_{mn}(\mathbf{a}) B_{nl}(\mathbf{y}; \mathbf{a}, t) \tag{77}$$

hold. The pdf equation (75) is now solvable, in principle, if initial and boundary conditions are set up properly. It is well known (see Soong, 1973; Keizer, 1987), that the pdf equation (75) represents a Markovian process if W_k is a Wiener process.

The conditions on the W_k are now further relaxed by only assuming that the increments of W_k are bounded. We consider jump processes independent of the continuous random processes acting on the Y_k. The pdf equation for this case can be deduced from (71) (see Pope, 1985). All that needs to be done is to set up the transition pdf F_1^c for jump processes on the right-hand side of (70). If we denote by $\Delta t/\tau$ the probability for a jump during the time interval Δt and denote by $T(\mathbf{y}', t|\mathbf{y}, t + \Delta t)$ the pdf for a change of $\mathbf{Y}$ from $\mathbf{y}'$ to $\mathbf{y}$ if a jump occurs, then it follows that the transition pdf is given by

$$F_1^c(\mathbf{y}'; \mathbf{a}, t + \Delta t) = \left(1 - \frac{\Delta t}{\tau}\right)\delta(\mathbf{y} - \mathbf{y}') + \frac{\Delta t}{\tau} T(\mathbf{y}'; \mathbf{a}, t|\mathbf{y}; \mathbf{a}, t + \Delta t). \tag{78}$$

Then (71) leads to

$$\frac{\partial F_1}{\partial t} = \frac{1}{\tau}\left\{\int d\mathbf{y}'\, F_1(\mathbf{y}'; \mathbf{a}, t) T(\mathbf{y}'; \mathbf{a}, t|\mathbf{y}; \mathbf{a}, t) - F_1(\mathbf{y}; \mathbf{a}, t)\right\}. \tag{79}$$

Note that τ can be regarded as the time scale of the jumps. Since continuous and discontinuous changes of $\mathbf{Y}$ are mutually exclusive, we can add the corresponding contributions to the change of the pdf and obtain the pdf equation for the system of stochastic differential equations

$$dY_j = A_j + B_{jk}\, dW_k + dJ_j, \qquad j = 1, \ldots, (l + 7), \tag{80}$$

where dJ_j is the increment due to the jump process, as follows:

$$\frac{\partial F_1}{\partial t} + \frac{\partial}{\partial y_j}\{H_j F_1\} = \frac{\partial^2}{\partial y_j \partial y_k}\{H_{jk} F_1\} + \frac{1}{\tau}\left\{\int d\mathbf{y}'\, F_1(\mathbf{y}') T(\mathbf{y}'|\mathbf{y}) - F_1\right\}. \tag{81}$$

This transport equation is solvable if initial and boundary conditions, as well as the properties of the continuous and discontinuous random processes, are specified.

3.3. Closure Models for the Pressure-Gradient Flux

The pressure gradient induces the flux

$$F_\alpha \equiv \left\langle \frac{\partial p}{\partial x_\alpha} \hat{f} \right\rangle = \left\langle \frac{\partial p'}{\partial x_\alpha} \middle| \rho = d, \mathbf{v} = \mathbf{v}, \Psi_j = \varphi_j \right\rangle f_1 + \frac{\partial \langle p \rangle}{\partial x_\alpha} f_1 \tag{82}$$

in velocity space. The flux due to the fluctuating pressure gradient cannot be expressed in terms of the single-point pdf and therefore requires a closure model. It was shown in Section 3.1 that the pressure gradient for incompressible flows depends on the velocity at all locations in physical space, and, furthermore, it can be shown (see Hanjalic and Launder, 1972) that the correlation involving $\partial p'/\partial x_\alpha$ consists of three parts given by

$$\frac{\partial p'}{\partial x_\alpha} = -\frac{\rho}{4\pi}\int d\mathbf{y} \frac{\partial}{\partial x_\alpha}\left(\frac{1}{|\mathbf{x} - \mathbf{y}|}\right)\frac{\partial v_\beta'}{\partial y_\gamma}\frac{\partial v_\gamma'}{\partial y_\beta} - \frac{\rho}{4\pi}\int d\mathbf{y} \frac{\partial}{\partial x_\alpha}\left(\frac{1}{|\mathbf{x} - \mathbf{y}|}\right)\frac{\partial \langle v_\beta \rangle}{\partial y_\gamma}\frac{\partial v_\gamma'}{\partial y_\beta} + \frac{\partial}{\partial x_\alpha} H(\mathbf{x}), \tag{83}$$

where $H(\mathbf{x})$ denotes the harmonic function required to satisfy the boundary conditions. The first contribution in (83) is called the "return to isotropy," the second contribution is called the "fast response" and the last boundary term (the terminology was introduced in the context of second-order closure schemes (Hanjalic and Launder, 1972; Lumley, 1978). The most advanced closure for (82) was developed by Haworth and Pope (1986, 1987) for incompressible flows with the total conditional flux including (82) and the viscous dissipation. No closures for the boundary term in (83), which is required for wall bounded flows, have appeared so far.

The Closure Model of Haworth and Pope (1986). This model incorporates both the pdf flux due to the fluctuating pressure gradient and viscous dissipation. It was developed for incompressible fluids using

the Langevin approach (formulation III). The system (65)–(68) is now specialized to

$$\frac{\partial X_\alpha}{\partial t} = V_\alpha, \qquad \frac{\partial V_\alpha}{\partial t} = -\frac{1}{R}\frac{\partial P}{\partial X_\alpha} + \nu \Delta V_\alpha + F_\alpha. \tag{84}$$

The corresponding Langevin-type stochastic differential equations (modeling the dynamics of X_α and V_α, P) were designed by Haworth and Pope as follows:

$$dX_\alpha = V_\alpha\, dt, \qquad dV_\alpha = \left(\nu \Delta \langle V_\alpha \rangle - \frac{1}{R}\frac{\partial \langle P \rangle}{\partial X_\alpha}\right) dt + G_{\alpha\beta}(V_\beta - \langle V_\beta \rangle)\, dt + (C_0 \varepsilon)^{1/2}\, dW_\alpha, \tag{85}$$

where dW_α is the increment of an isotropic Wiener process

$$\langle dW_\alpha \rangle = 0, \qquad \langle dW_\alpha\, dW_\beta \rangle = dt\, \delta_{\alpha\beta},$$

and ε denotes the expectation of the rate of dissipation of the kinetic energy of turbulence. It follows from (84) and (85) that

$$-\frac{1}{R}\frac{\partial P'}{\partial X_\alpha} + \nu \Delta V'_\alpha + F'_\alpha \cong G_{\alpha\beta}(V_\beta - \langle V_\beta \rangle)\, dt + (C_0 \varepsilon)^{1/2}\, dW_\alpha \tag{86}$$

represents the closure model. Two fundamental assumptions lead Haworth and Pope (1986) to this model:

(1) The effect of the fluctuations of the surrounding fluid depends linearily on velocity and is locally Markovian.
(2) The stochastic term is consistent with Kolmogorov's scaling law for the inertial subrange.

These two assumptions cannot be justified on a rigorous basis. The first assumption is inconsistent with the quadratic dependence of the fluctuating pressure gradient on the fluctuating velocity components as is apparent from (83). Turbulence is, strictly speaking, not a Markovian process, but the fluctuations in the inertial subrange are closely approximated by Markov processes (Monin and Yaglom, 1975). Considering the second assumption, we note that the stochastic term of the closure model (Wiener process) represents the stirring action of the surrounding fluid which is due to the fluctuating pressure gradient, viscous stresses, and external forces. This agitation is not restricted to the inertial subrange of the spectrum, whereas the model (86) takes into account subrange scaling only. Finally, it is important to notice that the closure (86) is not applicable to bounded variables such as the thermochemical scalars because no boundedness restriction can be implemented in linear models. However, the closure model (86) is tensorially consistent, realizable, and relaxes to a Gaussian pdf in the homogeneous limit. The final form of the closure model was established by constructing the tensor $G_{\alpha\beta}$ as a local function of Reynolds stress, mean rate of deformation, and dissipation rate. This constitutes a closure assumption and the form chosen by Haworth and Pope is linear in these moments, i.e.,

$$G_{\alpha\beta} = \alpha_1 \frac{1}{\tau}\delta_{\alpha\beta} + \alpha_2 \frac{1}{\tau} b_{\alpha\beta} + H_{\alpha\beta\gamma\delta}\frac{\partial \langle v_\gamma \rangle}{\partial x_\delta}, \tag{87}$$

where τ is the turbulent time scale ($\tau = k/\varepsilon$) and $H_{\alpha\beta\gamma\delta}$ is a linear function of the anisotropy tensor

$$b_{\alpha\beta} \equiv \frac{\langle v'_\alpha v'_\beta \rangle}{\langle v'_\gamma v'_\gamma \rangle} - \tfrac{1}{3}\delta_{\alpha\beta} \tag{88}$$

containing nine constants. Applying all exact symmetry and reduction properties, Haworth and Pope succeed in reducing the number of constants from eleven to six. These six constants are then determined with the aid of experiments in strained and unstrained homogeneous turbulent flows. The

model was applied to self-similar free shear layers and Haworth and Pope (1987) found that good agreement with experiments could be achieved for homogeneous and nonhomogeneous flows, if the constraint (Speziale, 1983) of proper transformation in the limit of two-dimensional turbulence was relaxed.

Closure Model for the "Return to Isotropy" Part of the Pressure-Gradient Term. It is straightforward to construct a closure model for (82) that simulates the return to isotropy aspect of the fluctuating pressure gradient, as Pope (1985) has shown. This is accomplished by pairwise interaction of material points with velocities υ' and υ'' in a sufficiently small neighborhood such that:

(1) $\upsilon^m \equiv \frac{1}{2}(\upsilon' + \upsilon'')$ remains constant and
(2) the difference $\Delta\upsilon \equiv \upsilon' - \upsilon''$ is reoriented randomly but $|\Delta\upsilon|$ remains constant.

The reorientation is carried out with uniform probability on a sphere with radius $|\Delta\upsilon|$ that is centered at υ^m in velocity space. This interaction model can be set up in the pdf formulation as follows: consider a volume $\Delta\upsilon$ in velocity space centered at υ and a time interval Δt and let the pdf $f_1(\upsilon; \mathbf{x}, t)$ be approximated by $N(\mathbf{x})$ elements. Let $N(\upsilon)$ be the number of elements with $\upsilon_\alpha \le v_\alpha(\mathbf{x}, t) \le \upsilon_\alpha + \Delta\upsilon_\alpha$ for $\alpha = 1, 2, 3$ and

$$\frac{N(\upsilon)}{N} \to f_1(\upsilon; \mathbf{x}, t) \qquad \text{as} \quad N \to \infty \quad \text{and} \quad \Delta\upsilon \to 0.$$

The change of the number of elements in $\Delta\upsilon$ at υ during Δt due to the stochastic reorientation of velocities is then

$$\frac{1}{\Delta t}\Delta N(\upsilon) = \Delta\dot{N}^+(\upsilon) - \Delta\dot{N}^-(\upsilon),$$

where $\Delta\dot{N}^+(\upsilon)$ is the number of elements added to the volume $\Delta\upsilon$ at υ and, analogously, $\Delta\dot{N}^-(\upsilon)$ is the number of elements removed from $\Delta\upsilon$ at υ during Δt. The number of added and removed elements can be established if the probability of interaction per unit time and the probability that the interaction of two elements produces an element in $\Delta\upsilon$ at υ or removes an element from this volume, are set up. Let τ denote the frequency of interaction (time scale of interaction) and let $f_2(\upsilon^{(i)}, \upsilon^{(j)}; \mathbf{x}, t)(\Delta\upsilon)^2$ be the probability of finding elements in $\Delta\upsilon$ at $\upsilon^{(i)}$ and elements in $\Delta\upsilon$ at $\upsilon^{(j)}$; then the assumption of statistical independence of finding elements in $\Delta\upsilon$ at $\upsilon^{(i)}$ from finding elements in $\Delta\upsilon$ at $\upsilon^{(j)}$ for $|\upsilon^{(i)} - \upsilon^{(j)}| > |\Delta\upsilon|$ is invoked. It follows that the equation

$$f_2(\upsilon^{(i)}, \upsilon^{(j)}) = f_1(\upsilon^{(i)}) f_1(\upsilon^{(j)}) \tag{89}$$

holds in analogy to the assumption of molecular chaos in the context of the Boltzmann equation (see Chapter 2.7 in Keizer (1987)). Finally the notion of transition pdf is introduced and

$$T(\upsilon^{(i)}, \upsilon^{(j)} \to \upsilon)\Delta\upsilon$$

denotes the probability that the interaction of an element $\upsilon^{(i)}$ with an element $\upsilon^{(j)}$ produces an element in $\Delta\upsilon$ at υ. It follows that

$$\Delta\dot{N}^+(\upsilon^{(i)}) = \frac{1}{2}\frac{N}{\tau}\left\{\sum_j\sum_k f_1(\upsilon^{(j)}) f_1(\upsilon^{(k)}) T(\upsilon^{(j)}, \upsilon^{(k)} \to \upsilon^{(i)}) + \sum_j\sum_k f_1(\upsilon^{(j)}) f_1(\upsilon^{(k)}) T(\upsilon^{(k)}, \upsilon^{(j)} \to \upsilon^{(i)})\right\}(\Delta\upsilon)^3$$

holds, and by restricting T to the symmetry $T(\upsilon^{(j)}, \upsilon^{(k)} \to \upsilon) = T(\upsilon^{(k)}, \upsilon^{(j)} \to \upsilon)$, we obtain

$$\Delta\dot{N}^+(\upsilon^{(i)}) = \frac{N}{\tau}\sum_j\sum_k f_1(\upsilon^{(j)}) f_1(\upsilon^{(k)}) T(\upsilon^{(j)}, \upsilon^{(k)} \to \upsilon^{(i)})$$

and likewise (for the removed elements)

$$\Delta\dot{N}^-(\upsilon^{(i)}) = \frac{N}{\tau}\sum_{j\neq i}\sum_{k\neq i} f_1(\upsilon^{(j)}) f_1(\upsilon^{(i)}) T(\upsilon^{(j)}, \upsilon^{(i)} \to \upsilon^{(k)}).$$

Passing to the limit $\Delta\upsilon \to 0$, $N \to \infty$ we get

$$\frac{\partial f_1}{\partial t}(\upsilon) = \frac{1}{\tau}\left\{\int d\upsilon' \int d\upsilon''\, f_1(\upsilon')f_1(\upsilon'')T(\upsilon', \upsilon'' \to \upsilon) - f_1(\upsilon)\right\}. \tag{90}$$

This is the general form of the effect of pairwise interaction of elements on the single-point pdf. It is very similar to the effect of a jump process in the Langevin equation (compare with (79)). There is, however, a subtle conceptual difference between (90) and (79): Since (90) describes the interaction of two elements, those elements cannot represent two realizations of a single stochastic differential equation since different realizations cannot interact with each other. Hence, (90) is outside the scope of the Langevin approach discussed in Section 3.2. The stochastic reorientation model can now be given in terms of the transition pdf T. The two geometrical properties characterizing this model lead to

$$T(\upsilon', \upsilon'' \to \upsilon) = \frac{1}{4\pi}\frac{1}{|\upsilon' - \upsilon''|}\delta(|\upsilon - \tfrac{1}{2}(\upsilon' + \upsilon'')| - |\upsilon' - \upsilon''|). \tag{91}$$

It is easy to see that T is the pdf with respect to υ and that T is concentrated on the sphere with radius $|\upsilon' - \upsilon''|$ centered at $\frac{1}{2}(\upsilon' + \upsilon'')$ in velocity space. The stochastic reorientation model is equivalent to Rotta's closure for the "return to isotropy" contribution to the pressure-gradient correlation on the level of second-order closures (see Rotta, 1951; Pope, 1985).

3.4. Closure Models for the Molecular Transport Terms

The molecular transport terms (see (63)) were shown to affect the pdf f_1 in physical space and in velocity-scalar space. Since the part accounting for the effect in physical space is negligible except in the close vicinity of fixed wall boundaries, we consider only the closure models for the effect of molecular transport on the single-point pdf f_1 in velocity–scalar space. The closure for the molecular transport terms is usually called a mixing model.

Linear Models. Dopazo (1975) put forward the closure assumption that the pdf flux in velocity-scalar space is a linear function of the probabilistic variables. This linear relation corresponds to quasi-Gaussian behavior of the flux. It is also inherent in the linear Langevin model of Haworth and Pope (1986), where a linear drift in velocity space accounts for the dissipation of mechanical energy produced by random external forcing. This model has serious drawbacks; in particular, it is unable to produce a continuous pdf in flows which are initially totally segregated. It is, however, valuable for theoretical reasons, because it can be shown to be the short time limit of the general nonlinear closure model discussed below (Kosaly, 1986; Kosaly and Givi, 1987).

Nonlinear Models. Models based on the interaction in velocity–scalar space of two or more fluid volumes (elements) depend in a nonlinear fashion on the pdf f_1. This can be deduced from the fact that the interaction of two or more elements requires the probability of finding those elements in a given neighborhood of the physical space. Presuming chaos locally, statistical independence prevails and the probability of finding elements is given by the product of the pdf f_1 at the chosen velocity and scalar values. The interaction model has already been established in equation (90) for the case of pairwise interaction. It remains to determine the transition pdf T for the present case. It follows from the properties of the molecular transport terms acting on the pdf in velocity–scalar space (see (63)), that any closure model must preserve normalization and mean values and reduce variances and covariances. Several authors have suggested expressions for the transition pdf T (see Dopazo, 1979; Janicka *et al.*, 1979; Pope, 1982), which can be given in the common form

$$T(\mathbf{y}', \mathbf{y}'' \to \mathbf{y}) = \int_0^1 d\alpha\, A(\alpha)\delta[\mathbf{y} - (1 - \alpha)\mathbf{y}' - \tfrac{1}{2}\alpha(\mathbf{y}' + \mathbf{y}'')], \tag{92}$$

where α is a random variable governed by the pdf $A(\alpha)$. This variable α controls the amount of mixing of the properties $\mathbf{y}$ taking place in a pairwise interaction (recall, that $\mathbf{y}$ represents the collection of probabilistic variables of the pdf). Several special models, defined in terms of $A(\alpha)$, have been developed.

Curl's (1963) *Model.* This model was originally derived for the pairwise interaction of droplets. It is given by

$$A(\alpha) = \delta(\alpha - 1) \tag{93}$$

and

$$T(\mathbf{y}', \mathbf{y}'' \to \mathbf{y}) = \delta[\mathbf{y} - \tfrac{1}{2}(\mathbf{y}' + \mathbf{y}'')]. \tag{94}$$

The definition of $A(\alpha)$ corresponds to complete mixing in each interaction. If two elements with properties $\mathbf{y}'$ and $\mathbf{y}''$ interact, they emerge with $\frac{1}{2}(\mathbf{y}' + \mathbf{y}'')$ after the interaction. It is computationally very efficient but has a serious drawback. This model is not capable of producing a continuous pdf if the initial condition is given as a collection of Dirac pseudofunctions, as would be the case for initially totally segregated flows (see Pope 1982).

The Dopazo Model (Dopazo, 1979; Janicka *et al.*, 1979). The basic idea of this model is to randomize the extent of mixing. The interaction of two elements produces incomplete mixing governed by $A(\alpha)$. The form of $A(\alpha)$ can be related to the local structure of mixing regions (Dopazo, 1979), which leads to intricate expressions for $A(\alpha)$. Typically the choice for $A(\alpha)$ is of the simplest possible form that produces a continuous pdf for initially totally segregated flows:

$$A(\alpha) = 1. \tag{95}$$

This mixing model found wide application, in particular in reacting flows (see Pope, 1985; Jones and Kollmann, 1987; Chen and Kollmann, 1989). It satisfies the mathematical constraints for moments, but all standardized moments

$$\mu_m = \frac{\langle y^m \rangle}{\langle y^2 \rangle^{m/2}}, \qquad m > 2,$$

diverge for $m > 4$ in the limit of decaying homogeneous turbulence (Pope, 1982). Hence, freely decaying homogeneous turbulence does not approach a Gaussian pdf with this mixing model.

Pope's (1982) *Model.* Pope noted that the Curl and Dopazo models mix elements independent of their mixing history. He suggested biasing the sampling of element pairs with the age of the elements (time elapsed between mixing interactions). This amounts to including an additional probabilistic variable age in the pdf. Hence, $f_1^*(\mathbf{y}, s; \mathbf{x}, t)$ is taken as the single-point pdf of $\mathbf{Y}$ and the time s between mixing interactions and $f_1(\mathbf{y}; \mathbf{x}, t)$ can be recovered as

$$f_1(\mathbf{y}; \mathbf{x}, t) = \int ds\, f_1^*(\mathbf{y}, s; \mathbf{x}, t).$$

The pdf $f_s(s)$ of the age variable is obviously

$$f_s(s; \mathbf{x}, t) = \int d\mathbf{y}\, f_1^*(\mathbf{y}, s; \mathbf{x}, t).$$

The age distribution can be changed if the sampling of elements for the mixing interaction is biased. The sampling bias $z(s)$ is defined as the relative probability of sampling an element with age s. It is normalized

$$\int ds\, z(s) f_s(s) = 1$$

and the pdf of finding two elements with $\mathbf{y}'$ and $\mathbf{y}''$ is now biased according to

$$f_1^{**}(\mathbf{y}'; \mathbf{x}, t) f_1^{**}(\mathbf{y}''; \mathbf{x}, t)\, d\mathbf{y}'\, d\mathbf{y}'',$$

where

$$f_1^{**}(\mathbf{y}; \mathbf{x}, t) = \int_0^\infty ds\, z(s) f_1^*(\mathbf{y}, s; \mathbf{x}, t) \tag{96}$$

is the pdf of the elements sampled for mixing. The mixing model appears now as

$$\frac{\partial f_1}{\partial t} = \frac{1}{\tau}\left\{\int d\mathbf{y}' \int d\mathbf{y}'' f_1^{**}(\mathbf{y}') f_1^{**}(\mathbf{y}'') T(\mathbf{y}', \mathbf{y}'' \to \mathbf{y}) - f_1^{**}(\mathbf{y})\right\}. \tag{97}$$

The choice of the sampling bias $z(s)$ enabled Pope (1982) to produce standardized moments that remain bounded in the limit of decaying homogeneous turbulence.

3.5. Time Scales

The closure models for the pressure correlations and the molecular-transport terms require a turbulent time scale τ. It is clear that the single-point pdf f_1 of density, velocity, and thermochemical scalars does not contain information on time or length scales. Two methods have been devised to provide the necessary information on time (or length) scales.

The Mean Rate of Dissipation. The first method provides the scale information by including a separate transport equation for the rate of dissipation:

$$\varepsilon = \left\langle \nu \frac{\partial v'_\alpha}{\partial x_\beta} \left(\frac{\partial v'_\alpha}{\partial x_\beta} + \frac{\partial v'_\beta}{\partial x_\alpha} \right) \right\rangle, \tag{98}$$

which in turn determines a turbulent time scale

$$\tau = C \frac{k}{\varepsilon}, \tag{99}$$

where $k \equiv \frac{1}{2}\langle v'_\alpha v'_\alpha \rangle$ denotes the kinetic energy of turbulence and C is a constant of order one. The continuous distribution of scales in the spectrum is therefore described by a single and global scale τ. The exact transport equation for the dissipation rate ε is dominated by a sensitive balance of production, destruction, and turbulent-transport terms, which are all nonclosed. The closure of this equation has been carried out in the context of second-order models (see Hanjalic and Launder, 1972; Lumley, 1978; Wilcox, 1989). It represents the least-justified part of closure models on the moment and pdf level.

Pdf Closures Including Scale Information. Scale information can be included in the pdf in two different ways. Meyers and O'Brien (1981) and Sirignano (1987) suggested including a scale-determining variable such as the gradient of scalars in the set of probabilistic variables of the single-point pdf. It follows that the single-point pdf then provides the scalar time scale

$$\tau_\phi \equiv \frac{\langle \phi'^2 \rangle}{\Gamma \langle (\nabla \phi')^2 \rangle} \tag{100}$$

since both numerator and denominator are integrals of the pdf of ϕ and $\nabla\phi$. Carrying this idea over to velocity, it becomes clear that the inclusion of all strain-rate components amounts to adding six probabilistic variables, which is rather expensive in any numerical method of solution. Adding the dissipation rate as a probabilistic variable leads to closure problems similar to the moment equations. This approach has been suggested by Pope (1985), who gave a Langevin formulation that ensured relaxation toward a log-normal pdf for the nonnegative variable dissipation rate in the absence of inhomogeneity. The second possibility of dealing with the scale problem is to consider multipoint pdfs. Ievlev (1973) and O'Brien (1980) discussed multipoint pdf transport equations and closure methods based on mathematical realizability conditions. Spatial multipoint pdf equations have received little attention so far due to the enormous computational cost for their solution. However, two-time pdf equations can be solved numerically and yield turbulent time scales. This is in fact the second way of including scale information in the pdf as pointed out by Pope (1985) and Kollmann and Wu (1987). The two-time pdf $F_2(\mathbf{v}', t'; \mathbf{v}, \mathbf{x}, t)$ satisfies a transport equation identical to (56) as shown by Kollmann and Wu (1987). The solution of this equation can be carried out using stochastic simulation techniques Time histories of velocity are recorded and their statistical evaluation leads to integral time scales τ because

$$R_{\alpha\beta}(\mathbf{x}, t, t') = \int d\mathbf{v}' \int d\mathbf{v}\, v_\alpha v'_\beta F_2(\mathbf{v}', t'; \mathbf{v}, \mathbf{x}, t) \tag{101}$$

leads to

$$\tau(\mathbf{x}, t) = \int_0^\infty dt' \frac{R_{\alpha\alpha}(\mathbf{x}, t + t')}{R_{\alpha\alpha}(\mathbf{x}, t, t)}. \tag{102}$$

Note that the dissipation rate ε can be recovered from

$$\varepsilon(\mathbf{x}, t) = C\frac{R_{\alpha\alpha}(\mathbf{x}, t, t)}{\tau}. \tag{103}$$

No separate equation for a scale-determining variable has to be solved. The application of this method to plane mixing layers by Kollmann and Wu (1987) shows promising agreement with measured velocity moments up to order three.

4. Applications and Extensions

Pdf methods have found the widest application in turbulent reacting flows. Both premixed and non-premixed systems were investigated. The progress made in the area of premixed turbulent combustion was reviewed recently by Pope (1987) and Borghi (1988). Hence only the case of non-premixed turbulent combustion will be considered here.

4.1. Turbulent Non-premixed Combustion at Low Mach Numbers

Turbulent non-premixed combustion is created by the interaction of one or several fuel streams with an oxidizer stream. The mass fraction Y_i of species i in such a reacting mixture is governed by (8) or (9). Bilger (1976, 1980) has shown that the energy equation written for the sensible enthalpy has, at low Mach numbers, the same structure as the species balance. Linear combinations of mass fractions and enthalpy (Shvab–Zeldovich coupling functions (see Williams, 1985)) can be found such that the chemical source terms are eliminated in all equations except one. Since elemental mass and mole fractions are always conserved and not uniformly constant in non-premixed flows, it follows that there always exists at least one conserved scalar among the variables describing the local thermodynamic state. Appropriate normalization with the values in the fuel and oxidizer streams leads to the mixture fraction ξ, which plays a central role in non-premixed combustion theory (see Bilger, 1988). An important consequence of this formulation is the fact that the density ρ now becomes a local function of the mixture fraction ξ and the other thermochemical variables. The Eulerian pdf $f_1(d, \upsilon, \varphi_1, \ldots, \varphi_l; \mathbf{x}, t)$ is therefore restricted by

$$f_1(d, \upsilon, \varphi_1, \ldots, \varphi_l) = f_1^*(\upsilon, \varphi_1, \ldots, \varphi_l)\delta(d - \rho(\varphi_1, \ldots, \varphi_l))$$

and the transport equation for f_1^* follows from (47) by integration over the values d of the density. Denoting by $\rho(\varphi_1, \ldots, \varphi_l)$ the local relation with the thermochemical scalars and setting $\Psi_1 \equiv \xi$, we obtain the Eulerian pdf equation

$$\begin{aligned}\rho(\varphi_1, \ldots, \varphi_l)\left\{\frac{\partial f_1^*}{\partial t} + \upsilon_\beta \frac{\partial f_1^*}{\partial x_\beta}\right\} + \sum_{j=1}^{l} \frac{\partial}{\partial \varphi_j}(\rho(\varphi_1, \ldots, \varphi_l) q_j(\varphi_1, \ldots, \varphi_l) f_1^*) \\ = \frac{\partial}{\partial \upsilon_\alpha}\left\langle\left(\frac{\partial p}{\partial x_\alpha} - \frac{\partial \tau_{\alpha\beta}}{\partial x_\beta} - \rho f_\alpha\right)\hat{f}\right\rangle - \sum_{j=1}^{l} \frac{\partial}{\partial \varphi_j}\left\langle \frac{\partial}{\partial x_\beta}\left(\rho \Gamma_j \frac{\partial \psi_j}{\partial x_\beta}\right)\hat{f}\right\rangle,\end{aligned} \tag{104}$$

where

$$\hat{f} \equiv \delta(\mathbf{v}(\mathbf{x}, t) - \upsilon) \prod_{j-1}^{l} \delta(\psi_j(\mathbf{x}, t) - \varphi_j). \tag{105}$$

Exactly the same equation follows from (56) for the Lagrangean pdf F_1^* (the asterisk is ommitted in the following). The application of pdf methods to non-premixed combustion problems depends crucially on the chemical mode. The chemistry of gas phase combustion is extremely complex and simplified model systems of reactions are therefore essential for the solvability of the resulting pdf equation. The pdf methods for non-premixed combustion are therefore classified according to the chemical models.

Equilibrium Models. Chemical equilibrium prevails locally to good approximation (Bilger, 1976) for turbulent reacting flows with fast reactions, which is the case if the time scales of the reactions are much smaller than the time scales of convection and diffusion (high Damköhler number). It follows (Bilger, 1976) that the local thermochemical state is then determined as the minimum of the Gibbs free

energy for a given mixture fraction, pressure, and enthalpy (sensible plus formation enthalpies). Turbulent combustion at low Mach numbers allows two further approximations:

(A) The pressure is constant in thermodynamic relations.
(B) Enthalpy is a linear function of mixture fraction.

The first approximation is based on the observation that, for low Mach numbers and small mean pressure gradients, pressure fluctuations are small

$$O\left(\frac{\langle p'^2\rangle^{1/2}}{\langle p\rangle}\right) \ll 1.$$

Hence we can neglect the pressure variations due to fluid mechanics in the thermochemical aspects of the reacting system. This does not hold for supersonic and rapidly expanding and compressing flows, where the pressure fluctuations can be of the same order of magnitude as the mean pressure itself. The second approximation can be seen to be a consequence of the energy equation. If the Mach number is much less than unity, the dissipation function in the energy equation (13) can be neglected; if the pressure is approximately constant, the substantial derivative of the pressure in the energy equation can also be neglected. Hence

$$\rho\frac{Dh}{Dt} \cong -\frac{\partial q_\alpha}{\partial x_\alpha}$$

is obtained. This form of the energy equation reduces to the same convection–diffusion equation for enthalpy as for the mixture fraction under the standard restrictions (Bilger, 1976) of the equilibrium flame sheet model. It can be argued (Bilger, 1976) that a linear relation between h and mixture fraction ξ exists sufficiently far away from boundaries, where h and ξ do not necessarily satisfy such a linear relation. Again, this approximation does not hold for supersonic flows where Φ becomes significant and the enthalpy ceases to be a conserved quantity. It follows now that the pdf equation, for turbulent flows involving fast reactions and low Mach numbers, contains only a single conserved scalar (mixture fraction) to account for combustion. The value of the mixture fraction uniquely determines the density, temperature, and composition so that expectations of these variables can be obtained by a straightforward integration. Pdf methods have been applied successfully to this case and the closely related turbulent transport of passive scalars (Kollmann and Janicka, 1982), but the full power of pdf methods has not been exploited in the transport of conserved scalars. Furthermore, the condition of high Damköhler numbers is too restrictive for many fuels (in particular hydrocarbons (see Bilger, 1988)).

Nonequilibrium Models. The inclusion of chemical nonequilibrium for reaction systems proceeding with finite rates requires careful analysis of the usually complex system of reactions in order to obtain a tractable system. The tools available for the reduction of complex systems of reactions are partial equilibrium for selected steps and constrained equilibrium, where the progress of reactions is assumed to take place in a series of quasi-equilibrium states subject to a set of constraints which are controlled by the rate-limiting reactions (Keck, 1978). These tools are not perfect and considerable insight into the detailed reaction mechanism and calculations of laminar flames are required to establish a reasonably accurate simplified mechanism (Kee and Peters, 1987; Peters and Williams, 1987; Rogg and Williams, 1988). Pdf methods were applied successfully to hydrogen–air flames (Chen and Kollmann, 1989a), CO–air flames (Pope and Correa, 1986), methane–air flames (Masri and Pope, 1989; Chen *et al.*, 1989), and propane–air flames (Jones and Kollmann, 1987; Chen and Kollmann, 1989b). Other reactants were treated by Givi *et al.* (1985) and Arroyo *et al.* (1988). We consider the case of turbulent methane combustion in jet flames in some detail to show the properties of pdf methods following Chen *et al.* (1989). The combustion of methane with air is described with the four-step mechanism of Peters and Kee (1987), which requires five scalar variables $\Psi_j(\mathbf{x}, t)$. They are defined as follows:

$$\Psi_1 \equiv \xi \text{ (mixture fraction)}, \qquad \Psi_2 \equiv n_{CH4},$$
$$\Psi_3 \equiv n_{CO}, \qquad \Psi_4 \equiv n,$$
$$\Psi_5 \equiv n_H$$

(n denotes the number of moles per unit volume). The pdf equation (104) is integrated over velocity space

$$\langle\rho\rangle\left\{\frac{\partial\tilde{f}_1}{\partial t}+\tilde{v}_\beta\frac{\partial\tilde{f}_1}{\partial x_\beta}+\sum_{j=1}^{I}\frac{\partial}{\partial\varphi_j}(q_j(\varphi_1,\ldots,\varphi_I)\tilde{f}_1)\right\}$$
$$=-\frac{\partial}{\partial x_\alpha}(\langle\rho\rangle\langle v_\alpha''|\Psi_j=\varphi_j\rangle\tilde{f}_1)-\left(\langle\rho\rangle\sum_{j=1}^{I}\frac{\partial}{\partial\varphi_j}\left\langle\frac{\partial}{\partial x_\beta}\left(\rho\Gamma_j\frac{\partial\psi_j}{\partial x_\beta}\right)\middle|\Psi_j=\varphi_j\right\rangle\tilde{f}_1\right) \tag{106}$$

and the density-weighted pdf $\tilde{f}_1$ defined by

$$\tilde{f}_1\equiv\frac{\rho(\varphi_1,\ldots,\varphi_I)}{\langle\rho\rangle}f_1(\varphi_1,\ldots,\varphi_I;\mathbf{x},t) \tag{107}$$

is used for essentially formal reasons. The turbulent fluxes and the time scale are determined from a second-order closure model (Dibble *et al.*, 1986). The closure for the flux is given by

$$-\langle\rho\rangle\langle v_\alpha''|\Psi_j=\varphi_j\rangle\tilde{f}_1\cong c_s\langle\rho\rangle\frac{\tilde{k}}{\tilde{\varepsilon}}\widetilde{v_\alpha''v_\beta''}\frac{\partial\tilde{f}_1}{\partial x_\beta}. \tag{108}$$

The mixing model (scalar-dissipation model) is the nonlinear interaction model of Dopazo (1979) and Janicka and Kollmann (1979) described in 3.3, equation (91). The rates of the four-step mechanism determine the source terms $q_j(\varphi_1,\ldots,\varphi_I)$, which control the motion of material points in scalar space due to combustion. The boundaries of the set of realizable states in scalar space are rather intricate (see Chen *et al.*, 1989). They satisfy all the conditions laid out in Section 3.2 for the pdf formulation. A detailed comparison of first- and second-order moments with the experiments of Masri *et al.* (1988) was carried out by Chen *et al.* (1989). A sample of two-dimensional pdfs and characteristic functions is presented in Figures 1–18. The flame considered is a turbulent jet flame burning methane with air

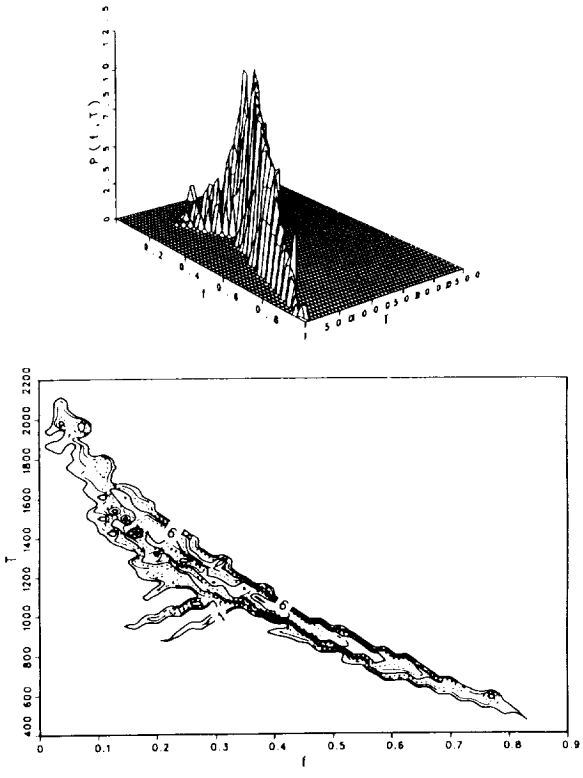

Figure 1. Pdf of mixture fraction and temperature in a turbulent methane–air non-premixed flame at $x/D = 20$ and $r/D = 1.11$.

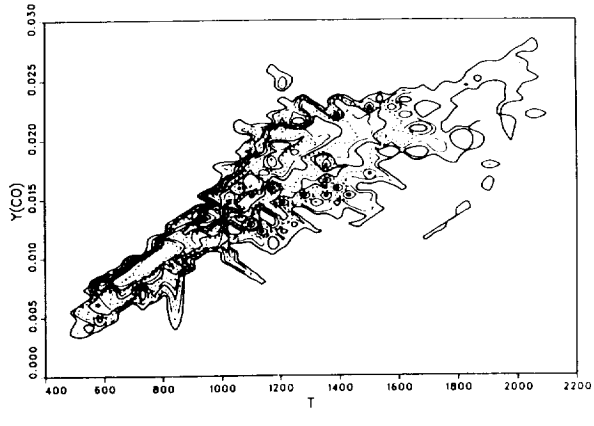

Figure 2. Pdf of CO mass fraction and temperature in a turbulent methane–air non-premixed flame at $x/D = 20$ and $r/D = 1.11$.

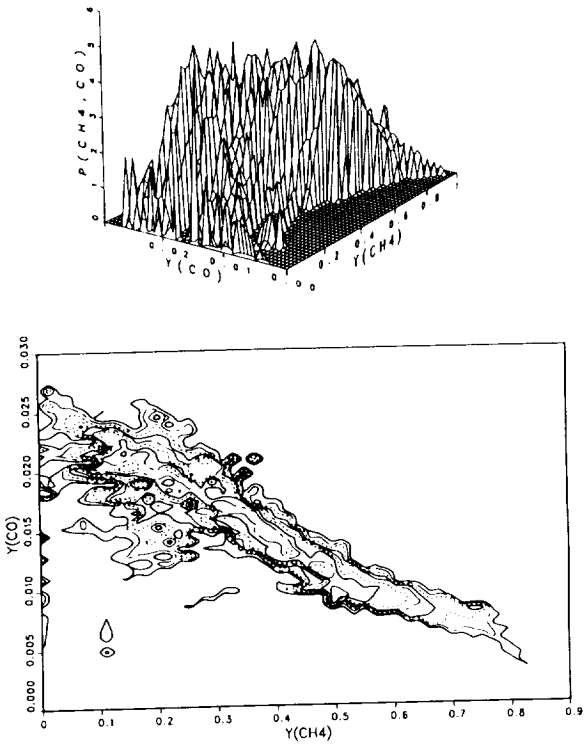

Figure 3. Pdf of CO and CH_4 mass fractions in a turbulent methane–air non-premixed flame at $x/D = 20$ and $r/D = 1.11$.

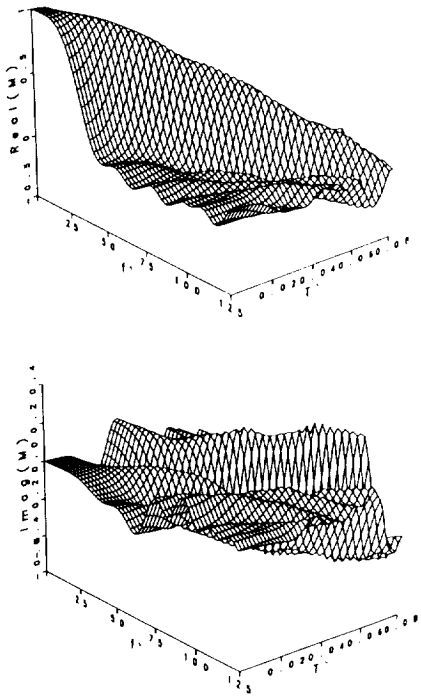

Figure 4. Real and imaginary parts of the characteristic function of mixture fraction and temperature at $x/D = 20$ and $r/D = 1.11$.

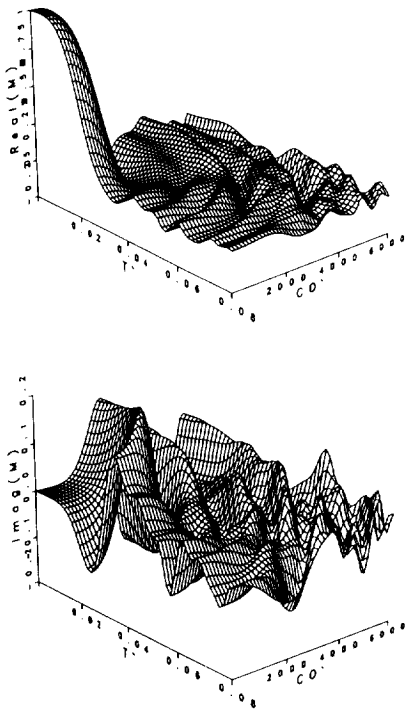

Figure 5. Real and imaginary parts of the characteristic function of CO mass fraction and temperature at $x/D = 20$ and $r/D = 1.11$.

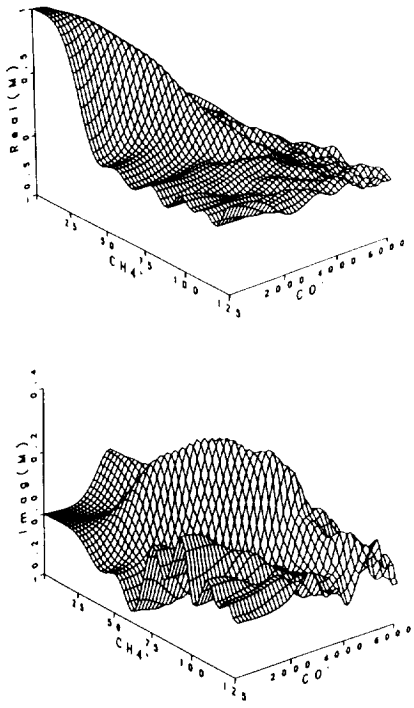

Figure 6. Real and imaginary parts of the characteristic function of CO and CH_4 mass fractions at $x/D = 20$ and $r/D = 1.11$.

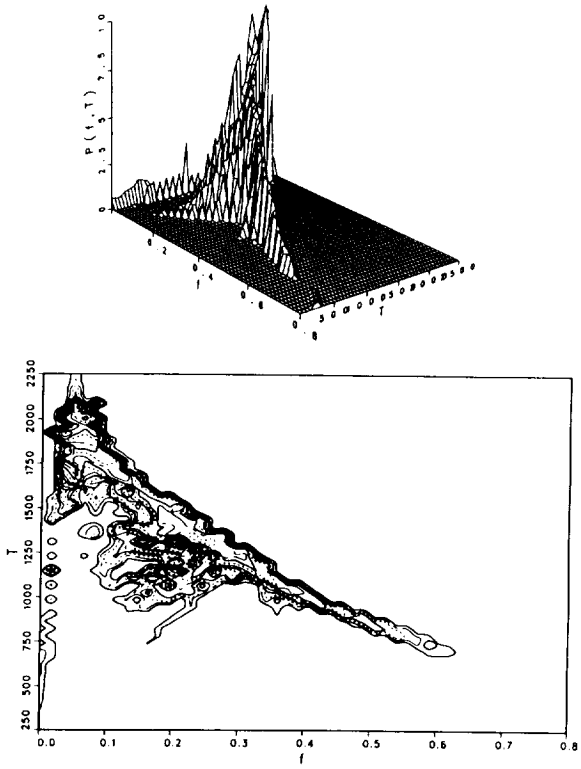

Figure 7. Pdf of mixture fraction and temperature in a turbulent methane–air non-premixed flame at $x/D = 20$ and $r/D = 1.49$.

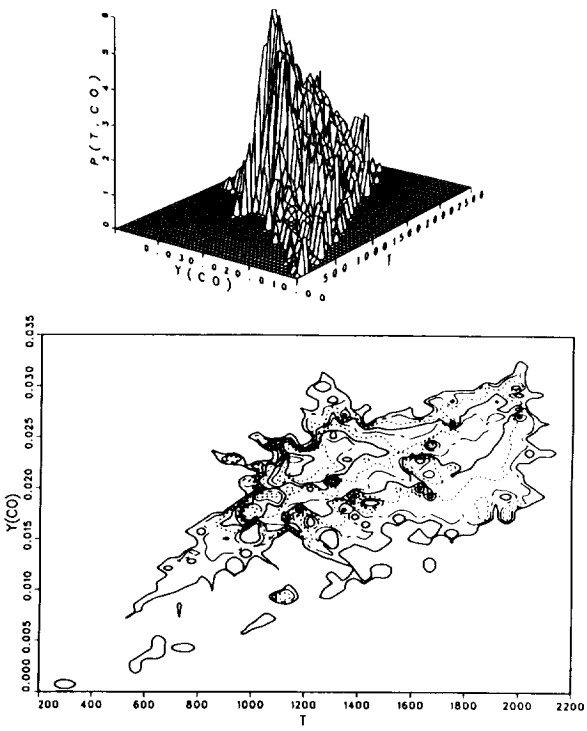

Figure 8. Pdf of CO mass fraction and temperature in a turbulent methane–air non-premixed flame at $x/D = 20$ and $r/D = 1.49$.

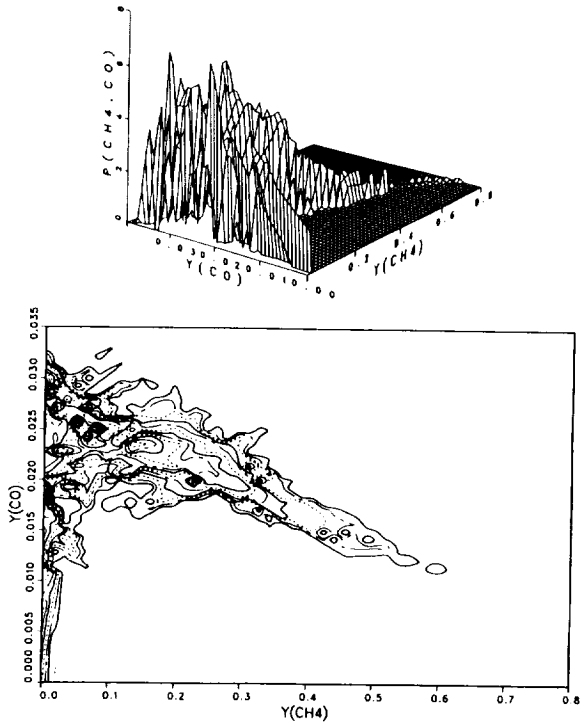

Figure 9. Pdf of CO and CH_4 mass fractions in a turbulent methane–air non-premixed flame at $x/D = 20$ and $r/D = 1.49$.

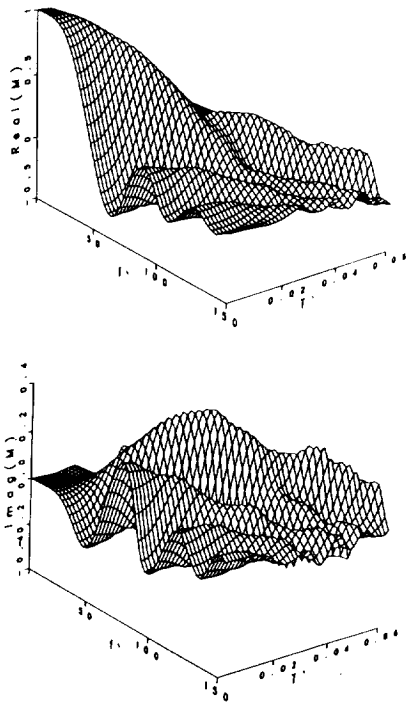

Figure 10. Real and imaginary parts of the characteristic function of mixture fraction and temperature at $x/D = 20$ and $r/D = 1.49$.

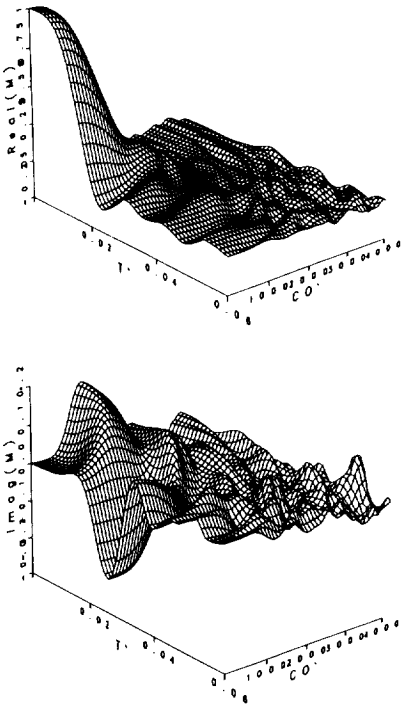

Figure 11. Real and imaginary parts of the characteristic function of CO mass fraction and temperature at $x/D = 20$ and $r/D = 1.49$.

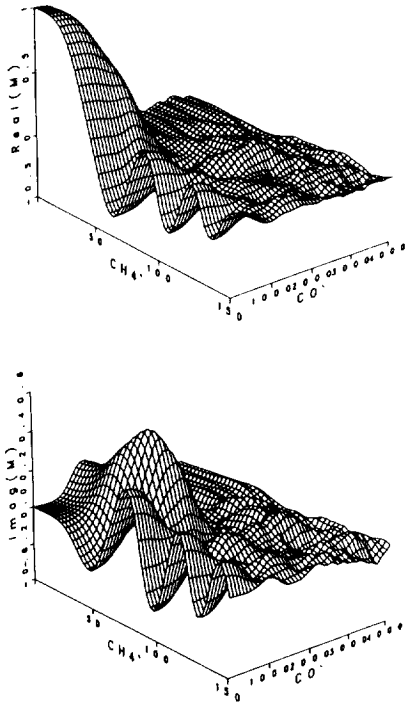

Figure 12. Real and imaginary parts of the characteristic function of CO and CH_4 mass fractions at $x/D = 20$ and $r/D = 1.49$.

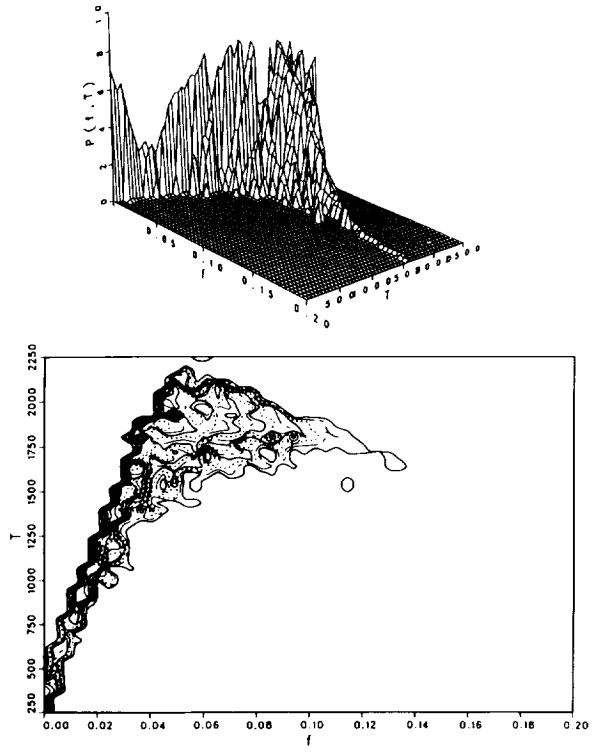

Figure 13. Pdf of mixture fraction and temperature in a turbulent methane–air non-premixed flame at $x/D = 20$ and $r/D = 2.07$.

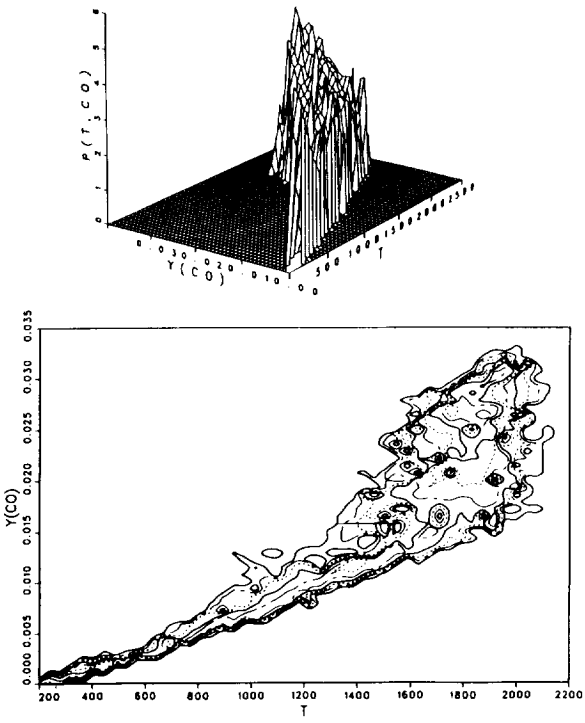

Figure 14. Pdf of CO mass fraction and temperature in a turbulent methane–air non-premixed flame at $x/D = 20$ and $r/D = 2.07$.

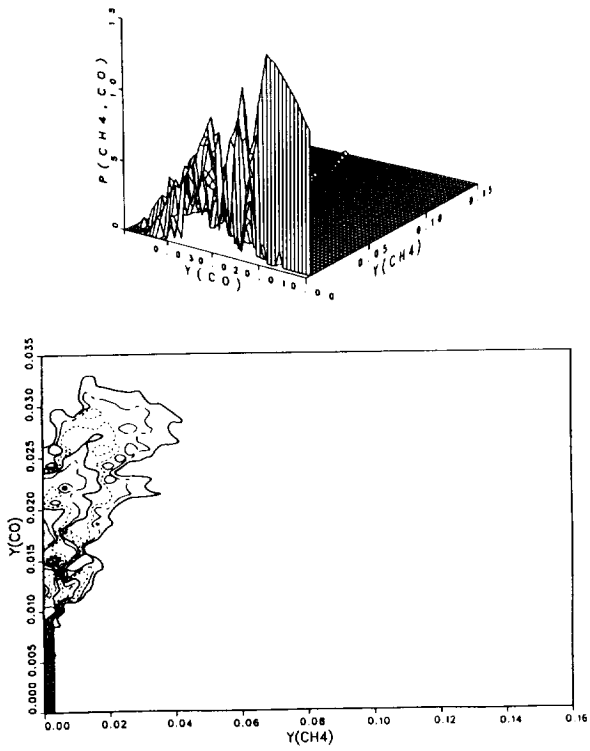

Figure 15. Pdf of CO and CH_4 mass fractions in a turbulent methane–air non-premixed flame at $x/D = 20$ and $r/D = 2.07$.

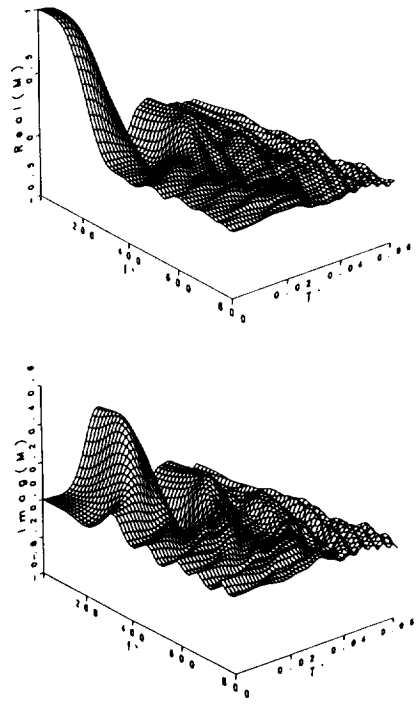

Figure 16. Real and imaginary parts of the characteristic function of mixture fraction and temperature at $x/D = 20$ and $r/D = 2.07$.

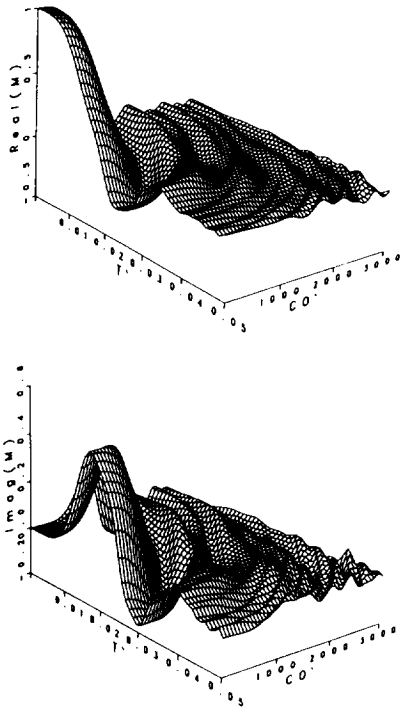

Figure 17. Real and imaginary parts of the characteristic function of CO mass fraction and temperature at $x/D = 20$ and $r/D = 2.07$.

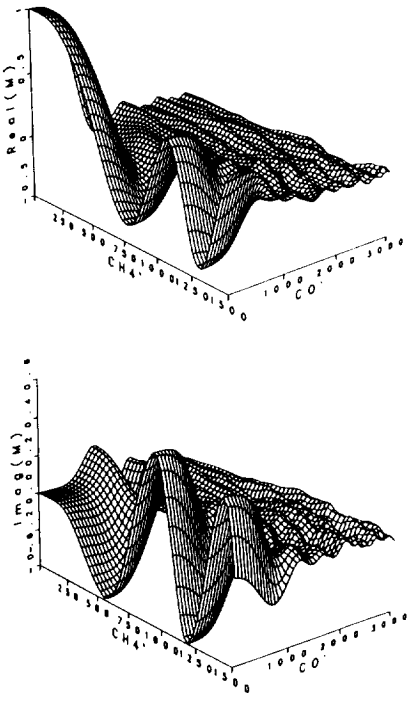

Figure 18. Real and imaginary parts of the characteristic function of CO and CH_4 mass fractions at $x/D = 20$ and $r/D = 2.07$.

from a coflowing stream. The inner diameter of the jet pipe is $D_i = 0.0072$ m and the bulk exit velocity of the fuel methane is $u_0 = 48$ m/s. The reaction is stabilized with a pilot flame (C_2H_2 and H_2) in the annulus between fuel jet and coflowing air stream ($D_o = 0.018$ m and $u_{air} = 15$ m/s). The solution of the pdf equation was carried out using a stochastic simulation technique (see Chen *et al.*, 1989). The cross-section at $x/D_i = 20$ is selected and results at three radial stations are presented in figures 1–18. The pdf for mixture fraction and temperature in Figure 1 ($r/D_i = 1.11$), Figure 7 ($r/D_i = 1.49$), and Figure 13 ($r/D_i = 2.07$) show the structural change of the pdf as the radial location is shifted outward. A significant amount of nonequilibrium is observed at $r/D_i = 1.49$ in Figure 7, where the pdf spreads over a range of 500 K on the rich side of the flame. Much less spread is seen on the lean side in Figure 13. The pdf of the CO mass fraction and temperature in Figures 2, 8, and 14 exhibits the change from a narrow pdf at $r/D_i = 1.11$ to a broad and doubly ridged form at $r/D_i = 1.49$ and finally to a club-like shape at $r/D_i = 2.07$. The pdf of CO and methane mass fractions in Figures 3, 9, and 15 reflects the amount of coexistence of these components. The pdf is spread over a wide range of methane mass fractions on the fuel rich side at $r/D_i = 1.11$, but gets gradually squeezed toward zero as the radial location is moved into the lean side of the flame zone. Figures 4–6, 10–12, and 16–18 contain the characteristic functions in separate graphs for real and imaginary parts corresponding to these pdfs. It is noticable that the characteristic functions are much smoother than the pdfs (no smoothing of pdfs or characteristic functions was performed). Furthermore, it should be remembered that discontinuities of the pdf appear as oscillations with decaying amplitude in the characteristic function. The characteristic function is real valued if the pdf is symmetric. Hence, the imaginary part of the characteristic function is a measure for the skewness of the pdf. Finally, note that the primed variables in the figures are the independent variables in Fourier space corresponding to the unprimed variables in scalar space. The characteristic function for mixture fraction and temperature in Figures 4, 10, and 14 shows a ridge, which decays with distance from the origin with increasing speed as the radial location is moved to the lean side of the raction zone. The characteristic function for CO and temperature in Figures 5, 11, and 17 is centered around the origin (real part) with quickly decaying waves, except at $r/D_i = 1.49$ indicating stronger discontinuity in the pdf. The characteristic function for CO and methane in Figures 6, 12, and 18 shows slowly decaying waves in real and imaginary parts as $r/D_i = 1.11$ and $r/D_i = 2.07$, but much less waviness at $r/D_i = 1.49$ which indicates a smoother pdf at this location.

This example shows clearly the degree of chemical nonequilibrium that can be present in a hydrocarbon flame. The fact, that all thermochemical variables are bounded, together with the unusual forms for the pdfs obtained in this example, demonstrates that assumptions like the quasi-Gaussian one are untenable for scalar pdfs.

4.2. Turbulent Supersonic Flows

Compressible turbulent flows pose new and challenging problems, in particular in the area of supersonic combustion. Pdf methods can be applied fruitfully to this type of turbulent flows, but the research effort is still in the beginning stage (Farshchi, 1989). The basic theory for the pdf approach is outlined here and possible ways of its application to supersonic combustion problems are discussed. The case of compressible nonreacting flows of an ideal gas is considered first.

Turbulent Supersonic Flows Without Reactions. The balances for mass, momentum, and energy set up in Section 2.1 are transformed to dimensionless variables. Mass balance appears in unchanged dimensionless variables ((6); only the Eulerian frame is used in the following), but momentum and energy balances contain several dimensionless parameters. The momentum balance is now given by

$$\rho \frac{Dv_\alpha}{Dt} = -\frac{\partial p}{\partial x_\alpha} + \frac{1}{\mathrm{Re}} \frac{\partial \tau_{\alpha\beta}}{\partial x_\beta} + B\rho f_\alpha, \tag{109}$$

where

$$\mathrm{Re} \equiv \frac{\rho_0 u_0 L}{\mu_0}, \qquad B \equiv \frac{f_0 L}{u_2^2}, \tag{110}$$

with ρ_0, u_0, L, μ_0, T_0, k_0, f_0 denoting the reference values. The stress tensor appears in unchanged

dimensionless variables (12). The energy balance emerges as an equation for the internal energy e in the form

$$\rho\frac{De}{Dt} = -(\gamma-1)(1+\gamma M_0^2 p)\frac{\partial v_\alpha}{\partial x_\alpha} + \gamma(\gamma-1)\frac{M_0^2}{\mathrm{Re}}\Phi - \frac{\gamma}{\mathrm{Pe}}\frac{\partial q_\alpha}{x_\alpha}, \tag{111}$$

where the ratio of specific heats γ was assumed constant and

$$M_0 \equiv \frac{u_0}{a_0}, \qquad a_0^2 = \gamma R T_0, \qquad \mathrm{Pe} = \mathrm{Re}\cdot\mathrm{Pr}, \qquad \mathrm{Pr} \equiv \frac{\mu_0 c_{p0}}{k_0}$$

are the Mach, Peclet, and Prandtl numbers for the reference state. The energy balance can be recast in terms of the specific (dimensionless) entropy

$$\rho\frac{Ds}{Dt} = -\frac{1}{\mathrm{Pe}}\frac{\partial}{\partial x_\alpha}\left(\frac{q_\alpha}{T}\right) + (\gamma-1)\frac{M_0^2}{\mathrm{Re}}\frac{\Phi}{T} - \frac{1}{\mathrm{Pe}}\frac{q_\alpha}{T^2}\frac{\partial T}{\partial x_\alpha}. \tag{112}$$

The dissipation function Φ in dimensionless form is given by (16) and the heat flux is

$$q_\alpha = -k\frac{\partial T}{\partial x_\alpha},$$

where $k(T)$ is the dimensionless conductivity. The ideal gas equation appears in dimensionless form as

$$\gamma M_0^2 p = \frac{1}{c_v}\rho e - 1. \tag{113}$$

Single point pdfs can now be defined in several ways for compressible flows (since mechanical and thermodynamic state are completely specified) if the velocity and two thermodynamic state variables are known. In the present case the following set of variables is considered (for a different set, see Farshchi (1989)): Velocity $\mathbf{v}$, density ρ, internal energy e, and rate of volume expansion $D \equiv \partial v_\alpha/\partial x_\alpha$. The tranport equation for D follows immediately from the momentum balance

$$\frac{DD}{Dt} = \frac{1}{\mathrm{Re}}\frac{\partial}{\partial x_\alpha}\left(\frac{1}{\rho}\frac{\partial \tau_{\alpha\beta}}{\partial x_\beta}\right) - \frac{\partial v_\alpha}{\partial x_\beta}\frac{\partial v_\beta}{\partial x_\alpha} + B\frac{\partial f_\alpha}{\partial x_\alpha} - \frac{\partial}{\partial x_\alpha}\left(\frac{1}{\rho}\frac{\partial p}{\partial x_\alpha}\right). \tag{114}$$

The definition of $\hat{f}$ (see (48)) is now modified as follows:

$$\hat{f} \equiv \delta(\mathbf{v}-\mathbf{v})\delta(\rho-d)\delta(e-u)\delta(D-\zeta), \tag{115}$$

and the pdf equation for compressible turbulent flow without reaction emerges as

$$\begin{aligned} d\left(\frac{\partial f_1}{\partial t} + v_\alpha\frac{\partial f_1}{\partial x_\alpha}\right) = {} & -\frac{\partial}{\partial v_\alpha}\left\{-\left\langle\frac{\partial p}{\partial x_\alpha}\hat{f}\right\rangle + \frac{1}{\mathrm{Re}}\left\langle\frac{\partial \tau_{\alpha\beta}}{\partial x_\beta}\hat{f}\right\rangle + Bd\langle f_\alpha\hat{f}\rangle\right\} \\ & + \frac{\partial}{\partial d}(d^2\zeta f_1) - \frac{\partial}{\partial u}\left\{-\frac{\gamma-1}{c_v}du\,\zeta f_1 + \gamma(\gamma-1)\frac{M_0^2}{\mathrm{Re}}\langle\Phi\hat{f}\rangle - \frac{\gamma}{\mathrm{Pe}}\left\langle\frac{\partial q_\alpha}{\partial c_\alpha}\hat{f}\right\rangle\right\} \\ & - \frac{\partial}{\partial\zeta}\left\{\frac{1}{\mathrm{Re}}\left\langle\frac{\partial}{\partial x_\alpha}\left(\frac{1}{\rho}\frac{\partial\tau_{\alpha\beta}}{\partial x_\beta}\right)\hat{f}\right\rangle - \left\langle\frac{\partial v_\alpha}{\partial x_\beta}\frac{\partial v_\beta}{\partial x_\alpha}\hat{f}\right\rangle + B\left\langle\frac{\partial f_\alpha}{\partial x_\alpha}\hat{f}\right\rangle - \left\langle\frac{\partial}{\partial x_\alpha}\left(\frac{1}{\rho}\frac{\partial p}{\partial x_\alpha}\right)\hat{f}\right\rangle\right\}. \end{aligned} \tag{116}$$

This form of the pdf equation contains information on a special time scale, namely the time scale of volume expansion. The inclusion of the inverse D of this time scale is the reason for the evolution-type structure of the pdf equation (116). The rate of volume expansion D could be eliminated, but then a pdf equation of the hyperbolic type would result.

Turbulent Supersonic Flows with Chemical Reactions. Turbulent flows at supersonic speed, with combustion reactions, lead to several new problems. The mixing of fuel and oxidizer becomes a problem of central importance because of the reduced residence times at high speeds and the effect of compressibility to reduce the turbulence level (see Papamoschou and Roshko, 1988; Papamoschou,

1989) and therefore the intensity of mixing. Turbulent flow at supersonic speed can be modified significantly by the interaction with shocks created outside the turbulent-flow field and random shocks (called shocklets (Johnson *et al.*, 1988)) created by supersonic turbulent shear layers. Pdf methods can be adapted to include the effects of compressibility and combustion. We consider first the case of infinitely fast reactions. It was shown in Section 4.1 (Equilibrium Models) that three variables determine the local state in this case: mixture fraction, pressure, and enthalpy. Pressure can vary significantly in supersonic flows and enthalpy is not conserved due to frictional heating in high shear regions. Hence, no further simplification, as in the case of low Mach number subsonic flames, is possible. The pdf f_1 defined in the previous section has to be modified to include the mixture fraction ξ:

$$f_1(\upsilon, \pi, \sigma, \zeta, \eta; \mathbf{x}, t) \equiv \langle \delta(\mathbf{v} - \upsilon)\delta(p - \pi)\delta(h - \sigma)\delta(D - \zeta)\delta(\xi - \eta)\rangle. \tag{117}$$

Ideal gas relations allow replacement of pressure and enthalpy with density and internal energy. Hence, a pdf transport equation similar to (116) is obtained with additional terms accounting for transport in mixture fraction space. Mean thermodynamic properties follow from the pdf f_1 by integration. The mean temperature for instance is given by

$$\langle T \rangle = \int d\pi \int d\sigma \int d\eta \; T(\pi, \sigma, \eta) f_1(\pi, \sigma, \eta),$$

where $T(\pi, \sigma, \eta)$ denotes the local relation of temperature to pressure, enthalpy, and mixture fraction. Extension to finite-rate chemistry can be carried out with the methods described the previous subsection. However, no closure models have been developed so far for (116), or its counterpart for reacting flows, and much work remains to be done.

Shock–Turbulence Interaction. The interaction of shocks with turbulence poses a formidable problem of practical importance (Billig and Dugger, 1969). So far, mostly moment closures (Kollmann *et al.*, 1985) have been used to predict mean fields in the region of interaction and mean shock properties and location were calculated with shock-capturing techniques. The application of pdf methods to supersonic flows with embedded shocks is a new area. Since shocks are near discontinuities for finite Reynolds/Peclet numbers (and approach genuine discontinuities as Reynolds/Peclet numbers go to infinity), it is natural to ask what the structure of the pdf equation will be in the presence of discontinuities. For the investigation of this question, a single balance equation for a scalar quantity $\Phi(x, t)$ is considered. The equation

$$\frac{\partial \Phi}{\partial t} + \frac{\partial F}{\partial x} - S = 0, \qquad \Phi(x, 0) = \Phi_0(x), \tag{118}$$

where $F(\Phi, x, t)$ is the flux and $S(\Phi, x, t)$ is the source term. This equation admits discontinuous solution in its weak form (Majda, 1984). If the initial condition is chosen randomly from a set of differentiable functions, then the statistical properties of the solution can be described in terms of the pdf $f_1(\varphi; x, t)$:

$$\hat{f} \equiv \delta(\Phi(x, t) - \varphi), \qquad f_1 = \langle \hat{f} \rangle.$$

If the flux F and the source S are local functions of Φ, and if the solution Φ remains at least once continuously differentiable, then the pdf equation follows from (47), i.e.,

$$\frac{\partial f_1}{\partial t} + \frac{\partial F}{\partial \Phi}\frac{\partial f_1}{\partial x} + \frac{\partial}{\partial \varphi}(S(\varphi) f_1) = \left\langle \frac{\partial^2 F}{\partial \Phi^2}\frac{\partial \Phi}{\partial x}\hat{f} \right\rangle. \tag{119}$$

However, the right-hand side is nonzero if the flux F is a nonlinear function of Φ. Its structure is not suited for the analysis of discontinuities and a different method must be used for this case. The theory of stochastic differential equations allows analysis of the scalar Φ taken at a fixed location x. The temporal increment of Φ is then

$$d\Phi = d\Phi_0 + dP + dW, \tag{120}$$

where $d\Phi_0$ is the deterministic and differentiable part of $d\Phi$, dP is the increment due to a jump process, and dW is the increment due to a continuous but not differentiable process. The differential

equation (118) leads to

$$d\Phi = -\frac{\partial F}{\partial x}\,dt + S\,dt.$$

The source term $S\,dt$ can now be viewed as the sum

$$S\,dt = S_0\,dt + dW \tag{121}$$

of the differentiable contribution $S_0\,dt$ and a continuous but nondifferentiable part dW. The flux term requires a closer look. If $F(\Phi)$ depends on Φ in a nonlinear fashion such that discontinuities form in finite time from smooth initial conditions, then there exist random and discrete-time instances when discontinuities cross the fixed location x. Hence, the derivative of the flux is the sum of a singular and a continuous part

$$\frac{\partial F}{\partial x} = \sum_{t_i \le t} [\![\Phi]\!]_i \delta(t - t_i) + \left(\frac{\partial F}{\partial x}\right)_c,$$

where $[\![\Phi]\!]_i$ denotes the jump height at time t_i and $(\partial F/\partial x)_c$ denotes the continuous part. Hence,

$$dP \equiv \sum_{t_i \le t} [\![\Phi]\!]_i\,dt\,\delta(t - t_i) \tag{122}$$

is the increment of a jump process and the increments in the stochastic differential equation are now identified as

$$d\Phi_0 \equiv \left(S_0 - \left(\frac{\partial F}{\partial x}\right)_c\right) dt$$

along with (121) and (122). The pdf equation for the solution process of (120) can be deduced from (81) as follows:

$$\frac{\partial f_1}{\partial t} + \frac{\partial}{\partial \varphi}\left\{\left(S_0 - \left(\frac{\partial F}{\partial x}\right)_c\right) f_1\right\} = \frac{1}{2}\frac{\partial^2}{\partial \varphi^2}\{B f_1\} + \frac{1}{\tau}\left\{\int d\Phi'\, f_1(\Phi') T(\Phi' \to \Phi) - f_1\right\} \tag{123}$$

if dW is specialized to a Wiener process. It becomes clear by inspection of this equation that the discontinuities crossing a given location x affect the evolution equation for the pdf in integral form appropriate for jump processes. This integral requires the probability of a jump from Φ' to Φ, denoted by $T(\Phi' \to \Phi)$, and the time scale τ for the appearance of discontinuities at x. The pdf equation derived from (120) does not provide this information, because only a single location x is considered and x-derivatives constitute therefore new unknowns.

This example showed that the appearance of shock waves with random location and strength produces an integral contribution to the pdf equation. It can be expected that the time scale and the transition pdf $T(\Phi' \to \Phi)$ are functionals of the flow variables. The explicit form of this functional relation is unknown at present.

5. Methods of Numerical Solution

The pdf $f_1(d, \upsilon, \varphi_1, \ldots, \varphi_m; \mathbf{x}, t)$ is apparently a function of a large number of independent variables. Classical methods of numerical solution such as finite-difference or finite-element algorithms become prohibitively expensive because the numerical effort for the solution grows rapidly with the dimension of the domain of definition (number of independent variables). However, stochastic simulation techniques can be shown to grow in numerical effort only linearily with the dimension of the domain of definition. Hence they offer the possibility of a numerical solution of the pdf equation for a significant number of variables (up to about ten with current computational capabilities). The development of stochastic simulation techniques for the solution of the pdf equation is essentially due to Pope (1985). The basic idea is to represent the pdf by a sufficiently large number of notional particles, whose motion in physical and velocity–scalar space is governed by modeled transport equations. The closure assumptions introduced for these dynamical equations (see Section 4) correspond to the closure assumptions constructed for the pdf equation. The numerical algorithm is based on a fractional-step method, where in each fractional step a numerical operator corresponding to a distinct physical or

chemical process is applied. The motion of the notional particles is thus calculated as time evolves. The pdf is then given approximately as a histogram of the properties of the notional particles in sufficiently small neighborhoods in physical space. A detailed discussion of this method can be found in Pope (1985). Several variants of this basic method have appeared. Jones and Kollmann (1987) and Chen and Kollmann (1989b) developed a hybrid method consisting of a finite-difference algorithm for a second-order closure for the velocity statistics and a stochastic simulation technique for the scalar pdf equation. Haworth and Pope (1987) extended their stochastic simulation technique to flows in general orthogonal coordinate systems and developed a second-order accurate method for Ito-type stochastic differential equations (Haworth and Pope, 1986).

6. Conclusions

Single-point pdf methods can be deduced from exact and closed equations on the functional level. The pdf at a single point or at a finite number of points can be viewed as the Fourier transform of the characteristic function which is in fact the characteristic functional taken at a special argument function. This has two important implications: there are two essentially equivalent ways to formulate the turbulence problem at a single point or a finite number of points and the pdf or characteristic function method are part of a general framework for the statistical treatment of turbulence based on a linear equation on the functional level. Finite-dimensional pdf equations, therefore, achieve partial and rigorous linearization without an approximation of certain nonlinear phenomena (such as convection and chemical reactions) by converting dependent variables into independent variables. This is in fact the main advantage of pdf methods over moment methods.

Pdf or characteristic function methods can be set up in Eulerian or Lagrangean frames and the choice of the frame is a matter of convenience. The single-point case was considered in detail. The equation for any pdf at a finite number of points is indeterminate because molecular transport (viscous and diffusive phenomena) and the pressure-gradient terms require information given at least one additional point for their description. Hence, a closure problem arises, which was formulated in terms of pdfs and characteristic functions. Under certain restrictions a third formulation using stochastic differential equations can be given. Several closure models were discussed and their properties were evaluated. None of these models is exact and they satisfy, at best, the mathematical condition of realizability and simulate some of the physical processes of the exact terms in the pdf equation.

Pdf methods have been applied to a variety of turbulent flows. In particular, turbulent flows with combustion are currently an active research area. The combustion of methane with air in a turbulent non-premixed jet flame was discussed and selected set of results for pdfs and characteristic functions was presented. The main conclusions that can be drawn from this particular application are the facts that pdf methods allow for the treatment of chemical nonequilibrium and that the calculated pdfs are very far from Gaussian shapes. Hence, no assumption of quasi-Gaussianity would suffice for the bounded scalar variables used in such a case.

Further developments of pdf methods may include compressible turbulent flows and the interaction of turbulence with shock waves. The basic formalism for the investigation of compressible turbulent flows both with and without combustion was laid out and a version of the pdf equation was given for flows without combustion. The interaction of turbulence with shock waves is a formidable problem. A simple example of a single scalar was discussed and the effect of discontinuities on the pdf was shown to appear as an integral contribution in the pdf equation.

References

Arroyo, P., Dopazo, C., Valiño, L., and Jones, W.P. (1988), Numerical Simulation of Velocity and Concentration Fields in a Continuous Flow Reactor, 10*th Int. Symp. Chem. Reaction Engin.*, Basle.

Averbukh, V.I., and Smolyanov, O.G. (1967), The Theory of Differentiation in Linear Topological Spaces, *Uspekhi Mat. Nauk*, **22**, 201.

Bilger, R.W. (1976), Turbulent Jet Diffusion Flames, *Progr. Energy Combust. Sci.*, **1**, 87.

Bilger, R.W. (1980), Turbulent Flows with Non-premixed Reactants, in *Turbulent Reacting Flows* (P.A. Libby and F.A. Williams, eds.), Springer-Verlag, Berlin.

Bilger, R.W. (1988), Turbulent Diffusion Flames, *Proc. 22nd Symp. (Int.) Combust.*, Seattle, to appear.

Billig, F.S., and Dugger, G.L. (1969), The Interaction of Shock Waves and Heat Addition in the Design of Supersonic Combustors, *Proc. 12th Symp. (Int.) Combust.*, The Combustion Institute, p. 1125.

Borghi, R. (1988), Turbulent Combustion Modelling, *Progr. Energy Combust. Sci.*, to appear.

Chen, J.-Y., and Kollmann, W. (1989a), Chemical Models for Pdf Modeling of Hydrogen–Air Non-Premixed Turbulent Flames, *Combust. Flame*, to appear.

Chen, J.-Y., and Kollmann, W. (1989b), Pdf Modeling of Chemical Mon-Equilibrium Effects in Turbulent Non-premixed Hydro-Carbon Flames, *Combust. Flame*, submitted.

Chen, J.-Y., Kollmann, W., and Dibble, R. W. (1989), Pdf Modeling of Turbulent Non-Premixed Methane Jet Flames, *Combust. Flame*, submitted.

Constantin, P, Foias, C., and Temam, R. (1985), *Attractors Representing Turbulent Flows*, Memoirs American Mathematical Society, No. 314, AMS, Providence, RI.

Curl, R.L. (1963), Dispersed Phase Mixing: I. Theory and Effects in Simple Reactors, *AIChE J.*, **9**, 175.

Daletskii, Y.L. (1962), Functional Integrals Connected with Operator Evolution Equations, *Uspekhi Mat. Nauk*, **17**, 3.

Dibble, R.W., Kollmann, W., Farshchi, M., and Schefer, R.W. (1986), Second Order Closure for Turbulent Non-Premixed Flames: Scalar Dissipation and Heat Release Effects, *Proc. 21st Symp. (Int.) Combust.*, The Combustion Institute, p. 1329.

Dopazo, C. (1975), Probability Function Approach for a Turbulent Axisymmetric Heated Jet. Centerline Evolution, *Phys. Fluids*, **18**, 397.

Dopazo, C. (1979), Relaxation of Initial Probability Density Functions in the Turbulent Convection of Scalar Fields, *Phys. Fluids*, **22**, 20.

Dopazo, C., and O'Brien, E.E. (1974), Functional Formulation of Non-Isothermal Turbulent Reactive Flow, *Phys. Fluids*, **17**, 1968.

Farshchi, M. (1989), A Pdf Closure Model for Compressible Turbulent Chemically Reacting Flow, Paper AIAA-89-0390.

Feller, M.N. (1986), Infinite-Dimensional Elliptic Equations and Operators of Levy Type, *Russ. Math. Surveys*, **41**, 119.

Foias, C. (1974), A Functional Approach to Turbulence, *Uspekhi Mat. Nauk*, **29**, 282.

Givi, P., Ramos, J.I., and Sirignano, W.A. (1985), Probability Density Function Calculations in Turbulent Chemically Reacting Round Jets, Mixing Layers and One-Dimensional Reactors, *J. Non-Equilib. Thermodyn.*, **10**, 75.

Hanjalic, K., and Launder, B.E. (1972), A Reynolds Stress Model of Turbulence and Its Application to Thin Shear Flows, *J. Fluid Mech.*, **52**, 609.

Haworth, D.C., and Pope, S.B. (1986), A Second Order Monte Carlo Method for the Solution of the Ito Stochastic Differential Equation, *Stochastic Anal. Appl.*, **4**, 151.

Haworth, D.C., and Pope, S.B. (1987), Monte Carlo Solutions of a Joint Pdf Equation for Turbulent Flows in General Orthogonal Coordinates, *J. Comput. Phys.*, **72**, 311.

Hopf, E. (1952), Statistical Hydromechanics and Functional Calculus, *J. Rational Mech. Anal.*, **1**, 87.

Hopf, E., and Titt, E.W. (1953), On Certain Special Solutions of the Φ-Equation of Statistical Hydromechanics, *J. Math. Mech.*, **2**, 587.

Ievlev, V.M. (1973), Equations for the Finite-Dimensional Probability Distributions of Pulsating Variables in a Turbulent Flow, *Soviet Phys. Dokl*, **18**, 117.

Janicka, J., Kolbe, W., and Kollmann, W. (1979), Closure of the Transport Equation for the Probability Density Function of Scalar Fields, *J. Non-equilib. Thermodyn.*, **4**, 27.

Johnson, J.A., Zhang, Y., and Johnson, L.E. (1988), Evidence of Reynolds Number Sensitivity in Supersonic Turbulent Shocklets, *AIAA J.*, **26**, 502.

Jones, W.P., and Kollmann, W. (1987), Multi-Scalar Pdf Transport Equations for Turbulent Diffusion Flames, in *Turbulent Shear Flows*, vol. 5 (Durst, F., *et al.*, eds.), Springer-Verlag, Berlin, p. 296.

Keck, J.C. (1978), Rate-Controlled Constrained Equilibrium Method for Treating Reactions in Complex Systems, in *Maximum Entropy Formalism* (Levine, R.D., *et al.*, eds.), MIT Press, Cambridge, MA.

Keizer, J. (1987), *Statistical Thermodynamics of Nonequilibrium Processes*, Springer-Verlag, Berlin.

Kollmann, W. (1987), Pdf-Transport Equations for Chemically Reacting Flows, *Proc. US–France Workshop on Turb. React. Flows*, Rouen, vol. 2, p. 20-1.

Kollmann, W., and Janicka, J. (1982), The Probability Density Function of a Passive Scalar in Turbulent Shear Flow, *Phys. Fluids*, **25**, 1755.

Kollmann, W., and Wu, A. (1987), Scalar–Velocity Pdf Equations for Turbulent Shear Flows, Paper AIAA-87-1348.

Kollmann, W., Haminh, H., and Vandromme, D. (1985), The Behaviour of Turbulence Anisotropy Through Shock Waves and Expansions, *Proc. Fifth Turbulent Shear Flows Conf.*, Cornell University.

Kosaly, G. (1986), Theoretical Remarks on a Phenomenological Model of Turbulent Mixing, *Comb. Sci. Technol.*, **49**, 227.

Kosaly, G., and Givi, P. (1987), Modeling of Turbulent Molecular Mixing, *Combust. Flame*, **70**, 101.

Levich, E., Levich, B., and Tsinober, A. (1984), Helical Structures, Fractal Dimensions and Renormalisation Group Approach in Homogeneous Turbulence, in *Turbulence and Chaotic Phenomena in Fluids* (Tatsumi, T., ed.), Elsevier, Amsterdam, p. 309.

Lewis, R.M., and Kraichnan, R.H. (1962), A Space–Time Functional Formalism for Turbulence, *Comm. Pure Appl. Math.*, **15**, 397.

Lindenberg, K., Seshadri, V., Shuler, K.E., and West, B.J. (1983), Langevin Equations with Multiplicative Noise: Theory and Applications to Physical Process, in *Probability Analysis and Related Topics*, vol. 3, Academic Press, New York, p. 81.

Lukacs, J. (1970), *Characteristic Functions*, Hafner, New York.
Lumley, J.L. (1978), Computational Modeling of Turbulent Flows, *Adv. Appl. Mech.*, **18**, 123.
Lundgren, T.S. (1967), Distribution Functions in the Statistical Theory of Turbulence, *Phys. Fluids*, **10**, 969.
Majda, A. (1984), *Compressible Fluid Flow and Systems of Conservation Laws in Several Space Dimensions*, Springer-Verlag, Berlin.
Mandelbrot, B.B. (1974), Intermittent Turbulence in Self-Similar Cascades: Divergence of High Moments and Dimension of the Carrier, *J. Fluid Mech.*, **62**, 331.
Masri, A.R., and Pope, S.B. (1989), Pdf Calculations of Piloted Turbulent Non-Premixed Flames of Methane, to appear.
Masri, A.M., Bilger, R.W., and Dibble, R.W. (1988), Turbulent Non-premixed Flames of Methane near Extinction: Mean Structure from Raman Measurements, *Combust. Flame*, **71**, 245.
Meyers, R.E., and O'Brien, E.E. (1981), The Joint Pdf of a Scalar and Its Gradient at a Point in a Turbulent Fluid, *Comb. Sci. Technol.*, **26**, 123.
Monin, A.S. (1962), Lagrangean Hydrodynamic Equations for Incompressible Viscous Fluids, *Prikl. Mat. Mekh.*, **26**, 320.
Monin, A.S., and Yaglom, A.M. (1975), *Statistical Fluid Mechanics*, vol. 2, MIT Press, Cambridge, MA.
O'Brien, E.E. (1980), The Probability Density Function (pdf) Approach to Reacting Turbulent Flows, in *Turbulent Reacting Flows* (Libby, P.A., and Williams, F.A., eds.), Springer-Verlag, Berlin.
Papamoschou, D. (1989), Structure of the Compressible Turbulent Shear Layer, Paper AIAA-89-0126.
Papamoschou, D., and Roshko, A. (1988), The Compressible Turbulent Shear Layer: An Experimental Study, *J. Fluid Mech.*, **197**, 453.
Peter, N., and Kee, R.J. (1987), The Computation of Stretched Diffusion Flames Using a Reduced Four-Step Mechanism, *Combust. Flame*, **68**, 17.
Peters, N., and Williams, F. A. (1987), The Asymptotic Structure of Stoichiometric Methane Air Flames, *Combust. Flame*, **68**, 185.
Pope, S.B. (1982), An Improved Turbulent Mixing Model, *Comb. Sci. Technol.*, **28**, 131.
Pope, S.B. (1985), Pdf Methods for Turbulent Reacting Flows, *Progr. Energy Comb. Sci.*, **11**, 119.
Pope, S.B. (1987), Turbulent Premixed Flames, in *Ann. Rev. Fluid Mech.*, vol. 19 (J.L. Lumley *et al.* eds.), p. 237.
Pope, S.B., and Correa, S.M. (1986), Joint Pdf Calculations of a Non-Equilibrium Turbulent Diffusion Flame, *Proc. 21st Symp. (Int.) Combust.*, The Combustion Institute, p. 1341.
Rogg, B., and Williams, F.A. (1988), Structure of Wet CO Flames with Full and Reduced Kinetic Mechanisms, *Proc. 22nd Symp. (Int.) Combust.*, The Combustion Institute, in press.
Rotta, J.C. (1951), Statistische Theorie Nichthomogener Turbulenz, *Z. Phys.*, **129**, 547.
Sirignano, W.A. (1987), Molecular Mixing in a Turbulent Flow: Some Fundamental Considerations, *Comb. Sci. Technol.*, **51**, 307.
Skorohod, A.V. (1974), *Integration in Hilbert Space*, Springer-Verlag, Berlin.
Soong, T.T. (1973), *Random Differential Equations in Science and Engineering*, Academic Press, New York.
Speziale, C.G. (1983), Closure Models for Rotating Two-Dimensional Turbulence, *Geophys. Astrophys. Fluid Dyn.*, **23**, 69.
Taylor, M. (1974), *Pseudo Differential Operators*, Lecture Notes in Mathematics, no. 416, Springer-Verlag, Berlin.
Truesdell, C.A. (1954), *The Kinematics of Vorticity*, Indiana University Publications in Science Series, no. 19. Indiana University Press, Bloomington, IN.
Vishik, M.I., Komech, A.I., and Fursikov, A.V. (1979), Some Mathematical Problems of Statistical Hydromechanics, *Russian Math. Surveys*, **34**, 149.
Wilcox, D.C. (1988), Reassessment of the Scale-Determining Equation for Advanced Turbulence Models, *AIAA J.*, **26**, 1299.
Williams, F.A. (1985), *Combustion Theory*, 2nd edition, Benjamin-Cummings, Menlo Park, CA.

Appendix II.

The Interaction of Turbulence and Chemical Kinetics.

W. Kollmann[1]

MAME Dept., University of California Davis, CA 95616

J.-Y. Chen[2]

Combustion Research Facility
Sandia National Laboratories, Livermore, CA 94551

Abstract

The interaction of turbulence and chemical kinetics is examined here with the emphasis on the influence of turbulence on chemical reactions. Both nonpremixed and premixed flames are considered. In particular, a nonpremixed methane turbulent jet flame is used to elucidate the complex nature of the interactions between turbulence and chemical kinetics. Furthermore, this example provides a useful evaluation of the mixing properties predicted by a probability density function (pdf) method.

[1] Research supported by NASA-Lewis Grant no. NAG 3-836 (R. Claus project monitor).

[2] Research supported by the United States Department of Energy, Office of Basic Energy Sciences, Division of Chemical Sciences.

1.0 Introduction

The interaction of turbulence and chemical reactions occurs in turbulent reacting flows over a wide range of flow conditions. Various degrees of interaction between turbulence and chemical reactions can lead to different phenomena. Weak interactions between turbulence and chemical reactions may simply modify the flame slightly causing wrinkles of flame surface (Williams, 1989). Strong interactions could cause a significant modification in both the chemical reactions and the turbulence. If chemical reactions cause small density changes in the flow, then the turbulence is weakly affected by the chemical process but the turbulence may still have strong influence on the chemical reactions. However, the purpose of combustion is generating heat; therefore, one expects large density changes (i.e., an order of magnitude) which can alter the fluid dynamics significantly. It has been observed experimentally that the entrainment process in mixing layers has been significantly altered by the heat release leading to different growth rates than those expected in constant density flows (Hermanson *et al.* 1985; Dimotakis, 1989). On the other hand, strong turbulence can strain the flames to a point that chemical reactions can no longer keep up with the mixing process causing the flame to extinguish. Some recent experiments by Masri *et al.* (1988) have revealed that local flame extinction can occur prior to the flame blow-out limit indicating a strong interaction between turbulence and chemistry.

To understand and quantify the complex interactions between turbulence and chemistry, it is useful to identify the relevant length and time scales in turbulent reacting flows. An overall characterization of the interactions between turbulence and chemical reactions can be obtained by plotting the Damköhler number (i.e., the ratio of flow time scale and reaction time scale) versus the Reynolds number over the whole range of length scales (Williams, 1989). Based on the length scales of flames and turbulence, two extreme regimes are identified. One extreme with the flame thickness much smaller than the smallest length of turbulence is identified as the flamelet regime. The other opposite extreme with thick flames compared to the smallest turbulence length is identified as the distributed reaction regime. The nature of the intermediate regimes between these two extremes is rather complex, and it is yet to be explored. Unfortunately, many practical combustion systems involve a wide range of operation conditions including the intermediate regimes.

The objective of this paper is to provide a fundamental understanding of the physics inherent in various processes causing turbulence to interact with chemical kinetics. In view of the importance of various practical chemical processes that occur in turbulent flows, the present paper is devoted mainly to the influence of turbulence on chemical kinetics. To provide a background of current theories in turbulent reacting flows, Section 2.0 reviews and summarizes the basic physics laws for chemical reactions in mixtures of ideal gases based on the Eulerian frame. The corresponding transformation to the Lagrangian frame is briefly discussed.

Section 3.0 is devoted to the main discussions on the influence of turbulence on chemical reactions. First the influence of turbulence on a binary reacting system (two species) is illustrated, and the degree of influence is characterized by the segregation parameters. Then the pdf transport equation of a single scalar is explored and an analytic solution is derived. This solution demonstrates the close relation between chemical reactions and the scalar dissipation.

Next, nonpremixed flames are considered and the appropriate measures of mixedness are introduced. The essential issue for modeling nonpremixed flames is highlighted by examining the closure problems in the current modeling methods. In particular, the mixing models in the pdf methods are examined in depth and future developments are indicated. The analysis of premixed flames is limited to the flamelet regime. Two proposed theories are reviewed: the Bray-Libby-Moss flamelet theory (Bray *et al.*, 1985) and the coherent flame theory of Marble and Broadwell (1977). The regime of flame sheet combustion clearly indicates the fundamental importance of surfaces embedded in turbulent flow field. Surfaces relevant to combustion flows are introduced and classified according to the underlying transport mechanisms. The relative progression velocity is shown to be dependent on a number of processes including diffusion, chemical rates and the local scalar gradients.

In Section 4.0, the intrinsic topology of surfaces embedded in a three dimensional space is discussed. The effect of chemical kinetics on turbulence is briefly described. Section 5.0 is devoted to the discussions of nonpremixed turbulent methane jet flames, which have been studied extensively by experiments and numerical simulations. The results from a stochastic simulation of the joint scalar pdf equation permit us to evaluate the mixedness parameters introduced in Section 3.0. It is shown that the mean chemical reaction rates can be larger or smaller than their corresponding $quasi-laminar$ values by several orders of magnitude indicating the strong influence of turbulence on chemical reactions. The last section summarizes the main findings from this study.

2.0 Basic Equations for Turbulent Reactive Flows

The current analysis of the interaction between turbulence and chemical reactions is restricted to Newtonian fluids in gaseous phase, to which the thermodynamic relations of ideal gases is applicable. Given compositions, two independent (intensive) thermodynamic variables, and velocity, one can determine the thermodynamic state of a reactive mixture. The governing transport equations for compositions, temperature, and velocity are dictated by the conservation laws of mass, energy, and momentum. In the Eulerian frame, these conservation equations can be written based on an observer fixed at an arbitrary location $\underline{x}$ in the flow field as function of time t. For some aspects of turbulent combustion, the physics can be better described based on the Lagrangian frame (following the fluid particles) than on the Eulerian frame. The relations that bridge the Eulerian and the Langrangian frames will be given at the end of this section.

Mass Balance:

Conservation of mass leads to the following transport equation for the density $\rho(\underline{x}, t)$ on the Eulerian frame

$$\frac{\partial \rho}{\partial t} + \frac{\partial}{\partial x_\alpha}(\rho v_\alpha) = 0, \tag{1}$$

where the repeated indexes mean summation over all possible states.

Species Balance:

We consider a mixture of N ideal gases with its compositions described in terms of mass fractions $Y_i(\underline{x},t)$. When chemical reactions occur, the mass fractions, Y_i, are not conserved, but consumed or produced according to their net production rates Q_i, which are determined by the reaction mechanism. Note that the net production rates, Q_i, depend only on the local thermodynamic variables; that is, Q_i do not contain time derivatives of thermodynamic variables or their integrals with respect to time or space. The transport equation for the mass fraction of the i-th species is then given by

$$\rho\frac{DY_i}{Dt} = -\frac{\partial J_\alpha^i}{\partial x_\alpha} + \rho Q_i, \qquad i = 1...N \tag{2}$$

where J_α^i denotes the diffusive flux in the α-coordinate. For multi-component reacting systems, the diffusive fluxes can be expressed in terms of functions containing gradients of species concentrations and their binary diffusion coefficients. If the i-th species is sufficiently diluted, its diffusion fluxes can be approximated by the Fick's diffusion law,

$$J_\alpha^i = -\rho\Gamma_i\frac{\partial Y_i}{\partial x_\alpha}, \tag{3}$$

where Γ_i is the diffusivity of the i-th species. For the purpose of this paper, we will use this approximation as it provides a very simple formula for calculating the diffusive fluxes in reacting flows.

Momentum balance

Newton's second law leads to the balance equation for momentum,

$$\rho\frac{Dv_\alpha}{Dt} = -\frac{\partial p}{\partial x_\alpha} + \frac{\partial \tau_{\alpha\beta}}{\partial x_\beta} + \rho f_\alpha, \tag{4}$$

where $\tau_{\alpha\beta}$ is the stress tensor and f_α is the external force per unit mass. For Newtonian fluids, the stress tensor obeys the following constitutive relation:

$$\tau_{\alpha\beta} = \mu(\frac{\partial v_\alpha}{\partial x_\beta} + \frac{\partial v_\beta}{\partial x_\alpha} - \frac{2}{3}\delta_{\alpha\beta}\frac{\partial v_\gamma}{\partial x_\gamma}), \tag{5}$$

where μ is the dynamic viscosity. An important feature of equation (5) is the linear relationship between the stresses and the rates of strain which are expressed as the velocity gradients.

Energy balance and state relations

Application of the first law of thermodynamics to a differential control volume leads to the energy balance equation in the Eulerian frame. This equation can be expressed in terms of several equivalent forms depending on the choice of the thermodynamic variables. If the specific enthalpy $h(\underline{x},t)$ is chosen, the energy conservation equation can be written as

$$\rho\frac{Dh}{Dt} = \frac{Dp}{Dt} + \Phi - \frac{\partial q_\alpha}{\partial x_\alpha}. \tag{6}$$

If the specific internal energy $e \equiv h - p/\rho$ is used, one can derive the following transport equation for e

$$\rho \frac{De}{Dt} = -p \frac{\partial v_\alpha}{\partial x_\alpha} + \Phi - \frac{\partial q_\alpha}{\partial x_\alpha}. \tag{7}$$

where Φ and q_α denote the dissipation function and the energy flux in the α-coordinate respectively. The dissipation function Φ is defined by

$$\Phi \equiv \tau_{\alpha\beta} \frac{\partial v_\alpha}{\partial x_\beta}, \tag{8}$$

which represents the heat generated by mechanical dissipation due to viscous friction. The energy flux q_α is expressed as a combination of conductive, diffusive, and radiative fluxes.

$$q_\alpha = -k \frac{\partial T}{\partial x_\alpha} - \rho \sum_{i=1}^{n} \frac{\bar{h}_i}{M_i} \Gamma_i \frac{\partial Y_i}{\partial x_\alpha} + q_\alpha^R. \tag{9}$$

For multi-component systems, with the ideal gas assumption, the mixture enthalpy is simply the sum of individual specific enthalpy weighted by its concentration

$$h = \sum_{i=1}^{n} \frac{\bar{h}_i}{M_i} Y_i, \tag{10}$$

where $\bar{h}_i$ is the molal enthalpy and M_i the molecular mass of the i-th component. The molal enthalpy $\bar{h}_i$ consists of two parts: the formation enthalpy $\bar{h}_i^0$ and the sensible enthalpy

$$\bar{h}_i = \bar{h}_i^0 + \int_{T_0}^{T} dT' \bar{c}_p(T'), \tag{11}$$

where $\bar{c}_p(T)$ denotes the molal specific heat at constant pressure. The above system of equations is completed if the ideal gas equation

$$p = \rho \Re T \sum_{i=1}^{n} \frac{Y_i}{M_i} \tag{12}$$

(where $\Re$ denotes the universal gas constant and M_i the molecular mass) is included and the chemical sources Q_i are specified.

So far we have presented the basic conservation laws in terms of mass fraction Y_i, enthalpy h, density ρ and velocity $\underline{v}$. This set of variables may not always be the most convenient ones, and a linear or nonlinear combination of these variables could be used for the treatment of turbulent reacting flows. For low Mach-number flows, it has been shown (Pope, 1985), by using a Taylor series expansion of the state relations, that chemical sources are, to the lowest order, independent of pressure fluctuations and that the substantial derivative of the pressure in the energy equation (6) can be neglected except under the condition of strong pressure

variations. Consequently, for low Mach number flows, the set of thermo-chemical variables $\Psi_i(\underline{x},t)$ obey a similar type of transport equations as

$$\rho\frac{D\psi_i}{Dt} = \frac{\partial}{\partial x_\alpha}\left(\rho\Gamma_i\frac{\partial\psi_i}{\partial x_\alpha}\right)+\rho q_i \quad , \; i = 1..l. \tag{13}$$

For combustion processes at constant pressure, the total number of thermo-chemical variables is simply $l = N + 1$.

Lagrangian frame

Studies of Chemical reactions in turbulent flows can also be carried out in the Lagrangian frame (Borghi, 1988), in which the observer follows an arbitrary material point of the fluid and monitors the evolution of this material point. This approach has some advantages because it is the natural frame for phenomena that are dominated by time history. Hence, the transformation rules between the Eulerian and Lagrangian frames will be given, and the structure of the conservation equations for the thermo-chemical variables Φ_i in the Lagrangian frame will be discussed briefly (Monin, 1962). In the Lagrangian frame, the independent variables are time t and $\underline{a}$, which is a variable used to identify the material point. The common choice for $\underline{a}$ is the position of a material point at the initial time t_0. The position of a material point in the Lagrangian frame is denoted by $\underline{X}(\underline{a},t)$ which can be used as a transformation function between the Eulerian and Lagrangian frames in the following manner

$$\underline{x} \;=\; \underline{X}(\underline{a},t) \quad and \quad \underline{a} \;=\; \underline{X}^{-1}(\underline{x},t),$$

where $\underline{X}^{-1}$ denotes the initial position of the material point which moves to the position $\underline{x}$ at time t. Here, the upper case letters denote the dependent variables in the Lagrangian frame and the lower case letters correspond to the same variables in the Eulerian frame. If the mapping function $\underline{X}$ and its inverse function $\underline{X}^{-1}$ are both twice continuously differentiable, both the time and spatial derivatives in the Eulerian frame can be transformed into the Lagrangian frame, and vice versa. For instance, the gradients of a variable can be transformed from one frame to the other frame according to (Truesdell, 1954)

$$\frac{\partial}{\partial x_\alpha} \;=\; \frac{1}{2J}\epsilon_{\alpha\beta\gamma}\epsilon_{\delta\eta\omega}\frac{\partial X_\beta}{\partial a_\eta}\frac{\partial X_\gamma}{\partial a_\omega}\frac{\partial}{\partial a_\delta} \tag{14}$$

and

$$\frac{\partial}{\partial a_\alpha} \;=\; \frac{J}{2}\epsilon_{\alpha\beta\gamma}\epsilon_{\delta\eta\omega}\frac{\partial X^{-1}_\beta}{\partial x_\eta}\frac{\partial X^{-1}_\gamma}{\partial x_\omega}\frac{\partial}{\partial x_\delta}, \tag{15}$$

where J denotes the Jacobian determinant

$$J \;=\; \frac{1}{6}\epsilon_{\alpha\beta\gamma}\epsilon_{\delta\eta\omega}\frac{\partial X_\delta}{\partial a_\alpha}\frac{\partial X_\eta}{\partial a_\beta}\frac{\partial X_\omega}{\partial a_\gamma} \tag{16}$$

Note that repeated subscripts imply summation and that $\epsilon_{\alpha\beta\gamma}$ is the permutation tensor. The transformation formula for the second and higher derivatives can be derived by using

Eqns. (14) and (15) repeatedly. In particular, the relation for the Laplacian is summarized here as

$$\Delta_x = \frac{1}{2J}\epsilon_{\alpha\beta\gamma}\epsilon_{\delta\eta\omega}\frac{\partial X_\zeta}{\partial a_\eta}\frac{\partial X_\phi}{\partial a_\omega}\frac{\partial}{\partial a_\delta}\left(\frac{1}{J}\frac{\partial X_\zeta}{\partial a_\beta}\frac{\partial X_\phi}{\partial a_\gamma}\frac{\partial}{\partial a_\alpha}\right). \tag{17}$$

The time derivatives in the Lagrangian frame are of fundamental interest because for a given material point, velocity and acceleration are, by definition, the time rates of change of position and velocity respectively. The latter terms appear in the Eulerian frame as the substantial or the Stokes derivative

$$\left(\frac{\partial}{\partial t}\right)_{\underline{a}} = \left(\frac{\partial}{\partial t}\right)_{\underline{x}} + v_\alpha(\underline{x},t)\frac{\partial}{x_\alpha} \equiv \frac{D}{Dt}. \tag{18}$$

The transformation rules (15)-(18) allow us to derive the transport equations for thermo-chemical variables in the Lagrangian frame based on those in the Eulerian frame. For instance, the transport equation (13) for $\Psi_i(\underline{x},t)$ can be transformed into the Lagrangian frame by using Eqns.(17) and (18), and the result is

$$\frac{\partial \Psi_i}{\partial t} = \frac{1}{2R_0}\epsilon_{\alpha\beta\gamma}\epsilon_{\delta\eta\omega}\frac{\partial X_\zeta}{\partial a_\eta}\frac{\partial X_\phi}{\partial a_\omega}\frac{\partial}{\partial a_\delta}\left(\frac{R^2\Gamma_i}{R_0}\frac{\partial X_\zeta}{\partial a_\beta}\frac{\partial X_\phi}{\partial a_\gamma}\frac{\partial \Psi_i}{\partial a_\alpha}\right)+Q_i,$$

$$i = 1..l. \tag{19}$$

Note that the nonlinear convective terms disappear, but the diffusion terms become highly nonlinear as $\underline{X}$ is a dependent variable in the Lagrangian frame. In deriving Eqn. (19), we have expressed the mass conservation law in the integrated form as

$$\frac{R(\underline{a},0)}{R(\underline{a},t)} = J, \tag{20}$$

where $R(\underline{a},t) = \rho(\underline{x},t)$ for $\underline{x} = \underline{X}(\underline{a},t)$. With this relation, the Jacobian J can be eliminated from the transport equations.

3.0 The Influence of Turbulence on Chemical Reactions.

In turbulent flows, chemical reactions proceed in an environment changing randomly in time and space. The fluctuating nature of mechanical and thermodynamic variables can have significant influence on the progress of chemical reactions. In this section, we will analyze this influence in detail by examining the mean reaction rate for a single irreversible chemical reaction involving only two reactive species. Under such a circumstance, the transport equation for the probability density function (pdf) of a single thermo-chemical variable can be solved for a non-decaying homogeneous turbulence. With the help of this solution, one can clarify the role of the correlation between the scalar and its gradients in describing the interactions between chemical reaction and turbulence.

The progress of chemical reactions in nonpremixed flames depends strongly on the degree of mixing between fuel and oxidizer. Turbulence can greatly enhance the mixing process and thus increase chemical reaction rates by several orders of magnitude. Due to the practical importance of nonpremixed flames, we will discuss in depth the mixing phenomenon and the theories that describe this important process. Furthermore, special attention will be given to the mixing models which are currently used in the pdf methods.

In premixed turbulent flames, the influence of turbulence on chemical reactions may be described as the combined effects of convection and distortion of the reaction zone. We will restrict our attention to the special case of thin reaction zones, which can be treated as flame sheets. As the concept of treating turbulent flames as an ensemble of laminar flamelets alleviates the need for detailed modeling of chemical reactions, we will provide some discussions on the kinematics and dynamics of surfaces moving through the turbulent flow field. Several types of surfaces relevant to turbulent combustion flows will be considered and the topological and geometrical properties of these surfaces will be analyzed.

3.1 Mean Chemical Reaction Rates in Turbulent Flows.

Let us consider the transport equation (2) for chemical species i. Density-weighted average of this equation leads to the mean transport equation for $\tilde{Y}_i$ as

$$\langle\rho\rangle(\frac{\partial\tilde{Y}_i}{\partial t}+\tilde{v}_\alpha\frac{\partial\tilde{Y}_i}{\partial x_\alpha})=-\frac{\partial}{\partial x_\alpha}(\langle\tilde{J}^i_\alpha\rangle+\langle\rho\rangle\widetilde{v''_\alpha Y''_i})+\langle\rho\rangle\tilde{\dot{w}}_i. \tag{21}$$

The most interesting quantity that will be addressed here is the mean chemical reaction rate $\tilde{\dot{w}}_i$ as it depends strongly on the temperature and species fluctuations. We begin with an analysis of this dependence for a bimolecular, irreversible reaction between two species A and B

$$A+B\rightarrow C.$$

The instantaneous kinetic source term $\dot{w}_i$ is written as

$$\dot{w}_A=\dot{w}_B=-kY_AY_B. \tag{22}$$

For simplicity, let us consider the case with a constant k first. Average of Eqn. (22) yields the mean kinetic source as

$$\tilde{\dot{w}}_A=-k(\tilde{Y}_A\tilde{Y}_B+\widetilde{Y''_AY''_B}).$$

It is clear that the influence of turbulence on the chemical reaction is reflected in the correlation $\widetilde{Y_A''Y_B''}$. Application of the Schwartz inequality leads to the upper bound for this correlation as

$$\widetilde{Y_A''Y_B''}^2 \leq \widetilde{Y_A''^2}\widetilde{Y_B''^2}.$$

With the inequality

$$\widetilde{Y_i''^2} \leq \tilde{Y}_i(1-\tilde{Y}_i) \ , \ i = A, B,$$

which is the consequence of Hausdorff's theorem (Akhiezer, 1965) on the moments of bounded random variables, one obtains the following relation

$$\widetilde{Y_A''Y_B''}^2 \leq \tilde{Y}_A(1-\tilde{Y}_A)\tilde{Y}_B(1-\tilde{Y}_B).$$

Hence, the upper bound for the mean chemical reaction can be derived as

$$|\tilde{\dot{w}}_A| \leq k(\tilde{Y}_A\tilde{Y}_B + \sqrt{\tilde{Y}_A(1-\tilde{Y}_A)\tilde{Y}_B(1-\tilde{Y}_B)}). \tag{23}$$

Therefore, turbulence can increase the mean sources $\tilde{\dot{w}}_A$ compared to the corresponding quasi-laminar values $\dot{w}(\tilde{Y}_i)$. However, the opposite effect is also possible; that is, turbulent fluctuations can also reduce the mean reaction rates. If the correlation $\widetilde{Y_A''Y_B''}$ is negative, it follows that

$$|\tilde{\dot{w}}_A| \leq |\dot{w}(\tilde{Y}_i)|,$$

which is the upper bound for the mean chemical source term. We can obtain a lower bound for $|\tilde{\dot{w}}_A|$ as follows. If the reactants A and B be totally segregated, the joint pdf of Y_A and Y_B is given by

$$f(y_A, y_B) = (1-\tilde{Y}_A)\delta(y_A)\delta(1-y_B) + \tilde{Y}_A\delta(1-y_A)\delta(y_B). \tag{24}$$

This pdf represents a special situation where species A and B do not coexist at the same spatial location, but they may have nonzero mean values. It can be shown that the fluctuations are maximal in this case. Physically, the flow consists of randomly distributed regions with only species A or species B but not with both, and the two species are separated by an infinitely thin interface. Straightforward integration of the instantaneous chemical reaction rate weighted by the pdf over the entire domain produces the following correlation

$$\widetilde{Y_A''Y_B''} = -\tilde{Y}_A\tilde{Y}_B.$$

It is clear that $\tilde{\dot{w}}_A = 0$ means zero reaction rate, because no mixing at the molecular level has taken place. We conclude that the mean reaction rate can have a wide range of values (but limited by the upper and lower bounds) which may be radically different from the corresponding quasi-laminar values.

Next, the case with a temperature dependent chemical reaction rate will be considered. We assume that k is given by the following Arrhenius form

$$k(T) = k_0 \exp(-\frac{T_E}{T}). \tag{25}$$

One parameter to measure the influence of turbulence on chemical reactions is the ratio of the mean reaction rate and its quasi-laminar counterpart as defined by

$$R \equiv \frac{\tilde{k}}{k(\tilde{T})}. \tag{26}$$

This expression can be further written in terms of of $T_E/\tilde{T}$ and the pdf of T as (Borghi, 1989)

$$R = \int_0^\infty dT \tilde{f}(T) g(T; \tilde{T}, T_E) \equiv \tilde{g}, \tag{27}$$

where the monotonically increasing function g is defined by

$$g(T) \equiv \exp\{-\frac{T_E}{\tilde{T}}(\frac{\tilde{T}}{T} - 1)\} = \exp(\frac{T_E}{\tilde{T}}) \cdot \exp(\frac{-T_E}{T}), \tag{28}$$

and it has the following properties: $g(0) = 0$, $g(\tilde{T}) = 1$ and $g(\infty) = \exp(T_E/\tilde{T}) \geq 1$. Due to the exponential dependence of chemical reaction rate on temperature, $g(T)$ increases rapidly with temperature. The rate of increase is given by the derivative of g,

$$\frac{dg}{dT}(T) = \frac{T_E}{T^2} g(T), \tag{29}$$

which has the value of $T_E/\tilde{T}^2$ at the mean temperature $\tilde{T}$. Under the condition of a large activation temperature with a low mean temperature, strong temperature fluctuations lead to large ratios $R \gg 1$, because the product of $g(T)$ and the pdf $\tilde{f}(T)$ increases drastically when $T \geq \tilde{T}$. It is also noted that the ratio R could be less than unity, but a reduction in the mean reaction rate can occur only when the pdf $\tilde{f}(T)$ is highly biased toward the low temperature side. These properties of the ratio R illustrate the effect of temperature fluctuations on the mean chemical reaction rate. The combined effect of temperature and composition fluctuations on the mean kinetic source terms will be addressed in Section 5.0 for a turbulent diffusion jet flame.

For high Reynolds number flows, the pdf transport equation for the set of l thermo-chemical variables governed by Eqn. (13) in the Eulerian frame or Eqn. (19) in the Lagrangian frame can be written as (Kollmann, 1989)

$$\langle\rho\rangle\{\frac{\partial \tilde{f}_1}{\partial t} + \tilde{v}_\beta \frac{\partial \tilde{f}_1}{\partial x_\beta} + \sum_{j=1}^{l} \frac{\partial}{\partial \varphi_j}(Q_j(\varphi_1, \cdots, \varphi_l)\tilde{f}_1)\} =$$

$$-\frac{\partial}{\partial x_\alpha}(\langle\rho\rangle\langle v_\alpha''|\Psi_j=\varphi_j\rangle\tilde{f}_1)$$

$$-\langle\rho\rangle\sum_{j=1}^{l}\sum_{k=1}^{l}\frac{\partial^2}{\partial\varphi_j\partial\varphi_k}(\langle\epsilon_{jk}|\Psi_j=\varphi_j\rangle\tilde{f}_1), \tag{30}$$

where the density-weighted pdf $\tilde{f}_1$ is defined by

$$\tilde{f}_1 \equiv \frac{\rho(\varphi_1,\cdots,\varphi_l)}{\langle\rho\rangle}f_1(\varphi_1,\cdots,\varphi_l;\underline{x},t). \tag{31}$$

and the scalar dissipation rates ϵ_{ij} in the conditional expectations are defined by

$$\epsilon_{ij} \equiv \Gamma\frac{\partial\Psi_i}{\partial x_\alpha}\frac{\partial\Psi_j}{\partial x_\alpha} \tag{32}$$

with $\Gamma_i=\Gamma_j=\Gamma$. For homogeneous turbulent flows, this equation reduces to

$$\langle\rho\rangle\{\frac{\partial\tilde{f}_1}{\partial t}+\sum_{j=1}^{l}\frac{\partial}{\partial\varphi_j}(Q_j(\varphi_1,\cdots,\varphi_l)\tilde{f}_1)\}=$$

$$-\langle\rho\rangle\sum_{j=1}^{l}\sum_{k=1}^{l}\frac{\partial^2}{\partial\varphi_j\partial\varphi_k}(\langle\epsilon_{jk}|\Psi_j=\varphi_j\rangle\tilde{f}_1). \tag{33}$$

The special case with a single scalar variable ($l=1$) is of particular interest. Integration over the scalar interval $[-\infty,\varphi]$ leads to

$$\frac{\partial\tilde{F}_1}{\partial t}+Q(\varphi)\tilde{f}_1+\frac{\partial}{\partial\varphi}\{\langle\epsilon_{11}|\Psi=\varphi\rangle\tilde{f}_1\}=0, \tag{34}$$

where $\tilde{F}_1$ is the distribution function associated with the pdf $\tilde{f}_1$. For statistically stationary turbulence, the time derivative can be eliminated from Eqn. (34) and the result is

$$Q(\varphi)\tilde{f}_1(\varphi)+\frac{d}{d\varphi}\{\langle\epsilon_{11}|\varphi\rangle\tilde{f}_1(\varphi)\}=0. \tag{35}$$

This equatuion can be solved analytically, and we obtain the following general solution

$$\langle\epsilon_{11}|\varphi\rangle\tilde{f}_1(\varphi)=C_N\cdot\exp\{-\int_{-\infty}^{\varphi}d\varphi'\frac{Q(\varphi')}{\langle\epsilon_{11}|\varphi'\rangle}\}, \tag{36}$$

where the constant C_N is determined by

$$N^{-1}=\int_{-\infty}^{\infty}d\varphi\frac{\exp\{-\int_{-\infty}^{\varphi}d\varphi'\frac{Q(\varphi')}{\langle\epsilon_{11}|\varphi'\rangle}\}}{\langle\epsilon_{11}|\varphi\rangle} \tag{37}$$

so that the integration of $\tilde{f}_1$ over $[-\infty, \infty]$ is unity. This solution has some interesting properties. First, we note that the influence of turbulence on the scalar pdf $\tilde{f}_1(\varphi)$ is expressed in terms of the conditional expectation of the scalar dissipation rate $\langle \epsilon_{11} | \varphi \rangle$. Applying scaling arguments to the scalar fluctuations, one concludes that ϵ_{11} and φ are statistically independent at high Reynolds numbers based on the Kolmogorov's hypotheses. If this is true, it follows that the pdf $\tilde{f}_1(\varphi)$ and its width are determined essentially by the source $Q(\varphi)$ and $\langle \epsilon_{11} \rangle$. A source $Q(\varphi)$ that is linear in φ can lead to the Gaussian pdf as time goes to infinity as expected in a homogeneous turbulence. However, this is true only for an unbounded variable φ. For bounded variables, such as mass fractions or concentrations, both the source Q and ϵ_{11} must be correlated with φ so that the pdf is confined to its allowable domain. This should be true even in the limit of infinite Reynolds number.

3.2 Nonpremixed Reacting Systems:

For nonpremixed turbulent flames, the effect of turbulence on chemical reactions is primarily through the enhancement of mixing. Mixing is defined as the inter-diffusion of different components on the molecular level. The mass fraction (mole fraction or concentration) of component i changes due to the unbalance of diffusive fluxes passing through the bounding surface of a control volume. The flux defined in Eqn. (3) and its divergence in Eqn. (2) are determined by the spatial gradients of mass fractions at the current time t. Hence, the Eulerian frame is most appropriate for the description of molecular diffusion. Chemical reactions on the other hand depend only on the local thermodynamic state, and, therefore, they are best described in the Lagrangian frame. It is clear that there is no definite preference to the Eulerian frame or the Lagrangian frame for the description of the combined effects of convection, diffusion, and reactions. So far, most theoretical treatments have been based on the Eulerian frame, but several recent approaches use the Lagrangian or a mixed Eulerian/Lagrangian formulation. Here we will consider the diffusion process in the Lagrangian frame first, and the mixed formulations will be given next.

The diffusive flux in the Lagrangian frame can be expressed as

$$J_\alpha^i = -\frac{1}{2} R_o \Gamma_i \epsilon_{\alpha\beta\gamma} \epsilon_{\delta\eta\omega} \frac{\partial X_\beta}{\partial a_\eta} \frac{\partial X_\gamma}{\partial a_\omega} \frac{\partial Y_i}{\partial a_\delta}, \tag{38}$$

which contains the Lagrangian deformation tensors, $\partial X_\alpha / \partial a_\beta$, and the Lagrangian gradients, $\partial / \partial a_\alpha$. The Lagrangian deformation tensors can be further expressed in terms of the Lagrangian deformation rates as follows:

$$\frac{\partial X_\alpha}{\partial a_\beta} = \delta_{\alpha\beta} + \int_0^t d\tau \frac{\partial V_\alpha}{\partial a_\beta}(\underline{a}, \tau).$$

Substitution of this expression into Eqn. (38) leads to

$$J_\alpha^i = -\frac{1}{2} R_o \Gamma_i \epsilon_{\alpha\beta\gamma} \epsilon_{\delta\eta\omega} (\delta_{\beta\eta} + \int_0^t d\tau \frac{\partial V_\beta}{\partial a_\eta}(\underline{a}, \tau))$$

$$(\delta_{\gamma\omega} + \int_0^t d\tau \frac{\partial V_\gamma}{\partial a_\omega}(\underline{a}, \tau)) \frac{\partial Y_i}{\partial a_\delta} \tag{39}$$

This equation shows that the influence of velocity fluctuations on the diffusive flux is through the deformation rate histories along the pathline of a material point $\underline{a}$. It is evident that in turbulent flows, the fluctuations of flux J_α^i are due to continuous changes of the mass fraction gradients and the deformation rate tensors. Note that the mass fraction gradient is time independent if the mass fraction Y_i itself is a material property (i.e., no diffusion and no sources). Hence, the temporal fluctuation of $\partial Y_i/\partial a_\alpha$ is solely due to the diffusion process and various production sources, such as chemical reactions. If the density changes are small, the fluctuations of the Lagrangian deformation rate tensors are dictated essentially by the conservation of momentum and mass. For large density fluctuations, significant modification of $\partial X_\alpha/\partial a_\beta$ is likely to happen due to the large fluctuations in the thermodynamic variables.

From system dynamics point of view, the evolution of turbulence can be described as a point in the phase space spanned by the Lagrangian position $\underline{X}(\underline{a})$ and the pressure $P(\underline{a})$. If the Reynolds number is sufficiently high, there exists a region in the phase space that attracts all the states of turbulence irrespective of their initial conditions. This phenomenon exhibits several interesting properties, which also appear in the strange attractors of low dimensional dynamical systems. In particular, the turbulent flows are shown to be very sensitive to their initial conditions. Consequently, the magnitude of the deformation rate tensor, $\partial X_\alpha/\partial a_\beta$, can be very large because material points that are initially close to each other can drift far apart due to turbulent motion.

The mixed formulation of the transport equation for the mass fraction Y_i is given by

$$R\left(\frac{\partial Y_i}{\partial t}\right)_{\underline{a}} = \frac{\partial}{\partial X_\alpha}(\rho\Gamma_i \frac{\partial Y_i}{\partial X_\alpha}) + RQ_i(\underline{a}, t). \tag{40}$$

This equation shows that following a material point, the time rate of change of Y_i is balanced by the diffusion process written in the Eulerian frame and by the chemical reactions expressed in the Lagrangian frame. The mixed formulation reduces to the kinetic rate equation for a closed reacting system in the absence of diffusion. The interpretation (but not the value) of the diffusive term is frame dependent. In the Eulerian frame only the mass fractions Y_i are dependent variables, and hence they are stochastic; in the Lagrangian frame, both Y_i and $\underline{X}$ are dependent variables, and hence both are stochastic. This suggests that modeling the processes in Eqn. (40) can be carried out in the Lagrangian frame with ratios of random variables as in Borghi's M.I.L. (1988) model.

Complete mixing is achieved if there is no scalar fluctuation. Therefore, nonzero scalar fluctuations indicate imperfect mixing, and they can be used as an indication of the degree of mixing (the mixedness) (Bilger 1976). In the Eulerian frame, the transport equation for the scalar variance can be expressed as following

$$\langle\rho\rangle\frac{\partial\widetilde{Y''^2}_i}{\partial t} + \langle\rho\rangle\tilde{v}_\alpha\frac{\partial\widetilde{Y''^2}_i}{\partial x_\alpha} = -\frac{\partial}{\partial x_\alpha}(\langle\rho\rangle\widetilde{v''_\alpha Y''^2_i})$$

$$-\langle\rho\rangle\widetilde{v''_\alpha Y''_i}\frac{\partial\tilde{Y}_i}{\partial x_\alpha} - \langle\rho\rangle\tilde{\epsilon}_i, \tag{41}$$

where

$$\langle\rho\rangle\tilde{\epsilon}_i \equiv \langle\rho\Gamma_i\frac{\partial Y_i}{\partial x_\alpha}\frac{\partial Y_i}{\partial x_\alpha}\rangle \tag{42}$$

denotes the density-weighted expectation of the scalar dissipation. As the scalar dissipation is always positive, it is clear that the scalar dissipation term reduces scalar variance; hence, it promotes mixing. This can be better described in terms of the mixing parameters defined as

$$\alpha_{ij} \equiv -\frac{\widetilde{Y_i''Y_j''}}{\tilde{Y}_i\tilde{Y}_j}\ , \quad i \leq j. \tag{43}$$

It is instructive to consider a binary reacting system which is homogeneous at the macro scales but not at the micro scales. For such a system, the following mathematic constraints are satisfied

$$Y_1'' + Y_2'' = 0\ ,\ \tilde{Y}_1 + \tilde{Y}_2 = 1,$$

$$\frac{\partial}{\partial x_\alpha} = 0, \quad and \quad \tilde{Y}_1 = constant.$$

Using the first two conditions, the mixing parameters for a binary system can be written as

$$\alpha_{12} = \frac{\widetilde{Y_1''^2}}{\tilde{Y}_1(1-\tilde{Y}_1)}\ ,\ 0 \leq \alpha_{12} \leq 1. \tag{44}$$

If the two species are totally segregated (i.e., no mixing at the molecular level), α_{12} is simply equal to one as the maximum value of $\widetilde{Y_1''^2}$ is $\tilde{Y}_1(1-\tilde{Y}_1)$. In the opposite case of perfect mixing, $\alpha_{12} = 0$. Using the transport equation (41), a time evolution equation for α_{12} can be derived as

$$\frac{\partial\alpha_{12}}{\partial t} = -\epsilon_1\tilde{Y}_1(1-\tilde{Y}_1),$$

which shows that α_{12} is always decreasing in time as the mixing process progresses at the molecular level. For reacting systems of multi-components, the values of α_{ij} are not simply bounded by zero and unity, and they may even change signs in the flow field according the correlations $\widetilde{Y_i''Y_j''}$ (see Section 5.0).

Mixing Models

The pdf methods (Pope, 1985; Borghi, 1988; Kollmann, 1989) offer an attractive framework for theoretical and computational studies of turbulent reacting flows since they do not require modeling of the mean chemical reaction rates. We will restrict our discussions to the single point pdf method. In particular, the joint scalar pdf method will be considered because the central issue in this paper is the influence of turbulence on chemistry. It has been demonstrated that the effect of turbulent mixing can be described by

$$\left(\frac{\partial\tilde{f}_1}{\partial t}\right)_{mix} = -\sum_{j=1}^{l}\sum_{k=1}^{l}\frac{\partial^2}{\partial\varphi_j\varphi_k}(\langle\epsilon_{jk}|\varphi_1,..,\varphi_l\rangle\tilde{f}_1), \tag{45}$$

which shows the joint scalar pdf is transported in the scalar space due to mixing and, more importantly, the shape of $\tilde{f}_1$ becomes narrower in time. It is worthy noting that the transport equation (45) represents a time-inverse diffusion process in the scalar space with the diffusion speed determined by the conditional expectation of the scalar dissipation rates. Consequently, the initial value problem posed by Eqn. (45) is difficult to solve by the traditional finite-difference methods as the numerical errors tend to grow exponentially. Fourier transformation of Eqn. (45) leads to the equation for the characteristic function m_1

$$\left(\frac{dm_1}{dt}\right)_{mix} = \sum_{j=1}^{l}\sum_{k=1}^{l} k_j k_k \langle \epsilon_{jk}|\underline{\varphi}\rangle * m_1,$$

where m_1 is defined by

$$m_1(\underline{k},t) = \int \cdots \int d\varphi_1 \cdots d\varphi_l \tilde{f}_1(\underline{\varphi},t)\exp(i\sum_{j=1}^{l} k_j\varphi_j),$$

and the asterisk denotes convolution. Restricting our consideration to $l = 1$ and assuming $\langle \epsilon_{11}|\varphi\rangle$ independent of φ, we obtain an analytic solution for $\tilde{f}_1$ as

$$\tilde{f}_1(\varphi,t) = \frac{1}{\sqrt{2\pi}}\int dk m_1(k,0)\exp\{ik\varphi + k^2\int_0^t d\tau\langle\epsilon_{11}\rangle(\tau)\}.$$

This solution indicates that if m_1 is initially non-Gaussian, high wave-number components can be amplified exponentially in time. This implies that the numerical errors in the high-wave-number range will grow exponentially, and eventually the solution becomes unstable. The major conclusion is that closure models for mixing should not be based on the time-inverse diffusion equation. Consequently, most mixing models developed so far are of integral form.

Integral Mixing Models

Any closure model for the mixing term in Eqn. (45) should possess as many as possible the important features of the exact term. Strict mathematic requirements demand the model to satisfy the following realizability conditions:

1. The pdf remains non-negative.
2. The pdf remains normalized.
3. The domain of definition of the pdf remains unchanged. (The values of pdf do not migrate outside the allowable domain, which are often dictated by the conservation laws.)

These realizability conditions ensure the solution of the modeled pdf equation satisfy all the basic mathematic constraints of a pdf. The physics of mixing must be introduced as additional requirements for the closure model. The exact equation (45) can be shown (Janicka *et al.*, 1979; Pope, 1985) to reduce the higher moments of a pdf such that in the limit $t \to \infty$ the Dirac pseudo-function is produced. A closure model that is able to fulfill the above requirements can be constructed as follows. Three basic assumptions are made here:

1. Mixing proceeds by pairwise interaction of fluid volumes (elements, notional particles) that are small compared to the volume of the flow domain.
2. Local chaos prevails so that the probability of finding $n \geq 2$ fluid volumes with specified properties in a given (small compared to the flow domain) neighborhood is the product of the n pdf values for these properties.
3. The time scale for the mixing process is independent of the scalar values involved in the mixing process.

It can be shown that a closure model that satisfies all these three assumptions has the following form (Kollmann, 1989)

$$\left(\frac{\partial \tilde{f}_1}{\partial t}\right)_{mix} = \frac{1}{\tau}\{\int_{\Re} d\underline{\varphi}' \int_{\Re} d\underline{\varphi}'' \tilde{f}_1(\underline{\varphi}')\tilde{f}_1(\underline{\varphi}'')T(\underline{\varphi}', \underline{\varphi}'' \rightarrow \underline{\varphi}) - \tilde{f}_1(\underline{\varphi})\}, \tag{46}$$

where $\Re$ denotes the domain of allowable scalar space. The essential properties of the mixing model are contained in the transition pdf T and the time scale τ. A general form of the transition pdf T can be cast as (Pope, 1985)

$$T(\underline{\varphi}', \underline{\varphi}'' \rightarrow \underline{\varphi}) = \int_0^1 d\alpha A(\alpha)\delta[\underline{\varphi} - (1-\alpha)\underline{\varphi}' - \frac{1}{2}\alpha(\underline{\varphi}' + \underline{\varphi}'')], \tag{47}$$

where $A(\alpha)$ is a pdf defined within $[0, 1]$. The random variable α controls the amount of mixing taking place during the pairwise interaction. The construction of the mixing model is now reduced to the specification of $A(\alpha)$ and the time scale τ. If we set

$$A(\alpha) = \delta(\alpha - 1), \tag{48}$$

Eqn. (47) reduces to Curl's (1963) droplet interaction model, which is computationally efficient but has well known deficiencies (Kollmann, 1989). Dopazo (1979) and Janicka *et al.* (1979) suggested

$$A(\alpha) = 1, \tag{49}$$

which randomizes the extent of mixing and overcomes the deficiency in Curl's model. Substitution of Eqn. (49) into Eqn. (47) yields a new form for T as

$$T(\underline{\varphi}', \underline{\varphi}'' \rightarrow \underline{\psi}) = \begin{cases} |\underline{\varphi}'' - \underline{\varphi}'|^{-1} & \text{for } \underline{\varphi} \in [\underline{\varphi}', \underline{\varphi}''] \\ 0 & \text{otherwise.} \end{cases} \tag{50}$$

Both Eqn. (49) and Eqn. (50) indicate that an equal probability is assigned to any value in the interval $[\underline{\varphi}', \underline{\varphi}'']$. This model has been applied to a wide range of flows (Pope, 1985; Jones and Kollmann, 1987; Chen and Kollmann, 1989,a,1990), but it causes the higher normalized moments,

$$\mu_m \equiv \frac{\langle \varphi^m \rangle}{\langle \varphi^2 \rangle^{\frac{m}{2}}},$$

($m \geq 4$) to diverge as time goes to infinity in decaying homogeneous turbulence (Pope, 1982). A possible remedy for this defficiency has been suggested by Pope (1982) as follows. If the probability of finding elements with the values $\underline{\varphi}$ at a given location is biased with the age of the element (time elapsed between mixing interactions normalized with an appropriate time scale), then bounded limits for the normalized moments μ_m can be achieved.

Time Scales

The time scale τ for the mixing event to take place depends on the turbulent flow field and the scalar field. If one assumes that the time scale ratios between the turbulent flow field and the scalar field,

$$R \equiv \frac{\langle \epsilon_{11} \rangle}{\langle \varphi'^2 \rangle} \frac{\tilde{k}}{\tilde{\epsilon}}, \tag{51}$$

are constant and independence of kinetic sources, then the time scale τ can be given by

$$\tau = C \cdot \frac{\tilde{k}}{\tilde{\epsilon}} \tag{52}$$

with C denoting a constant of order unity. This assumption was found to be reasonably good for nonreacting free-shear flows, but it becomes questionable for reacting flows (Borghi, 1988). There are several possible approaches to improve the model of time scales. First, the transport equation for the scalar dissipation can be included in the closure model (Lumley, 1978 and Dibble *et al.* 1986). Therefore, the effects of heat release on the scalar dissipation (or on the time scale) can be included in the model (Dibble *et al.*, 1986). However, this approach has not been successful. Alternatively, the time scale information can be carried by one of the variables in the pdf. This can be done by using the two-point pdf approach (Ievlev, 1973; Pope, 1985; Kollmann and Wu, 1987) or by including the scalar dissipation rate in the pdf (Meyers and O'Brien, 1981; Pope, 1989). Both approaches are currently under intense development.

3.3 Premixed Reacting Systems

The theory of laminar premixed flames is well developed (Williams, 1985). Laminar premixed flames with a high activation energy are thin, and their structure consists of a preheat zone with negligible combustion and a thin reaction zone (Pope 1987). The laminar flame speed u_L and the thickness ϵ_L can be determined entirely by the diffusivity Γ and the chemical time scale τ_c (Borghi, 1988). Flames with low activation energies are more complex, but the notions of flame speed and flame thickness are still valid. With the help of u_L and ϵ_L, the structures of turbulent premixed flames can be analyzed in the Klimov-Williams diagram (Borghi, 1988; Williams, 1989), where the ratio $k^{1/2}/u_L$ over l_t/ϵ_L or the Damkoehler number

$$D_a \equiv \frac{l_t}{k^{\frac{1}{2}}\tau_c} \tag{53}$$

over the Reynolds number

$$Re \equiv \frac{k^{\frac{1}{2}}l_t}{\nu} \tag{54}$$

is plotted (k denotes the kinetic energy of turbulence and l_t the turbulent macro-scale). Several important regimes can be identified. For large values of l_t/ϵ_L with low to moderate turbulence levels, turbulent premixed flames can be described as an ensemble of wrinkled flames. The effect of turbulence is essentially through the increase of flame front area per unit volume without significant changes in the flame structure. As turbulence intensity increases, pockets of fresh gases can form inside the burned product if the rate of pocket formation (determined by turbulence parameters) is approximately the same as the rate of pocket consumption (determined by chemical and turbulence parameters). This regime is called the corrugated flame regime (Peters, 1986). As turbulence intensity increases further, thick flames with their thickness larger than the micro scale of turbulence can form, and turbulence can significantly modify the local flame structure.

As discussed above, the effect of turbulence on premixed combustion ranges from distortion and wrinkles of thin flame fronts to complex interactions with thick combustion zones. Predictions of premixed turbulent flames have been explored by Pope (1987) with pdf methods, which are particularly well suited for the latter regime. However, traditional moment closure methods have been useful in treating the flame sheet combustion regime. Two models will be discussed briefly.

The BLM Model

The BLM model (Bray, Libby and Moss, 1985) proposed the concept that the progress of the reactions can be described by a single scalar variable c with certain assumptions. If the reaction zone is thin, then the pdf of the reaction progress variable can be approximately given by

$$\tilde{f}_1(c;\underline{x},t) = \alpha(\underline{x},t)\delta(c) + \beta(\underline{x},t)\delta(c-1) + \gamma(\underline{x},t)\tilde{f}_c(c;\underline{x},t) \tag{55}$$

with positive α, β, γ and the mathematic constraint

$$\alpha + \beta + \gamma = 1.$$

The coefficient α is the probability of observing reactants at the point $(\underline{x}, t)$; β is the probability of finding products, and γ represents the probability of a state within the reaction zone (flame sheet). The most important assumption in this model is

$$\gamma \ll 1, \tag{56}$$

which is valid for the thin flame sheet regime. The BLM model makes the full use of this fact so that the statistical moments can be expanded in terms of γ. It follows that

$$\alpha = 1 - \beta + O(\gamma)$$

and

$$\alpha = \frac{1 - \tilde{c}}{1 + \tau\tilde{c}} + O(\gamma),$$

where τ is the heat release parameter. The model consists of the transport equations for the mean progress variable $\tilde{c}$ and its variance. These equations need to be modeled, and their solutions determine the local pdf for c to first order in γ. Here, only the equation for $\tilde{c}$ is considered

$$\langle\rho\rangle\left(\frac{\partial\tilde{c}}{\partial t} + \tilde{v}_\alpha\frac{\partial\tilde{c}}{\partial x_\alpha}\right) = -\frac{\partial}{\partial x_\alpha}(\langle\rho\rangle\widetilde{v''_\alpha c''}) + \langle\rho\rangle\tilde{w}, \tag{57}$$

which contains two terms that need modeling, the turbulent flux $\widetilde{v''_\alpha c''}$ and the mean kinetic source $\tilde{w}$. Detailed modeling of the turbulent flux will not be repeated here and it can be found in Bray, Libby and Moss (1985). Since $w(0) = w(1) = 0$, one needs to estimate the contribution from the continuous part of the pdf $\tilde{f}_c$ (flame sheet contribution). A special form of $\tilde{f}_c$ can be constructed if the reaction zone consists of randomly convected, wrinkled, but unstrained laminar flamelets (Bray *et al.*, 1985). More recently, Bray *et al.* (1989) have proposed to model the mean reaction rate directly. Two approaches have been considered for this direct closure method. First, the mean reaction rate is represented as the product of the crossing frequency of the interface at a given point and the chemical reaction rate per crossing. Second, the mean source terms can be treated as the product of the average number of flamelets per unit length (in the neighborhood of the given point) and the chemical reaction rate per unit length. In both proposals, the essential issue becomes the modeling of the topology and geometry of an interface embedded in a turbulent flow. This aspect will be discussed in the next section.

The Coherent Flame Model

The basic concept of the coherent flame model proposed by Marble and Broadwell (1977) is the notion of laminar flamelets, which are transported and distorted by the turbulent flow field, but retain their identifiable structures. This concept provides an alternative way to model the mean reaction rate $\tilde{w}_i$. The key parameter in calculating the $\tilde{w}_i$ is the mean flame surface area density $\tilde{\Sigma}_f$ defined by (Darabiha *et al.*, 1989)

$$\Sigma_f \equiv \lim_{\delta V \to 0} \frac{\delta S}{\delta V},$$

where δS denotes the surface element and δV is the volume element centered at $\underline{x}$. This definition deserves further explanations. First, the reaction zone is represented by a surface on which the instantaneous reaction rate assumes a prescribed (nonzero) value. For finite Peclet and Damkoehler numbers, this surface is a differentiable manifold. Let's consider an arbitrary point $(\underline{x}, t)$ in the flow domain and let $K_{\underline{x}}(r)$ be a sphere of radius r (volume element δV) which is centered at $\underline{x}$. If the sphere intersects a flame surface, then we can find a radius r small enough so that the intersection of the surface with the sphere looks like a plane. Based on the properties of a differential manifold, there exist two possibilities for the instantaneous value of Σ_f. One possibility is $\underline{x}$ being on the surface; then

$$\Sigma_f \sim \frac{\pi r^2}{\frac{4\pi}{3} r^3} \sim \frac{1}{r} \to \infty \quad as \quad r \to 0.$$

The other possibility is $\underline{x}$ being outside the surface; then there exists a radius r_o such that

$$\Sigma_f \sim \frac{0}{\frac{4\pi}{3} r^3} = 0$$

for all $r \leq r_o$. Hence, Σ_f can have only the values ∞ and zero. It is not clear whether or not Σ_f has a mean value, because the value ∞ must associate with the zero probability in order to produce a nonzero mean. However, random variables can be constructed with the properties of Σ_f leading to a nonzero mean but no higher moments (Kollmann, 1989). Therefore, the properties of Σ_f are dependent on the characteristics of $\delta S/\delta V$ as the volume δV is shrunk to the point $\underline{x}$ under consideration.

The transport equation for the mean surface area per unit volume can be derived from the equation for the surface element with the assumption that the correlations on the right hand side exist, and the result is

$$\langle\rho\rangle\left(\frac{\partial \tilde{\Sigma}_f}{\partial t} + \tilde{v}_\alpha \frac{\partial \tilde{\Sigma}_f}{\partial x_\alpha}\right) = -\frac{\partial}{\partial x_\alpha}(\langle\rho\rangle \widetilde{v''_\alpha \Sigma''_f}) - \langle\rho\rangle n_\alpha n_\beta \widetilde{s_{\alpha\beta}\Sigma''_f}, \tag{58}$$

where $\underline{n}$ is the normal vector of the surface and $s_{\alpha\beta}$ denotes the strain rate. The source term poses an intricate closure problem as turbulence can change the flame surface area by straining, extinction, and mutual annihilation (Darabiha *et al.*, 1989). The proposed closure model for the mean reaction rate is then given by

$$\tilde{w}_i = v_{Di} \tilde{\Sigma}_f, \tag{59}$$

where v_{Di} is the volume consumption rate of species i per unit flame area and it is obtained from calculations for a laminar flame. Several refinements of Eqn. (59) can be made by including the dependence of v_{Di} on the strain rate and temperature, but they will not be addressed here.

3.4 Theory of Embedded Surfaces

It becomes clear from the previous sections that a certain class of surfaces embedded in turbulent flow fields plays a fundamental role in determining the progress of chemical reactions. Experimental data obtained from mixing layers and jets indicates that the topology of surfaces embedded in turbulent flows can be rather complicated (Dahm and Dimotakis, 1985; Dimotakis, 1989). A closer examination of the topology and geometry of surfaces is therefore warranted. Surfaces can be defined implicitly by

$$\Psi(\underline{x},t) - \Psi_o = 0,$$

where $\Psi(\underline{x},t)$ is a variable relevant to combustion. For nonpremixed combustion, Ψ can be the mixture fraction and Ψ_o its stoichiometric value. For premixed combustion Ψ can be the reaction progress variable and Ψ_o being its value at the maximum reaction rate. The variable Ψ is governed by the transport equation (2) which includes effects of convection, diffusion and production. Equation (2) leads to the following classification of iso-surfaces:

(A) If the flux J_α^i and the source Q_i are zero, then the surface is materially invariant. If the velocity $v_\alpha(\underline{x},t)$ is sufficiently smooth (at least once differentiable), then the topology of the surface is preserved in time, because the solution of Eqn. (2) provides a diffeomorphism of the surface. However, the geometrical properties (curvature, torsion etc.) of the surface can change drastically.

(B) If the flux J_α^i is nonzero but the source Q_i is zero, then the surface is not materially invariant but moves through the fluid with a speed determined by the local diffusive flux. The Fick's law Eqn. (3) for the diffusive flux implies that J_α^i is normal to the surface. It is possible that the topology of surfaces can be changed due to diffusive reconnection (Ashurst and Meiron, 1987).

(C) If both J_α^i and Q_i are nonzero, then in addition to the relative motion through the fluids, the surface can change its area due to the source term Q_i. Both topological and geometrical changes are possible.

(D) The surface moves with an arbitrarily defined velocity relative to the fluid. This is the most general case, in which both self-intersection and loss of orientability of the surface are possible. Furthermore, only the progression velocity on the surface needs to be defined.

Relative Progression Velocity of Iso-surfaces

The relative progression velocity at which the iso-surface moves relative to the fluid in case (C) can be expressed in terms of the diffusive flux and the source strength. To this end, we introduce the indicator function $I(\underline{x},t)$

$$I(\underline{x},t) = \begin{cases} 1 & \text{for } \Psi(\underline{x},t) \geq \Psi_o \\ 0 & \text{otherwise,} \end{cases} \tag{60}$$

and define the relative progression velocity $V(\underline{x},t)$ as

$$V n_\alpha \equiv v_\alpha - v_\alpha^s, \tag{61}$$

where v_α denotes the fluid velocity, v_α^s is the velocity of the iso-surface, and n_α is the normal vector of the iso-surface defined by

$$n_\alpha \equiv \frac{\nabla\Psi}{|\nabla\Psi|}, \qquad |\nabla\Psi| \neq 0. \tag{62}$$

It can be shown (Byggstoyl and Kollmann, 1986) that

$$\frac{\partial I}{\partial t} = -v_\alpha^s n_\alpha |\nabla\Psi| \delta(\Psi - \Psi_o) \tag{63}$$

and

$$\frac{\partial I}{\partial x_\alpha} = n_\alpha |\nabla\Psi| \delta(\Psi - \Psi_o). \tag{64}$$

Combining Eqns. (63) and (64) one obtains

$$\frac{\partial I}{\partial t} + v_\alpha^s \frac{\partial I}{\partial x_\alpha} = 0, \tag{65}$$

and

$$\frac{DI}{Dt} = V|\nabla\Psi|\delta(\Psi - \Psi_o). \tag{66}$$

From Eqn. (60), we can also express DI/Dt as

$$\frac{DI}{Dt} = \delta(\Psi - \Psi_o)\frac{D\Psi}{Dt}. \tag{67}$$

Eliminating DI/Dt from Eqn. (66) with Eqn. (67), we get an expression for V as

$$V = \frac{1}{|\nabla\Psi|}(-\frac{\partial J_\alpha^i}{\partial x_\alpha} + Q_i) \ , \quad \Psi(\underline{x}, t) = \Psi_o \tag{68}$$

with $|\nabla\Psi| \neq 0$. Equation (68) shows that the relative progression velocity depends essentially on the gradient of $\Psi(\underline{x}, t)$ at the location of the iso-surface. The treatment for case (D) is different because the relative progression velocity is given and an expression for v_α^s or its mean value is derived. This problem has been studied by Kerstein *et al.* (1988) for the special case with a constant V in homogeneous turbulence.

Topology of Embedded Surfaces

Properties of surfaces that do not change under continuous one-to-one mapping are topologically invariant (i.e., a homeomorphism). We note first that the iso-surfaces that are interested in turbulent combustion are 'closed', i.e., they do not have boundaries (holes) as a consequence of the smooth (differentiable) variation of the defining scalars. Now let's consider the homeomorphisms defined only on the surfaces. The relevant topological properties are (Seifert and Threlfall, 1934; Rushing, 1973):

(1) Connectedness: The number of closed, connected surface components that form the complete surface.
(2) Orientability: An orientable surface possesses at each point a unique normal vector or a unique orientation (sense of rotation). Closed, non-orientable surfaces which are embedded in a three-dimensional Euclidean space must intersect themselves.
(3) Genus: The number of closed cuts that can be made without disintegrating the surface into disconnected parts. For instance, a sphere has a genus value of zero and a torus has a genus value of one.

Surfaces can be shown to be homeomorphic to spheres with attached handles (tori) and crosscaps (Moebius bands attached to circular holes in the sphere). Furthermore, surfaces can be triangularized and then analyzed by calculating the Euler characteristic function

$$\chi \equiv V - E + F, \tag{69}$$

where V denotes the number of vertices, E is the number of edges and F is the number of triangles. χ is a topological invariant (hence the same for the original and the triangularized surface) and changes with the number of handles and crosscaps. It can be shown that two surfaces, either orientable or non-orientable, are homeomorphic if they have the same characteristic function (Seifert and Threlfall, 1934).

Surfaces embedded in a topological space, such as in a three dimensional Euclidean space, can also be classified according to their structures. This leads to the consideration of homeomorphisms defined for the embedding space and for the surface. Surfaces with the same orientability and characteristic can be further classified according to the types of knots, links and braids present (Moran, 1983). Links and braids may be of particular importance in turbulent shear flows with and without combustion. Flow visualizations in plane mixing layers show that braided vortical structures are the linking mechanisms between the large-scale structures and the lateral vortices. Furthermore, in these braided vortical structures, there are tube-like domains, where viscous interaction occurs. Therefore, topological change can take place if these braided structures are brought together sufficiently close by the convection process.

Gibson (1968) pointed out the importance of extremal sets of scalars in turbulent flows and showed that they appear as isolated points (local extrema and saddle points) and lines (saddle lines). Consequently, Kerstein (1982) used this result to construct a model for an iso-surface as the boundary of the Voronoi tesselation created by the extremal points. The Voronoi tesselation is essentially a simplicial complex and, therefore, it is amenable to the methods of algebraic topology. Here, a fascinating problem arises which warrants future investigation: the relation of interface topology to the distribution of extremal points in turbulent flows. Closely related to the geometric topology of interfaces is the measure and dimension of such surfaces. Fractal concepts have been proposed (Gouldin, 1988; Srinivasan *et al.*, 1989) to explain the variation of surface area with scales, but the question is far from settled (Miller and Dimotakis, 1989).

4.0 The Influence of Chemical Reactions on Turbulence

The dynamics of turbulence can be affected by chemical reactions if the heat release due to chemical reactions is large enough to cause noticeable density changes. This implies that significant density fluctuations can be expected for strongly exothermic gas-phase reactions. The turbulent velocity field can be modified by the chemical reactions via two processes. First, density fluctuations can modify the acceleration of fluid particles; that is, the light-weight fluid particles are accelerated faster than the heavy-weight fluid particles even under the same pressure gradient and the viscous stresses. Second, the pressure field can be modified via the state relation, which links pressure, density and temperature together. These two processes are difficult to model and they will not be considered here (Pope, 1985; Borghi, 1988; Williams, 1989; Bray *et al.*, 1989).

5.0 Pdf Modeling of Nonpremixed Methane Jet Flames

The interactions of turbulence with finite rate chemistry will be examined here, particularly, in turbulent nonpremixed methane jet flames. As our current computer capabilities do not permit a detailed chemical scheme to be incorporated in turbulent combustion models, simplified reaction mechanisms are needed. Peters and Kee (1987) developed a simplified mechanism for methane-air combustion based on the assumptions of a steady state for certain intermediate components and the partial equilibrium for two reaction steps. The simplified mechanism contains the following four global steps

$$CH_4 + 2H + H_2O \rightleftharpoons CO + 4H_2, \qquad (I)$$

$$CO + H_2O \rightleftharpoons CO_2 + H_2, \qquad (II)$$

$$2H + M \rightleftharpoons H_2 + M, \qquad (III)$$

$$O_2 + 3H_2 \rightleftharpoons 2H + 2H_2O \qquad (IV)$$

With the assumption of equal diffusivity, this mechanism requires five scalar variables $\Psi_j(\underline{x}, t)$ to determine the local thermodynamic state. They are chosen as follows: $\Psi_1 \equiv \xi$ (mixture fraction), $\Psi_2 \equiv n_{CH4}$, $\Psi_3 \equiv n_{CO}$, $\Psi_4 \equiv n$, $\Psi_5 \equiv n_H$, where n denotes the number of moles per unit mass. To explore the pdf methods, we use a combined scheme which consists of a Reynolds stress closure (details are in Dibble *et al.*, 1986) and the joint scalar pdf model for Eqn. (30). The Reynolds stress closure provides the mean transport properties and the time scale that are needed in the pdf model. In return, the pdf yields the mean density. The turbulent flux in Eqn. (30) is modeled by a gradient type formula

$$-\langle\rho\rangle\langle v''_\alpha|\Psi_j = \varphi_j\rangle\tilde{f}_1 \cong c_s\langle\rho\rangle\frac{\tilde{k}}{\tilde{\epsilon}}\widetilde{v''_\alpha v''_\beta}\frac{\partial\tilde{f}_1}{\partial x_\beta}. \qquad (70)$$

We incorporated the nonlinear interaction model to model the effects of molecular mixing as discussed in Section 3.2 for Eqn. (46). The effects of chemical reactions on the pdf are modeled by by moving the pdf position in the scalar space according to the chemical reaction rates of (I) to (IV) (detailed expressions can be found in Peters and Kee, 1987).

The boundaries of the set of realizable states in the scalar space are rather intricate but can be defined mathematically (Chen *et al.*, 1989). A detailed comparison of the first and second order moments with the experiments of Masri *et al.* (1988) can be found in Chen *et al.* (1989). The numerical solutions enable us to evaluate the mixedness parameters defined in equation (43) and to compare the mean reaction rates with their corresponding quasi-laminar rates.

The mixedness parameter α_{ij} is plotted at $x/D = 20$ for several combinations of reactants as shown in Fig. 1 to Fig. 3. We note first that the α_{ij} are not positive definite for multi-component (more than two) mixtures in contrast to those in a binary mixture. It follows from the definition of α_{ij} that negative values indicate that both components exceed the local mean, whereas positive values indicate that one of the components exceeds the local mean and the other component is below the the mean. Positive mixedness values indicate, therefore, the lack of mixing and negative values correspond to the state of good mixing.

Fig. 1 reveals the degree of mixing between CH_4 and several other components. It is clear from this figure that CH_4 is not well mixed with the intermediate components and the product H_2O in the inner parts of the flame, but they become mixed in the outer parts of the flame. Therefore, reaction (I) proceeds in the forward direction if CH_4 is well mixed with H and H_2O and in the backward direction if CH_4 is well mixed with CO and H_2. However, the forward rate is larger than the backward rate over the cross section (see Fig. 4). The mixedness of CO with the components involved in step II is shown in Fig. 2. It is clear that mixing is good for all three components in the outer parts of the flame.

The mixedness of O_2 with the active components involved in step IV is positive throughout the jet indicating the lack of mixing. The comparison of the mean reaction rates with the quasi-laminar rates for the four steps I to IV is presented in Fig. 4 to Fig. 7 showing clearly the strong influence of turbulence. In particular, the second step in Fig. 5 and the third step in Fig. 6 illustrate that turbulence can greatly enhance the average rates. On the other hand, turbulence can also reduce the average rate compared to the quasi-laminar rate as evident in Fig. 7.

6.0 Conclusions

The interaction of turbulence and chemical reactions is a complex phenomenon that can cause significant modification in both the turbulence and the chemical reactions. For chemical reactions with negligible heat release, this interaction has only one direction; that is, turbulence will modify the chemical rates, but the reactions have no influence on the flow field. However, the purpose of combustion is to generate heat in a short period of time; therefore, combustion processes usually cause strong density variations. Hence, the turbulence will experience strong influence by the chemical processes and vise versa.

The influence of turbulence on the chemical reactions is the main topic in this paper. First, the basic governing equations of the dynamics in turbulent combustion are outlined in the Eulerian frame. The corresponding transformation to the Lagrangian frame has been presented with the aid of the Lagrangian position field. It was shown that in the Lagrangian frame, the transport equation for a thermo-chemical variable does not contain the nonlinearity due to convection, but the diffusive flux appears as a highly nonlinear process depending on the time histories of the Lagrangian strain rate.

The influence of turbulence on the chemical processes is expressed by the statistical moments that appear in the mean reaction rate. Upper and lower bounds for the mean reaction rate were obtained for a binary mixture. It was shown that the mean reaction rate can have values radically different from the quasi-laminar values (reaction rate at the mean properties). The influence of temperature fluctuations on the mean chemical reaction rate is shown to be significant for reactions with large activation energies at a low mean temperature. Furthermore, it was shown that the pdf equation for a single reactive scalar can be solved for a homogeneous turbulence. The solution indicates that for bounded scalar variables, a scalar and its dissipation rate must be correlated in order to satisify the realizability conditions.

The analysis of nonpremixed flames illustrated the important role of mixing in determining the progress of chemical reactions. Mixedness parameters were introduced and the mixing models for the single point pdf methods were discussed. The main conclusions drawn from the studies of nonpremixed reacting systems are that the mixing models must satisfy realizability conditions and that they must represent the effect of turbulent mixing correctly at least for lower order moments. Furthermore, the current model for the turbulent time scale associated with the mixing process is rather crude as it neglects the possible modification due to heat release. Several approaches for overcoming these shortcomings are indicated.

The treatment of premixed systems was restricted to the flame sheet regime. In this regime, the effect of turbulence is essentially through the distortion of the thin flame sheet leading to increased flame surface area. Predictive models for premixed turbulent flames are discussed.

The interaction of turbulence and chemical reactions in nonpremixed and premixed combustion can also be described in terms of the effects of turbulence on surfaces, in particular, the flame surfaces. Hence, the basic dynamical and topological properties of surfaces were introduced. It was shown that for flame surfaces, both the diffusive flux and the chemical sources can alter the relative progression velocity of such surfaces. Finally, the topological classification of embedded surfaces was discussed briefly.

We used nonpremixed turbulent methane-air jet flames as an example to illustrate the

mixing properties predicted by a pdf method. It was shown that the mean reaction rates can be larger or smaller than the quasi-laminar rates by orders of magnitude due to the effect of turbulence. From the computation results, the predicted mixedness parameters were examined showing that they are not positive-definite as in binary systems.

References.

Akhiezer, N. I. (1965), *The classical moment problem*, Oliver and Boyd, Edinburgh and London.

Ashurst, W. T. and Meiron, D. (1987), *Numerical Study of Vortex Reconnection*, Phys. Rev. Lett. 58, 1632

Bilger, R. W. (1976), *Turbulent Jet Diffusion Flames*, Progr. Energy Comb. Sci. 1, 87

Borghi, R. (1988), *Turbulent Combustion Modelling*, Progr. Energy Comb. Sci., 14, 245.

Bray, K. N. C., Libby, P. A. and Moss, J. B. (1985), *Unified Modeling Approach for Premixed Turbulent Combustion*, Comb. Flame, 61, 87

Bray, K. N. C., Champion, M. and Libby, P. A. (1989), *The Interaction between Turbulence and Chemistry in Premixed Turbulent Flames*, Lecture Notes in Engin., vol.40, Springer V.,541

Byggstoyl, S. and Kollmann, W. (1986), *Stress transport in the rotational and irrotational zones of turbulent shear flows*, Phys. Fluids 29,1432

Chen, J.-Y. and Kollmann, W. (1990), *Chemical Models for Pdf Modeling of Hydrogen-air Nonpremixed Turbulent Flames*, Comb. Flame, **79**, 75.

Chen, J.-Y. and Kollmann, W. (1989a), *Pdf Modeling of Chemical Non- equilibrium Effects in Turbulent Nonpremixed Hydro-carbon Flames*, 22nd Symp. (Int.) Comb., The Combustion Institute, 645.

Chen, J.-Y., Kollmann, W. and Dibble, R. W. (1989), *Pdf Modeling of Turbulent Nonpremixed Methane Jet Flames*, Comb. Sci. Technol. 64, 315.

Curl, R. L. (1963), *Dispersed Phase Mixing: I. Theory and Effects in Simple Reactors*, A.I.Ch.E. J. **9**, 175.

Dahm, W. J. A. and Dimotakis, P. E. (1985), *Measurements of Entrainment and Mixing in Turbulent Jets*, AIAA-85-0056.

Darabiha, N., Giovangigli, V., Trouve, A., Candel, S. and Esposito, E. (1989), *Coherent flame description of turbulent premixed ducted flames*, Lecture Notes in Engineering, vol.40, Springer V., 591.

Dibble, R. W., Kollmann, W., Farshchi, M. and Schefer, R. W. (1986), *Second Order Closure for Turbulent Nonpremixed Flames: Scalar Dissipation and Heat Release Effects*, 21st Symp. (Int.) Comb., The Comb. Inst., 1329.

Dimotakis, P. E. (1989), *Turbulent Free Shear Layer Mixing*, AIAA-89-0262.

Dopazo, C. (1979), *Relaxation of initial Probability Density Functions in the Turbulent Convection of Scalar Fields*, Physics Fluids bf 22, 20.

Gibson, C. H. (1968), *Fine structure of scalar fields mixed by turbulence, I. Zero gradient points and minimal gradient surfaces*, Phys. Fluids **11**, 2305.

Gouldin, F. C. (1988), *Interpretation of jet mixing using fractals*, AIAA J. **26**, 1405.

Hermanson, J. C., Mungal, M. G. and Dimotakis, P. E. (1985), *Heat Release Effects on Shear Layer Growth and Entrainment*, AIAA-85-0142.

Ievlev, V. M. (1973), *Equations for the Finite-dimensional Probability Distributions of Pulsating Variables in a Turbulent Flow*, Sov. Phys. Dokl. **18**, 117.

Janicka, J., Kolbe, W. and Kollmann, W. (1979), *Closure of the Transport Equation for the Probability Density Function of Scalar Fields*, J. Non-equil. Thermodyn. **4**, 27.

Jones, W. P. and Kollmann, W. (1987), *Multi-scalar Pdf Transport Equations for Turbulent Diffusion Flames*, in Turbulent Shear Flows vol. 5 (Durst, F et al., ed.s), Springer Verlag, 296.

Kerstein, A. R. (1982), *Percolation of scalar iso-surfaces in turbulent flow, with application to flame blow-off*, Unpublished Sandia-report.

Kerstein, A. R., Ashurst, W. T. and Williams, F. A. (1988), *Field equation for interface propagation in an unsteady homogeneous flow field*, Phys. Rev. A **37**, 2728.

Kollmann, W. (1989), *Pdf-transport Equations for Chemically Reacting Flows*, Proc. US -France Workshop on Turb. React. Flows, Rouen,vol.2, 20-1

Kollmann, W. and Wu, A. (1987), *Scalar-velocity Pdf Equations for Turbulent Shear flows*, AIAA-87-1348.

Lumley, J. L. (1978), *Computational Modeling of Turbulent Flows*, Adv. Appl. Mech. **18**, 123.

Marble, F. E. and Broadwell, J. E. (1977), *The coherent flame model for turbulent chemical reactions*, Project Squid Tech. Rep. TRW-9-PU, Purdue Univ., Indiana.

Masri, A. M., Bilger, R. W. and Dibble, R. W. (1988), *Turbulent Non- premixed Flames of Methane near Exstinction: Mean Structure from Raman Measurements*, Comb. Flame **71**, 245.

Meyers, R. E. and O'Brien, E. E. (1981), *The Joint Pdf of a Scalar and its Gradient at a Point in a Turbulent Fluid*, Comb. Sci. Technol. **26**, 123.

Miller, P. L. and Dimotakis, P. E. (1989), *Stochastic geometric properties of scalar interfaces*, ASME Fluids Engin. Conf., La Jolla.

Monin, A. S. (1962), *Lagrangean Hydrodynamic Equations for Incompressible Viscous Fluids*, Prikl. Mat. Mekh. **26**, 320.

Moran, S. (1983), *The Mathematical Theory of Knots and Braids*, North Holland, Amsterdam.

Peters, N. (1986), *Laminar flamelet concepts in turbulent combustion*, 21st Symp. (Int.) Comb., Munich.

Peters, N. and Kee, R. J. (1987), *The Computation of Stretched Diffusion Flames using a Reduced Four-Step Mechanism*, Comb. Flame **68**, 17.

Pope, S.B. (1982), *An Improved Turbulent Mixing Model*, Comb. Sci. Technol. **28**, 131.

Pope, S.B. (1985), *Pdf Methods for Turbulent Reacting Flows*, Progr. Energy Comb. Sci. **11**, 119.

Pope, S.B. (1987), *Turbulent Premixed Flames*, Ann. Rev. Fluid Mech.,vol.19, (J.L. Lumley et al. ed.s), 237.

Pope, S.B. (1989), *The stochastic velocity-dissipation model applied to turbulent shear flows*, Proc. Seventh Symp. Turbulent Shear Flows, Stanford Univ.

Rushing, B. (1973), *Topological Embeddings.*, Academic Press.

Seifert, H. and Threlfall, W. (1934), *Lehrbuch der Topologie*, Chelsea, New York.

Srinivasan, K. R., Ramshankar, R. and Meneveau, C. (1989), *Mixing, entrainment and fractal dimension of surfaces in turbulent flow*, Proc. Roy. Soc. London A, **421**, 79.

Truesdell, C. A. (1954), *The Kinematics of Vorticity*, Indiana Univ. Publ. Science, ser. no. **19**.

Williams, F. A. (1985), *Combustion Theory*, 2nd edition, Benjamin-Cummings, Menlo Park. CA.

Williams, F. A. (1989), *Structure of flamelets in turbulent reacting flow and influence of combustion on turbulence fields*, Lecture Notes in Engineering, vol.40, Springer V., 195.

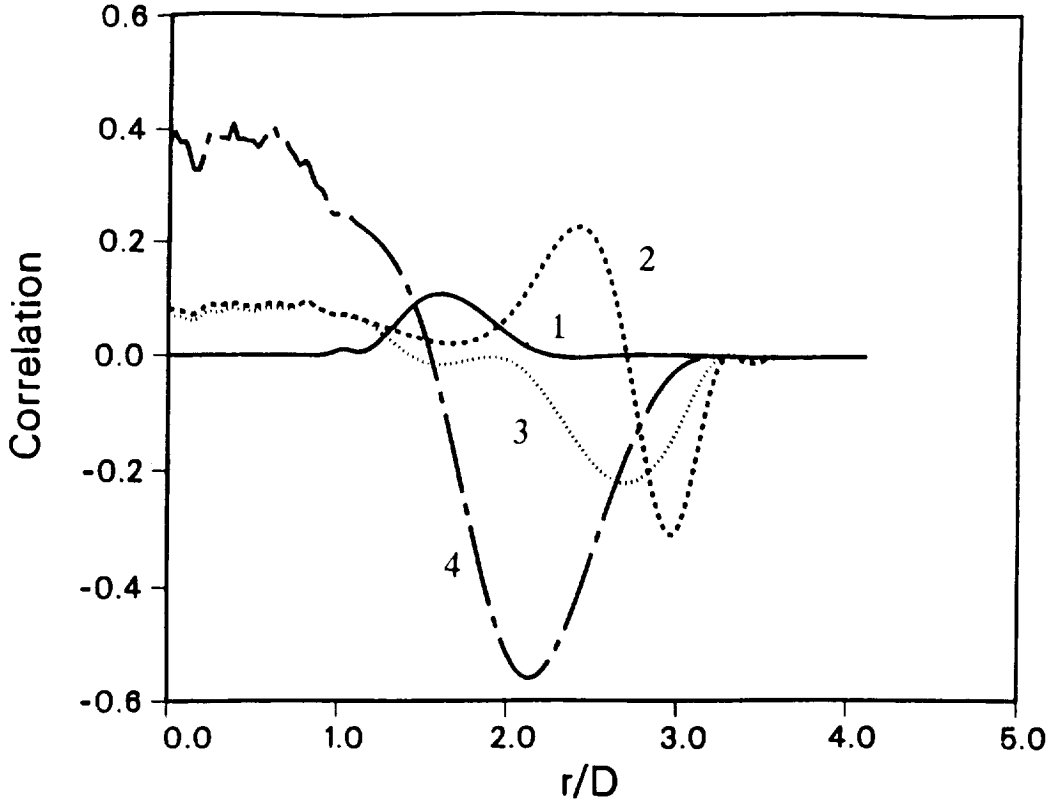

Fig. 1. Mixedness parameter α_{ij} in a turbulent methane-air nonpremixed flame at $x/D = 20$ using the four step mechanism of Peters and Kee (1987) for:

$1 = CH_4$ and H. $3 = CH_4$ and CO.

$2 = CH_4$ and H_2O. $4 = CH_4$ and H_2.

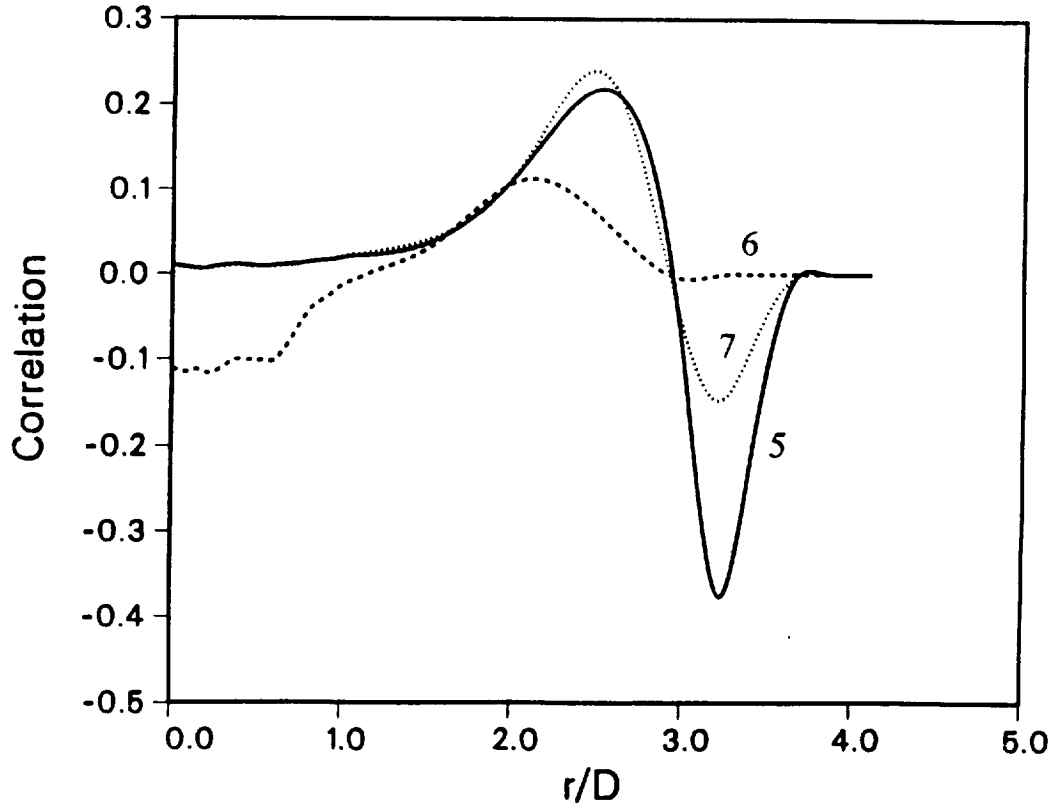

Fig. 2. Mixedness parameter α_{ij} in a turbulent methane-air nonpremixed flame at $x/D = 20$ using the four step mechanism of Peters and Kee (1987) for:

$5 = CO$ and H_2O. $6 = CO$ and H_2. $7 = CO$ and CO_2.

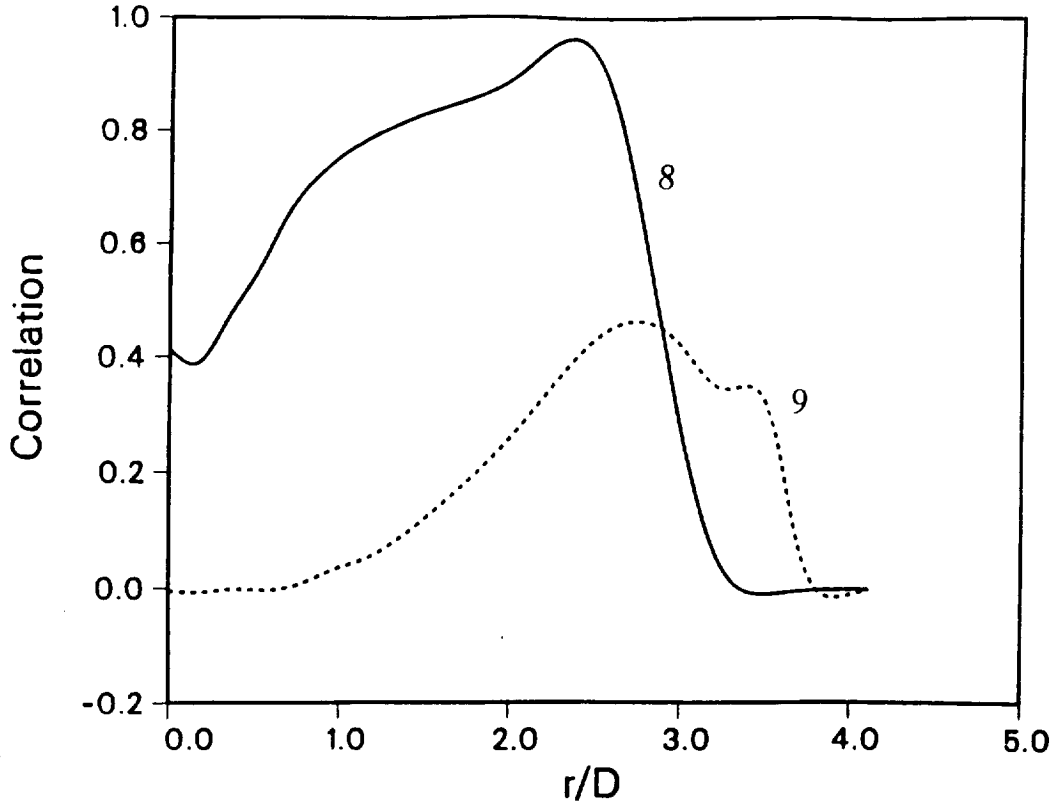

Fig. 3. Mixedness parameter α_{ij} in a turbulent methane-air nonpremixed flame at $x/D = 20$ using the four step mechanism of Peters and Kee (1987) for:

8 = O_2 and H_2. 9 = O_2 and H_2O.

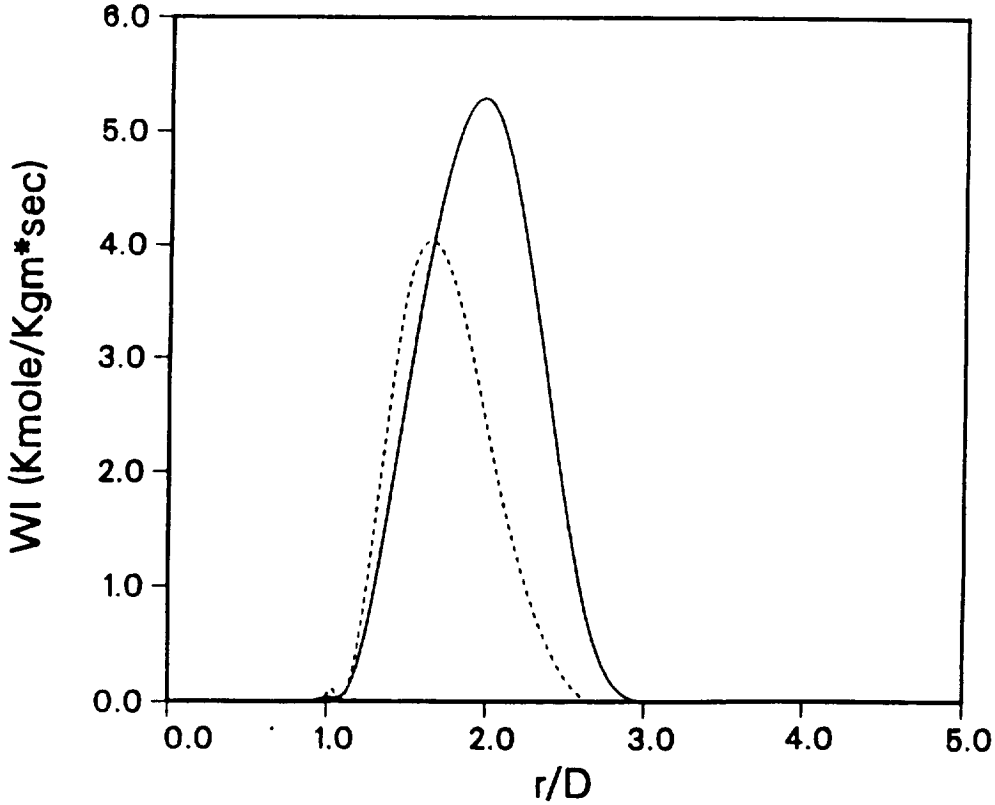

Fig. 4. Mean kinetic source (full line) and quasi-laminar source (broken line) in a turbulent methane-air nonpremixed flame at $x/D = 20$ for reaction I of the four step mechanism of Peters and Kee (1987).

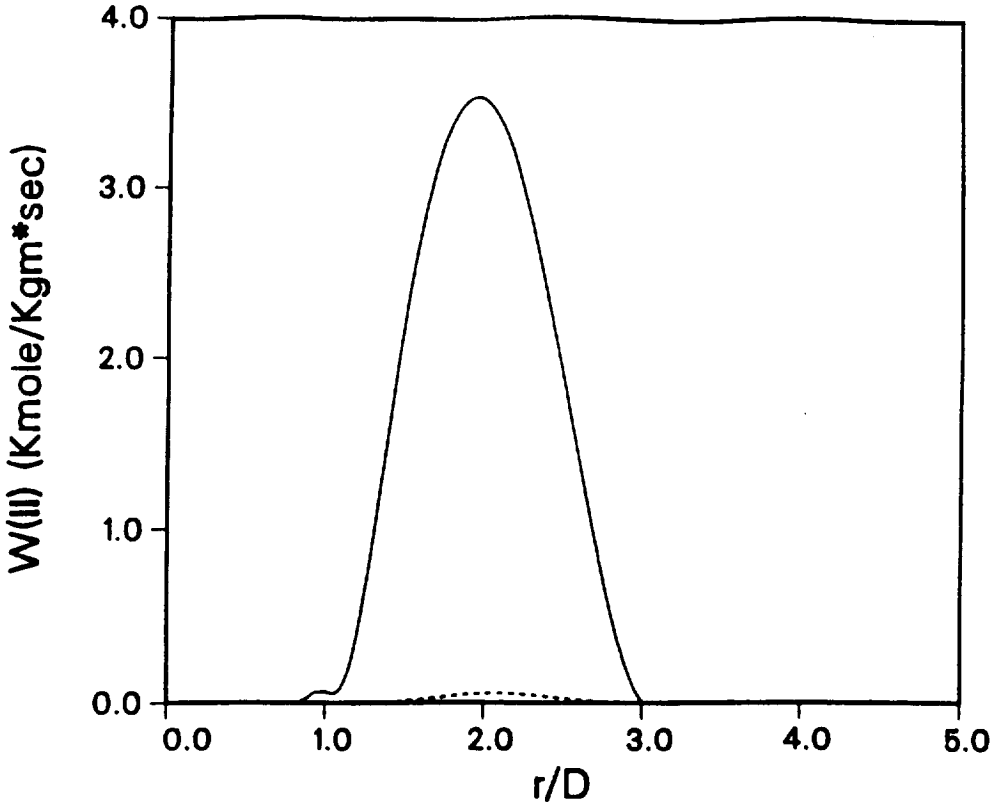

Fig. 5. Mean kinetic source (full line) and quasi-laminar source (broken line) in a turbulent methane-air nonpremixed flame at $x/D = 20$ for reaction II of the four step mechanism of Peters and Kee (1987).

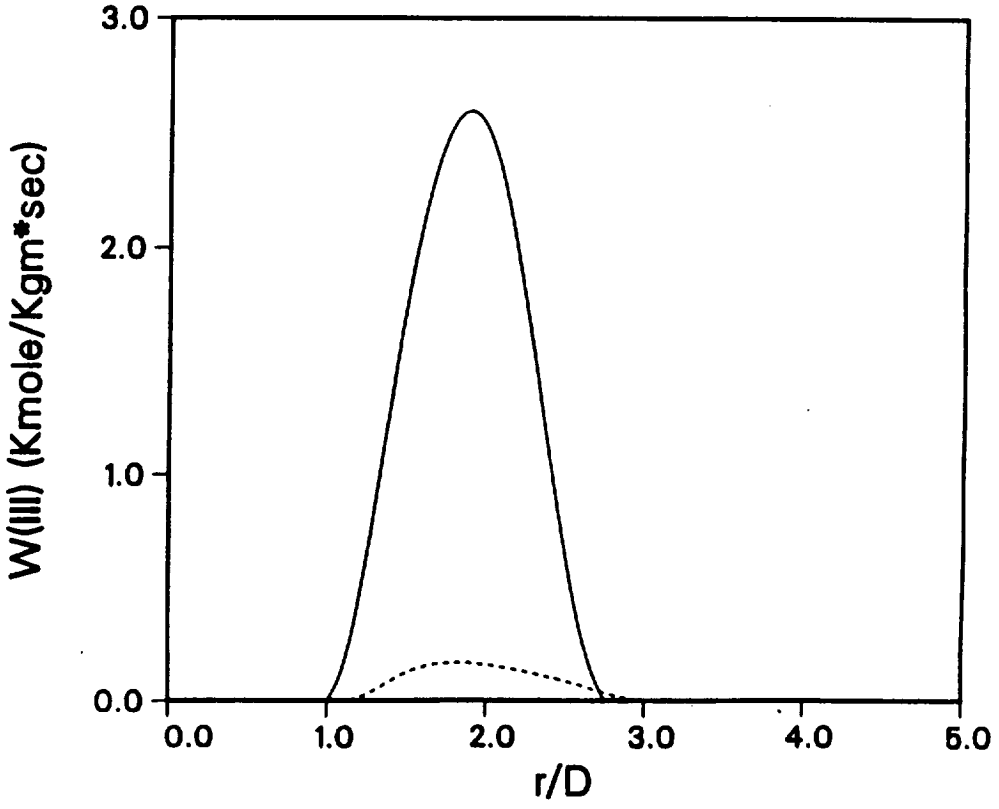

Fig. 6. Mean kinetic source (full line) and quasi-laminar source (broken line) in a turbulent methane-air nonpremixed flame at $x/D = 20$ for reaction III of the four step mechanism of Peters and Kee (1987).

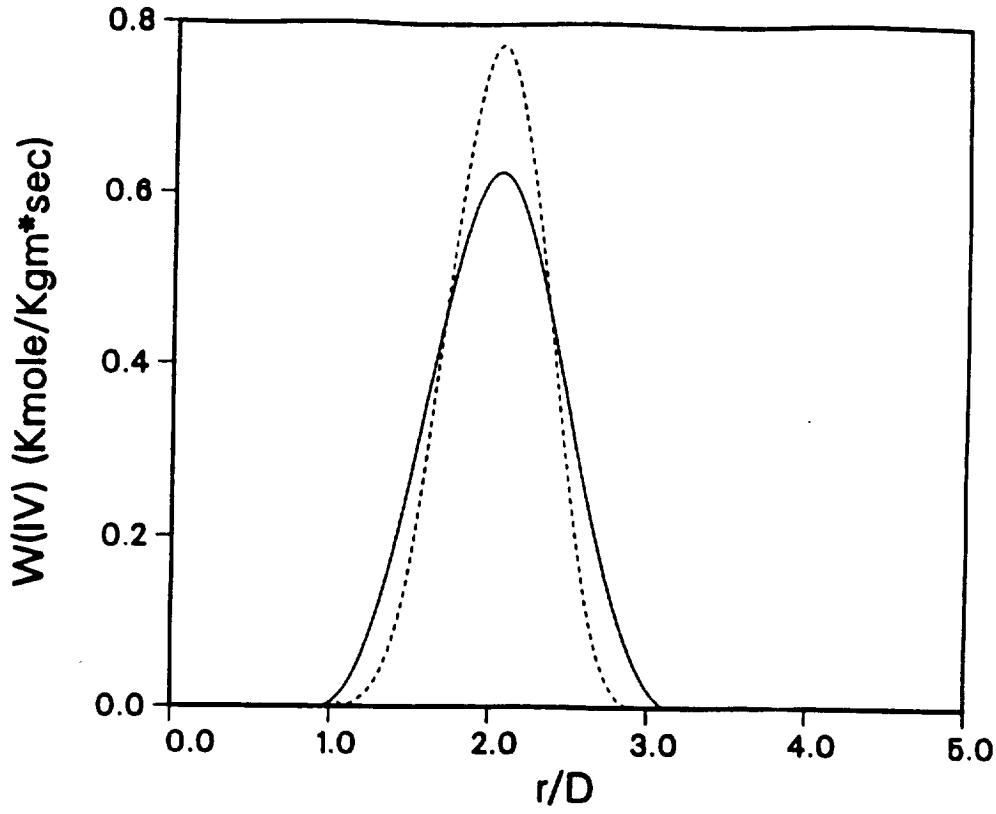

Fig. 7. Mean kinetic source (full line) and quasi-laminar source (broken line) in a turbulent methane-air nonpremixed flame at $x/D = 20$ for reaction IV of the four step mechanism of Peters and Kee (1987).

Appendix III.

Mapping methods for pdf equations.

W. Kollmann[1], MAME Dept., University of California Davis, CA.95616, USA.

Contents:

1.0 Introduction.
- 1.1 The basic laws as mapping equations.

2.0 Basic considerations.
- 2.1 Function spaces.
- 2.2 Local and global mappings.
- 2.3 A reduction property for multi-dimensional mappings.

3.0 Transport equations for pdfs and cdfs.

4.0 Mapping method for the one-dimensional case.
- 4.1 The Chen-Kraichnan method.
- 4.2 Mapping method for the characteristic function.

5.0 Mapping methods for multi-dimensional pdfs.
- 5.1 The fundamental mapping equations.
- 5.2 Mapping method in the spatial frame.
- 5.3 Mapping method in the material frame.
- 5.4 Mapping method for two-point pdfs.

6.0 Conclusions.

[1] Research supported by NASA-Lewis Grant NAG 3-836, R. Claus project monitor.

1.0 Introduction.

Kraichnan's idea to apply mappings as tool in constructing closures for pdf equations (Chen et al. 1989, Kraichnan 1990, Feng 1991, Pope 1991, Valiño et al. 1991) proved very successful for the case of a single scalar variable in homogeneous turbulence. It is not yet clear how powerful this approach is for the case of more than one variable (Pope, 1991). The rigorous theory on the functional level requires the determination of the probability measure governing the dynamics of turbulent flows. This measure is defined in a function space, that contains the set of all realizable flow fields. It can be constructed as a measure relative to a Gaussian measure or any other reference measure. It follows that the probability measure can be regarded as the image of a Gaussian measure. The underlying mapping contains, therefore, the essential information on turbulence. It is apparent that turbulence can be viewed as the mapping of appropriately defined function spaces. The structure of those function spaces and the mapping relating them deserve closer scrutiny.

The notion of a mapping can be exploited in two distinct ways:

I. The mapping is known and both the original and the image variables are the unknowns. The prime example for this case is the linear map provided by Fourier transform which can be extended to functionals. The resulting equation for the case of the probability functional is the Hopf/Kolmogorov equation for the characteristic functional.

II. The mapping is unknown and either the original or the image variable is known. The prime example for this case is Kraichnan's method which is based on the well known relation between mapped and original pdf depending on a single variable

$$f(\varphi) = \frac{f_G(\eta)}{|\frac{dX}{d\eta}|}$$

where $\varphi = X(\eta, t)$ and $f_G(\eta)$ is the Gaussian pdf. The extension of this method to the multi-dimensional case and to functionals is not obvious. The task of constructing a mapping between function spaces can be daunting and it is instructive to consider several examples to illustrate the properties of mappings. Fourier transformation, regarded as solution of the so far unspecified mapping equation, provides an example for the mapping of the space L^2 of square integrable functions defined in R^3 onto itself

$$\Psi(\underline{z}) = \frac{1}{(2\pi)^3} \int_{R^3} d\underline{x} \exp(i\underline{x}.\underline{z}) \Phi(\underline{x})$$

where $\underline{x}, \underline{z} \in R^3$ and $\Phi(\underline{x}), \Psi(\underline{z}) \in L^2(R^3)$. The image field $\Psi(\underline{z})$ is a complex valued square integrable function defined on R^3. The value of the image field Ψ at a location $\underline{z} \in R^3$ depends on the values of the argument field Φ at all locations $\underline{x} \in R^3$. Hence has the mapping induced by Fourier transformation functional (or nonlocal) character. Mappings of this type are denoted by

$$\Psi(\underline{z}, t) = X[\Phi(.); \underline{z}, t]$$

where the semi-colon separates functional arguments from parameters. A different example is provided by

$$\Psi(\underline{z}) = \exp(\Phi(\underline{z}))$$

which has local character. Locations in argument and image fields are the same and a change of the argument field $\Phi(\underline{z}')$ at a location $\underline{z}' \neq \underline{z}$ has no influence on the value of the image field at $\underline{z}$. Local mappings are denoted by

$$\Psi(\underline{z}, t) = \mathcal{X}(\Phi(\underline{Y}(\underline{z}, t)), \underline{z}, t)$$

where

$$\underline{Y} : R^3 \rightarrow R^3$$

is a mapping of R^3 onto itself. It is clear that the computational effort for functional and local mapping can be expected to be widely different. The comparison of a functional mapping with the probability functional indicates that the image domain for the mapping is a function space whereas the image domain for the probability functional is the unit interval. This indicates that the computational effort for the calculation of the mapping may be equal or larger than the effort for the probability functional. However, it should be noted that the Gaussian characteristic functional can be set up explicitely and the notion of the determinant can be extended to the case of countable infinite many variables (see Muldowney, 1987 and Skorohod, 1974), thus offering an avenue for theoretical investigations.

Three aspects of turbulence involving mappings will be discussed in detail before the mapping equation is investigated. First, the basic laws (mass and momentum balances) are set up as equations determining a mapping of the flow domain at a reference time onto the domain at a later time. This mapping is a diffeomorphism as long as the smoothness of the solution of the Navier-Stokes equations is insured. In addition, incompressible flows generate a measure preserving diffeomorphism due to the particular form of mass balance. This mapping is, however, fundamentally different from the mapping employed by Chen et al. (1989) who map the phase space spanned by the solutions of the Navier-Stokes equations onto a reference space equipped with a Gaussian measure. Second, the properties of Gaussian measures are reviewed and finally transformations of the function space containing the solutions of the Navier-Stokes and Euler systems are discussed.

The mapping method suggested by Chen et al. (1989) is the reviewed for the one-dimensional case. It is shown that it corresponds to a convolution of the characteristic function and the mapping equation for it is derived. The multi- dimensional case is then considered in detail.

1.1 The basic laws as mapping equations.

The basic laws for a single incompressible fluid are introduced in the material (or Lagrangean) frame. The independent variables in the material frame are defined as time $0 \leq t \leq T$ and label $a \in A$, where A is the label space to be defined. The label identifies uniquely a material point in the flow field. There are many ways of defining a label and for each definition a different set of variables emerges. The present definition for the label space A is the position of all fluid material points at a reference time zero. The label space is now the fluid volume at the reference time zero

$$A \equiv \{\underline{X} : \textit{ Position of a material point at } t = 0\} \tag{1.1}$$

and the mapping $\underline{X} : A \rightarrow D(t)$ is assumed to have the following properties (Kreiss and Lorenz, 1989): $\underline{X}(\underline{a}, t)$ is for $\underline{a} \in A$ and a nonzero time interval a smooth (continuously differentiable) function satisfying

(i) $\underline{X}(\underline{a}, 0) = \underline{a}$

(ii) If $\underline{a} \neq \underline{b}$ then $\underline{X}(\underline{a}, t) \neq \underline{X}(\underline{b}, t)$ for $t \geq 0$.

(iii) The mapping $\underline{a} \rightarrow \underline{X}(\underline{a}, t)$ has a smooth inverse $\underline{X}^{-1}$.

The set of independent variables in the material (sometimes also called referential frame for the present chioce of the label space) frame consists therefore of time t and the position $\underline{a}$) at time zero. Note that the size of the time interval for which the mapping $\underline{X}$ remains smooth is related to the existence of smooth solutions of the Navier-Stokes equations. There is no general existence proof for three-dimensional flows except for finite time intervals, whose length depends on the inital data, and we must keep in mind that the smoothness may break down in finite time and the conditions (ii) and (iii) for the mapping of the label space onto the fluid volume at later time may be violated. The position $\underline{X}(t, \underline{a})$ of a material point is considered a dependent variable in the material frame.

The time rate of change keeping the label variable $\underline{a}$ constant is in the material frame the time rate of change measured by an observer moving with the material point. It follows that velocity is defined by

$$\underline{V}(t, \underline{a}) \equiv \frac{\partial \underline{X}}{\partial t} \tag{1.2}$$

and acceleration by

$$\underline{C}(t, \underline{a}) \equiv \frac{\partial \underline{V}}{\partial t} \tag{1.3}$$

Mass balance in classical mechanics is the requirement that mass cannot be created or destroyed and appears as $J = 1$ or

$$\epsilon_{\alpha\beta\gamma}\epsilon_{\delta\eta\omega}\frac{\partial X_\alpha}{\partial a_\delta}\frac{\partial X_\beta}{\partial a_\eta}\frac{\partial X_\gamma}{\partial a_\omega} = 6 \tag{1.4}$$

where J denotes the Jacobian of the mapping $\underline{X}(\underline{a}, t)$. Momentum balance is the consequence of Newton's second law and can be shown to govern the temporal evolution of the mapping

$\underline{X}(\underline{a},t)$ by

$$\frac{\partial^2 X_\alpha}{\partial t^2} = -\frac{1}{2R}\epsilon_{\alpha\beta\gamma}\epsilon_{\delta\eta\omega}\frac{\partial X_\beta}{\partial a_\eta}\frac{\partial X_\gamma}{\partial a_\omega}\frac{\partial P}{\partial a_\delta} + \frac{\nu}{2}\epsilon_{\theta\beta\gamma}\epsilon_{\delta\eta\omega}\frac{\partial X_\zeta}{\partial a_\eta}\frac{\partial X_\phi}{\partial a_\omega}\frac{\partial}{\partial a_\delta}\left(\frac{\partial X_\zeta}{\partial a_\beta}\frac{\partial X_\phi}{\partial a_\gamma}\frac{\partial^2 X_\alpha}{\partial a_\theta \partial t}\right) + G_\alpha \tag{1.5}$$

It follows that the material frame version of the Navier-Stokes system set up in terms of position and pressure fields can be regarded as the equations determining a measure-preserving mapping $\underline{X}(\underline{a},t) : \ D(0) \rightarrow \ D(t)$ (where $D(0)$ denotes a measurable subset of the flow domain at time zero) of the flow domain at the reference time onto the domain at a later time. This mapping is smooth as long as the solution remains smooth. The role of the pressure in this system is to preserve the measure of any measurable subset of the flow domain. This property is lost in compressible flows where the volume of a materially invariant subset of the flow field may change in time. The notion of mappings can be applied to compressible flows with suitable extension of the variables to include mass and energy densities.

The mapping equations (1.4) and (1.5) show that the dynamics of a nonlinear phenomenon can be viewed as the evolution of a mapping governed by a nonlinear system of equations. The solution of (1.4) and (1.5) allows to determine the image of any measurable subset of the original flow domain as a function of time.

2.0 Basic Considerations.

The notion of mappings can be extended to relations between function spaces and a general equation for such a mapping can be derived. It is worth noting that the mapping equation for a single variable governed by the linear diffusion equation and taken at a single point is linear (Chen et al., 1989 and Pope 1991) but not exact. It will be shown in chapter 4.0 that this is due to the requirement that the single point statistics of the image of the Gaussian random fields is equal to the single point statistics of the unknown turbulent fields. The extension of this closure procedure to multi-variables and multi- point pdfs and the passage to the functional level requires some preparations. This will be done in the present chapter. It is well known that the Lebesgue measure has no extension to infinitely many variables, hence there is no obvious extension of the cdf equation (derived in the next chapter) to the functional level since it contains multi-dimensional integrals whose limit for infinitely many variables is not defined. The pdf equation on the other hand can be (at least formally) extended to the functional level. It follows that the pdf equation and its Fourier transform (characteristic function) are the appropriate starting point for the development of mapping methods for the multi-dimensional case. Furthermore, it is possible to set up explicitely the Gaussian measure for infinitely many variables in terms of its characteristic functional and there exists a well defined equation for the characteristic functional of the turbulence measure. It is possible to define properly measures relative to a Gaussian measure (Skorohod, 1974). If the turbulence measure is defined in such a way, all that is left to determine is the distortion of the Gaussian measure necessary to produce the turbulence measure. This is nothing but a mapping of the function spaces containing the Gaussian fields and the turbulence fields. It is clear that these two function spaces justify attention.

2.1 Function spaces.

Consider a compact flow domain denoted by $D(t) \subset R^3$ with boundary $\partial D(t)$. The boundary is assumed to be orientable and sufficiently smooth such that a normal vector exists nearly everywhere. The surface area for the boundary ∂D must satisfy

$$0 < \int_{\partial D} dA < \infty$$

and the volume of the flow domain is obviously bounded. $D(t)$ is the domain of definition for the turbulence fields. The domain of definition for the Gaussian reference fields is $\hat{D} \equiv R^3$. Cartesian coordinate systems are introduced in both domains and denoted by $\underline{x} \in D(t)$ and $\underline{\hat{x}} \in \hat{D}$ respectively. Various functions of scalar, vector and tensor character will be defined on D and called turbulence fields. Functions defined on $\hat{D}$ will be called reference or argument fields. Various sets of fields will be considered and they will be embedded in various function spaces. The most important Banach and Hilbert spaces will be discussed briefly. A class of Banach spaces is given by

$$L^p(D) \equiv \{\Phi(\underline{x}) | \Phi : D \rightarrow R^1, \Phi \; measureable, \int_D d\underline{x} |\Phi(\underline{x})|^p < \infty\}$$

with norm

$$\|\Phi\|_{L^p(D)} \equiv \{\int_D d\underline{x} |\Phi(\underline{x})|^p\}^{\frac{1}{p}}$$

which is a Hilbert space for $p = 2$ with scalar product

$$(\Phi, \Psi) \equiv \int_D d\underline{x} \Phi(\underline{x}) \Psi(\underline{x})$$

A different class of function spaces can be constructed by requiring differentiability up to a certain order. These spaces are called Sobolev spaces and are defined by

$$W^{m,p}(D) \equiv \{\Phi(\underline{x}) | D^\alpha \Phi \in L^p, |\alpha| \leq m\}$$

where $D^i \equiv \partial / \partial x_i$ denotes the differential operator and

$$D^\alpha \equiv \frac{\partial^{|\alpha|}}{\partial x_1^{\alpha_1} \cdots \partial x_n^{\alpha_n}}$$

with $|\alpha| \equiv \sum_{i=1}^n \alpha_i$ and $\alpha_i \geq 0$. The norm is defined by

$$\|\Phi\|_{m,p,D} \equiv \sum_{|\alpha| \leq m} \|D^\alpha \Phi\|^2_{L^p(D)}$$

For $p = 2$ a Hilbert space is obtained with scalar product

$$(\Phi, \Psi)_{m,D} \equiv \sum_{|\alpha| \leq m} \int_D d\underline{x} D^\alpha \Phi D^\alpha \Psi$$

The general properties of these spaces can be found in the literature on functional analysis.

2.2 Local and global mappings.

The aim of this chapter is to discuss the properties of mappings of a separable Hilbert space $\hat{H} = \{\hat{\Phi}(\hat{\underline{x}}) | \hat{\Phi} : \hat{D} \rightarrow R^1, \hat{\Phi}\ continuous\}$ with scalar product $(\hat{\Phi}, \hat{\Psi})_H$ onto another separable Hilbert space H (separable means that the space has a countably infinite basis). The elements of $\hat{H}$ are the reference or argument fields and the elements of H are the image fields. The basic requirement for mapping methods is that the statistics of the image fields agree at least at one or several points with the turbulence fields. If they agree on all points of the flow domain an exact solution of the Hopf-Kolmogorov equation (see Vishik and Fursikov, 1988) is obtained. This aspect will be discussed in chapter 4.0. The space H containing the image fields is embedded in the Sobolev space $H^m(D)$. The mapping $X : \hat{H} \rightarrow H(D)$ will be time dependent because the image fields must be time dependent in order to simulate the properties of turbulent fields. The mapping is denoted by

$$\Phi(\underline{x}, t) = X[\hat{\Phi}(.); \underline{x}, t]$$

where the semicolon separates argument fields from parameters. The argument field $\hat{\Phi}(\hat{\underline{x}}) \in \hat{H}$, the values of the parameters $\underline{x} \in D(t)$ and $t \geq 0$ determine uniquely the image field $\Phi(\underline{x}, t) \in H(D)$ and the argument field, the location in the flow domain and time can be varied independently. Consider now a modified argument field $\hat{\Phi}(\hat{\underline{x}}) + \epsilon h_\delta(\hat{\underline{x}} - \hat{\underline{x}}_o)$ where $h_\delta \in \hat{H}$, $\epsilon > 0$ and

$$h_\delta(\hat{\underline{x}} - \hat{\underline{x}}_o) = \begin{cases} \geq 0 & \text{for } |\hat{\underline{x}} - \hat{\underline{x}}_o| \leq \delta > 0 \\ 0 & \text{otherwise} \end{cases}$$

and $h \in C^\infty(R^3)$ such that

$$\int_{R^3} d\hat{\underline{x}} h_\delta(\hat{\underline{x}} - \hat{\underline{x}}_o) = 1$$

holds. The image fields at the same location $\underline{x}$ and the same time t are denoted by $\Phi(\underline{x}, t) = X[\hat{\Phi}(.); \underline{x}, t]$ and $\Psi(\underline{x}, t) = X[\hat{\Phi}(.) + \epsilon h_\delta(.); \underline{x}, t]$. Two cases are now possible:

(A) $\Psi(\underline{x}, t) \neq \Phi(\underline{x}, t)$ for nearly all $\hat{\underline{x}} \in \hat{\Omega}$ and $\epsilon > 0$. The value of the image field at a given location $\underline{x} \in D(t)$ depends on the values of the argument field at nearly all locations $\hat{\underline{x}} \in \hat{\Omega}$. This implies that X depends on $\hat{\Phi}(.)$ in functional fashion.

(B) There exists a subset $\hat{\Omega}_o \subset \hat{\Omega}$ such that $\Psi(\underline{x}, t) = \Phi(\underline{x}, t)$ holds for $\hat{\underline{x}} \in \hat{\Omega}_o$ and $\mu_3(\hat{\Omega} - \hat{\Omega}_o) < C\delta^3$ with $C < \infty$ as $\delta \rightarrow 0$ for all $\underline{x} \in D(t)$. This implies the existence of a relation

$$\hat{\underline{x}} = \underline{Y}(\underline{x}, t)$$

such that the mapping X is local, i.e.

$$\Phi(\underline{x}, t) = X(\hat{\Phi}(\underline{Y}(\underline{x}, t)); \underline{x}, t), \quad \underline{x} \in D(t)$$

The special case of a local mapping

$$\Phi(\underline{x}, t) = X(\hat{\Phi}(\underline{Y}(\underline{x}, t)); t)$$

is called $\underline{x}$-autonomous and

$$\Phi(\underline{x}, t) = X(\hat{\Phi}(\underline{Y}(\underline{x}, t)))$$

is called fully autonomous.

2.2.1 Properties of global maps.

Global maps are characterized by the property that the change of the argument field in a small neighbourhood of any point $\underline{\hat{x}}_o \in \hat{D}$ leads to a change of the value of the image field at a fixed location $\underline{x} \in D$. This functional dependence indicates that it must be possible to express the mapping X in terms of a functional. This can be achieved using a special construction which leads to a subset of the set of global mappings. Consider an arbitrary functional

$$\Lambda[\hat{\Phi}] : \hat{H}(\hat{D}) \rightarrow R^1$$

The value $\Lambda[\hat{\Phi}]$ is then independent of $\underline{\hat{x}} \in \hat{D}$ and derivatives with respect to location vanish. Suppose now that Λ is Frechet-differentiable in $\hat{H}$

$$(\frac{\delta \Lambda}{\delta \hat{\Phi}(\underline{\hat{x}})}, h) = \lim_{\epsilon \rightarrow 0} \frac{\partial}{\partial \epsilon} \Lambda[\hat{\Phi} + \epsilon h]$$

for $\hat{\Phi}$, $h \in \hat{H}$. Then is the first Frechet-derivative of Λ a generalized function of the location $\underline{\hat{x}}$. It follows that

$$\frac{\delta \Lambda}{\delta \hat{\Phi}(\underline{\hat{x}})} \equiv X^*[\hat{\Phi}(.); \underline{x}], \quad \hat{\Phi} \in \hat{H}$$

provides a mapping of the argument space $\hat{H}$ into some function space $H^*(\hat{D})$ because keeping the argument field fixed and varying the location $\underline{x} \in D$ produces a scalar field whose smoothness properties depend on the functional Λ. A second step is required for the construction of global mappings based on functionals. We need to define a mapping $\underline{Y} : D(t) \rightarrow \hat{D}$ which is bijective, local and sufficiently smooth. Then we can express the location in $D(t)$ in terms of the location in $\hat{D}$ by

$$\underline{\hat{x}} = \underline{Y}(\underline{x}, t)$$

If the functional Λ is defined in such a way that the fields generated by its Frechet-derivative are always contained in the space $H^m(\hat{D})$ for $m \geq 0$ and combining the derivative with the mapping $\underline{Y}(\underline{x}, t)$ of the domains we can define a mapping by

$$X[\hat{\Phi}(.); \underline{x}, t] \equiv \frac{\delta \Lambda[\hat{\Phi}(.)]}{\delta \hat{\Phi}(\underline{Y}(\underline{x}, t))}$$

It is clear that global mapping do not require a mapping of the domains and for this reason is the present construction rather special.

2.2.2 Properties of local maps.

The value $\Phi(\underline{x},t)$ of the image field depends on the value of the argument field $\hat{\Phi}$ at a unique location $\hat{\underline{x}} = \underline{Y}(\underline{x},t)$. If the argument field is modified at any other location no change of $\Phi(\underline{x},t)$ is observed. Hence is

$$\Phi(\underline{x},t) = X(\hat{\Phi}(\underline{Y}(\underline{x},t),\underline{x},t)$$

a strictly local map. Differentiation of the image field can be carried out using the rules of standard calculus. For instance, the time derivative emerges as

$$\frac{\partial \Phi}{\partial t}(\underline{x},t) = \frac{\partial X}{\partial \hat{\Phi}} \frac{\partial \hat{\Phi}}{\partial Y_\alpha} \frac{\partial Y_\alpha}{\partial t} + \frac{\partial X}{\partial t}$$

and likewise for the spatial derivative. Higher derivatives follow from repeated application of these operations.

2.3 A reduction property for multi-dimensional mappings.

The closure problem for mappings can be viewed as the construction of a global map corresponding to the local map which is to be determined as the solution of the mapping equation. The relation of the global map to the local map needs clarification since they act on the same class of reference and turbulence fields. If the global map is known we can calculate the statistics at any number of points as the image of of Gaussian statistics. Hence, we can calculate the statistics at a single point which implies that there exists a relation between the mapping for a single variable and the mapping for many variables containing the single point. This relation can be obtained as follows. Pdfs posses a well known reduction property given by

$$f_1(\varphi_N) = \int_{-\infty}^{\infty} d\varphi_1 \cdots \int_{-\infty}^{\infty} d\varphi_{N-1} f_N(\varphi_1,\cdots,\varphi_N)$$

which must be retained if the pdfs are transformed Gaussians. Let the local mapping be $X : R^1 \rightarrow \Omega$, where Ω denotes the range of the scalar defined at a single point in the flow field $D(t)$, and the global (N-dimensional) mapping $\underline{X}^N : R^N \rightarrow \Omega^N$, then are the one-dimensional pdf and the N-dimensional pdf given by

$$f(y) = \frac{f_G(\eta)}{\frac{\partial X}{\partial \eta}}$$

and

$$f_N(y_1,\cdots,y_N) = \frac{f_G(\eta_1,\cdots,\eta_N)}{det\left(\frac{\partial X_i}{\partial \eta_j}\right)}$$

respectively where $y = X(\eta)$ and $\underline{y} = \underline{X}(\eta_1, \cdots, \eta_N)$ hold. Application to the reduction property for pdfs leads to

$$\frac{f_G(\eta)}{\frac{\partial X}{\partial \eta}} = \int_{-\infty}^{\infty} d\varphi_1 \cdots \int_{-\infty}^{\infty} d\varphi_{N-1} det\left(\frac{\partial X_i}{\partial \eta_j}\right)_{N-1} \frac{f_G(\eta_1, \cdots, \eta_N)}{det\left(\frac{\partial X_i}{\partial \eta_j}\right)_N}$$

where the subscripts on the Jacobian matrices indicate the rank. Since the Gaussian reference measure is the product of N one-dimensional measures it follows that

$$\frac{\partial X}{\partial \eta}^{-1} = \int_{-\infty}^{\infty} d\varphi_1 \cdots \int_{-\infty}^{\infty} d\varphi_{N-1} \frac{det\left(\frac{\partial X_i}{\partial \eta_j}\right)_{N-1}}{det\left(\frac{\partial X_i}{\partial \eta_j}\right)_N} \prod_{i=1}^{N-1} f_G(\eta_i)$$

holds. Denoting by $dG_i \equiv d\eta_i f_G(\eta_i)$ the differential of the standard Gaussian measure (zero mean and unit variance) we get

$$\left(\frac{\partial X}{\partial \eta}\right)^{-1} = \int_{-\infty}^{\infty} dG_1 \cdots \int_{-\infty}^{\infty} dG_{N-1} \frac{det\left(\frac{\partial X_i}{\partial \eta_j}\right)_{N-1}}{det\left(\frac{\partial X_i}{\partial \eta_j}\right)_N}$$

as reduction property for mappings. It is worth noting that this relation can be extended to infinitely many variables since the Gaussian has a well defined limit. It is easy to show that the reduction property appears in the form (note that $\eta \equiv \eta_N$)

$$\left(\frac{\partial X}{\partial \eta}\right)^{-1} = \int_{-\infty}^{\infty} dG(\eta_1) \cdots \int_{-\infty}^{\infty} dG(\eta_{N-1}) \left(\frac{\partial}{\partial \eta_N} X_N(\eta_1, \cdots, \eta_N)\right)^{-1}$$

if the Jacobian matrices are triangular. This particular form of the reduction property expresses the one-dimensional map for the N^{th} variable η_N in terms of the global or N-dimensional map for all variables $\eta_1, \cdots, \eta_N$. It depends obviously on the Gaussian reference measure.

3.0 Transport equations for pdfs and cdfs.

Transport equations for pdfs and cdfs can be obtained using the notions of step functions and pseudo-functions. The starting point are the basic differential equations set up in the spatial (Eulerian) frame with respect to a Cartesian system of coordinates. Mass balance is given by

$$\frac{\partial v_\alpha}{\partial x_\alpha} = 0 \tag{3.1}$$

and momentum balance by

$$\frac{\partial v_\alpha}{\partial t} + v_\beta \frac{\partial v_\alpha}{\partial x_\beta} = -\frac{1}{\rho}\frac{\partial p}{\partial x_\alpha} + \nu \frac{\partial^2 v_\alpha}{\partial x_\beta \partial x_\beta} \tag{3.2}$$

A passive scalar obeys

$$\frac{\partial \Phi}{\partial t} + v_\beta \frac{\partial \Phi}{\partial x_\beta} = Q(\Phi) + \Gamma \frac{\partial^2 \Phi}{\partial x_\beta \partial x_\beta} \tag{3.3}$$

The flow domain is denoted by Ω and its boundary by $\partial\Omega$. Consider now N distinct points $\underline{x}^{(i)} \in \Omega$. We derive first the cumulative distribution function (cdf) of the values of velocity ans scalar at those N points in the flow domain. We define the step function

$$\hat{F}_N \equiv \Pi_{i=1}^{N} H(\varphi_i - \Phi(\underline{x}^{(i)}, t)) H(\underline{v}_i - \underline{v}(\underline{x}^{(i)}, t)) \tag{3.4}$$

where N denotes the number of points in the flow field, H denotes the Heaviside function

$$H(x) \equiv \begin{cases} 1 & \text{for } x \geq 0 \\ 0 & \text{for } x < 0 \end{cases}$$

and the step function of a vector argument is the product of the step functions of the components. It is easy to show that the expectation of $\hat{F}_N$ is the cdf F_N

$$\langle \hat{F}_N \rangle = F_N(\underline{v}_1, \cdots, \underline{v}_N, \varphi_1, \cdots, \varphi_N; \underline{x}^{(1)}, \cdots, \underline{x}^{(N)}, t) \tag{3.5}$$

of the variables $\underline{v}(\underline{x}^{(i)}, 1)$, $\Phi(\underline{x}^{(i)}, t)$ at the N points in the flow field. The necessary tools for the derivation of the transport equations are the spatial and temporal derivatives of the step function $\hat{F}_N$. Implicit differentiation leads to

$$\frac{\partial \hat{F}_N}{\partial t} = -\sum_{i=1}^{N} \{ \frac{\partial v_\alpha}{\partial t}(\underline{x}^{(i)}, t) \frac{\partial \hat{F}_N}{\partial v_\alpha^i} + \frac{\partial \Phi}{\partial t}(\underline{x}^{(i)}, t) \frac{\partial \hat{F}_N}{\partial \varphi_i} \} \tag{3.6}$$

and

$$\frac{\partial \hat{F}_N}{\partial x_\alpha^{(j)}} = -\frac{\partial v_\beta}{\partial x_\alpha^{(j)}}(\underline{x}^{(j)}, t) \frac{\partial \hat{F}_N}{\partial v_\beta^j} - \frac{\partial \Phi}{\partial x_\alpha^{(j)}}(\underline{x}^{(j)}, t) \frac{\partial \hat{F}_N}{\partial \varphi_j} \tag{3.7}$$

where the summation convention applies to Greek subscripts.

Pressure.

The pressure $p(\underline{x},t)$ can be eliminated from the momentum balance according to

$$-\triangle p = \frac{\partial v_\alpha}{\partial x_\beta}\frac{\partial v_\beta}{\partial x_\alpha}$$

with boundary conditions

$$\frac{\partial p}{\partial n_\alpha} = h_\alpha(\underline{v})$$

on $\partial\Omega$. The solution of this Poisson equation for $p(\underline{x},t)$ can be given in the form

$$p(\underline{x},t) = -\frac{1}{4\pi}\int_\Omega d\underline{y} G(\underline{x},\underline{y})\frac{\partial v_\alpha}{\partial y_\beta}\frac{\partial v_\beta}{\partial y_\alpha} + B(\underline{x},t) \tag{3.8}$$

where $G(\underline{x},\underline{y}) = |\underline{x}-\underline{y}|^{-1}$ is the Poisson kernel and $B(\underline{x},t)$ is a harmonic function ensuring that the boundary conditions are satisfied. It follows from this solution that pressure depends in functional form on velocity, it depends on time in autonomous form via velocity and it depends on location $\underline{x}$ parametrically. Hence $p(\underline{x},t) = p[\underline{v}(.,t);\underline{x}]$ and

$$\frac{\partial p}{\partial t} = \dot{p}[\underline{v}(.,t),\frac{\partial \underline{v}}{\partial t}(.,t);\underline{x}] \tag{3.9}$$

and the Frechet-derivative of pressure with respect to velocity is given by

$$\frac{\delta}{\delta v_\alpha(\underline{y},t)}p[\underline{v}(.,t);\underline{x}] = -\frac{1}{2\pi}\frac{\partial^2 G(\underline{x},\underline{y})}{\partial y_\alpha \partial y_\beta}v_\beta(\underline{y},t)$$

if no boundaries are present. This derivative represents the change of pressure at $\underline{x}$ due to a change of the velocity component v_α at $\underline{y}$.

Transport equation for $\hat{F}_N$.

The transport equation for $\hat{F}_N$ follows from the differentiation rules and the Navier-Stokes system. We get

$$\frac{\partial \hat{F}_N}{\partial t} + \sum_{i=1}^N v_\alpha(\underline{x}^{(i)},t)\frac{\partial \hat{F}_N}{\partial x_\alpha^{(i)}} + \sum_{i=1}^N\{\Gamma\triangle^{(i)}\Phi\frac{\partial \hat{F}_N}{\partial \varphi_i} + \nu\triangle^{(i)}v_\alpha\frac{\partial \hat{F}_N}{\partial v_\alpha^i}\}$$

$$+\sum_{i=1}^N\{Q(\Phi_i)\frac{\partial \hat{F}_N}{\partial \varphi_i} - \frac{\partial}{\partial x_\alpha^{(i)}}p[\underline{v}(.,t);\underline{x}]\frac{\partial \hat{F}_N}{\partial v_\alpha^i}\} = 0 \tag{3.10}$$

This equation can be viewed as the condition that the value of the cdf $\hat{F}_N$ remains constant for points in phase space (the product of flow domain, scalar space and velocity spaces) that move with the velocity $(v_\alpha(\underline{x}^{(i)},t), \Gamma\triangle^{(i)}\Phi + Q(\Phi), \nu\triangle^{(i)}v_\alpha - \partial p/\partial x_\alpha)$.

Preliminary form of the transport equation for the cdf F_N.

Averaging of the transport equation for $\hat{F}_N$ leads at once to the equation for the cdf F_N. Its preliminary form is given by

$$\frac{\partial F_N}{\partial t} + \sum_{i=1}^{N} \langle v_\alpha(\underline{x}^{(i)}, t) \frac{\partial \hat{F}_N}{\partial x_\alpha^{(i)}} \rangle + \sum_{i=1}^{N} \{ \Gamma \langle \triangle^{(i)} \Phi \frac{\partial \hat{F}_N}{\partial \varphi_i} \rangle + \nu \langle \triangle^{(i)} v_\alpha \frac{\partial \hat{F}_N}{\partial v_\alpha^i} \rangle \}$$

$$+ \sum_{i=1}^{N} \{ \langle Q(\Phi_i) \frac{\partial \hat{F}_N}{\partial \varphi_i} \rangle - \langle \frac{\partial}{\partial x_\alpha^{(i)}} p[\underline{v}(.,t); \underline{x}] \frac{\partial \hat{F}_N}{\partial v_\alpha^i} \rangle \} = 0 \tag{3.11}$$

All expectations appearing in this equations need to be evaluated to provide expressions containing the cdf F_k. If $k \leq N$ the term is called closed otherwise it is nonclosed and represents an additional unknown.

Flux in physical space.

Mass balance holds at every point $\underline{x}^{(i)}$ and this implies

$$\langle v_\alpha(\underline{x}^{(i)}, t) \frac{\partial \hat{F}_N}{\partial x_\alpha^{(i)}} \rangle = \frac{\partial}{\partial x_\alpha^{(i)}} \langle v_\alpha(\underline{x}^{(i)}, t) \hat{F}_N \rangle$$

The flux is now according to the definition of the angular brackets given by

$$\langle v_\alpha(\underline{x}^{(i)}, t) \hat{F}_N \rangle =$$

$$\int d\Phi(\underline{x}^{(1)}) \cdots \int d\underline{v}(\underline{x}^{(N)}) v_\alpha(\underline{x}^{(i)}) \hat{F}_N f_N(\underline{v}(\underline{x}^{(1)}), \cdots, \Phi(\underline{x}^{(N)}); \underline{x}^{(1)}, \cdots, \underline{x}^{(N)}, t)$$

The definition of $\hat{F}_N$ implies

$$\langle v_\alpha(\underline{x}^{(i)}, t) \hat{F}_N \rangle = \int_{-\infty}^{\varphi_1} d\Phi_1 \cdots \int_{-\infty}^{\underline{v}^N} d\underline{v}^N v_\alpha^i f_N(\underline{v}^1, \cdots, \Phi_N; \underline{x}^{(1)}, \cdots, \underline{x}^{(N)}, t)$$

The relation

$$f_N = \frac{\partial^{4N} F_N}{\partial v_1^1 \cdots \partial \Phi^N}$$

leads to

$$\langle v_\alpha(\underline{x}^{(i)}, t) \hat{F}_N \rangle = \int_{-\infty}^{v_\alpha^i} dv_\alpha^i v_\alpha^i \frac{\partial F_N}{\partial v_\alpha^i}$$

and partial integration results in

$$\langle v_\alpha(\underline{x}^{(i)}, t) \hat{F}_N \rangle = v_\alpha^i F_N - \int_{-\infty}^{v_\alpha^i} dv_\alpha^i F_N \tag{3.12}$$

which is closed. It can be shown easily that it is consistent with the corresponding expression in the pdf equation.

Diffusive flux in scalar space.

The flux in scalar space is given by $\langle \Delta^{(i)}\Phi \hat{F}_N \rangle$ which is by definition

$$\langle \Delta^{(i)}\Phi \hat{F}_N \rangle = \int d\Phi^1 \cdots \int d\underline{v}^N \int d(\Delta^{(i)}\Phi)$$

$$\Delta^{(i)}\Phi \Pi_{j=1}^N H(\varphi_j - \Phi^j) H(\underline{v}^j - \underline{v}^j) f_{N+1}(\Phi^1, \cdots, \underline{v}^j, \Delta^{(i)}\Phi, t)$$

Introducing the conditional pdf f_c defined by

$$f_{N+1}(\Phi^1, \cdots, \underline{v}^N, \Delta^{(i)}\Phi) = f_c(\Delta^{(i)}\Phi | \Phi^1, \cdots, \underline{v}^N) f_N(\Phi^1, \cdots, \underline{v}^N)$$

leads to

$$\langle \Delta^{(i)}\Phi \hat{F}_N \rangle = \int_{-\infty}^{\varphi_1} d\Phi^1 \cdots \int_{-\infty}^{\underline{v}^N} d\underline{v}^N \langle \Delta^{(i)}\Phi | \Phi(\underline{x}^{(1)}) = \Phi^1, \cdots, \underline{v}(\underline{x}^{(N)}) = \underline{v}^N \rangle \frac{\partial^{4N} F_N}{\partial \Phi^1 \cdots \partial \underline{v}^N} \tag{3.13}$$

as final result. A new unknown $\langle \Delta^{(i)}\Phi | \cdots \rangle$ appears and the flux in scalar space is, therefore, nonclosed. Consistency with the pdf equation follows at once from the equation above by differentiation. It is important to notice the fundamental difference between the cases $N = 1$ and $N > 1$. The term actually appearing in the transport equation for the cdf is

$$\frac{\partial}{\partial \varphi_i} \langle \Delta^{(i)}\Phi \hat{F}_N \rangle$$

which is for $N = 1$ obviously a differential term

$$\frac{\partial}{\partial \varphi_i} \langle \Delta^{(i)}\Phi \hat{F}_1 \rangle = \frac{\partial}{\partial \varphi_i} \int_{-\infty}^{\varphi_i} d\Phi^i \langle \Delta^{(i)}\Phi | \Phi(\underline{x}^{(i)}) = \Phi^i \rangle \frac{\partial F_1}{\partial \Phi^i}$$

given by (see Pope, 1991)

$$\frac{\partial}{\partial \varphi_i} \langle \Delta^{(i)}\Phi \hat{F}_1 \rangle = \langle \Delta^{(i)}\Phi | \Phi(\underline{x}^{(i)}) = \varphi_i \rangle \frac{\partial F_1}{\partial \varphi^i}$$

whereas for $N > 1$ the integral character is preserved since the single derivative removes only one of the integrals.

Viscous flux in velocity space.

The viscous flux in velocity space is completely analogue to the diffusive flux in scalar space. It follows from (13) that

$$\langle \Delta^{(i)} v_\alpha \hat{F}_N \rangle = \int_{-\infty}^{\varphi_1} d\Phi^1 \cdots \int_{-\infty}^{\underline{v}^N} d\underline{v}^N \langle \Delta^{(i)} v_\alpha | \Phi(\underline{x}^{(1)}) = \Phi^1, \cdots, \underline{v}(\underline{x}^{(N)}) = \underline{v}^N \rangle \frac{\partial^{4N} F_N}{\partial \Phi^1 \cdots \partial \underline{v}^N} \tag{3.14}$$

holds. The flux is nonclosed and consistent with the pdf equation.

Source flux in scalar space.

The source term $Q(\Phi, \underline{v})$ is assumed to be a local function of the scalar $\Phi(\underline{x}^{(i)}, t)$ and the velocty $\underline{v}(\underline{x}^{(i)}, t)$ It follows from (3.13) that

$$\langle Q \hat{F}_N \rangle = \int_{-\infty}^{\varphi_1} d\Phi^1 \cdots \int_{-\infty}^{\underline{v}^N} d\underline{v}^N Q(\Phi^i, \underline{v}^i) \frac{\partial^{4N} F_N}{\partial \Phi^1 \cdots \partial \underline{v}^N}$$

holds. This expression can be simplified if the source term Q depends only on Φ^i and $\underline{v}^i$ because partial integration removes the differentiation with respect to all the other variables and we get

$$\langle Q \hat{F}_N \rangle = \int_{-\infty}^{\varphi_i} d\Phi^i \int_{-\infty}^{\underline{v}^i} d\underline{v}^i Q(\Phi^i, \underline{v}^i) \frac{\partial^4 F_N}{\partial \Phi^i \partial \underline{v}^i} \tag{3.15}$$

which is a closed term. For the special case that the source Q depends on Φ^i only we obtain for the derivative appearing in the cdf equation

$$\frac{\partial}{\partial \varphi_i} \langle Q \hat{F}_N \rangle = Q(\varphi_i) \frac{\partial F_N}{\partial \varphi_i}$$

Consistency with the pdf equation becomes evident by differentiation of (3.15).

Pressure flux in velocity space.

It follows from the functional dependence of p on the velocity $\underline{v}$ that the pressure gradient is a nonlocal function of $\underline{v}$. Hence we can apply (3.13) and get

$$\langle \frac{\partial p}{\partial x_\alpha^{(i)}} \hat{F}_N \rangle = \int_{-\infty}^{\varphi_1} d\Phi^1 \cdots \int_{-\infty}^{\underline{v}^N} d\underline{v}^N \langle \frac{\partial p}{\partial x_\alpha^{(i)}} | \Phi(\underline{x}^{(1)}) = \Phi^1, \cdots, \underline{v}(\underline{x}^{(N)}) = \underline{v}^N \rangle \frac{\partial^{4N} F_N}{\partial \Phi^1 \cdots \partial \underline{v}^N} \tag{3.16}$$

This result is nonclosed.

Cdf equation in terms of conditional fluxes.

The expressions (3.12) to (3.16) can be used to obtain a new version of the transport equation for the cdf F_N

$$\frac{\partial F_N}{\partial t} + \sum_{i=1}^{N} \{ v_\alpha^i \frac{\partial F_N}{\partial x_\alpha^{(i)}} - \int_{-\infty}^{v_\alpha^i} dv_\alpha^i \frac{\partial F_N}{\partial x_\alpha^{(i)}} \} +$$

$$\sum_{i=1}^{N} \{ \Gamma \frac{\partial}{\partial \varphi_i} \int_{-\infty}^{\varphi_1} d\Phi^1 \cdots \int_{-\infty}^{\underline{v}^N} d\underline{v}^N \langle \Delta^{(i)} \Phi | \Phi(\underline{x}^{(1)}) = \Phi^1, \cdots \rangle \frac{\partial^{4N} F_N}{\partial \Phi^1 \cdots \partial \underline{v}^N}$$

$$+ \nu \frac{\partial}{\partial v_\alpha^i} \int_{-\infty}^{\varphi_1} d\Phi^1 \cdots \int_{-\infty}^{\underline{v}^N} d\underline{v}^N \langle \Delta^{(i)} v_\alpha | \Phi(\underline{x}^{(1)}) = \Phi^1, \cdots \rangle \frac{\partial^{4N} F_N}{\partial \Phi^1 \cdots \partial \underline{v}^N} \}$$

$$+ \sum_{i=1}^{N} \{ \frac{\partial}{\partial \varphi_i} \int_{-\infty}^{\varphi_i} d\Phi^i \int_{-\infty}^{\underline{v}^i} d\underline{v}^i Q(\Phi^i, \underline{v}^i) \frac{\partial^4 F_N}{\partial \Phi^i \partial \underline{v}^i}$$

$$- \frac{\partial}{\partial v_\alpha^i} \int_{-\infty}^{\varphi_1} d\Phi^1 \cdots \int_{-\infty}^{\underline{v}^N} d\underline{v}^N \langle \frac{\partial p}{\partial x_\alpha^{(i)}} | \Phi(\underline{x}^{(1)}) = \Phi^1, \cdots \rangle \frac{\partial^{4N} F_N}{\partial \Phi^1 \cdots \partial \underline{v}^N} \} = 0 \qquad (3.17)$$

This version is not suitable for the limit $N \to \infty$ since it contains the N-dimensional Lebesgue measure for which no limit exists. However, the transport equation (3,17) has several noteworthy properties. First we note the special case of a single scalar in homogeneous turbulence with $Q(\Phi)$. It follows that the cdf for the single scalar satisfies

$$\frac{\partial F}{\partial t} + \{ \Gamma \langle \Delta \Phi | \Phi = \varphi \rangle + Q(\varphi) \} \frac{\partial F}{\partial \varphi} = 0 \qquad (3.18)$$

which is non-integral with respect to the scalar value φ. The hyperbolic equation (3.18) expresses the fact that the value of the cdf remains constant for points moving with the velocity $\Gamma \langle \Delta \Phi | \Phi = \varphi \rangle + Q(\varphi)$. We conclude that the structure of the cdf equation for $N = 1$ and $N > 1$ is fundamentally different and methods developed for $N = 1$ cannot be expected to carry over to $N > 1$ without major modifications.

Pdf equation in terms of conditional fluxes.

The transport equation for the cdf can be used to obtain the equation for the pdf f_N by differentiation according to

$$f_N = \frac{\partial^{4N} F_N}{\partial v_1^1 \cdots \partial \Phi^N}$$

It follows that the pdf is governed by

$$\frac{\partial f_N}{\partial t} + \sum_{i=1}^{N} v_\alpha^i \frac{\partial f_N}{\partial x_\alpha^{(i)}} +$$

$$\sum_{i=1}^{N}\{\Gamma\frac{\partial}{\partial\varphi_i}[\langle\Delta^{(i)}\Phi|\Phi(\underline{x}^{(1)})=\Phi^1,\cdots\rangle f_N]+\nu\frac{\partial}{\partial v_\alpha^i}[\langle\Delta^{(i)}v_\alpha|\Phi(\underline{x}^{(1)})=\Phi^1,\cdots\rangle f_N]\}$$

$$+\sum_{i=1}^{N}\{\frac{\partial}{\partial\varphi_i}[Q(\Phi^i,\underline{v}^i)f_N]-\frac{\partial}{\partial v_\alpha^i}[\langle\frac{\partial p}{\partial x_\alpha^{(i)}}|\Phi(\underline{x}^{(1)})=\Phi^1,\cdots\rangle f_N]\}=0 \qquad (3.19)$$

which is formally of local (non-integral) character in scalar-velocity space. It reduces for a single scalar in homogeneous turbulence to the well known equation

$$\frac{\partial f}{\partial t}+\frac{\partial}{\partial\varphi}\{[\Gamma\langle\Delta\Phi|\Phi=\varphi\rangle+Q(\varphi)]f\}=0 \qquad (3.20)$$

which can be regarded as the condition that the divergence of a flux in the phase space spanned by time and the scalar space is zero. Equation (3.20) and its generalisation to higher dimensions (3.19) can be regarded as balance equations for the "mass" per unit "volume" f_N. The coefficients of f_N can be interpreted as velocity components and f_N will remain nonnegative and its integral unity.

4.0 Mapping method for the one-dimensional case.

The mapping method suggested by Chen et al. (1989) has two distinct advantages over the previously constructed models. It produces the Gaussian pdf as asymptotic limit for decaying turbulence and agrees very well with DNS results for pure mixing in homogeneous turbulence. The derivation of the mapping equation will be reviewed and its variant for the characteristic function will be discussed.

4.1 The Chen-Kraichnan method.

The starting point for the Chen-Kraichnan method is the pdf equation for a single scalar $\Phi(\underline{x},t)$ given by

$$\frac{\partial f}{\partial t}+\langle v_\alpha\rangle\frac{\partial f}{\partial x_\alpha}+\frac{\partial}{\partial\varphi}(Qf)=-\frac{\partial}{\partial x_\alpha}(\langle v'_\alpha|\Phi(\underline{x},t)=\varphi\rangle f)-\frac{\partial}{\partial\varphi}(\langle\Gamma\triangle\Phi|\Phi=\varphi\rangle f) \tag{4.1}$$

which reduces for homogeneous turbulence to

$$\frac{\partial f}{\partial t}+\frac{\partial}{\partial\varphi}\{F_\varphi f\}=0 \tag{4.2}$$

The equation for the corresponding cdf is according to ch.3.

$$\frac{\partial F}{\partial t}+F_\varphi\frac{\partial F}{\partial\varphi}=0 \tag{4.3}$$

The velocity in scalar space is defined by

$$F_\varphi\equiv Q+\langle\Gamma\triangle\Phi|\Phi(\underline{x},t)=\varphi\rangle \tag{4.4}$$

It governs the dynamics of pdf and cdf. The probabilistic argument space of pdf and cdf is the range of values the scalar Φ can assume at any point $(\underline{x},t)$. Let this space be the unit interval $[0,1]$. There are two slightly different ways for the development of a mapping method.

Method I.: A mapping $X:\ R^1\rightarrow[0,1]$ is defined by two conditions. First, the value of the cdf at the image variable $X(\eta)$ is equal to the value of the standard Gaussian cdf at the argument variable η

$$F(X(\eta,\underline{x},t))=F_G(\eta) \tag{4.5}$$

and second, the mapping is monotonically increasing

$$X(\eta_1)<X(\eta_2)\quad for\quad \eta_1<\eta_2 \tag{4.6}$$

Mapping the domain of definition of the single point cdf implies that the value of the scalar $\Phi(\underline{x},t)$ is the image of a variable ranging on $(-\infty,\infty)$. Hence will the mapping in general depend on the location in the flow field and on time. The first condition (4.5) implies the existence of a Gaussian random variable Ψ such that

$$F_G(\eta)=Prob\{\Psi\leq\eta\}$$

holds. The argument variable is now extended to a Gaussian random field such that the Gaussian random variable is the Gaussian field at a location $\underline{\zeta}\equiv\underline{Y}(\underline{x},t)$. Note that this extension is completely arbitrary and the mapping X does not determine the relation between the locations of the image variable $\Phi(\underline{x},t)$ and the argument variable $\Psi(\underline{\zeta})$. The second condition (4.6) is a direct consequence of the monotonicity of the cdfs.

The probabilistic interpretation of the first condition (4.5) using

$$F(X(\eta,\underline{x},t)) = Prob\{\Phi(\underline{x},t) < X(\eta,\underline{x},t)\}$$

and

$$F_G(\eta) = Prob\{\Psi(\underline{\zeta}) < \eta\}$$

is given by

$$Prob\{\Phi(\underline{x},t) < X(\eta,\underline{x},t)\} = Prob\{\Psi(\underline{\zeta}) < \eta\}$$

which can be regarded as

$$Prob\{\Phi(\underline{x},t) < \varphi\} = Prob\{X(\Psi(\underline{\zeta}),\underline{x},t) < \varphi\} \tag{4.7}$$

It should be noted that the mapping thus constructed is local in the sense that any change of the Gaussian argument field $\Psi(\underline{\zeta})$ at any location $\underline{\zeta} \neq \underline{Y}(\underline{x},t)$ has no influence on the mapping. We note that there are three fields involved in this version of the mapping method:

1) The turbulent field $\Phi(\underline{x},t)$.

2) The Gaussian argument field $\Psi(\underline{\zeta})$.

3) The (local) image field $\hat{\Phi}(\underline{x},t) \equiv X(\Psi(\underline{\zeta}),\underline{x},t)$ where $\zeta = \underline{Y}(\underline{x},t)$ holds. The image field is called surrogate field (Pope, 1991).

It follows from the fact that the mapping relates only single point statistics to Gaussian statistics that no scale information will be determined by this version of the mapping method. The mapping $\underline{Y}$ relating the locations of turbulent and argument fields is so far undetermined.

The mapping equation is now derived from the first condition (4.5) by differentiating with respect to time. It follows that

$$\frac{\partial F}{\partial t} + \frac{\partial X}{\partial t}\frac{\partial F}{\partial \varphi} = 0 \tag{4.8}$$

must hold since the reference distribution is time independent. Comparison with (4.3) and (4.4) leads to

$$\frac{\partial X}{\partial t} = Q + \langle \Gamma \triangle \Phi | \Phi(\underline{x},t) = \varphi \rangle \tag{4.9}$$

The closure model is completed by requiring that the conditional expectation of the turbulent field is equal to the conditional expectation of the image of the Gaussian reference field (surrogate field)

$$\frac{\partial X}{\partial t} \tilde{=} Q(\varphi) + \langle \Gamma \triangle \hat{\Phi} | \hat{\Phi}(\underline{x},t) = \varphi \rangle \tag{4.10}$$

The most important property of this mapping equation is the fact that the Gaussian reference measure allows explicit calculation of the conditional expectations in terms of the mapping and correlations of the Gaussian reference field. The derivatives of the image field can be expressed in terms of the reference field as follows

$$\frac{\partial \hat{\Phi}}{\partial x_\alpha} = \frac{\partial}{\partial x_\alpha} X(\Psi(\underline{Y}(\underline{x},t),t),t)$$

and thus

$$\frac{\partial \hat{\Phi}}{\partial x_\alpha} = \frac{\partial X}{\partial \varphi}\frac{\partial \Psi}{\partial \zeta_\beta}\frac{\partial Y_\beta}{\partial x_\alpha} \tag{4.11}$$

holds. If the so far undetermined relation between the locations in physical and reference spaces $\underline{Y}$ is restricted to a stretching transformation uniform in physical space we get

$$\frac{\partial Y_\beta}{\partial x_\alpha} = \delta_{\alpha\beta} m(t) \tag{4.12}$$

where m is time dependent. Denoting the derivatives of the mapping with

$$X' \equiv \frac{\partial X}{\partial \varphi}, \quad \frac{\partial X}{\partial t} \equiv \dot{X} \tag{4.13}$$

we get

$$\frac{\partial \hat{\Phi}}{\partial x_\alpha} = X'\frac{\partial \Psi}{\partial \zeta_\beta}\frac{\partial Y_\beta}{\partial x_\alpha} \tag{4.14}$$

and for the Laplacian

$$\frac{\partial^2 \hat{\Phi}}{\partial x_\alpha \partial x_\alpha} = m^2\left(X''\frac{\partial \Psi}{\partial \zeta_\alpha}\frac{\partial \Psi}{\partial \zeta_\alpha} + X'\frac{\partial^2 \Psi}{\partial \zeta_\alpha \partial \zeta_\alpha}\right) \tag{4.15}$$

The conditional expectation of the Laplacain can be established explicitly in terms of the mapping X and correlations of the Gaussian reference field if and only if the derivatives of the mapping are completely specified by the condition $\Phi(\underline{x}) = \varphi$. This implies that the mapping must be local, i.e. the variation of the reference field at locations $\underline{\zeta}' \neq \underline{\zeta}$ has no influence on $X(\Psi(\underline{\zeta}), t)$. It follows then from $\Psi(\underline{\zeta}) = \eta$ being the unique inverse image of $\hat{\Phi}(\underline{x}, t) = \varphi$ that

$$\langle\frac{\partial^2 \hat{\Phi}}{\partial x_\alpha \partial x_\alpha}|\hat{\Phi}(\underline{x}) = \varphi\rangle = m^2\left(X''\langle\frac{\partial \Psi}{\partial \zeta_\alpha}\frac{\partial \Psi}{\partial \zeta_\alpha}|\Psi(\underline{\zeta}) = \eta\rangle + X'\langle\frac{\partial^2 \Psi}{\partial \zeta_\alpha \partial \zeta_\alpha}|\Psi(\underline{\zeta}) = \eta\rangle\right) \tag{4.15}$$

holds. The correlations of the Gaussian reference maesure can be evaluated as follows

$$\langle\frac{\partial \Psi}{\partial \zeta_\alpha}\frac{\partial \Psi}{\partial \zeta_\alpha}|\Psi(\underline{\zeta}) = \eta\rangle = \langle\frac{\partial \Psi}{\partial \zeta_\alpha}\frac{\partial \Psi}{\partial \zeta_\alpha}\rangle \tag{4.16}$$

and

$$\langle\frac{\partial^2 \Psi}{\partial \zeta_\alpha \partial \zeta_\alpha}|\Psi(\underline{\zeta}) = \eta\rangle = -\eta\frac{\langle\frac{\partial \Psi}{\partial \zeta_\alpha}\frac{\partial \Psi}{\partial \zeta_\alpha}\rangle}{\langle\Psi^2\rangle} \tag{4.17}$$

The variance $\langle\Psi^2\rangle$ of the reference measure can be set to unity without restricting the generality of the result. This completes the closure of the mapping equation. The resulting equation determining the mapping is thus given by

$$\frac{\partial X}{\partial t} = Q(\eta) + m^2\Gamma\langle\frac{\partial \Psi}{\partial \zeta_\alpha}\frac{\partial \Psi}{\partial \zeta_\alpha}\rangle(X'' - \eta X')$$

This result was first obtained by Chen et al. (1989) and generalized by Pope (1991) to several variables using the fact that the N-variate pdf can be represented as the product of N conditional pdfs.

Method II.: A general transformation of the domain of definition of the pdf equation (4.2) is considered. The domain of definition is the space $S \equiv \Re \times [0,T]$ which is the image space of the mapping $\underline{X} : R^1 \times [0,T] \rightarrow S$ (T denotes the time interval considered and $\Re$ is the range of the values of Φ). The mapping is then written as

$$t = X_t(\eta,\tau), \quad \varphi = X_\Phi(\eta,\tau) \tag{4.18}$$

The mapping must possess a unique inverse satisfying the same smoothness conditions as $\underline{X}$

$$\tau = X_t^{-1}(\varphi,t), \quad \eta = X_\Phi^{-1}(\varphi,t) \tag{4.19}$$

and it must have a positive Jacobian. The mapping equations are established in two steps: First the pdf equation in the reference domain is set up and then the mapping condition that this pdf is Gaussian is introduced. The function f^T defined by

$$f^T(\eta,\tau) \equiv f(X_\Phi(\eta,\tau), X_t(\eta,\tau)) \tag{4.20}$$

is the pdf in the reference variables, but it is not pdf with respect to η since it it is not necessarily normalized. The transport equation for f^T requires the transformation of the derivatives in (4.2) given by

$$\frac{\partial}{\partial t} = \frac{\partial X_\Phi^{-1}}{\partial t}\frac{\partial}{\partial \eta} + \frac{\partial X_t^{-1}}{\partial t}\frac{\partial}{\partial \tau}$$

and

$$\frac{\partial}{\partial \varphi} = \frac{\partial X_\Phi^{-1}}{\partial \varphi}\frac{\partial}{\partial \eta} + \frac{\partial X_t^{-1}}{\partial \varphi}\frac{\partial}{\partial \tau}$$

The inverse transformation can be expressed in terms of the mapping itself (see Courant (1968), vol.II, ch.III, sect.4) and we obtain

$$\frac{\partial}{\partial t} = \frac{1}{J}\left(\frac{\partial X_\Phi}{\partial \tau}\frac{\partial}{\partial \eta} - \frac{\partial X_\Phi}{\partial \eta}\frac{\partial}{\partial \tau}\right) \tag{4.21}$$

and

$$\frac{\partial}{\partial \varphi} = \frac{1}{J}\left(-\frac{\partial X_t}{\partial \tau}\frac{\partial}{\partial \eta} + \frac{\partial X_t}{\partial \varphi}\frac{\partial}{\partial \tau}\right) \tag{4.22}$$

where J denotes the Jacobian defined by

$$J \equiv \frac{\partial X_\Phi}{\partial \tau}\frac{\partial X_t}{\partial \eta} - \frac{\partial X_\Phi}{\partial \eta}\frac{\partial X_t}{\partial \tau} \tag{4.23}$$

The pdf equation in the reference variables follows now in the form

$$\frac{\partial X_\Phi}{\partial \tau}\frac{\partial f^T}{\partial \eta} - \frac{\partial X_\Phi}{\partial \eta}\frac{\partial f^T}{\partial \tau} + \{\frac{\partial X_t}{\partial \eta}\frac{\partial}{\partial \tau} - \frac{\partial X_t}{\partial \tau}\frac{\partial}{\partial \eta}\}(F_\varphi^T f^T) = 0 \tag{4.24}$$

where $F_\varphi^T \equiv F_\varphi(X_\Phi(\eta,\tau), X_t(\eta,\tau))$. The mapping X_Φ, X_t is now in part fixed by the requirement that the pdf with respect to the reference variables is Gaussian

$$\frac{\partial X_\Phi}{\partial \eta} f^T(\eta,\tau) = f_G(\eta) \tag{4.25}$$

or with (4.20)

$$f(\varphi,t) = \frac{f_G(\eta)}{\frac{\partial X_\Phi}{\partial \eta}}$$

where $\varphi = X_\Phi(\eta,\tau)$ holds. The derivatives of f^T can be expressed in terms of f_G and we obtain

$$\frac{\partial f^T}{\partial \eta} = -\frac{f_G}{(\frac{\partial X_\Phi}{\partial \eta})^2}\left[\eta\frac{\partial X_\Phi}{\partial \eta} + \frac{\partial^2 X_\Phi}{\partial \eta^2}\right] \tag{4.26}$$

and

$$\frac{\partial f^T}{\partial \tau} = -\frac{f_G}{(\frac{\partial X_\Phi}{\partial \eta}^2}\frac{\partial^2 X_\Phi}{\partial \eta \partial \tau} \tag{4.27}$$

It follows that the Gaussian cancels out of the pdf equation which can be recast as

$$\left(-\eta\frac{\partial X_\Phi}{\partial \eta} - \frac{\partial^2 X_\Phi}{\partial \eta^2} + \frac{\partial X_\Phi}{\partial \eta}\frac{\partial}{\partial \eta}\right)\left(\frac{\partial X_\Phi}{\partial \tau} - F_\varphi^T\frac{\partial X_t}{\partial \tau}\right) + \frac{\partial X_\Phi}{\partial \eta}\frac{\partial}{\partial \tau}\left(F_\varphi^T\frac{\partial X_t}{\partial \eta}\right) - F_\varphi^T\frac{\partial X_t}{\partial \eta}\frac{\partial^2 X_\Phi}{\partial \eta \partial \tau} = 0 \tag{4.28}$$

If we set (compare to (4.10))

$$\frac{\partial X_\Phi}{\partial \tau} = F_\varphi^T\frac{\partial X_t}{\partial \tau} \tag{4.29}$$

it then follows from the pdf equation that

$$\frac{\partial}{\partial \tau}\left(F_\varphi^T\frac{\partial X_t}{\partial \eta}\right) = F_\varphi^T\frac{\partial X_t}{\partial \eta}\frac{\frac{\partial^2 X_\Phi}{\partial \eta \partial \tau}}{\frac{\partial X_\Phi}{\partial \eta}} \tag{4.30}$$

must also be satisfied. There are now two distinct possibilities for the mapping: We can restrict the temporal map to $X_t(\eta,\tau) = X_t(\tau)$ which then implies that $\partial X_t/\partial \eta = 0$ and the second mapping equation (4.30) is trivially satisfied. Hence, the condition that the reference measure is Gaussian does not determine the scale factor $\partial X_t/\partial \tau$. In the second case where the dependence of X_t on η is retained we find that the second mapping equation (4.30) determines the temporal evolution of X_t but not the variation with respect to η which is set arbitrarily by the initial condition.

4.2 Mapping method for the characteristic function.

The characteristic function corresponding to the pdf $f(\varphi, t)$ is defined as the Fourier transform

$$m(\zeta, \underline{x}, t) = \frac{1}{\sqrt{2\pi}} \int d\varphi f(\varphi, \underline{x}, t) \exp(i\varphi\zeta) \tag{4.31}$$

If we regard the pdf as the image of a Gaussian via $\varphi = X(\eta, t)$ we can transform the integral and obtain

$$m(\zeta, \underline{x}, t) = \frac{1}{\sqrt{2\pi}} \int d\eta \frac{\partial X}{\partial \eta} f(X(\eta, t), \underline{x}, t) \exp(i\zeta X(\eta))$$

It follows from the properties of the mapping $X(\eta)$ that

$$m(\zeta, \underline{x}, t) = \frac{1}{\sqrt{2\pi}} \int d\eta f_G(\eta) \exp(i\zeta X(\eta)) \tag{4.32}$$

holds. If we introduce the characteristic function of the Gaussian $m_G(\zeta)$ we find that the characteristic functions are related by

$$m(\zeta, \underline{x}, t) = \frac{1}{\sqrt{2\pi}} \int d\eta \int d\omega m_G(\omega) \exp\{i(\zeta X(\eta) - \omega\eta)\} \tag{4.33}$$

and we can regard

$$Y(\zeta, \omega, t) \equiv \frac{1}{\sqrt{2\pi}} \int d\eta \exp\{i(\zeta X(\eta, t) - \omega\eta)\} \tag{4.34}$$

as mapping function. It is straightforward to derive the transport equation for Y from (4.34) and the equation for X given by (4.10)

$$\frac{\partial Y(\zeta, \omega, t)}{\partial t} = m^2 \langle \nabla\Psi \cdot \nabla\Psi \rangle \{-\omega^2 Y(\zeta, \omega) + \frac{\partial}{\partial \omega}(\omega Y) +$$

$$\int d\kappa \int d\xi \kappa\xi Y(\zeta, \kappa) Y(\zeta, \xi) Y(-\zeta, \omega - \kappa - \xi)\} + i\zeta \int d\kappa \tilde{Q}(\kappa - \omega) Y(\zeta, \kappa) \tag{4.35}$$

where $\tilde{Q}$ is the Fourier transform of the source term Q. This equation is apparently nonlinear and its usefulness depends essentially of the way the limit of zero fluctuations is approached. It follows from the definition of Y (4.34) that the Gaussian characteristic function is approached if the mapping Y approaches the Dirac-function

$$Y(\zeta, \omega, t) \to \delta(\zeta - \omega) \quad as \quad X(\eta) \to \eta$$

This property eliminates Y from consideration since it leads back to the awkward properties of the time inverse diffusion equation whose solution must reduce the width of the solution profile as time evolves. However, a simple modification of the definition of the mapping

$$Z(\zeta, \eta, t) \equiv \frac{1}{\sqrt{2\pi}} \exp(i\zeta(X(\eta, t) - \eta) \tag{4.36}$$

leads to the limit

$$Z(\zeta,\eta,t) \rightarrow \frac{1}{\sqrt{2\pi}}, \quad as \quad t \rightarrow \infty$$

and the corresponding transport equation appears in the form

$$\frac{\partial Z}{\partial t} = i\tilde{Q}(\eta)\zeta Z + m^2\Gamma\langle\frac{\partial\Psi}{\partial\zeta_\alpha}\frac{\partial\Psi}{\partial\zeta_\alpha}\rangle\{\frac{\partial^2 Z}{\partial\eta^2} - \frac{1}{i\zeta Z}\left(\frac{\partial Z}{\partial\eta}\right)^2 - i\eta\zeta Z - \eta\frac{\partial Z}{\partial\eta}\} \tag{4.37}$$

We note the absence of integral terms but the presence of nonlinear terms. The characteristic function can be recovered from

$$m(\zeta;\underline{x},t) = \int d\omega m_G(\omega)\int d\eta Z(\zeta,\eta;\underline{x},t)\exp(i(\zeta-\omega)\eta) \tag{4.38}$$

In conclusion we note that there is considerable freedom in setting up a mapping procedure. The usefulness depends on two aspects: The approach of zero fluctuations and the number of independent variables, which becomes critical if more than a single probabilistic variable in the pdf is considered.

5.0 Mapping method for the multi-dimensional pdfs.

The extension of mapping methods to multi-dimensional pdfs requires some preparations. We begin with a fundamental property of the pdf equation and its consequence for mapping methods. The pdf equation is regarded as a first order pde and a slight modification of the characteristic theory of this class of equations (see Courant and Hilbert, vol.II (1962), ch.II) leads to the basic result. It will be shown that it is not necessary to resort to the cdf equation (as done by Pope, 1991) for the development of mapping methods.

5.1 Fundamental mapping equations.

Suppose the pdf $f_M(\varphi_1,\cdots,\varphi_M,t) = Prob\{\varphi_i \le \Phi_i \le \varphi_i + d\varphi_i, i = 1(1)M\}$ depends on M probabilistic variables, i.e. f_M integrates to unity with respect to $\varphi_1,\cdots,\varphi_M$, and time. The transport equation for f_M is then given by

$$\frac{\partial f_M}{\partial t} + \sum_{i=1}^{M} \frac{\partial}{\partial \varphi_i}[\langle R_i|\Phi_1 = \varphi_1,\cdots\rangle f_M] = 0 \tag{5.1}$$

where the fluxes R_i are subject to the conditions that random variables Φ_i assume the values φ_i for $i = 1(1)M$. The particular structure of the conditional expectations $\langle R_i|\cdots\rangle$ is not important for the following assertion. Consider now a local mapping $\underline{X} : R^M \to \Re^M$, where $\Re^M$ denotes the range of the variables Φ_i for $i = 1(1)M$,

$$\varphi_i = X_i(\eta_1,\cdots,\eta_M,t), \quad i = 1(1)M$$

such that the Jacobian J defined by

$$J \equiv det\left(\frac{\partial X_i}{\partial \eta_j}\right) > 0 \tag{5.2}$$

remains positive. Let $f_G(\eta_1,\cdots,\eta_M)$ be M-variate Gaussian and let

$$f_M^*(X_1(\eta_1,\cdots,\eta_M,t),\cdots,X_M(\eta_1,\cdots,\eta_M,t),t) = \frac{f_G(\eta_1,\cdots,\eta_M)}{J(\eta_1,\cdots,\eta_M,t)} \tag{5.3}$$

be the pdf defined by f_G and the Jacobian J. We will prove that f_M^* satisfies the transport equation

$$\left(\frac{\partial f_M^*}{\partial t}\right)_{\underline{\varphi}} + \sum_{i=1}^{M} \frac{\partial}{\partial \varphi_i}\left(\frac{\partial X_i}{\partial t} f_M^*\right) = 0 \tag{5.4}$$

where $\varphi_i = X_i(\eta_1,\cdots,\eta_M,t)$.

Proof: The time rate of change of f_M^* for $\underline{\eta}$ kept constant follows at once from implicit differentiation

$$\left(\frac{\partial f_M^*}{\partial t}\right)_{\underline{\eta}} = \left(\frac{\partial f_M^*}{\partial t}\right)_{\underline{\varphi}} + \sum_{i=1}^{M}\left(\frac{\partial f_M^*}{\partial \varphi_i}\right)_t \left(\frac{\partial X_i}{\partial t}\right)_{\underline{\eta}}$$

where $\varphi_i = X_i(\eta_1,\cdots,\eta_M,t)$ was used. Differentiation of the right hand side of (5.3) leads to

$$\frac{\partial}{\partial t}\left(\frac{f_G}{J}\right)_{\underline{\eta}} = -\frac{f_G}{J^2}\left(\frac{\partial J}{\partial t}\right)_{\underline{\eta}}$$

Using (5.3) we get

$$\frac{\partial}{\partial t}\left(\frac{f_G}{J}\right)_{\underline{\eta}} = -f_M^*\left(\frac{1}{J}\frac{\partial J}{\partial t}\right)_{\underline{\eta}}$$

The time rate of change of the Jacobian is given as a sum of determinants by

$$\frac{\partial J}{\partial t} = \sum_{k=1}^{M} \begin{vmatrix} \frac{\partial X_1}{\partial \eta_1} & \cdots & \frac{\partial \dot{X}_k}{\partial \eta_1} & \cdots & \frac{\partial X_M}{\partial \eta_1} \\ \cdot & & \cdot & & \cdot \\ \frac{\partial X_1}{\partial \eta_M} & \cdots & \frac{\partial \dot{X}_k}{\partial \eta_M} & \cdots & \frac{\partial X_M}{\partial \eta_M} \end{vmatrix}$$

where the notation

$$\dot{X}_i \equiv \left(\frac{\partial X_i}{\partial t}\right)_{\underline{\eta}}$$

was used for the time derivative. Consider now a differentiable function $F(X_1, \cdots, X_M)$ where the arguments are functions $X_i(\eta_1, \cdots, \eta_M, t)$ and set up

$$\frac{\partial F}{\partial \eta_i} = \sum_{k=1}^{M} \frac{\partial F}{\partial X_k} \frac{\partial X_k}{\partial \eta_i}$$

Cramer's rule leads to an expression for the derivatives with respect to the X_i

$$J \frac{\partial F}{\partial X_i} = \begin{vmatrix} \frac{\partial X_1}{\partial \eta_1} & \cdots & \frac{\partial F}{\partial \eta_1} & \cdots & \frac{\partial X_M}{\partial \eta_1} \\ \cdot & & \cdot & & \cdot \\ \frac{\partial X_1}{\partial \eta_M} & \cdots & \frac{\partial F}{\partial \eta_M} & \cdots & \frac{\partial X_M}{\partial \eta_M} \end{vmatrix}$$

where the derivatives of F appear in the ith column. Setting $F \equiv \dot{X}_i$ and summing over $i = 1(1)M$ produces

$$J \sum_{i=1}^{M} \frac{\partial \dot{X}_i}{\partial X_i} = \sum_{k=1}^{M} \begin{vmatrix} \frac{\partial X_1}{\partial \eta_1} & \cdots & \frac{\partial \dot{X}_k}{\partial \eta_1} & \cdots & \frac{\partial X_M}{\partial \eta_1} \\ \cdot & & \cdot & & \cdot \\ \frac{\partial X_1}{\partial \eta_M} & \cdots & \frac{\partial \dot{X}_k}{\partial \eta_M} & \cdots & \frac{\partial X_M}{\partial \eta_M} \end{vmatrix}$$

which is identical with the time rate of change of the Jacobian. It follows that

$$\left(\frac{1}{J}\frac{\partial J}{\partial t}\right)_{\underline{\eta}} = \sum_{i=1}^{M} \frac{\partial \dot{X}_i}{\partial X_i}$$

holds. Combining the results for the left and the right hand sides and using

$$\varphi_i = X_i(\eta_1, \cdots, \eta_M, t)$$

leads to the conclusion that f_M^*, as defined by (5.3), satisfies

$$\left(\frac{\partial f_M^*}{\partial t}\right)_{\underline{\varphi}} + \sum_{i=1}^{M} \frac{\partial f_M^*}{\partial \varphi_i} \dot{X}_i + \sum_{i=1}^{M} f_M^* \frac{\partial \dot{X}_i}{\partial \varphi_i} = 0$$

or

$$\left(\frac{\partial f_M^*}{\partial t}\right)_{\underline{\varphi}} + \sum_{i=1}^{M} \frac{\partial}{\partial \varphi_i}\left(\frac{\partial X_i}{\partial t} f_M^*\right) = 0$$

as claimed.

Note that the particular properties of the Gaussian reference measure did not enter the proof, only its time independence was used. It follows that any other time independent reference measures such as the measure with beta-function density, suitable for bounded scalars, could be used. Comparison of (5.4) with (5.1) shows that this result allows the set up of the mapping equations for any number of variables. It follows that $f_M = f_M^*$ holds if

$$\frac{\partial X_i}{\partial t} = \langle R_i | \Phi_1 = \varphi_1, \cdots \rangle, \quad i = 1(1)M \tag{5.5}$$

and the initial and boundary conditions for (5.1) and (5.4) are the same. The relations (5.5) are the central result for mapping methods. It is instructive to compare (5.5) with the dynamic equations for the scalars $\Phi_i(\underline{x}, t)$. The scalars are governed by

$$\frac{\partial \Phi_i}{\partial t}(\underline{x}, t) = R_i(\underline{x}, \Phi_1(\underline{x}, t), \cdots, \Phi_M(\underline{x}, t), t)$$

for $i = 1(1)M$ and the right hand sides R_i do not depend on the parameters $\varphi_1, \cdots, \varphi_M$. Note that the dynamic equations may be taken at different points in the flow field and the location vectors $\underline{x}$ are then labelled accordingly. The mapping equations (5.5) contain the conditional expectation of the same right hand sides R_i but the expectations depend on the conditioning parameters $\varphi_1, \cdots, \varphi_M$. The dependence on the location is now parametric if all scalars are taken at the same point.

The generalisation of (5.3) to time dependent reference measures

$$f_M^*(X_1(\eta_1, \cdots, \eta_M, t), \cdots, X_M(\eta_1, \cdots, \eta_M, t), t) = \frac{f_G(\eta_1, \cdots, \eta_M, t)}{J(\eta_1, \cdots, \eta_M, t)} \tag{5.3'}$$

leads to a modified equation for f_M^*. The dependence of the reference measure on time is established for the case of a non-degenerate M-variate Gaussian given by

$$f_M^*(\eta_1, \cdots, \eta_M; t) = \{(2\pi)^M det(M_{ij})\}^{-\frac{1}{2}} \exp\{-\frac{1}{2} \sum_{i=1}^{M} \sum_{j=1}^{M} (\eta_i - \mu_i(t)) M_{ij}^{-1} (\eta_j - \mu_j(t))\}$$

in terms of the time dependence of its mean value vector $\underline{\mu}(t)$ and covariance matrix $M_{ij}(t)$. The equation for the pdf defined by (5.3') can be shown to be

$$\left(\frac{\partial f_M^*}{\partial t}\right)_{\underline{\varphi}} + \sum_{i=1}^{M} \frac{\partial}{\partial \varphi_i}\left(\frac{\partial X_i}{\partial t} f_M^*\right) = f_M^* \frac{\partial \log(f_G)}{\partial t} \tag{5.4'}$$

The derivative for the logarithm of the reference density f_G can be established if the particular form of f_G is known. It follows for the Gaussian that

$$\frac{\partial \log(f_G)}{\partial t} = \sum_{i=1}^{M} \frac{\partial \log(f_G)}{\partial \mu_i} \frac{\partial \mu_i}{\partial t} + \sum_{i=1}^{M} \sum_{j=1}^{M} \frac{\partial \log(f_G)}{\partial M_{ij}^{-1}} \frac{\partial M_{ij}^{-1}}{\partial t}$$

holds. It follows from the pdf equation (5.1) that a time dependent reference measure is inappropriate if the right hand side of the pdf equation is zero.

The properties of the flux equations (5.5) depend essentially on the formulation of the basic laws. Their particular structure will be analyzed in the following sections for the spatial and material frames. The case of two-point pdfs will then receive special attention to illustrate the properties of mapping methods that are able to produce scale information.

5.2 Mapping method in the spatial frame.

The evaluation of the conditional expectations requires now the knowledge of the the particular properties of the fluxes R_i. The random variables Φ_i are now regarded as the the values of stochastic fields at one or more than one points $\underline{x}^{(j)}$ in the flow field D. At each point $\underline{x}^{(i)}, i = 1(1)N$ in D a set of K variables $\Phi_j, j = 1(1)K$ consisting of velocity, scalars and other variables is taken as the probabilistic variables in the pdf. The notation is modified $\Phi_j^{(i)} \equiv \Phi_j(\underline{x}^{(i)}, t)$ to indicate the location in the flow field. Accordingly are the fluxes and the components of the mapping denoted by $R_j^{(i)}$, $X_j^{(i)}$. The fluxes $R_j^{(i)}$ can be split into a local and integral contribution

$$R_j^{(i)} = L_j^{(i)}(\Phi_l^{(i)}, \frac{\partial \Phi_k^{(i)}}{\partial x_\alpha^{(i)}}, \cdots) + N_j^{(i)}(\Phi_k, \frac{\partial \Phi_k}{\partial x_\alpha}, \cdots) \tag{5.6}$$

where the lack of a superscript in the integral contribution indicates that it depends on any location in the flow field. It should be noted that the presence of spatial derivatives in the $R_j^{(i)}$ required the extension to stochastic fields. Examples for the local and integral contributions can be found by inspection of the basic laws (3.1) to (3.3) and (3.8). It is easy to see that

$$L_j^{(i)} = \nu \frac{\partial^2 \Phi_j}{\partial x_\alpha^{(i)} \partial x_\alpha^{(i)}}$$

is local and

$$N_j^{(i)} = -\frac{1}{4\pi} \int_D d\underline{y} \frac{\partial}{\partial x_j^{(i)}} G(\underline{x}^{(i)}, \underline{y}) \frac{\partial v_\alpha}{\partial y_\beta} \frac{\partial v_\beta}{\partial y_\alpha}$$

is integral and, therefore, nonlocal. The Gaussian random variables representing the arguments of the mapping are also regarded as the values of stochastic fileds at N locations $\underline{\zeta}^{(i)}$, $i = 1(1)N$ in the domain of definition R^3 of the fields Ψ_j, $j = 1(1)K$. The argument fields $\Psi_j(\underline{\zeta})$, $j = 1(1)K$ are homogeneous Gaussian fields with time independent statistical properties. The extension of the random variables to stochastic fields taken at N points in the

respective domains of definition implies that there must be a relation of these N points in R^3 for the Gaussian argument fields to the corresponding N points in the flow domain D for the image fields. This mapping $\underline{Y} : [D]^N \rightarrow [R^3]^N$ is denoted by

$$\underline{\zeta}^{(i)} = \underline{Y}^{(i)}(\underline{x}^{(1)}, \cdots, \underline{x}^{(N)}, t) \tag{5.7}$$

It is time dependent and was defined as pure stretching in the case of single point pdfs (see (4.12)). It is important to notice that $\underline{Y}$ is not determined at this point and the subsequent development will show that $\underline{Y}$ may depend on the mapping $X_j^{(i)}$.

The fundamental requirement of mapping methods is now that the conditional expectations of the turbulent fields $\Phi_j^{(i)}(\underline{x}^{(i)}, t)$ is equal to the expectations of the images of the Gaussian argument fields $\Psi_i(\underline{\zeta}^{(j)})$, $i = 1(1)K$, $j = 1(1)N$. If we denote the fluxes taken at the image fields with $\hat{R}_j^{(i)}$

$$\hat{R}_j^{(i)} = R_j^{(i)}(X_1^{(1)}(\Psi_1^{(1)}, \cdots), \cdots, X_K^{(N)}(\Psi_1^{(1)}, \cdots), \underline{x}^{(1)}, \cdots, \underline{x}^{(N)}, t) \tag{5.8}$$

and

$$\hat{\Phi}_j^{(i)} = X_j^{(i)}(\Psi_1^{(1)}(\underline{Y}^{(1)}(\underline{x}^{(1)}, \cdots, \underline{x}^{(N)}, t)), \cdots, \Psi_K^{(N)}(\underline{Y}^{(N)}(\underline{x}^{(1)}, \cdots, \underline{x}^{(N)}, t)), \underline{x}^{(1)}, \cdots, \underline{x}^{(N)}, t) \tag{5.9}$$

for $i = 1(1)N$, $j = 1(1)K$, we can write the mapping closure as

$$\langle R_j^{(i)} | \Phi_1^{(1)} = \varphi_1^{(1)}, \cdots \rangle = \langle \hat{R}_j^{(i)} | \Psi_1^{(1)} = \eta_1^{(1)}, \cdots \rangle \tag{5.10}$$

where the fact that the mapping has a positive Jacobian was used to express the conditions on the image variables in terms of the argument variables. The equations

$$\frac{\partial X_j^{(i)}}{\partial t}(\eta_1^{(1)}, \cdots, \eta_K^{(N)}, \underline{x}^{(1)}, \cdots, \underline{x}^{(N)}, t) = \langle \hat{R}_j^{(i)} | \Psi_1^{(1)} = \eta_1^{(1)}, \cdots \rangle, \quad j = 1(1)K, \quad i = 1(1)N \tag{5.11}$$

(with appropriate change of notation compared to (5.5)) are called flux equations. Introducing the the representation (5.6) for the fluxes leads to

$$\frac{\partial X_j^{(i)}}{\partial t} = \langle \hat{L}_j^{(i)} | \Psi_1^{(1)} = \eta_1^{(1)}, \cdots \rangle + \langle \hat{N}_j^{(i)} | \Psi_1^{(1)} = \eta_1^{(1)}, \cdots \rangle \tag{5.12}$$

The presence of nonlocal contributions $N_j^{(i)}$ needs some attention, because they contain the values of the turbulent fields at locations $\underline{y} \neq \underline{x}^{(i)}$ for all $i = 1(1)N$, where they are not image of a Gaussian argument field since the mapping (being local i.e. only defined for the $\underline{x}^{(i)}, i = 1(1)N$) is not defined. Extending the mapping to nonlocal (or functional) character does not make sense since no tractable mapping equation would emerge. The only avenue open on the level of N-point pdfs is the construction of an additional closure for the nonlocal

terms (such a closure was outlined by Chen et al. (1989)). This aspect of mapping methods will not be discussed in the present chapter.

It is important to notice that the pdf f_M^* defined by (5.3) is not solution of the pdf transport equation (3.19) for $N > 1$ or non-homogeneous turbulence if the mapping $X_j^{(i)}$ is only applied to the probabilistic variables $\Phi_j^{(i)}$. This is a consequence of the fact that the locations $\underline{x}^{(i)}$ in the spatial frame are parameters and not probabilistic variables since there is no transport equation governing them. However, it is clear from the structure of the convective term in (3.19) that the notion of the mapping can be extended to include $\underline{Z} : [R^3]^N \rightarrow [D]^N$ which is determined by

$$\frac{\partial Z_j^{(i)}}{\partial t} = X_j^{(i)}(\eta_1^{(1)}, \cdots, \eta_K^{(N)}, \underline{x}^{(1)}, \cdots, \underline{x}^{(N)}, t) \tag{5.13}$$

for $j = 1, 2, 3$ and $i = 1(1)N$, where the supscripts of $X_j^{(i)}$ are arranged such that $j = 1, 2, 3$ correpond to the velocity vector. The closure is completed by requiring that $\underline{Z}$ is the inverse map of $\underline{Y}$ introduced in (5.7)

$$Z_j^{(i)} = \left(Y_j^{(i)}\right)^{-1} \tag{5.14}$$

It is now apparent that we must require that $\underline{Y} : [D]^N \rightarrow [R^3]^N$ has a unique inverse. It follows then that the mapping $\underline{Y}$ for the domains of definition is in general a function of the same set of independent varaiables as the mapping $\underline{X}$ of the range of values.

5.3 Mapping method in the material frame.

The basic laws in the material frame can be given in mixed (spatial-material) notation as follows

$$\frac{\partial}{\partial t} X_\alpha(\underline{a}, t) = V_\alpha(\underline{a}, t) \tag{5.15}$$

as kinematic condition and

$$\frac{\partial V_\alpha}{\partial X_\alpha} = 0 \tag{5.16}$$

$$\frac{\partial V_\alpha}{\partial t} = -\frac{1}{\rho}\frac{\partial P}{\partial X_\alpha} + \nu \frac{\partial^2 V_\alpha}{\partial X_\beta \partial X_\beta} \tag{5.17}$$

$$\frac{\partial \Phi}{\partial t} = Q(\Phi) + \Gamma \frac{\partial^2 \Phi}{\partial X_\beta \partial X_\beta} \tag{5.18}$$

where $\underline{X}(\underline{a}, t)$, $\underline{V}(\underline{a}, t)$, $P(\underline{a}, t)$ and $\Phi(\underline{a}, t)$ denote now position, velocity, pressure and scalar in the material frame as function of the label variable $\underline{a} \equiv \underline{X}(\underline{a}, 0)$ and time t. The time derivative is now the substantial derivative with the label $\underline{a}$ kept fixed. It was shown in section 1.1 that the implicit derivatives with respect to the actual location can be expressed in terms of derivatives with respect to the independent variable $\underline{a}$, but the resulting expressions are highly nonlinear and will be invoked only if necessary. The set of dependent variables

consists now of position $\underline{X}$, velocity $\underline{V}$ and scalar Φ and the mapping equations developed in section 5.1 can be applied without modifications. It is worth noting that the minimal set of dependent variables appearing in the spatial frame (section 5.2) requires an extension of the mapping and results in the same set of variables for the mapping as in the material frame. The components of the mapping $X_j^{(i)}$ (not to be confused with location $\underline{X}$ in the material frame) are ordered such that $X_j^{(i)}$ corresponds to location for $j = 1,2,3$, to velocity for $j = 4,5,6$ and to the scalar for $j = 7$ and the superscript indicates the material point $\underline{a}^{(i)} \in D(0)$. The flow domain $D(t)$ is a function of time and represents the range of the dependent variable position $\underline{X}$ whereas $D(0)$ is the domain of definition of all dependent variables $\underline{X}$, $\underline{V}$ and Φ.

The random variables Φ_i appearing in the pdf equation (5.1) are now regarded as the the values of stochastic fields at one or more than one labels $\underline{a}^{(j)} \in D(0)$. At each label $\underline{a}^{(i)}, i = 1(1)N$ in $D(0)$ a set of K variables $\Phi_j, j = 1(1)K$ consisting of position $\underline{X}$, velocity $\underline{V}$ and the scalar Φ is taken as the set of probabilistic variables in the pdf. The notation is modified as in section 5.2 to $\Phi_j^{(i)} \equiv \Phi_j(\underline{a}^{(i)}, t)$ to indicate the location in the initial flow field. The fluxes and the components of the mapping are denoted by $R_j^{(i)}$, $X_j^{(i)}$ as before. The fluxes $R_j^{(i)}$ can be split into a local and integral contribution

$$R_j^{(i)} = L_j^{(i)}(\Phi_l^{(i)}, \frac{\partial \Phi_k^{(i)}}{\partial X_\alpha^{(i)}}, \cdots) + N_j^{(i)}(\Phi_k, \frac{\partial \Phi_k}{\partial X_\alpha}, \cdots) \tag{5.19}$$

where the lack of a superscript in the integral contribution indicates that it depends on any location in the flow field (mixed spatial-material notation is used for the fluxes). The Gaussian random variables representing the arguments of the mapping are also regarded as the values of stochastic fields at time t and at N labels $\underline{\zeta}^{(i)}$, $i = 1(1)N$ in the domain of definition R^3 of the fields Ψ_j, $j = 1(1)K$. The argument fields $\Psi_j(\underline{\zeta}, t)$, $j = 1(1)K$ are homogeneous and stationary Gaussian fields. The mapping $\underline{Y}$ introduced in the spatial frame by (5.7) appears naturally in the material frame. Recalling that the mapping $X_j^{(i)}$ represents for $j = 1,2,3$ the position of the material point (i)

$$X_j(\underline{a}^{(i)}, t) = X_j^{(i)}(\Psi_1^{(1)}, \cdots, \Psi_K^{(N)}; \underline{a}^{(1)}, \cdots, \underline{a}^{(N)}, t)$$

we note that at time $t = 0$

$$X_j^{(i)}(\Psi_1^{(1)}, \cdots, \Psi_K^{(N)}; \underline{a}^{(1)}, \cdots, \underline{a}^{(N)}, 0) = a_j^{(i)} \tag{5.20}$$

must hold. The condition of a positive Jacobian for the mapping $X_j^{(i)}$ implies that there exists a unique inverse which is for $j = 1,2,3$ the Gaussian distributed argument position field at $\underline{\zeta}^{(i)}$

$$\Psi_j(\underline{\zeta}^{(i)}) = \{X_j^{(i)}\}^{-1}(\varphi_1^{(1)}, \cdots, \varphi_K^{(N)}; \underline{a}^{(1)}, \cdots, \underline{a}^{(N)}, t)$$

$(j = 1,2,3)$. For $t = 0$ we set

$$\zeta^{(i)} = \{X_j^{(i)}\}^{-1}(\varphi_1^{(1)}, \cdots, \varphi_K^{(N)}; \underline{a}^{(1)}, \cdots, \underline{a}^{(N)}, 0) \tag{5.21}$$

and (5.20) implies that $\{X_j^{(i)}\}^{-1}(\cdots,0)$ depends only on the label $\underline{a}^{(i)}$. Hence, we have found a mapping

$$\zeta_j^{(i)} = Y_j^{(i)}(\underline{a}^{(i)}) \tag{5.22}$$

defined by

$$Y_j^{(i)}(\underline{a}^{(i)}) \equiv \{X_j^{(i)}\}^{-1}(\varphi_1^{(1)},\cdots,\varphi_K^{(N)};\underline{a}^{(1)},\cdots,\underline{a}^{(N)},0) \tag{5.23}$$

which is independent of time. In summary we note that all argument fields are stationary and homogeneous Gaussian fields. The deterministic conditions (5.20) and (5.21) at time zero are enforced as initial conditions for the mapping $X_j^{(i)}$ which approaches appropriate constants for $t \to 0$, thus producing marginal Dirac pdfs for position. There is no need to introduce time dependent reference measures.

The fundamental requirement of mapping methods is now that the conditional expectations of the turbulent fields $\Phi_j^{(i)}(\underline{a}^{(i)},t)$ is equal to the expectations of the images of the Gaussian argument fields $\Psi_i(\underline{\zeta}^{(j)})$, $i = 1(1)K$, $j = 1(1)N$. If we denote the fluxes taken at the image (surrogate) fields with $\hat{R}_j^{(i)}$

$$\hat{R}_j^{(i)} = R_j^{(i)}(X_1^{(1)}(\Psi_1^{(1)},\cdots),\cdots,X_K^{(N)}(\Psi_1^{(1)},\cdots),\underline{a}^{(1)},\cdots,\underline{a}^{(N)},t) \tag{5.24}$$

and

$$\hat{\Phi}_j^{(i)} = X_j^{(i)}(\Psi_1^{(1)}(\underline{Y}^{(1)}(\underline{a}^{(1)})),\cdots,\Psi_K^{(N)}(\underline{Y}^{(N)}(\underline{a}^{(N)})),\underline{a}^{(1)},\cdots,\underline{a}^{(N)},t) \tag{5.25}$$

for $i = 1(1)N$, $j = 1(1)K$, we can write the mapping closure as

$$\langle R_j^{(i)}|\Phi_1^{(1)} = \varphi_1^{(1)},\cdots\rangle = \langle \hat{R}_j^{(i)}|\Psi_1^{(1)} = \eta_1^{(1)},\cdots\rangle \tag{5.26}$$

where the fact that the mapping has a positive Jacobian was used to express the conditions on the image variables in terms of the argument variables. The equations

$$\frac{\partial X_j^{(i)}}{\partial t}(\eta_1^{(1)},\cdots,\eta_K^{(N)},\underline{a}^{(1)},\cdots,\underline{a}^{(N)},t) = \langle \hat{R}_j^{(i)}|\Psi_1^{(1)} = \eta_1^{(1)},\cdots\rangle, \quad j = 1(1)K, \quad i = 1(1)N \tag{5.27}$$

are called flux equations as in section 5.2. Introducing the the representation (5.6) for the fluxes leads to

$$\frac{\partial X_j^{(i)}}{\partial t} = \langle \hat{L}_j^{(i)}|\Psi_1^{(1)} = \eta_1^{(1)},\cdots\rangle + \langle \hat{N}_j^{(i)}|\Psi_1^{(1)} = \eta_1^{(1)},\cdots\rangle \tag{5.28}$$

The presence of nonlocal contributions $N_j^{(i)}$ presents the same difficulty as in the spatial frame since they contain the values of the turbulent fields at labels $\underline{a} \neq \underline{a}^{(i)}$ for al l $i = 1(1)N$.

5.4 Mapping method for two-point pdfs.

The mapping methods developed in the previous sections will be applied to a special case of particular importance. We consider the pdf taken at two points in homogeneous turbulence and restrict attention to position and velocity desribed in the material frame. The pdf equation (3.19) appears now in the form

$$\frac{\partial f_2}{\partial t}+\sum_{i=1}^{2} v_\alpha^i \frac{\partial f_2}{\partial x_\alpha^{(i)}}+\sum_{i=1}^{2}\frac{\partial}{\partial v_\alpha^i}\{[\langle \nu\triangle^{(i)}v_\alpha|\Phi(\underline{x}^{(1)})=\Phi^1,\cdots\rangle-\langle\frac{\partial p}{\partial x_\alpha^{(i)}}|\Phi(\underline{x}^{(1)})=\Phi^1,\cdots\rangle]f_2\}=0 \tag{5.29}$$

where the subscript indicates that two points are considered. Homogeneity in physical space implies that f_2 depends on $\underline{r}\equiv\underline{x}^{(2)}-\underline{x}^{(1)}$ but not on $\underline{x}\equiv\frac{1}{2}(\underline{x}^{(2)}+\underline{x}^{(1)})$ and it follows that the pdf equation is reduced to

$$\frac{\partial f_2}{\partial t}+(v_\alpha^2-v_\alpha^1)\frac{\partial f_2}{\partial r_\alpha}+\sum_{i=1}^{2}\frac{\partial}{\partial v_\alpha^i}\{[\langle \nu\triangle^{(i)}v_\alpha|\Phi(\underline{x}^{(1)})=\Phi^1,\cdots\rangle-\langle\frac{\partial p}{\partial x_\alpha^{(i)}}|\Phi(\underline{x}^{(1)})=\Phi^1,\cdots\rangle]f_2\}=0 \tag{5.30}$$

The pdf f_2 depends on relative position $\underline{r}$, velocity at two points $\underline{v}^{(i)}$, $i=1,2$ and time t. The image space S of the mapping $X_j^{(i)}$ is, therefore, spanned by the range of these variables. Since no boundaries are present for homogeneous flows it follows that the image space is given by $S=R^9$. The argument variables are all Gaussian random variables and this implies that the domain of definition of the mapping $X_j^{(i)}$ is also given by R^9. Hence, $X_j^{(i)}: R^9\to R^9$. We denote the mapping of the relative position with $\underline{Z}: R^9\to R^3$ and the mapping onto the velocity space with $\underline{X}^{(i)}: R^9\to R^3$, $i=1,2$. The image variables are now regarded as values of stochastic fields at two labels $\underline{a}^{(i)}$, $i=1,2$.

$$\Phi_j^{(i)}=\begin{cases} X_j(\underline{a}^{(2)},t)-X_j(\underline{a}^{(1)},t)\equiv\triangle X_j(\underline{a}^{(1)},\underline{a}^{(2)},t) \\ V_j(\underline{a}^{(i)},t), & \text{i=1,2}\end{cases}$$

and likewise for the argument variables

$$\Psi_j^{(i)}=\begin{cases} \Psi_j(\underline{\zeta}^{(2)},t)-\Psi_j(\underline{\zeta}^{(1)},t)\equiv\triangle\Psi_j(\underline{\zeta}^{(1)},\underline{\zeta}^{(2)},t) \\ \Psi_j(\underline{\zeta}^{(i)},t), & \text{i=1,2}\end{cases}$$

The mappings relate the argument and image variables

$$\triangle\underline{X}(\underline{a}^{(1)},\underline{a}^{(2)},t)=\underline{Z}(\triangle\underline{\Psi},\underline{\Psi}^{(1)},\underline{\Psi}^{(2)};\underline{a}^{(1)},\underline{a}^{(2)},t) \tag{5.31}$$

and

$$\underline{V}(\underline{a}^{(i)},t)=\underline{X}^{(i)}(\triangle\underline{\Psi},\underline{\Psi}^{(1)},\underline{\Psi}^{(2)};\underline{a}^{(1)},\underline{a}^{(2)},t) \tag{5.32}$$

where the label $\underline{a}$ in physical space and the domain of definition of the argument fields are related by the time independent mapping $\underline{Y}$ given by (5.22). The flux equations follow at once from section 5.3 in the form

$$\frac{\partial Z_j}{\partial t}=X_j^{(2)}-X_j^{(1)},\quad j=1,2,3 \tag{5.33}$$

and

$$\frac{\partial X_j^{(i)}}{\partial t} = \langle \hat{L}_j^{(i)} | \Delta\Psi_1 = \eta_1, \cdots \rangle + \langle \hat{N}_j^{(i)} | \Delta\Psi_1 = \eta_1, \cdots \rangle, \quad i = 1, 2 \tag{5.34}$$

The implicit form of the local and nonlocal parts of the conditional fluxes follow from (5.17) as

$$\langle \hat{L}_\alpha^{(i)} | \Delta\Psi_1 = \eta_1, \cdots \rangle = \langle \nu \frac{\partial^2 X_\alpha^{(i)}}{\partial Z_\beta \partial Z_\beta} | \Delta\Psi_1 = \eta_1, \cdots \rangle \tag{5.35}$$

and

$$\langle \hat{N}_\alpha^{(i)} | \Delta\Psi_1 = \eta_1, \cdots \rangle = -\langle \frac{1}{\rho} \frac{\partial}{\partial Z_\alpha} \hat{P}[\underline{X}(.,t), \underline{V}(.,t)] | \Delta\Psi_1 = \eta_1, \cdots \rangle \tag{5.36}$$

where the pressure is a functional of position and velocity according to (3.8) which can be translated into the material frame without difficulty. However, position and velocity in $P[\underline{X}(.,t), \underline{V}(.,t)]$ cannot be expressed in terms of any argument fields because the mapping is defined for two labels only.

The evaluation of the local part of the flux equation is rather complicated and will be outlined without explicit calculation of all expressions. Furthermore, it will be assumed that the mappings do not depend parametrically on the labels $\underline{a}^{(i)}, i = 1, 2$ and the dependence on the labels is via the map $\underline{Y}$ only (the maps $\underline{Z}$ ans $\underline{X}^{(i)}$ are autonomous with respect to label). The position field is dependent variable and the mapping is defined for two different labels. This implies that the implicit derivatives with respect to actual position must be expressed in terms of derivatives in terms of labels. The Laplacian is thus according to section 1.1 given by

$$\frac{\partial^2 X_\alpha^{(i)}}{\partial Z_\beta \partial Z_\beta} = \frac{1}{2} \epsilon_{\theta\beta\gamma} \epsilon_{\delta\eta\omega} \frac{\partial Z_\zeta}{\partial a_\eta} \frac{\partial Z_\phi}{\partial a_\omega} \frac{\partial}{\partial a_\delta} \left(\frac{\partial Z_\zeta}{\partial a_\beta} \frac{\partial Z_\phi}{\partial a_\gamma} \frac{\partial X_\alpha^{(i)}}{\partial a_\theta} \right) \tag{5.37}$$

The argument fields $\Delta\underline{\Psi}$ and $\underline{\Psi}^{(i)}, i = 1, 2$ depend on the label $\underline{a}$ via the map $\underline{Y}(\underline{a})$ and parametrically as indicated in (5.31) and (5.32). It is now more convenient to expand (5.37) into

$$\frac{\partial^2 X_\alpha^{(i)}}{\partial Z_\beta \partial Z_\beta} = \frac{1}{2} \epsilon_{\theta\beta\gamma} \epsilon_{\delta\eta\omega} \frac{\partial Z_\zeta}{\partial a_\eta} \frac{\partial Z_\phi}{\partial a_\omega} \frac{\partial Z_\zeta}{\partial a_\beta} \frac{\partial Z_\phi}{\partial a_\gamma} \frac{\partial^2 X_\alpha^{(i)}}{\partial a_\theta \partial a_\delta} + \epsilon_{\theta\beta\gamma} \epsilon_{\delta\eta\omega} \frac{\partial Z_\zeta}{\partial a_\eta} \frac{\partial Z_\phi}{\partial a_\omega} \frac{\partial Z_\zeta}{\partial a_\beta} \frac{\partial X_\alpha^{(i)}}{\partial a_\theta} \frac{\partial^2 Z_\phi}{\partial a_\gamma \partial a_\delta} \tag{5.38}$$

Implicit differentiation leads to

$$\frac{\partial Z_\alpha}{\partial a_\beta} = \frac{\partial Z_\alpha}{\partial \varphi_\delta} \frac{\partial \Psi_\delta}{\partial \zeta_\gamma} \frac{\partial Y_\gamma}{\partial a_\beta} + \frac{\partial Z_\alpha}{\partial \varphi_\delta^{(1)}} \frac{\partial \Psi_\delta^{(1)}}{\partial \zeta_\gamma} \frac{\partial Y_\gamma}{\partial a_\beta} + \frac{\partial Z_\alpha}{\partial \varphi_\delta^{(2)}} \frac{\partial \Psi_\delta^{(2)}}{\partial \zeta_\gamma} \frac{\partial Y_\gamma}{\partial a_\beta} \tag{5.39}$$

where $\underline{Z}(\underline{\varphi}, \underline{\varphi}^{(1)}, \underline{\varphi}^{(2)}, t)$. The mappings $\underline{Z}$ and $\underline{X}^{(i)}$ were assumed to be local. This implies that the derivatives $\partial Z_\alpha / \partial \varphi_\delta \cdots$ as well as $\partial Y_\gamma / \partial a_\beta$ (since it is the inverse of $\underline{Z}$ at time zero) are completely determined by the conditions $\Delta\underline{\Psi} = \underline{\eta} \cdots$ and the conditional expectation applies to the derivatives of the Gaussian argument fields $\Delta\underline{\Psi} \cdots$ only. The second derivatives follow from repeated application of (5.39). The conditional expectation of the Laplacian emerges as complicated combination of products of first and second derivatives of the mappings $\underline{Z}$ and $\underline{X}^{(i)}$. The degree of nonlinearity is clearly given by the nonlinearity of the momentum balance (1.5).

6.0 Conclusions.

Several conclusions can be drawn from the mapping methods discussed in the present paper.

1. Mapping methods applied to velocity pdfs require additional closure assumptions since the pressure depends in functional (integral) form on velocity.

2. Random variables which are regarded as values of stochastic fields at particular locations require an additional mapping for these locations in the domains of definition of image (turbulent) and argument (Gaussian) fields.

3. The computational effort for the flux equations is approximately M-times the effort for the pdf equation where M is the number of probabilistic variables of the pdf. Mapping methods are, therefore, not competitive for $M > 1$.

References.

Adler, R.J. (1981), "The geometry of random fields", J. Wiley, New York.

Chen, H., Chen, S. and Kraichnan, R.H. (1989), "Probability distribution of a stochastically advected scalar field", Phys. Rev. Lett., **62**, 2657.

Courant, R. and Hilbert, D. (1962), "Methods of Mathematical Physics", vol.II, Wiley-Interscience.

Courant, R. (1968), "Differential and integral calculus", vol.II, Wiley-Interscience.

Feng, G. (1991), "Mapping closure and non-Gaussianity of the scalar probability density functions in isotropic turbulence", Phys. of Fluids A, **3**, 2438.

Feng, G. and OBrien, E.E. (1991), "A mapping closure for multi-species Fickian diffusion", Phys. of Fluids A, **3**, 956.

Kraichnan, R.H. (1990), "Models for Intermittency in Hydrodynamic Turbulence", Phys. Rev. Lett. **65**, 575.

Kreiss, H.O. and Lorentz, J. (1989), "Initial-Boundary Value Problems and the Navier-Stokes Equations", Academic Press.

Lumley, J.L. (1970), "Stochastic tools in Turbulence", Academic Press.

Muldowney, P. (1987), "A general theory of integration in function spaces", Longman Scientific & Technical.

Pope, S.B. (1991), "Mapping closures for turbulent mixing and reaction", Theoret. and Computat. Fluid Dynamics **2**, 255.

Skorohod, A.V. (1974), "Integration in Hilbert Space", Springer Verlag, New York.

Valiño, L., Ros, J. and Dopazo, C. (1991), "Monte-Carlo implementation and analytic solution of an inert-scalar turbulent-mixing test problem using a mapping closure", Phys Fluids A, **3**, 2191.

Vishik, M.J. and Fursikov, A.V. (1988), "Mathematical Problems of Statistical Hydromechanics", Kluwer Academic Publ.

Appendix IV.

Prediction of compressible turbulent reacting flows.

P. Eifler[1], MAME Dept., University of California Davis, CA.95616. USA.

W. Kollmann[2], MAME Dept., University of California Davis, CA.95616. USA.

Contents:

1.0 Introduction.

2.0 Pdf transport equation for compressible flows.

2.1 Compressibility effects.

2.2 Closure model.

3.0 Prediction of supersonic hydrogen flames.

3.1 Initial conditions.

4.0 Results and comparison with experiments.

4.1 Parametric study of the compressibility model (26).

4.2 Mean values and correlations.

4.3 One-dimensional pdfs.

4.4 Two-dimensional pdfs.

5.0 Conclusions.

---

[1] Exchange student from Aachen, Germany, supported by DAAD

[2] Research supported by NASA-Lewis Grant NAG 3-836, R. Claus project monitor.

1.0 Introduction.

The prediction of compressible turbulent reacting flows requires careful consideration of all possible formulations of the basic laws to produce a set of equations suitable for pdf methods. The first step is, therefore, devoted to the study of possible formulations of the pdf method for compressible turbulent flows with combustion reactions. This aspect of the research work was carried out in a previous grant and is documented in the report by Farshchi et al. (1991). The second step is the development of closure models for this type of flow with particular emphasis on the effect of compressibility. The pdf method can be based on the transport equation for the pdf of thermo-chemical scalars plus variables measuring the rate of relative volume expansion or the material derivative of the pressure (see Farshchi et al., 1991). The pdf approach offers the possibility of treating chemical non-equilibrium in rigorous fashion, which is particularly important for high speed flows characterized by high shearing rates and short residence times. The progress achieved in the development of a closure model for the pdf equation valid in this situation and the successful application of this model to supersonic hydrogen flames will be discussed in detail.

2.0 Pdf transport equation for compressible flows.

The single point pdf equation for scalar variables determining the local thermodynamic state is considered. Turbulent flow at supersonic speed can be modified significantly by compressibility and the interaction with shocks created outside the turbulent flow field and random shocks (shocklets, Johnson et al., 1973) generated in supersonic turbulent shear layers. Pdf methods can be adapted to cope with the effects of compressibility including random discontinuities and combustion. We consider the case of infinitely fast reactions, in which three variables determine the local state: Mixture fraction, pressure and enthalpy or any other equivalent set of thermodynamic variables. Pressure can vary significantly in supersonic flows and enthalpy is not conserved due to frictional heating in high shear regions. Hence, no further simplification, as in the case of low Mach number subsonic flames, is possible. The single point pdf f_1 is then set up for the velocity $\underline{v}$, density ρ, or a local function of density such as $log(\rho)$ which will be used below, internal energy u, relative rate of volume expansion D and mixture fraction ξ (a choice that was found to be advatageous by Farshchi et al., 1991)

$$f_1(\underline{v}, d, u, \zeta, \eta; \underline{x}, t) \equiv \langle \delta(\underline{v} - \underline{v})\delta(\rho - d)\delta(\epsilon - u)\delta(D - \zeta)\delta(\xi - \eta) \rangle \tag{1}$$

The transport equation for this pdf can be obtained using standard methods and emerges in the form

$$d(\frac{\partial f_1}{\partial t} + v_\alpha \frac{\partial f_1}{\partial x_\alpha}) = -\frac{\partial}{\partial v_\alpha}\{-\langle \frac{\partial p}{\partial x_\alpha}\hat{f}\rangle + \frac{1}{Re}\langle \frac{\partial \tau_{\alpha\beta}}{\partial x_\beta}\hat{f}\rangle + Bd\langle f_\alpha \hat{f}\rangle\}$$

$$+\frac{\partial}{\partial d}(d^2\zeta f_1) - \frac{\partial}{\partial u}\{-\frac{\gamma - 1}{c_v}du\zeta f_1 + \gamma(\gamma - 1)\frac{M_0^2}{Re}\langle \Phi \hat{f}\rangle - \frac{\gamma}{Pe}\langle \frac{\partial q_\alpha}{\partial x_\alpha}\hat{f}\rangle\}$$

$$-\frac{\partial}{\partial \zeta}\{\frac{1}{Re}\langle \frac{\partial}{\partial x_\alpha}(\frac{1}{\rho}\frac{\partial \tau_{\alpha\beta}}{\partial x_\beta})\hat{f}\rangle - \langle \frac{\partial v_\alpha}{\partial x_\beta}\frac{\partial v_\beta}{\partial x_\alpha}\hat{f}\rangle + B\langle \frac{\partial f_\alpha}{\partial x_\alpha}\hat{f}\rangle - \langle \frac{\partial}{\partial x_\alpha}(\frac{1}{\rho}\frac{\partial p}{\partial x_\alpha})\hat{f}\rangle\} - \frac{\partial}{\partial \eta}\langle \frac{\partial}{\partial x_\alpha}(\rho\Gamma\frac{\partial \zeta}{\partial x_\alpha})\hat{f}\rangle \tag{2}$$

Mean thermodynamic properties follow from the pdf f_1 by integration using the local relation determined by equilibrium considerations. The mean pressure for instance is given by

$$\langle p \rangle = \int dd \int du \int d\eta p(d,u,\eta) f_1(d,u,\eta)$$

where $p(d,u,\eta)$ denotes the local relation of pressure to density, internal energy and mixture fraction. The calculation of this type of local relation is straightforward. The relations for other thermodynamic variables such as composition and temperature to the pdf variables density, internal energy and mixture fraction were established using the equilibrium code STANJAN (Reynolds, 1986).

2.2 Closure model for the pdf equation.

The pdf equation to be considered is the result of integration of (2) over velocity space. It is given in terms of the density-weighted pdf $\tilde{f}_1$ defined by (Kollmann, 1990)

$$\tilde{f}_1 \equiv \frac{\rho(\varphi_1,\cdots,\varphi_l)}{\langle\rho\rangle} f_1(\varphi_1,\cdots,\varphi_l;\underline{x},t) \tag{3}$$

where $\underline{\varphi}$ corresponds to the scalar variables $(\rho, \epsilon, D, \zeta)$ and $l = 4$. The integrated pdf transport equation for the set of l thermo-chemical variables follows from (2) for high Reynolds numbers in the form

$$\langle\rho\rangle\{\frac{\partial\tilde{f}_1}{\partial t} + \tilde{v}_\beta\frac{\partial\tilde{f}_1}{\partial x_\beta} - \frac{\partial}{\partial d}(d\zeta\tilde{f}_1)\} + \frac{\partial}{\partial u}\{-\langle\rho\rangle\frac{\gamma-1}{c_v}u\zeta\tilde{f}_1 + \gamma(\gamma-1)\frac{M_0^2}{Re}\langle\Phi\hat{f}\rangle\}$$

$$+\frac{\partial}{\partial\eta}\{-\langle\frac{\partial v_\alpha}{\partial x_\beta}\frac{\partial v_\beta}{\partial x_\alpha}\hat{f}\rangle + B\langle\frac{\partial f_\alpha}{\partial x_\alpha}\hat{f}\rangle - \langle\frac{\partial}{\partial x_\alpha}(\frac{1}{\rho}\frac{\partial p}{\partial x_\alpha})\hat{f}\rangle\} = -\frac{\partial}{\partial x_\alpha}(\langle\rho\rangle\langle v_\alpha''|\Psi_j=\varphi_j\rangle\tilde{f}_1)$$

$$-\frac{\partial}{\partial u}\frac{\gamma}{Pe}\langle\frac{\partial q_\alpha}{\partial x_\alpha}\hat{f}\rangle - \frac{\partial}{\partial\zeta}\frac{1}{Re}\langle\frac{\partial}{\partial x_\alpha}(\frac{1}{\rho}\frac{\partial\tau_{\alpha\beta}}{\partial x_\beta})\hat{f}\rangle - \frac{\partial}{\partial\eta}\langle\frac{\partial}{\partial x_\alpha}(\rho\Gamma\frac{\partial\zeta}{\partial x_\alpha})\hat{f}\rangle \tag{4}$$

The terms on the right hand side can be shown to contain dominant terms describing turbulent mixing in scalar space which has the well known structure of a time-inverse diffusion process

$$\left(\frac{\partial\tilde{f}_1}{\partial t}\right)_{mix} = -\sum_{j=2}^{l}\sum_{k=2}^{l}\frac{\partial^2}{\partial\varphi_j\partial\varphi_k}(\langle\epsilon_{jk}|\Psi_j=\varphi_j\rangle\tilde{f}_1) \tag{5}$$

and the scalar dissipation rates ϵ_{ij} in the conditional expectations are defined by

$$\epsilon_{ij} \equiv \Gamma\frac{\partial\Psi_i}{\partial x_\alpha}\frac{\partial\Psi_j}{\partial x_\alpha} \tag{6}$$

with equal diffusivities $\Gamma_i = \Gamma_j = \Gamma$ for simplicity. Note that no such term acts in the first scalar direction which corresponds to the variation of density.

2.3 Mixing Model.

Any closure model for the mixing process described by (5) should share as many properties as possible with the exact term. It should preserve normalisation and mean values and decrease variances and covariances. The pdf should remain nonnegative and should not spread outside the domain of realizable states. The pair interaction model for the $l-1$ (note that one of the scalars does not mix as it corresponds to the density, which does not diffuse) scalar variables is defined by

$$\left(\frac{\partial \tilde{f}_1}{\partial t}\right)_{mix} = \frac{1}{\tau}\{\int_{\Re} d\underline{\varphi}' \int_{\Re} d\underline{\varphi}'' \tilde{f}_1(\underline{\varphi}')\tilde{f}_1(\underline{\varphi}'')T(\underline{\varphi}', \underline{\varphi}'', \underline{\varphi}) - \tilde{f}_1(\underline{\varphi})\} \tag{7}$$

It is assumed that all scalars are appropriately normalized such that the scalar space (set of all realizable states) $\Re$ is a subset of an $l-1$-dimensional unit cube. It should be noted that $\Re$ may have intricate boundaries as a consequence of realizability conditions that mass fractions cannot become negative or exceed unity and that they must add to unity. The transition pdf $T(\underline{\varphi}', \underline{\varphi}'', \underline{\varphi})$ must satisfy the requirements

$$T(\underline{\varphi}', \underline{\varphi}'', \underline{\varphi}) = T(\underline{\varphi}', \underline{\varphi}'', \underline{\varphi}' + \underline{\varphi}'' - \underline{\varphi}) \tag{8}$$

and

$$T(\underline{\varphi}', \underline{\varphi}'', \underline{\varphi}) = 0 \ for \ \varphi \notin N(\underline{\varphi}', \underline{\varphi}'') \tag{9}$$

The central part of the condition (9) is the construction of the neighbourhood $N(\underline{\varphi}', \underline{\varphi}'')$ which is the interval $[\varphi', \varphi'']$ in the single scalar case. N can be at most the cube $C_{l-1} \equiv \{\underline{\varphi} : \varphi_i \in [\varphi_i', \varphi_i''], i = 2, l\}$ defined by $\underline{\varphi}'$ and $\underline{\varphi}''$ for pairwise interaction according to our assumption of normalisation of the scalars. Realizability requires that the mixed states are in $\Re$, hence

$$N \subseteq C_{l-1} \cap \Re \tag{10}$$

must hold. Symmetry

$$\underline{\varphi} \in N \ \Leftrightarrow \ \underline{\varphi}' + \underline{\varphi}'' - \underline{\varphi} \in N \tag{11}$$

must be imposed to insure the properties of a mixing model. Furthermore is T pdf with respect to $\underline{\varphi}$

$$\int_{\Re} d\underline{\varphi} T(\underline{\varphi}', \underline{\varphi}'', \underline{\varphi}) = 1 \tag{12}$$

Conditions (8)-(12) do not define the mixing model uniquely but represent a class of models. It is important to realize that the structure of the scalar domain $\Re$ modifies the neighbourhood N unless N is reduced to the line connecting $\underline{\varphi}'$ and $\underline{\varphi}''$. If $\underline{\varphi}'$ and $\underline{\varphi}''$ are close to the boundary of $\Re$ the neighbourhood is essentially the connecting line due to (10), but if the poi are inside $\Re$ and far away from its boundary then may N be the cube C_{l-1}. The transit pdf T determines the particular form of the mixing model and is set up in the present case as

$$T(\underline{\varphi}', \underline{\varphi}'', \underline{\varphi}) = G(\underline{\zeta})H(\underline{\varphi}', \underline{\varphi}'', \underline{\varphi}) \tag{13}$$

where

$$H(\underline{\varphi}', \underline{\varphi}'', \underline{\varphi}) = \begin{cases} \frac{1}{\mu_{l-1}(N)} & \text{for } \underline{\varphi} \in N(\underline{\varphi}', \underline{\varphi}'') \\ 0 & \text{otherwise} \end{cases} \tag{14}$$

and $\mu_{l-1}(N)$ is the $l-1$-dimensional volume of $N(\underline{\varphi}', \underline{\varphi}'')$ and $\underline{\zeta}$ denotes the centered variable

$$\zeta_i \equiv \frac{2}{\mu_{l-1}(N)^{\frac{1}{l-1}}}[\varphi_i - \frac{1}{2}(\varphi_i' + \varphi_i'')], \quad i = 2, l \tag{15}$$

It follows that T satisfies

$$\int_N d\underline{\zeta} G(\underline{\zeta}) = 2^{l-1} \tag{16}$$

and

$$G(\underline{\zeta}) = G(-\underline{\zeta}) \tag{17}$$

The present choice for the function $G(\underline{\zeta})$ is a constant determined by the condition (16) which can be regarded as the condition to assign equal probability to all possible outcomes of the mixing interaction of two fluid elements. The mixing model for (5) is thus set up.

2.4 Compressibility Effects.

It is advantageous to set up the closure model representing the effects of compressibility in the Lagrangean frame as stochastic differential equations. The basic laws are written in abbreviated form

$$\frac{d \log \rho}{dt} = -D \tag{18}$$

for mass balance

$$\frac{d D}{dt} = Q_D \tag{19}$$

for the balance equation for the relative rate of volume expansion

$$\frac{d E}{dt} = Q_E \tag{20}$$

for the energy equation in terms of the internal energy per unit mass and finally

$$\frac{d \zeta}{dt} = Q_\zeta \tag{21}$$

for the mixture fraction, where d/dt denotes the material derivative and $D \equiv \nabla \cdot \underline{v}$ the relative rate of volume expansion. The right hand side terms are conveniently set up in the Eulerian frame (which can be considered implicit Lagrangean expressions). The basic laws combined with the constitutive relations for Newtonian fluids lead to the explicit form of the Q_i given by

$$Q_D \equiv \frac{1}{Re} \frac{\partial}{\partial x_\alpha}(\frac{1}{\rho} \frac{\partial \tau_{\alpha\beta}}{\partial x_\beta}) - \frac{\partial}{\partial x_\alpha}(\frac{1}{\rho} \frac{\partial p}{\partial x_\alpha}) - \frac{\partial v_\alpha}{\partial x_\beta} \frac{\partial v_\beta}{\partial x_\alpha} + \frac{\partial q_\alpha}{\partial x_\alpha} \tag{22}$$

where q_α denotes the energy flux vector,

$$Q_E \equiv -\gamma(\gamma-1)M_a^2(1+p)D + \frac{1}{Re}\gamma(\gamma-1)M_a^2\Phi - \frac{\gamma}{Re\,Pr}\frac{\partial q_\alpha}{\partial x_\alpha} \tag{23}$$

and where Φ is the dissipation function.

$$Q_\zeta \equiv \frac{1}{Re\,Sc}\frac{\partial}{\partial x_\alpha}(\rho\Gamma\frac{\partial\zeta}{\partial x_\alpha}) \tag{24}$$

The general form of the closure model (24) for the pdf equation given above (4) (which contains the dynamics of the variables density, internal energy, relative rate of volume expansion and mixture fraction) is set up using the form of stochastic differential equation

$$dY_i = A_i dt + b_{ij}dW_j + dJ_i \tag{25}$$

The stochastic nature of (25) is given by dW_i, which is the increment of a normalized random process (such as the Wiener process), and dJ_i, which is the increment corresponding to a jump process. The closure for the equations (19) - (21) will discussed for each of them in some detail.

I. The time rate of change of the relative rate of volume expansion consists of three contributions: The increment due molecular transport which is regarded as mixing, the increment due to the passage of isentropic compression and expansion waves past the material point considered, and the passage of random shock waves past the material point considered.

The first contribution ΔD_{mix} is represented by the mixing model (7) together with the requirement that T is constant in its domain of definition. It can be shown that the viscous term in (22) implies indeed that D is subject to diffusion. Hence will D participate in the mixing model described in the previous chapter. The second contribution is modelled according to an Ornstein-Uhlenbeck process

$$\Delta D_{is} = \{c_{\rho 1}f(M_a)\frac{\Delta t}{\tau}\}^{\frac{1}{2}}\eta - c_{\rho 2}f(M_a)\frac{\Delta t}{\tau}(D-\langle D\rangle) \tag{26}$$

where $c_{\rho 1} = 1.0$ and $c_{\rho 2} = 0.5$ are constants (the values given here are arbitrarily chosen and a systematic variation is discussed in a later section) and

$$f(M_a) = M_a^2$$

is an empirical function of the local Mach-number. It ensures that the increment of D vanishes as the Mach-number goes to zero. The first part of ΔD is a Wiener process (η is a Gaussian random variable with zero mean and unit variance) representing the random stirring effect of isentropic compression and expansion waves moving past the material point considered. The second part is a drift term ensuring the existence of a steady state. Finally, we note that τ is

the turbulent time scale provided by the second order closure (see Dibble et al., 1986). The model for Q_D has now the form

$$Q_D \Delta t \doteq \Delta D_{mix} + \Delta D_{is} + \Delta D_{sh} \tag{27}$$

where the first and the second contributions have been established. The last term represents the random occurrence of shocks. This contribution is nearly singular and corresponds to the derivative of a Dirac-pseudofunction in the inviscid limit. There is no model for it at present and a way of treating random shocks will be discussed in the section II below.

II. Mass balance (18) does not require closure and contains only a drift term

$$d \log \rho = -D \, dt \tag{28}$$

as long as the relative rate of volume expansion remains sufficiently smooth. The case of random shocks leads to a singularity for D and will be treated as separate contribution to $d\log(\rho)/dt$ in the form of a jump process. If the local Mach-number is greater than unity, shocks may appear with the maximal strength given by the normal shock relation

$$G(M_a) = \begin{cases} \frac{M_a^2 - 1}{1 + \frac{\gamma - 1}{2} M_a^2} & \text{for } M_a \geq 1 \\ 0 & \text{otherwise.} \end{cases} \tag{29}$$

and the increment dJ_1 for the jump process representing the random shocks is modelled by

$$dJ_1 = G(M_a) \frac{\tilde{\epsilon}}{\tilde{k}} N_s(\frac{dt}{\tau}) \eta \tag{30}$$

where $N_s(\phi)$ denotes a nonegative integer random variable representing the number of shocks arriving at the material point in ϕ dimensionless time units and $0 \leq \eta \leq 1$ is the random variable giving the dimensionless shock strength. The current model for $N_s(o)$ is a Poisson process and η is a random variable with uniform distribution. The complete increment for the logarithm of density is thus given by

$$\Delta \log \rho \doteq - D \Delta t + dJ_1 + \Delta D_{dis} \tag{31}$$

where the last contribution is due to frictional heating at constant pressure. This contribution is given by

$$\Delta D_{dis} = \rho(\zeta, u + \Delta u, p) - \rho(\zeta, u, p)$$

where Δu is the increment of internal energy due to frictional heating. Finally, we note that $\log \rho$ does not participate in the mixing process.

III. The increment for the internal energy consists of several contributions

$$Q_E \Delta t \doteq \Delta u_{mix} + \Delta u_{is} + \{-\gamma(\gamma - 1) M_a^2 (1 + p) D + \frac{1}{Re} \gamma(\gamma - 1) M_a^2 \Phi\} \Delta t + \Delta u_{sh} \tag{32}$$

The first part is due to heat conduction and is therefore part of the mixing model applied to internal energy. The second part of the increment is due to the isentropic expansion and compression waves passing the point considered and can be written as

$$\Delta u_{is} = u(\zeta, s, \rho + \Delta\rho) - u(\zeta, s, \rho)$$

where $\Delta\rho = -D\Delta t$ denotes the change of density as a result of the change in the relative rate of volume expansion. The third part contains the pressure work term and the frictional heating contribution. The dissipation function consists of

$$\Phi = \nu\left(\frac{\partial\tilde{u}}{\partial y}\right)^2 + \tilde{\epsilon}$$

for flows of boundary layer type. The last contribution is due to the random arrival of shocks at the material point considered.

3.0 Prediction of supersonic hydrogen flames.

The closure model developed in the previous chapter was applied to the prediction of supersonic hydrogen flames burning in coflowing stream of air. The flow configuration was a round H_2 jet with a coflowing stream of air at higher temperature than the fuel. The prediction requires accurate initial data which will be discussed next.

3.1 Initial conditions.

The flow conditions of the first test case of Evans et al. (1978) are shown in Fig.1.

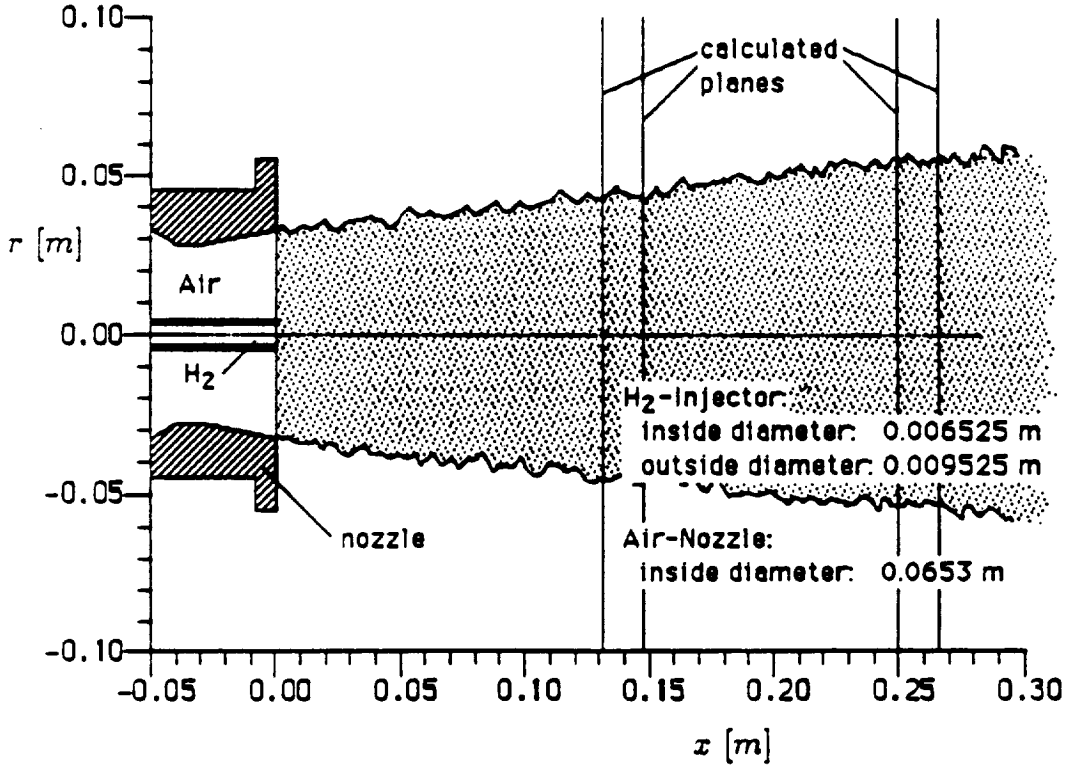

Fig.1 Flow geometry for the supersonic H_2-air flame.

Cold hydrogen at $T_{H_2} = 251K$ is injected at the axis of a circular supersonic air flow generated by a convergent-divergent nozzle. The air temperature is given by $T_{air} = 1495K$. This temperature is achieved by burning hydrogen upstream of the nozzle and then adding oxygen to the hot products to produce $X_{O_2} = 0.21$ mole fraction corresponding to air. The air flow contains, therefore, a high percentage of water as product of the heating process ($X_{H_2O} = 0.281$). The boundary conditions and the nozzle geometry are summarized in Table 1.

Exit condition		:	H_2-Jet	Outer Jet
Mach Number	Ma	:	2.0	1.9
Temperatur, K	T	:	251.0	1495.0
Mean Velocity, m/s	u_m	:	2432	1510
Pressure, MPa	p	:	0.1	0.1
Mass Fraction				
	Y_{H_2}	:	1.000	0.000
	Y_{O_2}	:	0.000	0.241
	Y_{N_2}	:	0.000	0.478
	Y_{H_2O}	:	0.000	0.281

Table 1. Initial data.

The calculation of the turbulent nonpremixed flame is carried out with the hybrid method developed by Chen and Kollmann (1988). The first step in the solution procedure is the calculation of the thermo-chemical properties, which are stored in a table for the later use in the solution of the pdf equation. The results of this calculation were reported by Farshchi et al. (1991). The next step is the set up of the initial (or entrance) conditions appropriate for the first test case of Evans et a. (1978). The initial velocity profile is shown in Fig.2 where the symbols indicate the initial location of the grid points.The H_2 stream contains 30 grid points and the coflowing air stream 18 points.

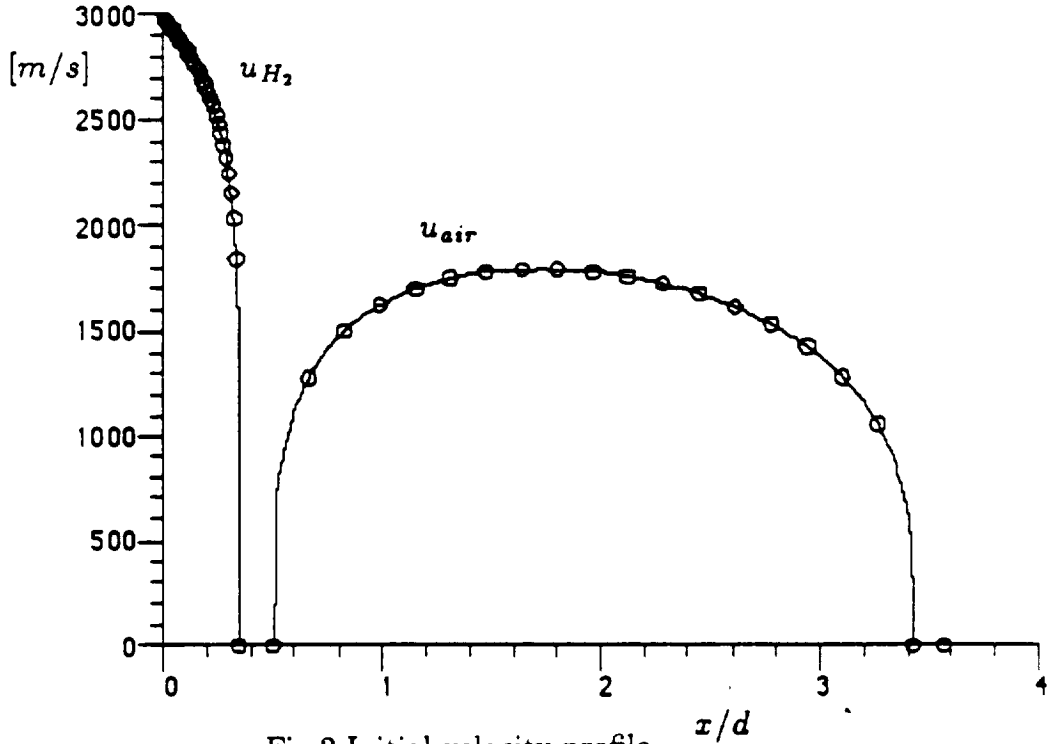

Fig.2 Initial velocity profile.

4.0 Results and comparison with experiments.

The thermo-chemical properties of the reacting mixture of H_2 and air are determined from the condition of chemical equilibrium constrained with pressure and internal energy. This assumption is unrealistic for many situations in supersonic flows, but it is the logical first step in the development of prediction models for such flows. The extension to chemical non-equilibrium has been carried out for zero Mach-number flames (see Chen and Kollmann, 1988, 1990) and, once the questions concerning compressibility effects on the turbulence structure have been sorted out, the results obtained for zero Mach-number flames can be applied to supersonic flows.

The fuel considered in the present prediction was a mixture of hydrogen and nitrogen ($Y_{H2} = 0.22335$ and $Y_{N2} = 0.77665$, in order to raise the stoichiometric value of mixture fraction from $\zeta_{st} = 0.0283$ for pure hydrogen fuel to $\zeta_{st} = 0.113$. The pure hydrogen case was also considered but only results for the former case will be presented.

The pdf equation is solved using a stochastic simulation technique (see Pope, 1985 for details) together with a second order closure model for the first and second order moments of the velocity field (Dibble et al., 1986) including modifications accounting for compressibility effects (Zeman, 1989) on the dissiaption rate based on direct simulation results by Lele (1989).

4.1 Parametric study of the compressibility model (26).

The compressibility model (26) represents the random passage of compression and expansion waves passing the material point considered. The function $f(M_a) = M_a^2$ is an ad hoc model for the unknown dependence of this model on the Mach-number. It is clear from the consideration of the low Mach-number limit that this function must be nonnegative and vanish as the Mach-number approaches zero. These two properties are obviously satisfied by this function. The model (26) contains furthermore two constants $c_{\rho 1}$ and $c_{\rho 2}$ for which no information is available at this time. Hence two reference values $c_{\rho 1=1.0}$ and $c_{\rho 2} = 0.5$ were chosen and a systematic variation of the constants was carried out to learn how the solution depends on them. The results for one of two sets of runs are presented in Fig.3 to Fig.16 varying the constant $c_{\rho 1}$. There is only a limited amount of experimental data available in Evans et al. (1978), which consist of Pitot pressure measurements and some composition information at two cross sections. The Pitot pressure results at the first station $x/D = 13.8$ in Fig.3 shows clearly that increasing the value of $c_{\rho 1}$ leads to significant improvement. It should be noted, however, that perfect agreement is not to be expected near the axis where the temperature of the fuel is below the minimal temperature of $T = 296K$ for which thermodynamic data were available and the equilibrium relations could be established. The initial temeperature of the fuel stream had to be set to this temperature and not the temperature of the experiments. The profiles for the mean velocity (which is calculated using a second order closure model solved parallel to the stochastic simulation procedure for the pdf equation) in F0g.4, the mean density in Fig.5, the mean temperature in Fig.6, the mean internal energy in Fig. 7, the mean mixture fraction in Fig.8 and the mean value for the relative rate of volume expansion D in Fig.9 show the corresponding variation with $c_{\rho 1}$. The mean value for D in Fig.9 is apparently zero, with some numerical noise which is typical for stochastic simulation techniques, visible.

The results for the second axial station at $x/D = 26.2$ confirm the tendency that emerged at the first staion. The agreement between the calculated and the measured Pitot pressure in Fig.10 is quite good except near the axis for reasons explained above. Only the mean temperature in Fig.13 and the mean density in Fig.12 show a strong dependence on $c_{\rho 1}$. The mean dilation in Fig.16 is again close to zero indicating the there is no significant turning of the mean streamlines occurring. The mean composition for fuel and oxidiser in Fig. 17 and Fig.18 shows reasonable agreement between calculation and measurements.

4.2 Mean values and correlations.

The mean values for the scalar fields and the velocity field are presented at $x/D = 15.5$ in Fig.19 to Fig.36. Pdf methods allow the calculation of any moment of the probabilistic variables of the pdf and the order of the moment is only limited by numerical accuracy. The mean values for the thermodynamic variables show that the mean internal energy (Fig.20) is minimal at the axis since the enthalpy of formation for the fuel is negative. Mean density in Fig.21 and mean temperature in Fig.22 are similar to the results obtained for low Mach-number jet flames (Chen and Kollmann, 1988). The mean pressure, however, is not constant across the supersonic flame as can be seen in Fig.23. A small pressure depression at the location of the flame is apparent and the pressure in the cold fuel is higher than the ambient pressure. The mean velocity in Fig. 24 shows that at $x/D = 15.5$ most of the initial velocity difference has been smoothed out and only small mean strain rates are present. The Reynolds stress components in Fig.25 indicate the presence of two shear layers between the fuel jet and the coflowing air jet and the air jet and stagnant surrounding air. The mean dissipation rate in Fig.26 reflects only the inner shear layer formed between fuel and coflowing air jets. The correlations of thermodynamic variables have several interesting features. Mixture fraction and internal energy are mostly negatively correlated (Fig.28) since the internal energy for the fuel is negative but the mixture fraction for the fuel is maximal (unity). The correlations of mixture fraction and density (Fig.29) and internal energy and density (Fig.32) change sign over the cross section. The correlations with the relative rate of volume expansion are rather small and rather noisy Fig.30, 33, 35 and 36).

4.3 One-dimensional pdfs.

The information on the various pdfs for the thermodynamic scalars is contained in fig.37 to fig.56 at $x/D = 15.5$ for five radial stations. The pdf for mixture fraction in Fig.37 to Fig.41 shows the change of sign of the skewness as the flow is traversed. The pdf of the internal energy in Fig.42 to Fig.46 has a shape similar to the pdf of mixture fraction with the opposite sign for the skewness. The pdf for density in Fig.47 to Fig.51 shows the appearance of entrained heated air at radial stations greater than $x/D = 84$ (Fig.49) which emerges as spike around $\rho = 0.23$. The pdf of the relative rate of volume expansion in Fig. 52 to Fig.56 is close to the Gaussian which due to the model equation (26) simulating an Ornstein-Uhlenbeck process.

4.4 Two-dimensional pdfs.

The effect of compressibility becomes apparent if two-dimensional pdfs are considered. The comparison of the one-dimensional pdfs for mixture fraction and internal energy (or any other thermodynamic variable except enthalpy, which is a linear function of mixture fraction at $M_a = 0.0$, and mixture fraction) does not lead to unambigous conclusions, because the local relation between those variables, that holds at zero Mach-number, is nonlinear. The Ornstein-Uhlenbeck process described in chapter 2.4 as model for the random fluctuations of the relative rate of volume expansion leads to a broadening of the pdf for thermodynamic variables and mixture fraction, which would be related locally in incompressible flows. The pdf of mixture fraction and internal energy shows some broadening due to compressibility as Fig.57 to Fig.61 prove. However, the pdf of density and mixture fraction in Fig.62 to Fig.66 exhibits a much more pronounced broadening in particular in shear layer between fuel and heated air at $x/D = 0.27$ in Fig.62. The pdf of density and internal energy in Fig.67 to Fig.71 confirms this fact. The pdf containing the relative rate of volume expansion D as one of the variables allow some insight into the properties of the model suggested in equation (26). The pdfs for internal energy and D in Fig.72 to Fig.76 and in particular the pdfs for density and d in Fig.77 to Fig.81 show that The statistics of those variables are not Gaussian but the marginal pdf for D is close to Gaussian.

5.0 Conclusions.

It was shown that pdfs for three scalar variables describing the local thermodynamic state in a compressible reacting flow can be determined as solutions of model equation that simulates the effects of convection, turbulent diffusion, chemical reactions and reversible and irreversible compression and expansion processes occuring randomly in a turbulent flow at high speed. The limited amount of experimental information does not allow to draw a final conclusion concerning the accuracy of the calculations, but it is clear that pdf predictions of compressible reacting flows are feasible. There are, however, several problems awaiting solution. In particular the role of the fluctuating pressure containing several different modes (acoustic mode, entropy mode) and the significance of chemical non-equilibrium need to be investigated. Pdf methods are especially well suited for the latter because they allow rigorous treatment of nonlinear and local processes.

References.

Chen, J.-Y. and Kollmann, W. (1988), *Pdf Modeling of Chemical Non- equilibrium Effects in Turbulent Non-premixed Hydro-carbon Flames*, Proc. 22nd Symp. (Int.) Comb., The Comb. Institute, 645.

Chen, J.-Y. and Kollmann, W. (1990), *Chemical Models for Pdf Modeling of Hydrogen-air Non-premixed Turbulent Flames*, Comb. Flame **79**, 75.

Dibble, R.W., Farshchi, M., Kollmann, W. and Schefer, R. W. (1986), *Second Order Closure for Turbulent Nonpremixed Flames: Scalar Dissipation and Heat Release Effect*, Proc. 21st Symp. (Int.) Comb., The Comb. Institute, 1329.

Dimotakis, P.E., (1989), *Turbulent Free Shear Layer Mixing*, AIAA-89-0262.

Evans, J.S., Schexnayder, C.J. and Beach, H.L. (1978), *Application of a Two - Dimensional Parabolic Computer Program to Prediction of Turbulent Reacting Flows*, NASA Technical Paper no. 1169.

Farshchi, M., (1986), *Prediction of Heat Release Effects on a Mixing Layer*, AIAA-Paper 86-0058

Farshchi, M., Kollmann, W. and Shirani, E.(1991), *Supersonic Turbulent Reacting Flow Modelling and Calculation.*, NEAR Report for NASA-Lewis Contract NAS 3-25633.

Johnson, D.A and Rose, W.C., (1973), *Measurements of Turbulence Transport Properties in a Supersonic Boundary Layer Flow Using Laser Velocimeter and Hot Wire Anemometer Techniques*, AIAA J., **13**, 512.

Kollmann, W. (1990), *The pdf approach to turbulent flow*, Theoret. Comput. Fluid Dynamics **1**, 249.

Lele, S.K., (1989), *Direct Numerical Simulation of Compressible Shear Flows*, AIAA-89-0374, Jan. 1989, Reno, Nevada.

Pope, S.B. (1985), *Pdf Methods for Turbulent Reacting Flows*, Progr. Energy Comb. Sci. **11**, 119.

Reynolds, W.C. (1986), *The element potential method for chemical equilibrium analyisi: STANJAN*, version 3, Dept. Mech. Engineering, Stanford University.

Zeman, O., (1989), *Dilatation Dissipation: The Concept and Application in Modeling Compressible Mixing Layers*, CTR Manuscript 100, Stanford University.

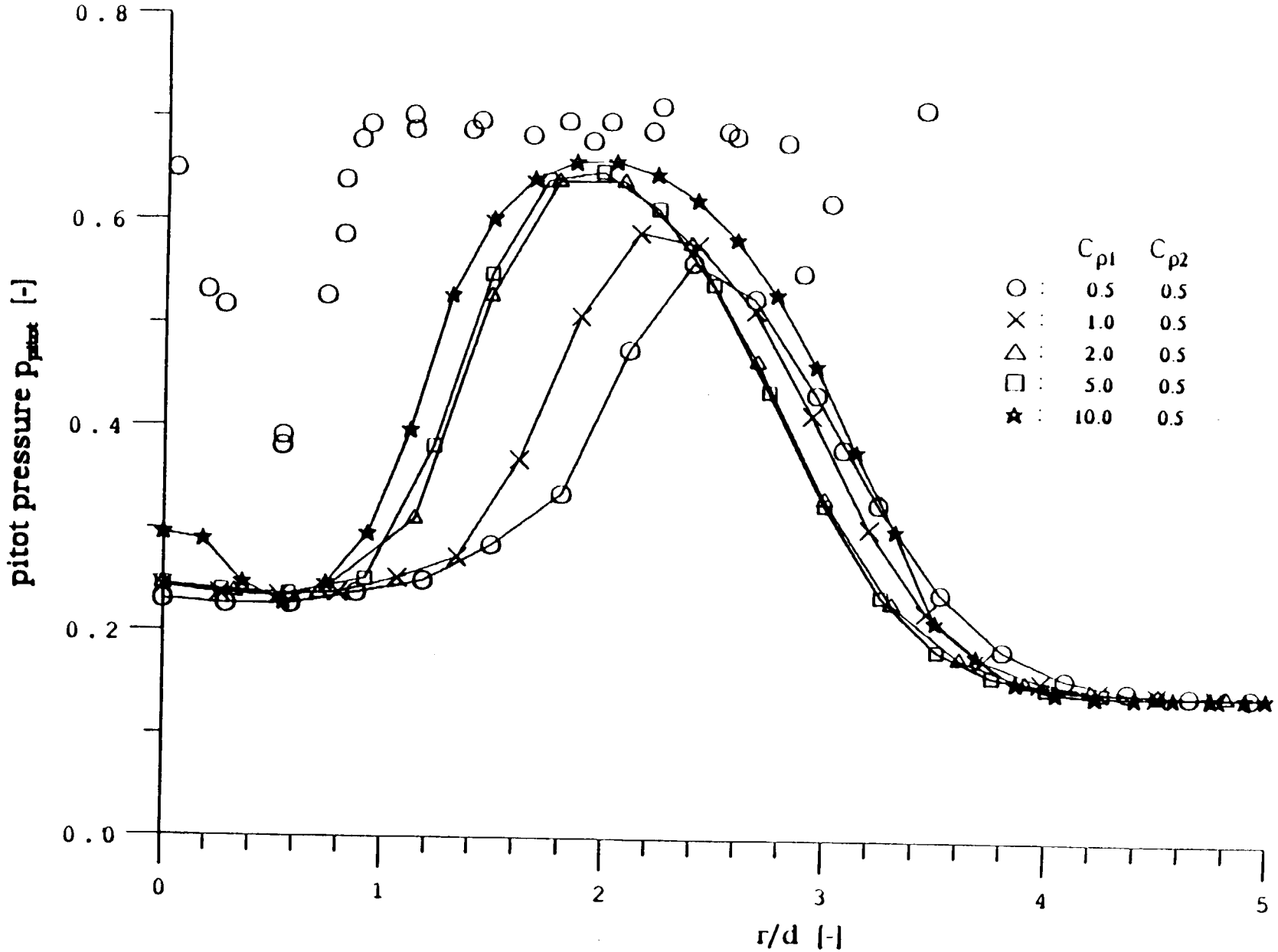

Fig. 3. Coaxial turbulent supersonic jet flame burning H_2 with air. Parametric study of the compressibility term for the stochastic simulation of the relative rate of volume expansion (equation (26)). Mean Pitot pressure at $x/D = 13.8$. Open circles are the measurements of Evans et al. (1978).

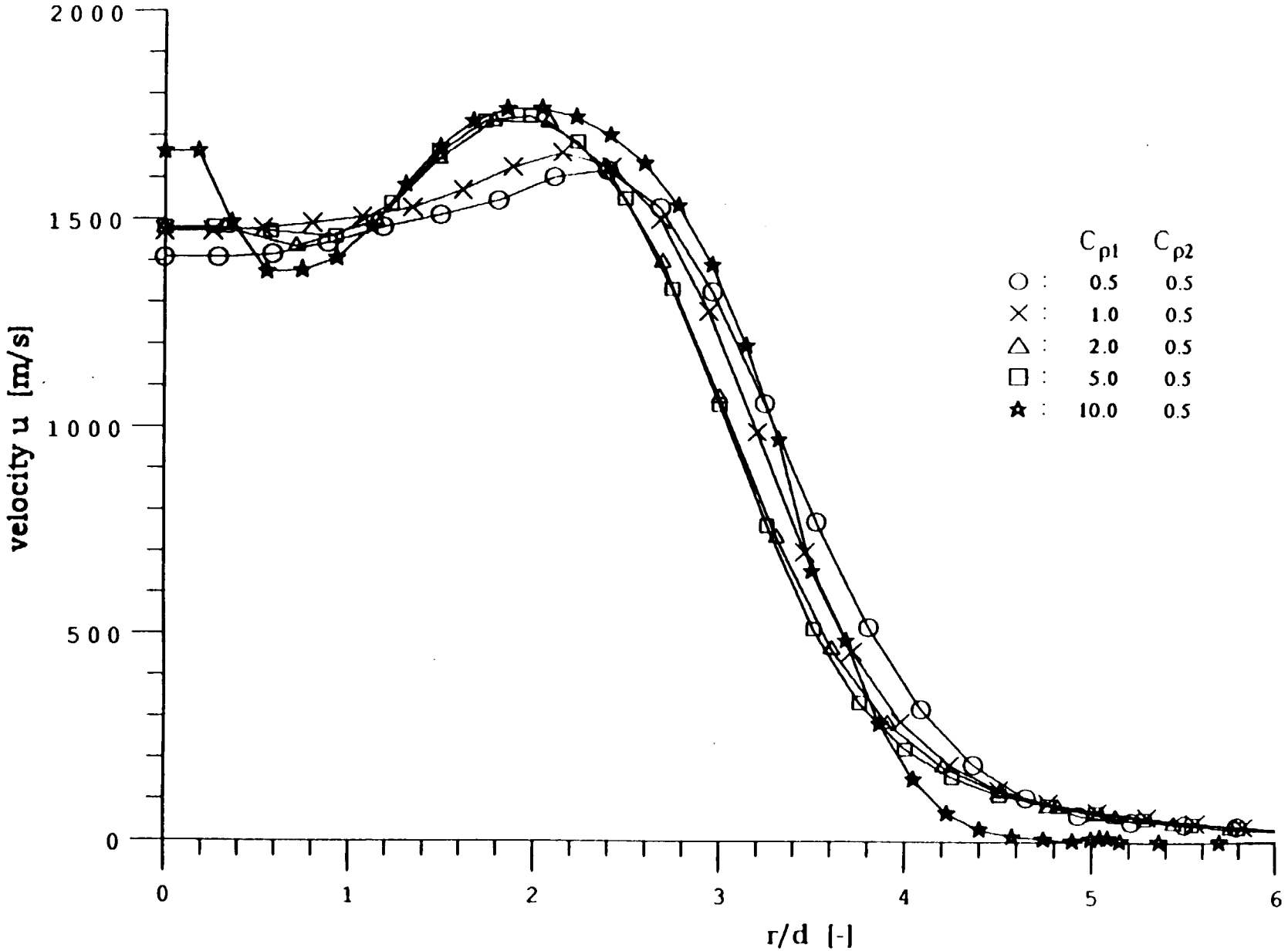

Fig. 4. Coaxial turbulent supersonic jet flame burning H_2 with air. Parametric study of the compressibility term for the stochastic simulation of the relative rate of volume expansion (equation (26)). Mean velocity at $x/D = 13.8$.

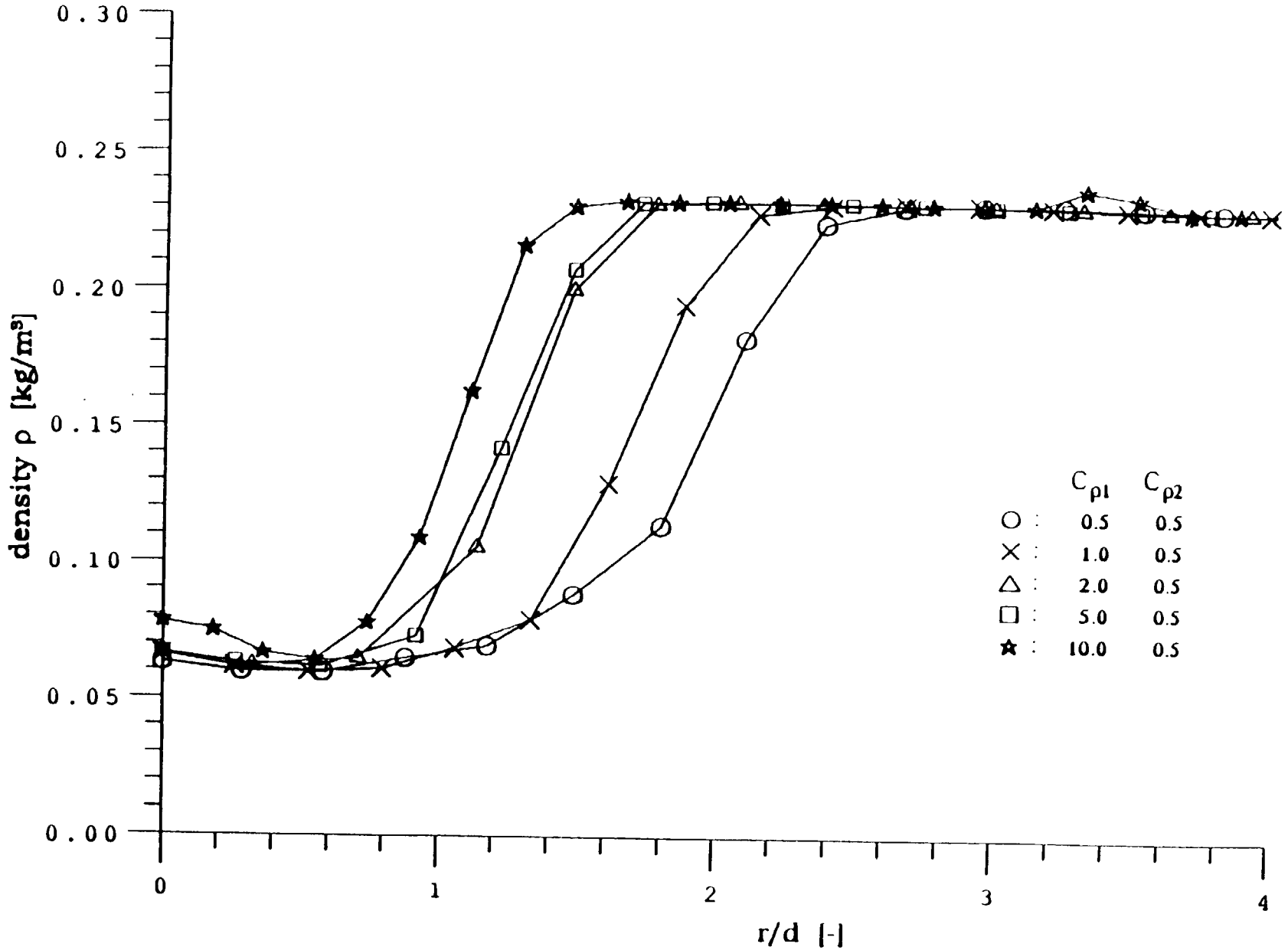

Fig. 5. Coaxial turbulent supersonic jet flame burning H_2 with air. Parametric study of the compressibility term for the stochastic simulation of the relative rate of volume expansion (equation (26)). Mean density at $x/D = 13.8$.

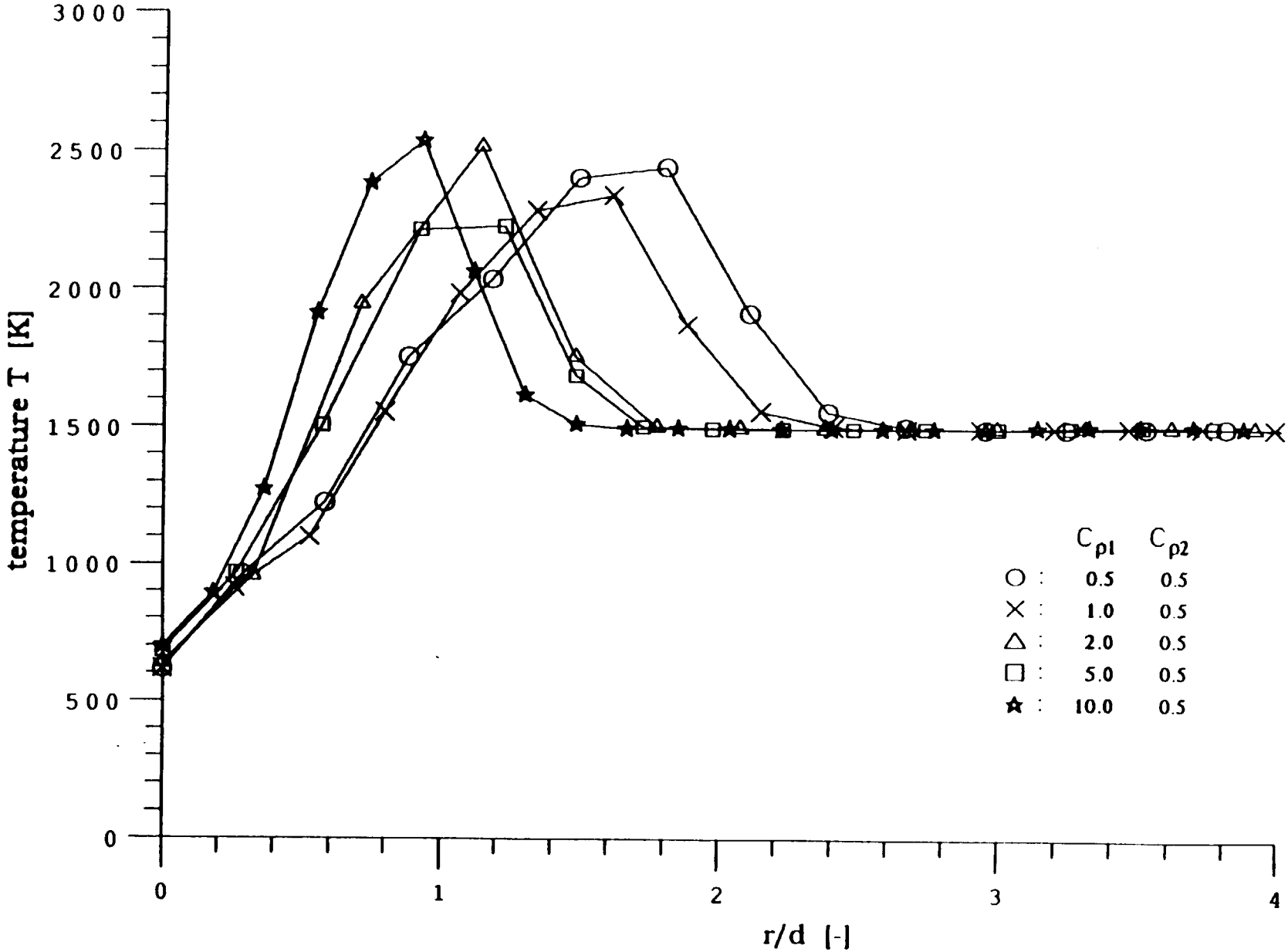

Fig. 6. Coaxial turbulent supersonic jet flame burning H_2 with air. Parametric study of the compressibility term for the stochastic simulation of the relative rate of volume expansion (equation (26)). Mean temperature at $x/D = 13.8$.

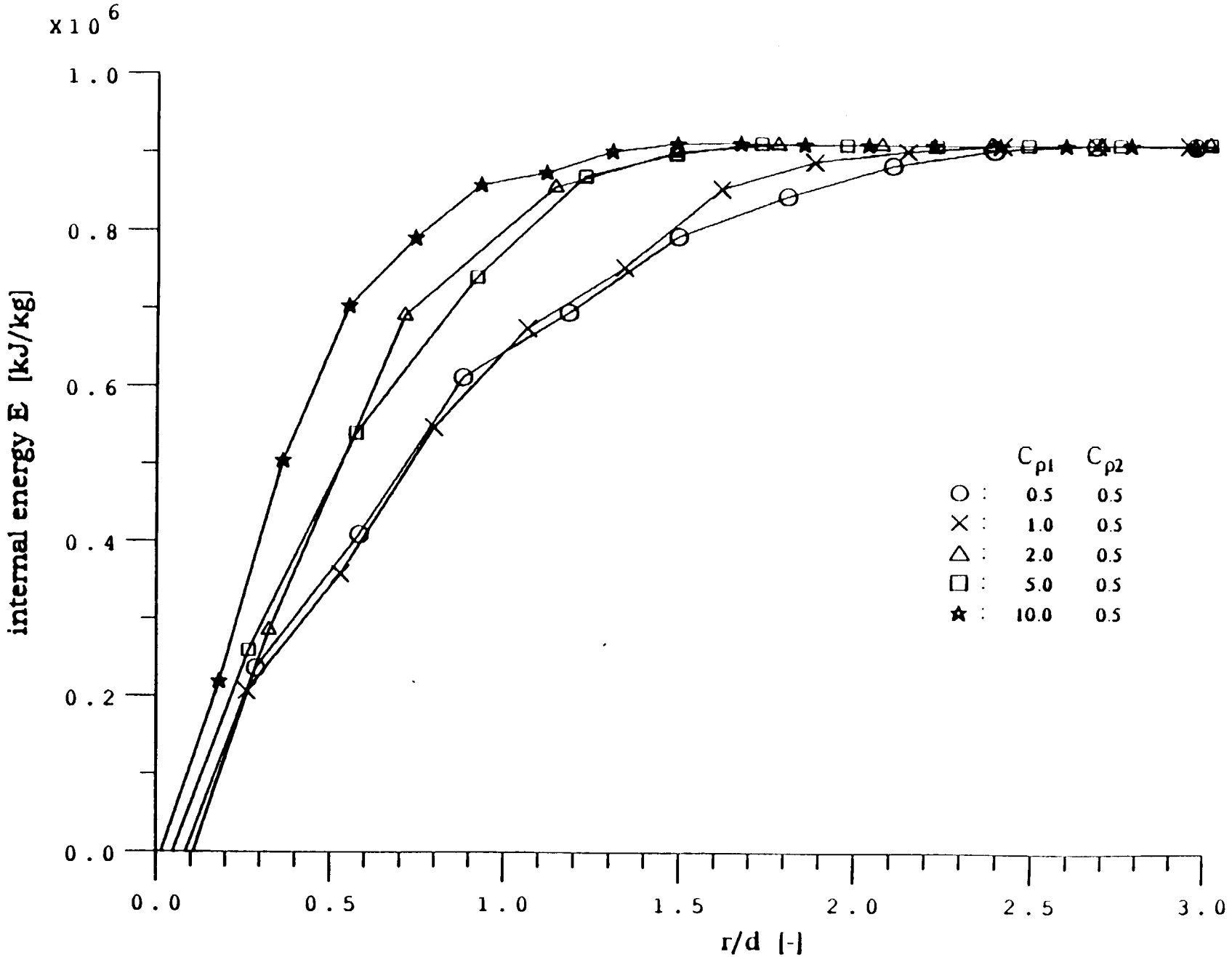

Fig. 7. Coaxial turbulent supersonic jet flame burning H_2 with air. Parametric study of the compressibility term for the stochastic simulation of the relative rate of volume expansion (equation (26)). Mean internal energy at $x/D = 13.8$.

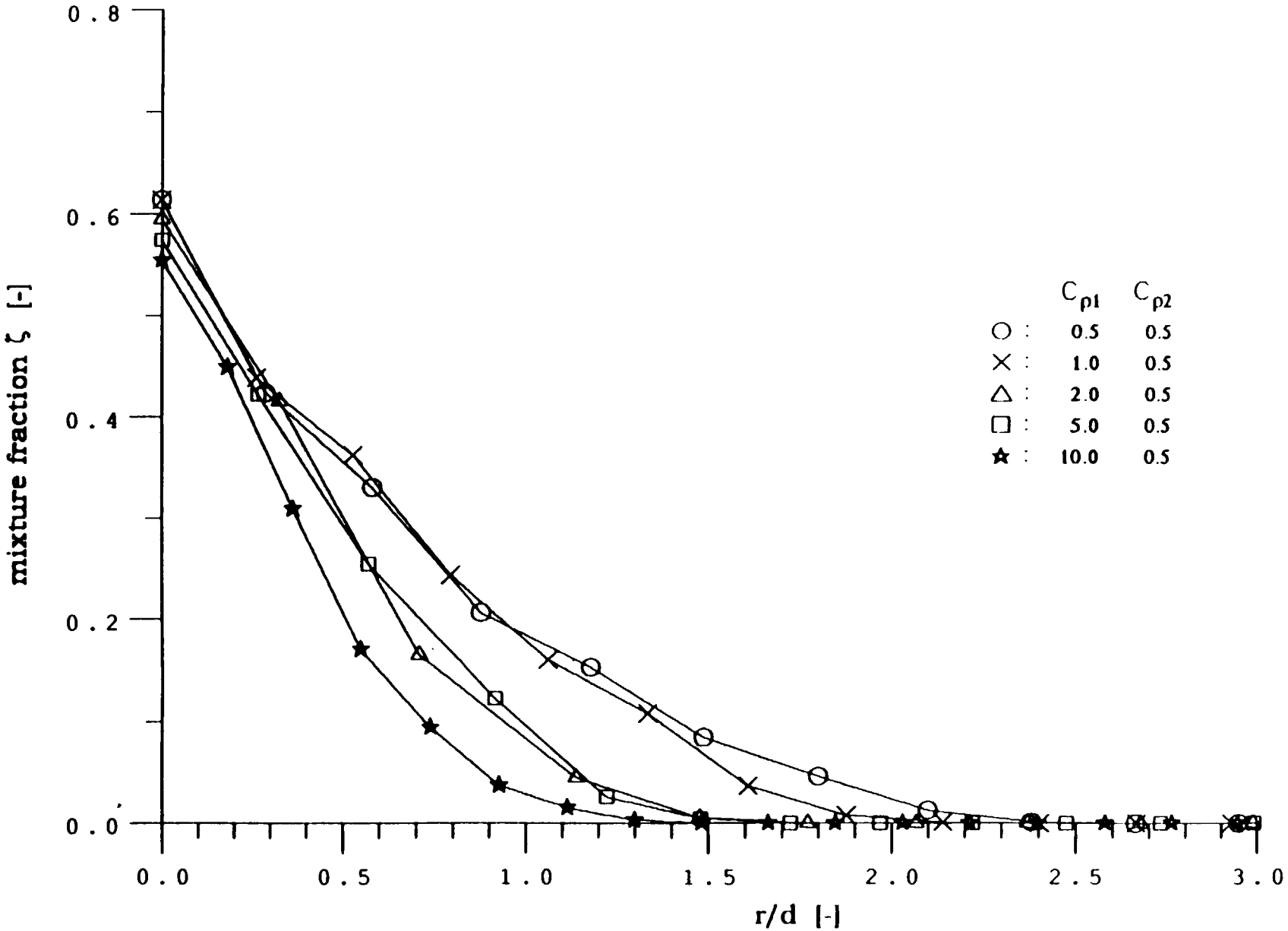

Fig. 8. Coaxial turbulent supersonic jet flame burning H_2 with air. Parametric study of the compre ibility term for the stochastic simulation of the relative rate of volume expansion (equation (26)). Mean mixture fraction at $x/D = 13.8$.

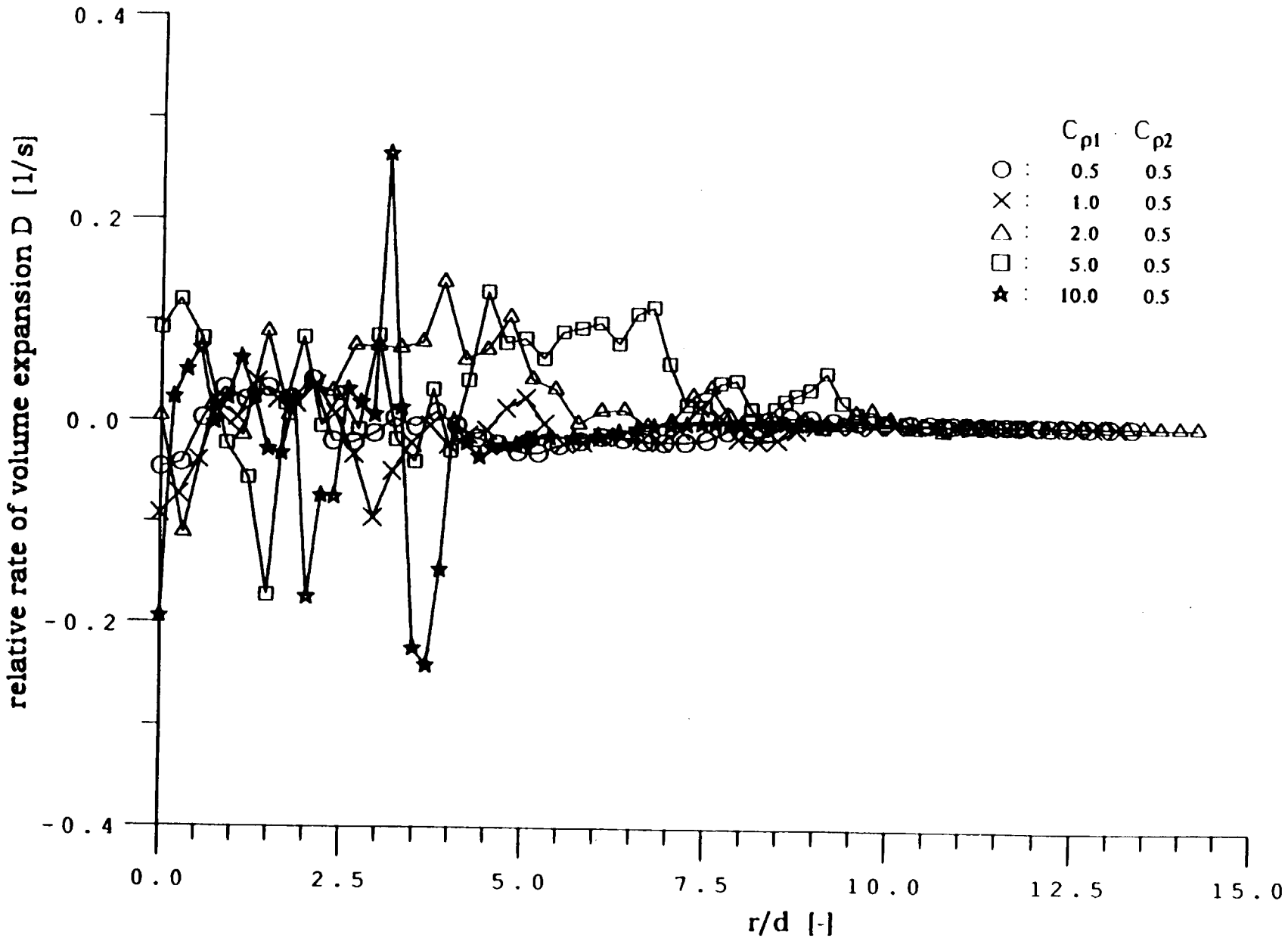

Fig. 9. Coaxial turbulent supersonic jet flame burning H_2 with air. Parametric study of the compressibility term for the stochastic simulation of the relative rate of volume expansion (equation (26)). Mean relative rate of volume expansion at $x/D = 13.8$.

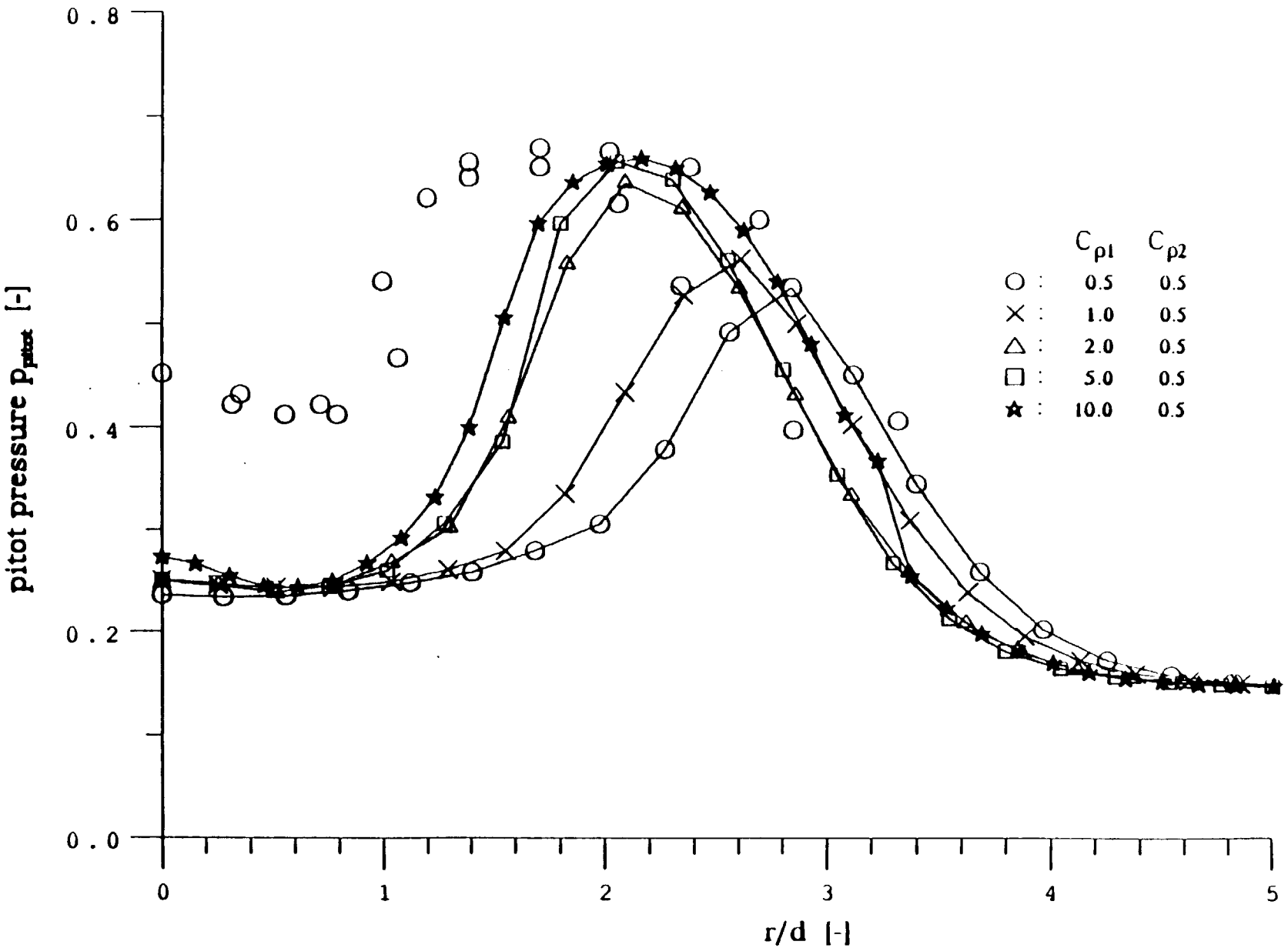

Fig. 10. Coaxial turbulent supersonic jet flame burning H_2 with air. Parametric study of the compressibility term for the stochastic simulation of the relative rate of volume expansion (equation (26)). Mean Pitot pressure at $x/D = 26.2$. Open circles are the measurements of Evans et al. (1978).

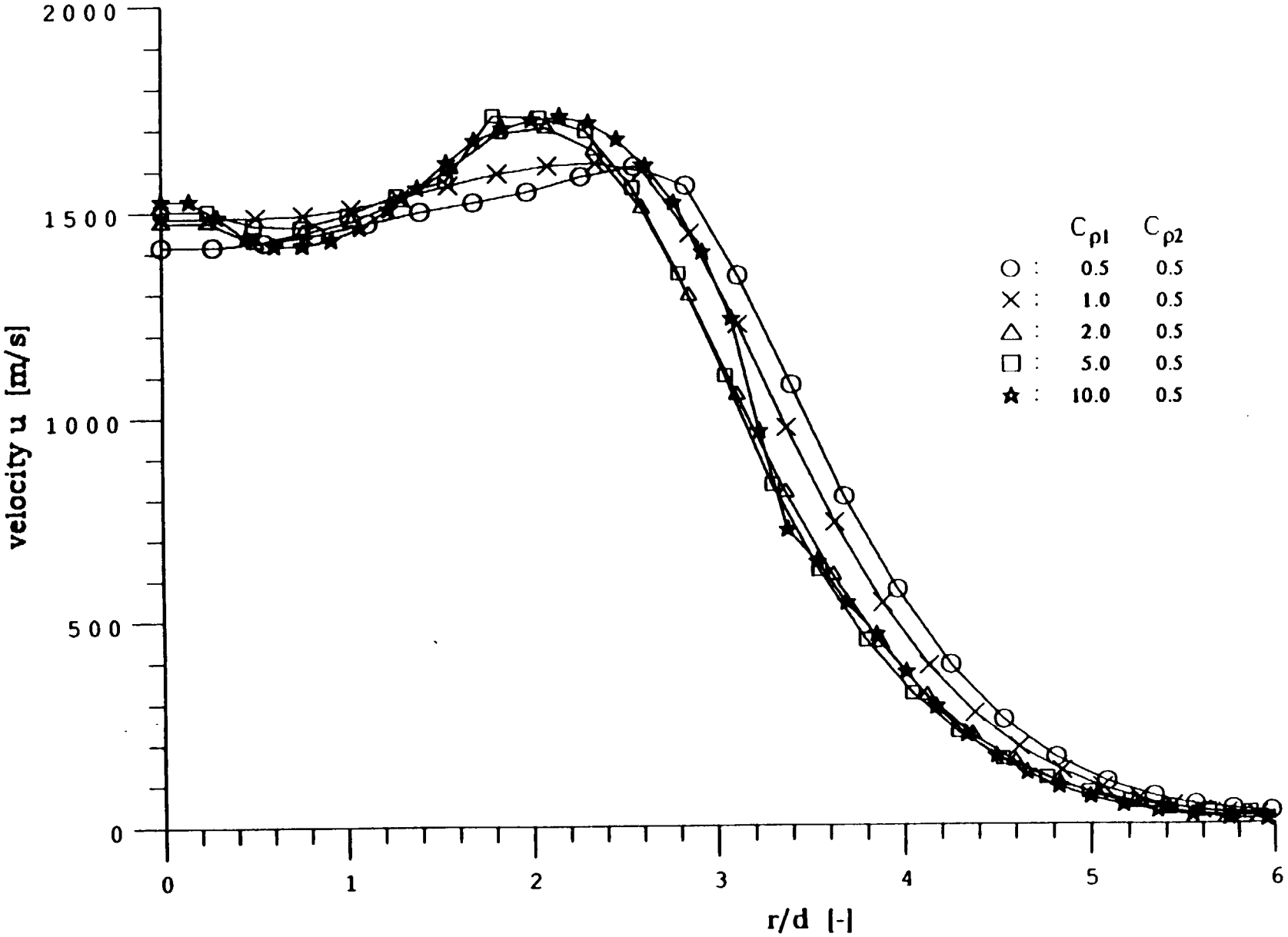

Fig. 11. Coaxial turbulent supersonic jet flame burning H_2 with air. Parametric study of the compressibility term for the stochastic simulation of the relative rate of volume expansion (equation (26)). Mean velocity at $x/D = 26.2$.

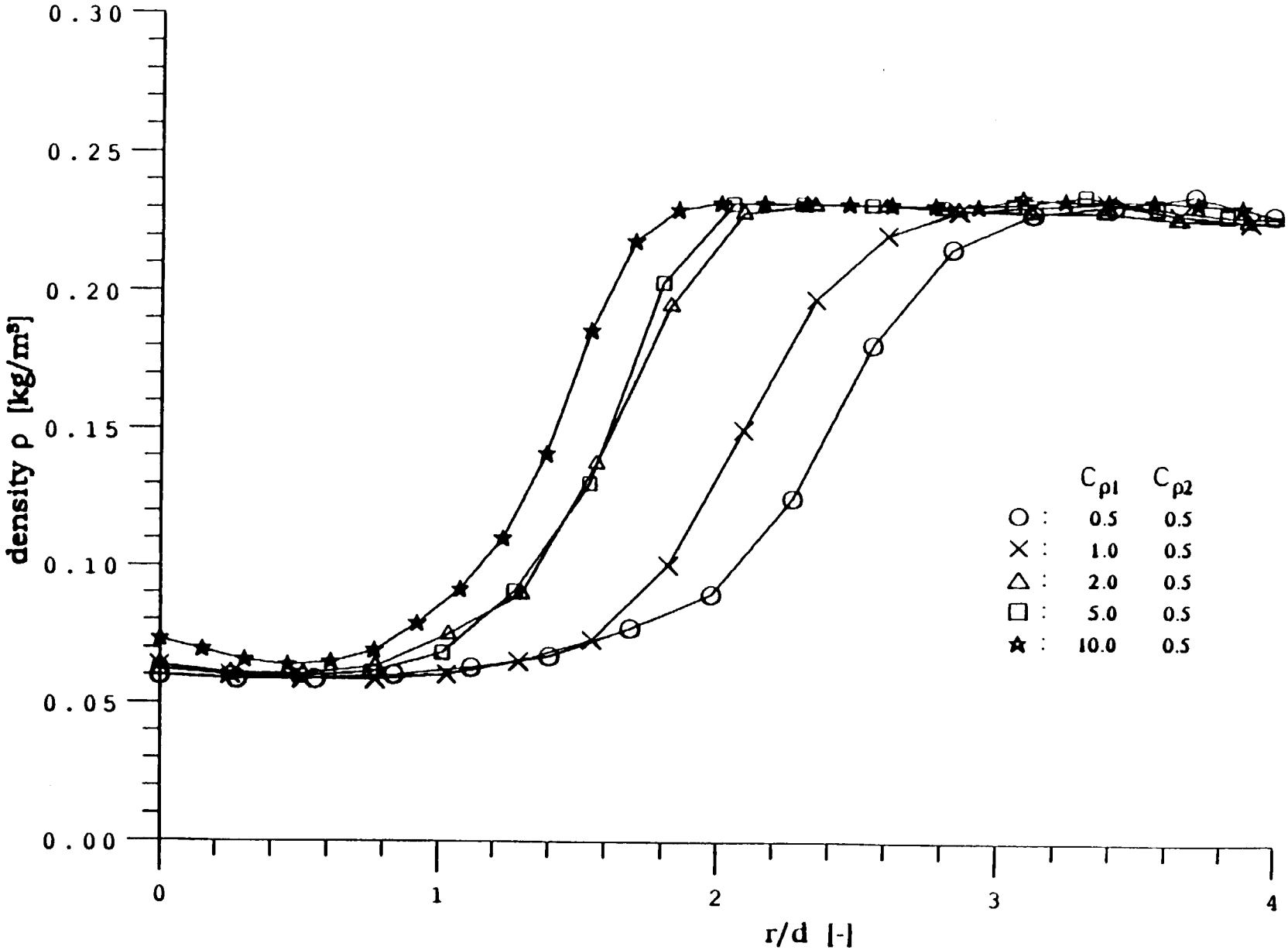

Fig. 12. Coaxial turbulent supersonic jet flame burning H_2 with air. Parametric study of the compressibility term for the stochastic simulation of the relative rate of volume expansion (equation (26)). Mean density at $x/D = 26.2$.

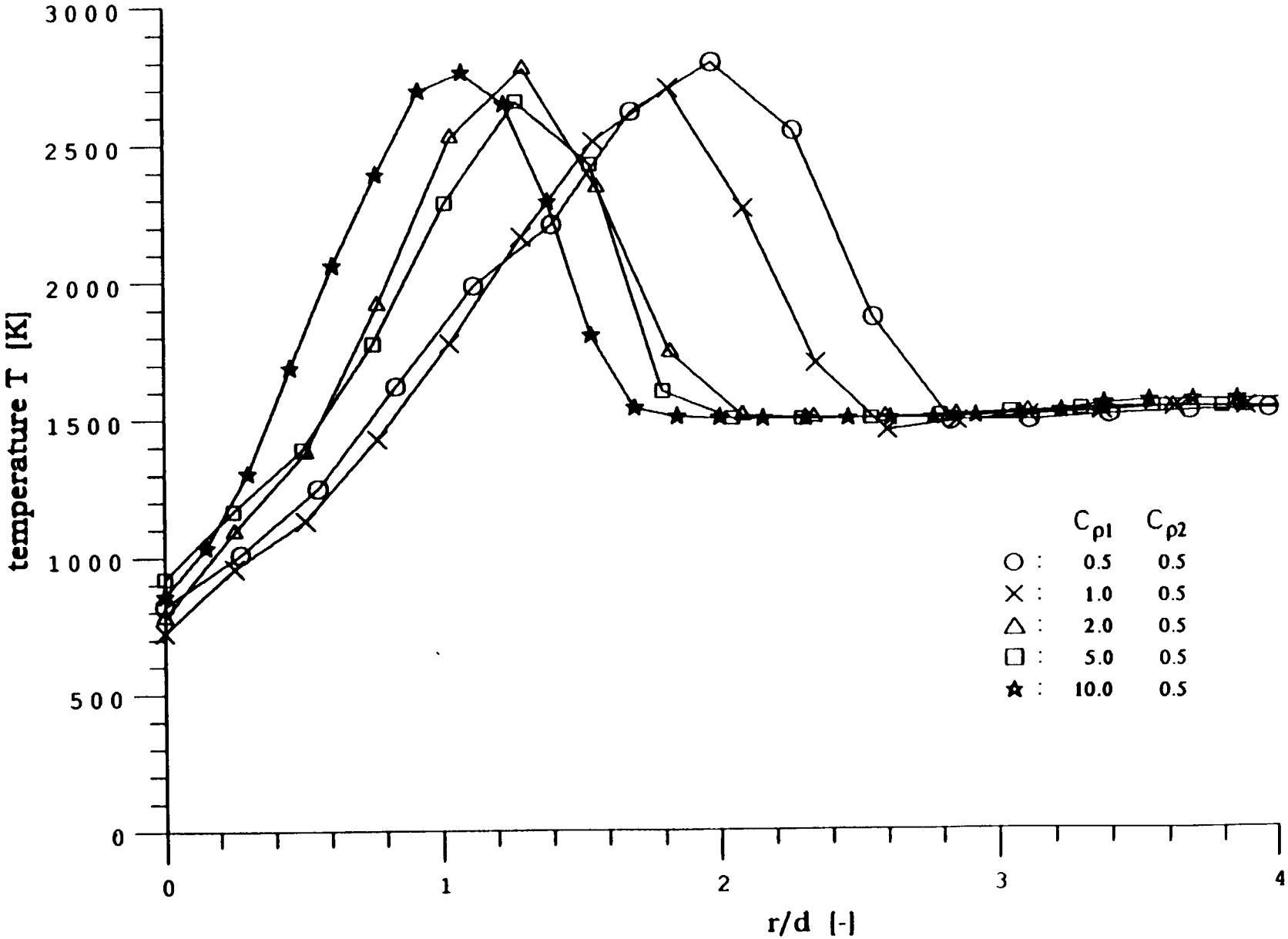

Fig. 13. Coaxial turbulent supersonic jet flame burning H_2 with air. Parametric study of t compressibility term for the stochastic simulation of the relative rate of volume expansion (equation (26)). Mean temperature at $x/D = 26.2$.

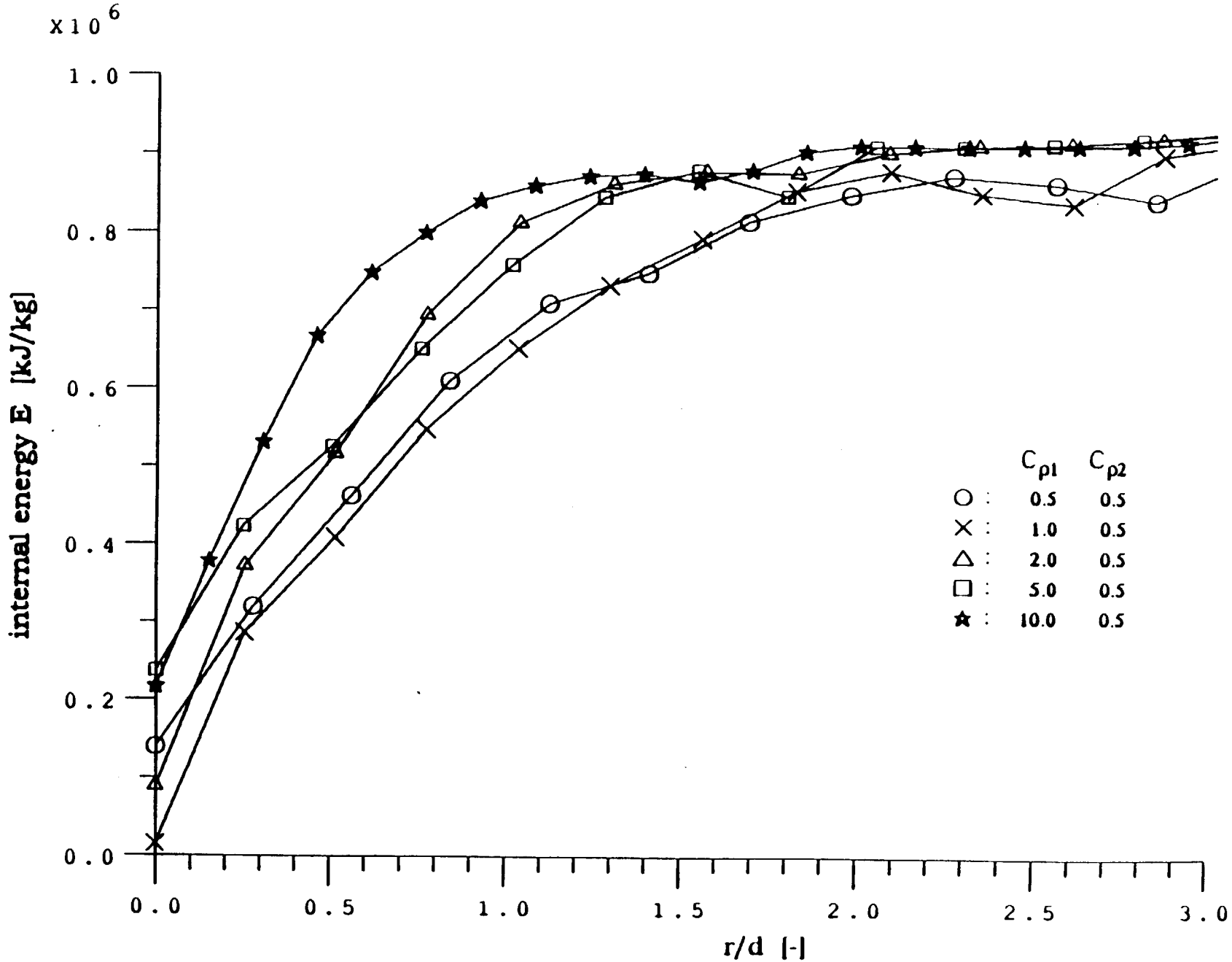

Fig. 14. Coaxial turbulent supersonic jet flame burning H_2 with air. Parametric study of the compressibility term for the stochastic simulation of the relative rate of volume expansion (equation (26)). Mean internal energy at $x/D = 26.2$.

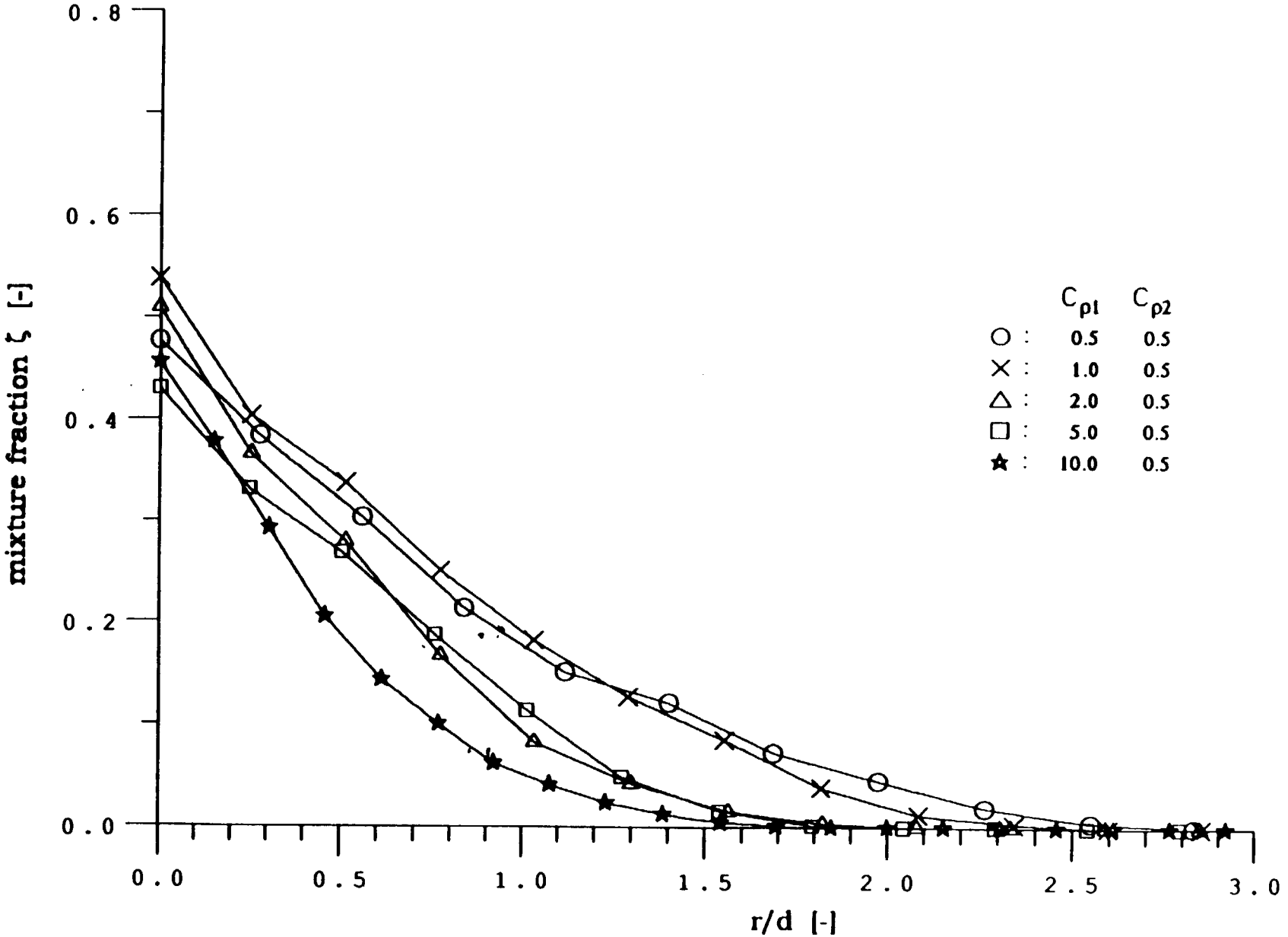

Fig. 15. Coaxial turbulent supersonic jet flame burning H_2 with air. Parametric study of the compressibility term for the stochastic simulation of the relative rate of volume expansion (equation (26)). Mean mixture fraction at $x/D = 26.2$.

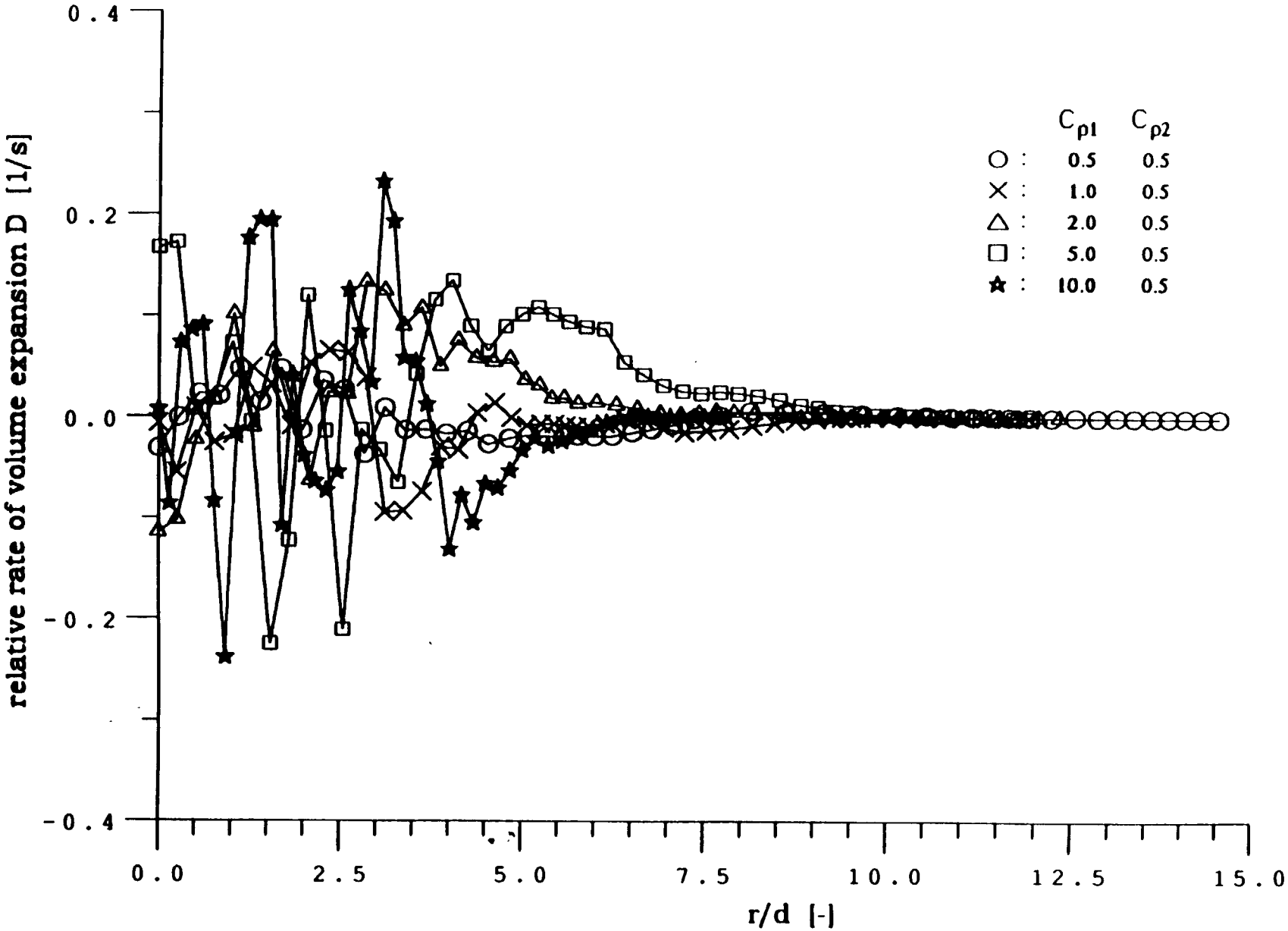

Fig. 16. Coaxial turbulent supersonic jet flame burning H_2 with air. Parametric study of the compressibility term for the stochastic simulation of the relative rate of volume expansion (equation (26)). Mean relative rate of volume expansion at $x/D = 26.2$.

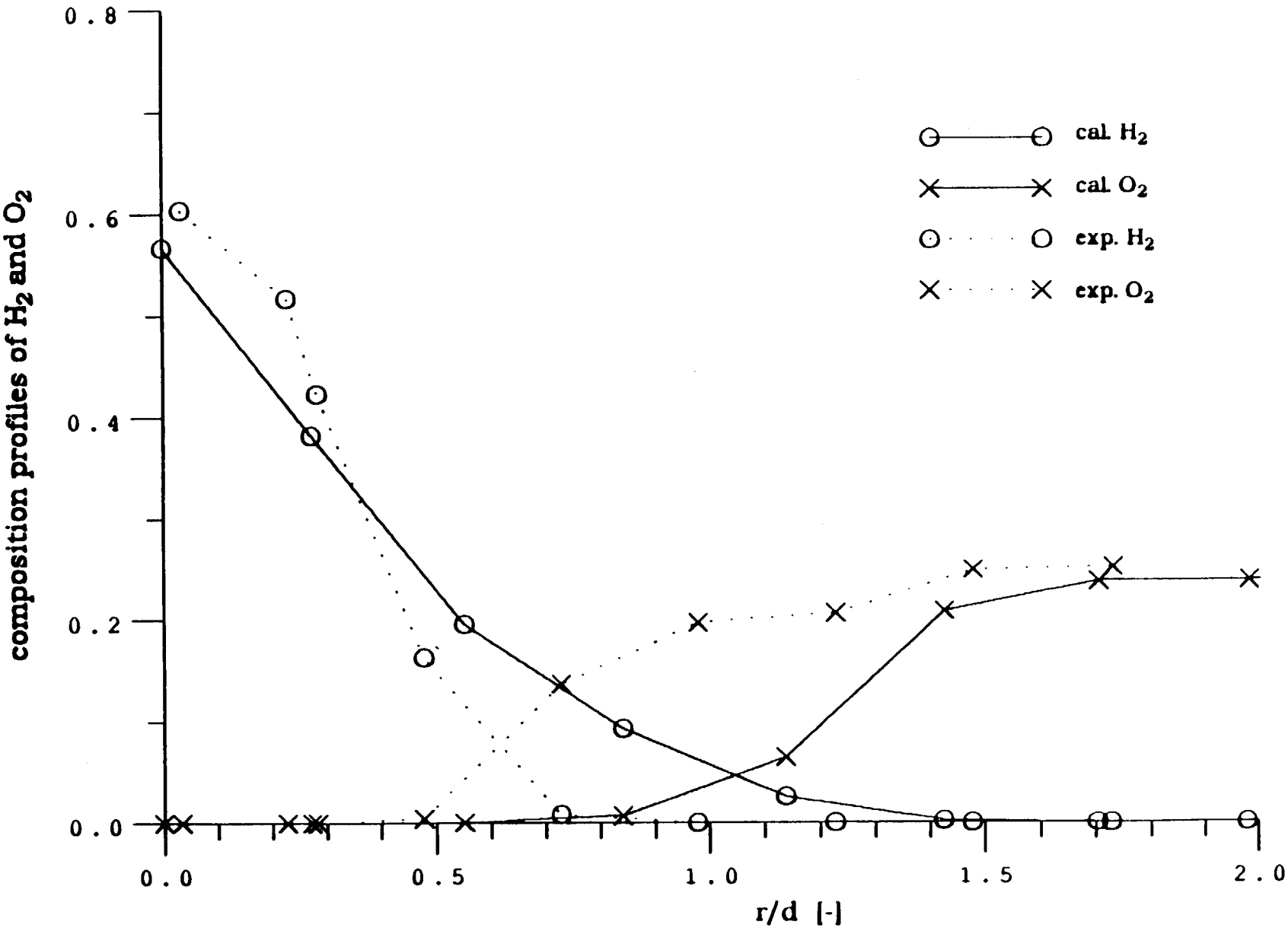

Fig. 17. Coaxial turbulent supersonic jet flame burning H_2 with air. Mean mass fractions at $x/D = 15.5$ for $c_{\rho 1} = 1.0$ and $c_{\rho 2} = 0.5$ compared to the experiments of Evans et al. (1978).

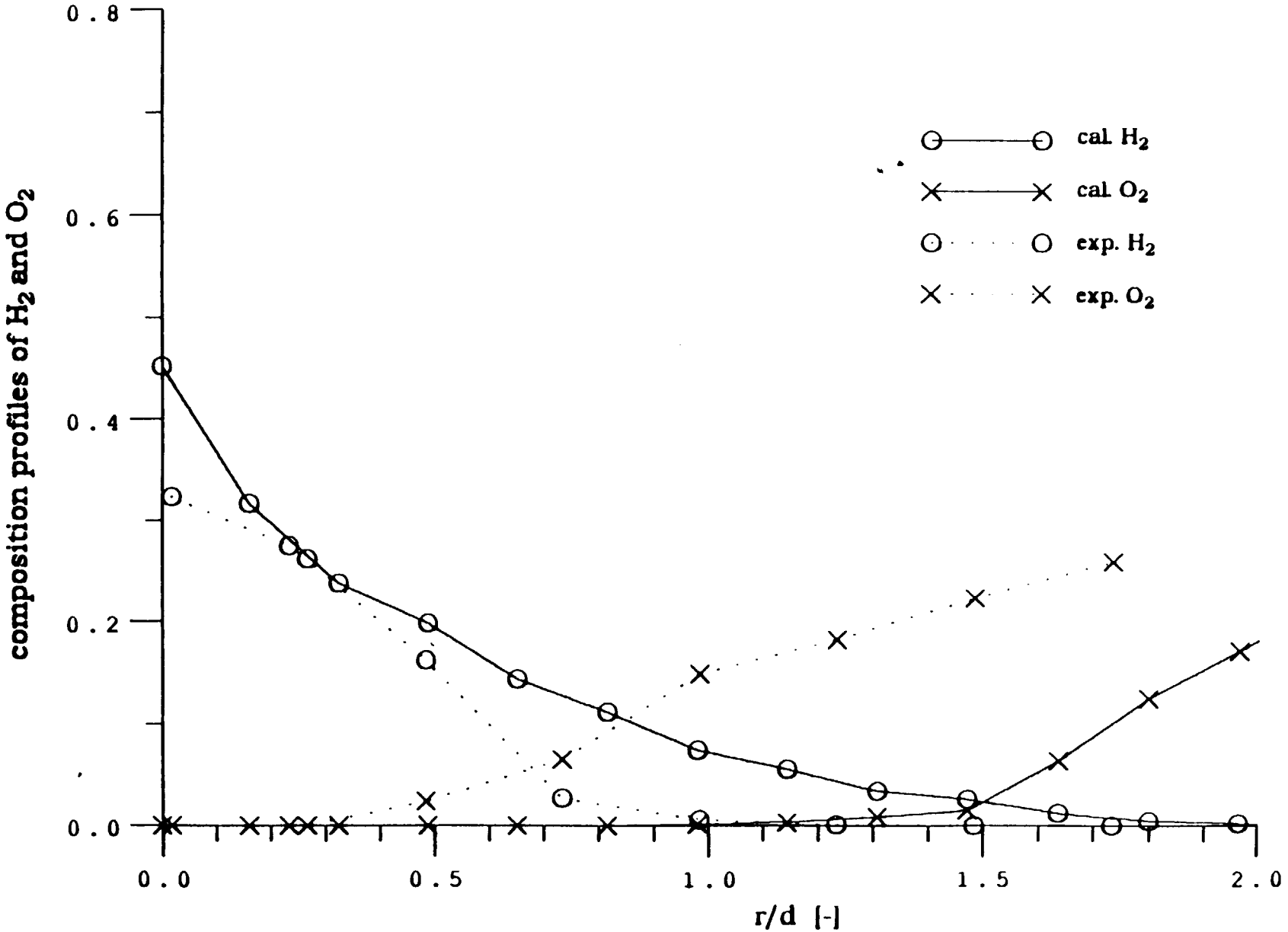

Fig. 18. Coaxial turbulent supersonic jet flame burning H_2 with air. Mean mass fractions at $x/D = 27.9$ for $c_{\rho 1} = 1.0$ and $c_{\rho 2} = 0.5$ compared to the experiments of Evans et al. (1978).

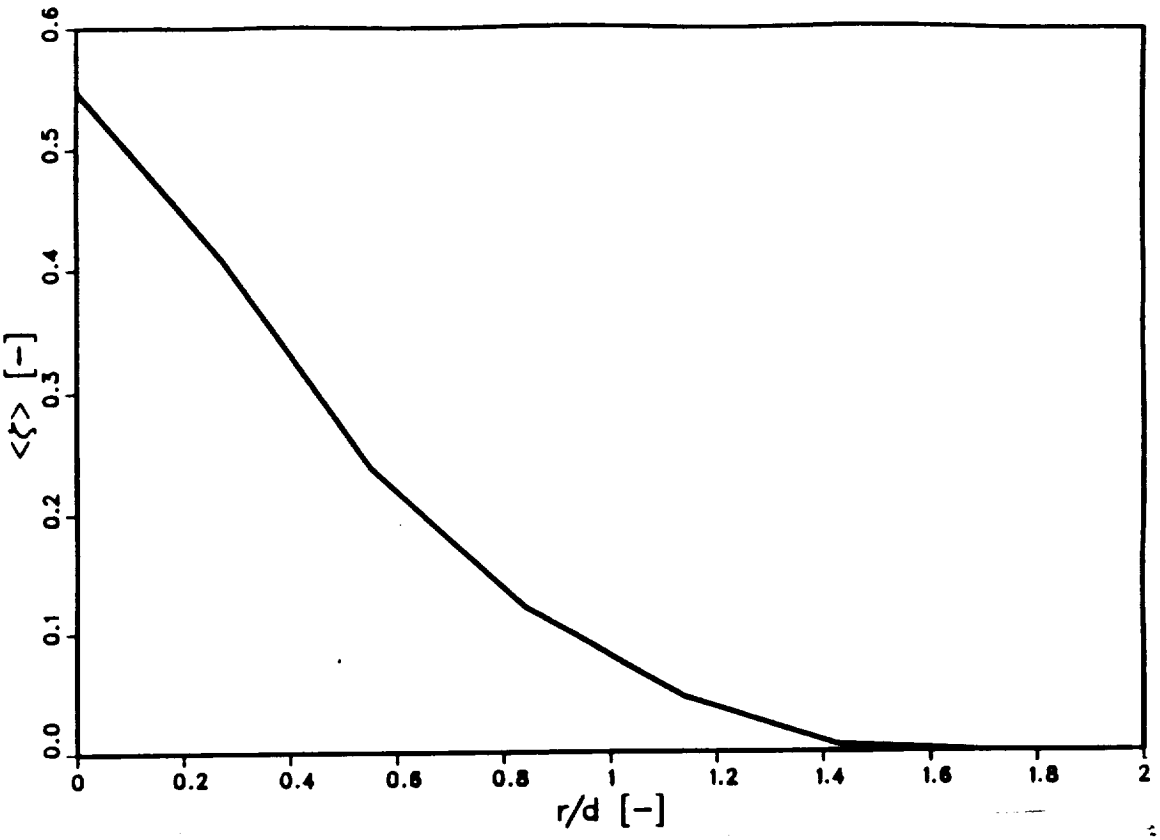

Fig. 19. Coaxial turbulent supersonic jet flame burning H_2 with air. Mean mixture fraction at $x/D = 15.5$ for $c_{\rho 1} = 1.0$ and $c_{\rho 2} = 0.5$.

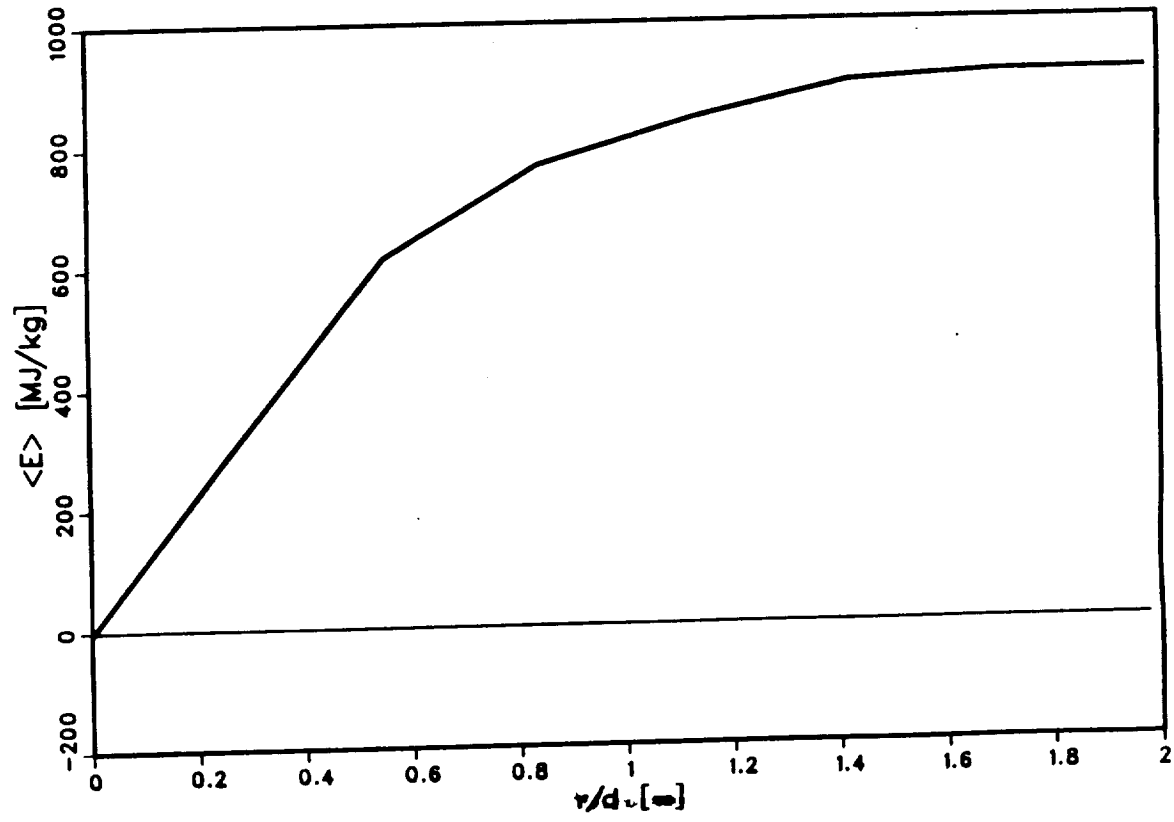

Fig. 20. Coaxial turbulent supersonic jet flame burning H_2 with air. Mean internal energy at $x/D = 15.5$ for $c_{\rho 1} = 1.0$ and $c_{\rho 2} = 0.5$.

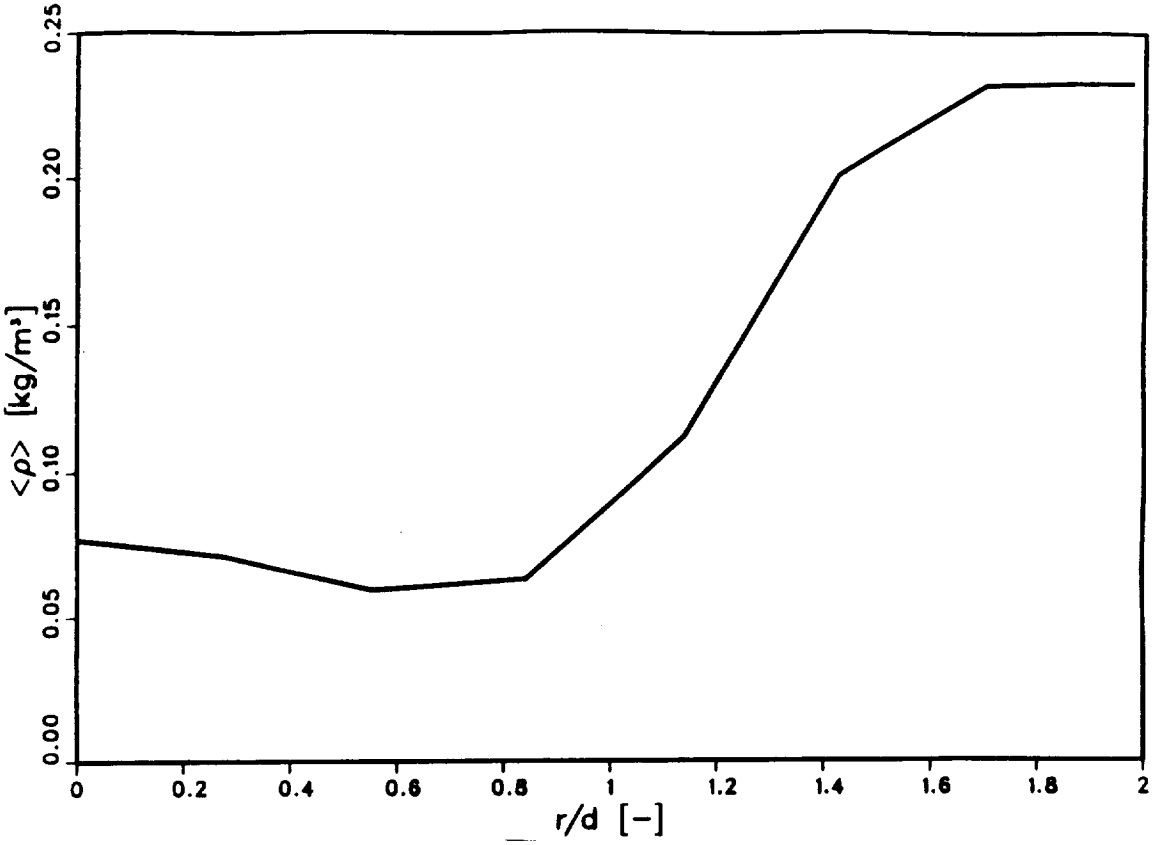

Fig. 21. Coaxial turbulent supersonic jet flame burning H_2 with air. Mean density at $x/D = 15.5$ for $c_{\rho 1} = 1.0$ and $c_{\rho 2} = 0.5$.

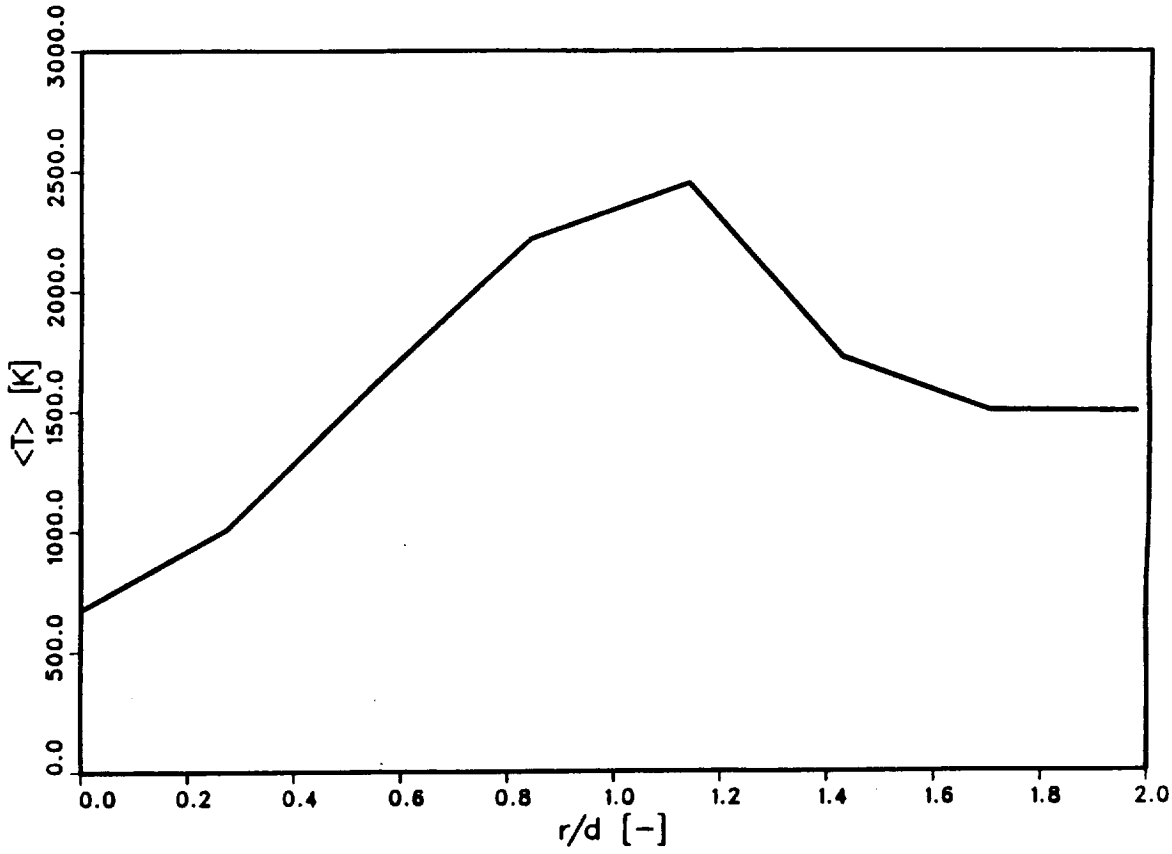

Fig. 22. Coaxial turbulent supersonic jet flame burning H_2 with air. Mean temperature at $x/D = 15.5$ for $c_{\rho 1} = 1.0$ and $c_{\rho 2} = 0.5$.

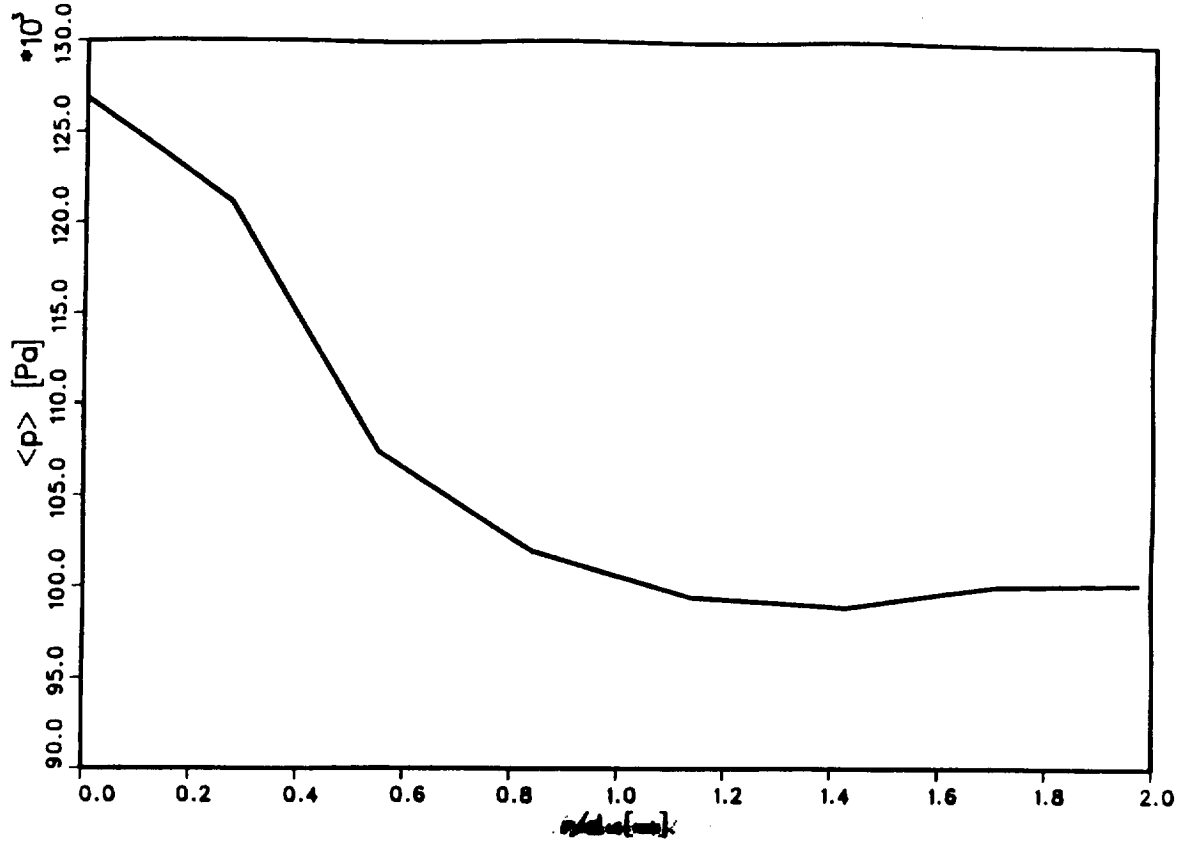

Fig. 23. Coaxial turbulent supersonic jet flame burning H_2 with air. Mean pressure at $x/D = 15.5$ for $c_{\rho 1} = 1.0$ and $c_{\rho 2} = 0.5$.

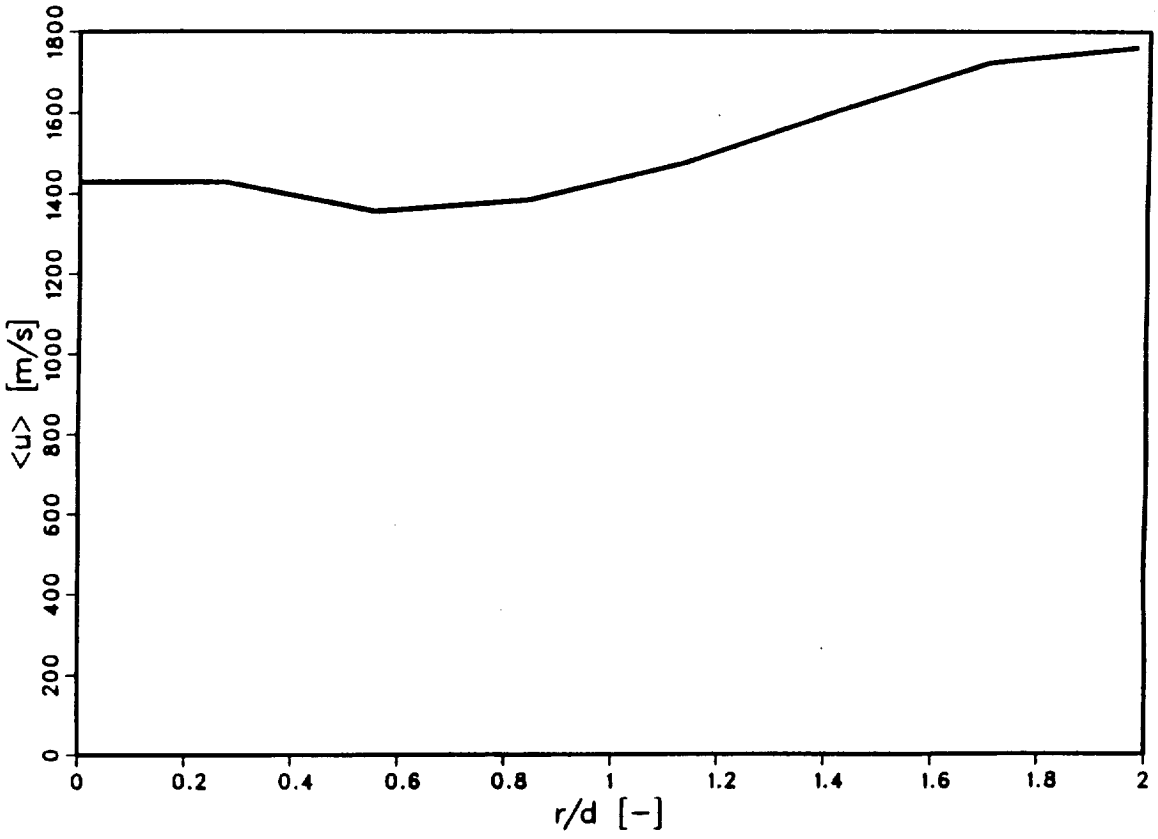

Fig. 24. Coaxial turbulent supersonic jet flame burning H_2 with air. Mean velocity at $x/D = 15.5$ for $c_{\rho 1} = 1.0$ and $c_{\rho 2} = 0.5$.

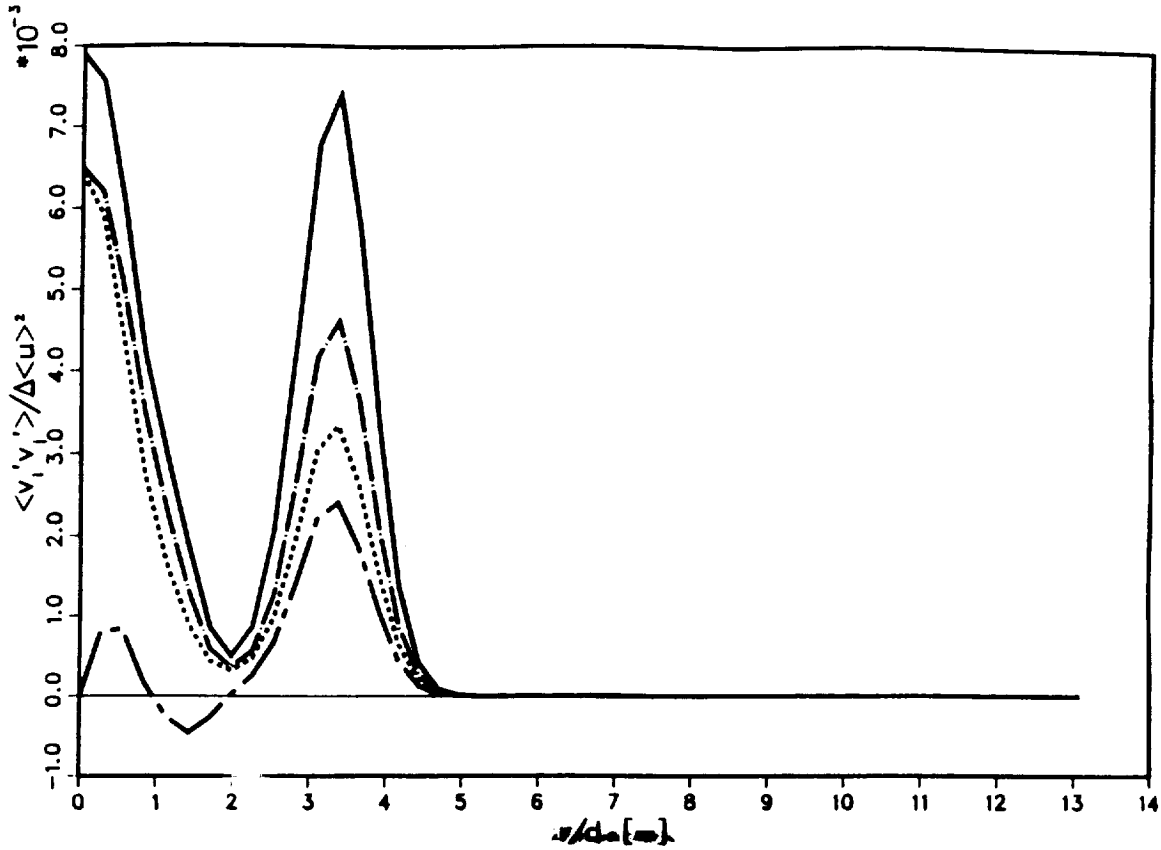

Fig. 25. Coaxial turbulent supersonic jet flame burning H_2 with air. Reynolds stress components at $x/D = 15.5$ for $c_{\rho 1} = 1.0$ and $c_{\rho 2} = 0.5$.

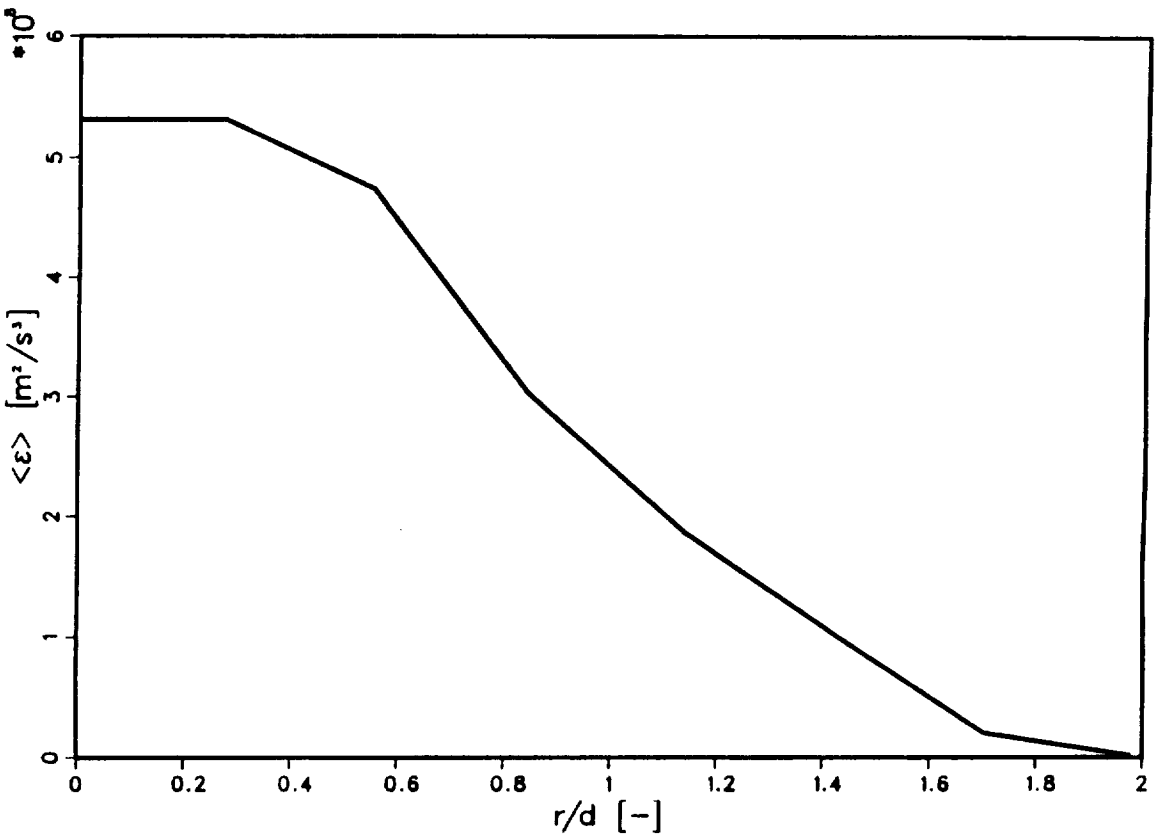

Fig. 26. Coaxial turbulent supersonic jet flame burning H_2 with air. Mean Dissipation rate at $x/D = 15.5$ for $c_{\rho 1} = 1.0$ and $c_{\rho 2} = 0.5$.

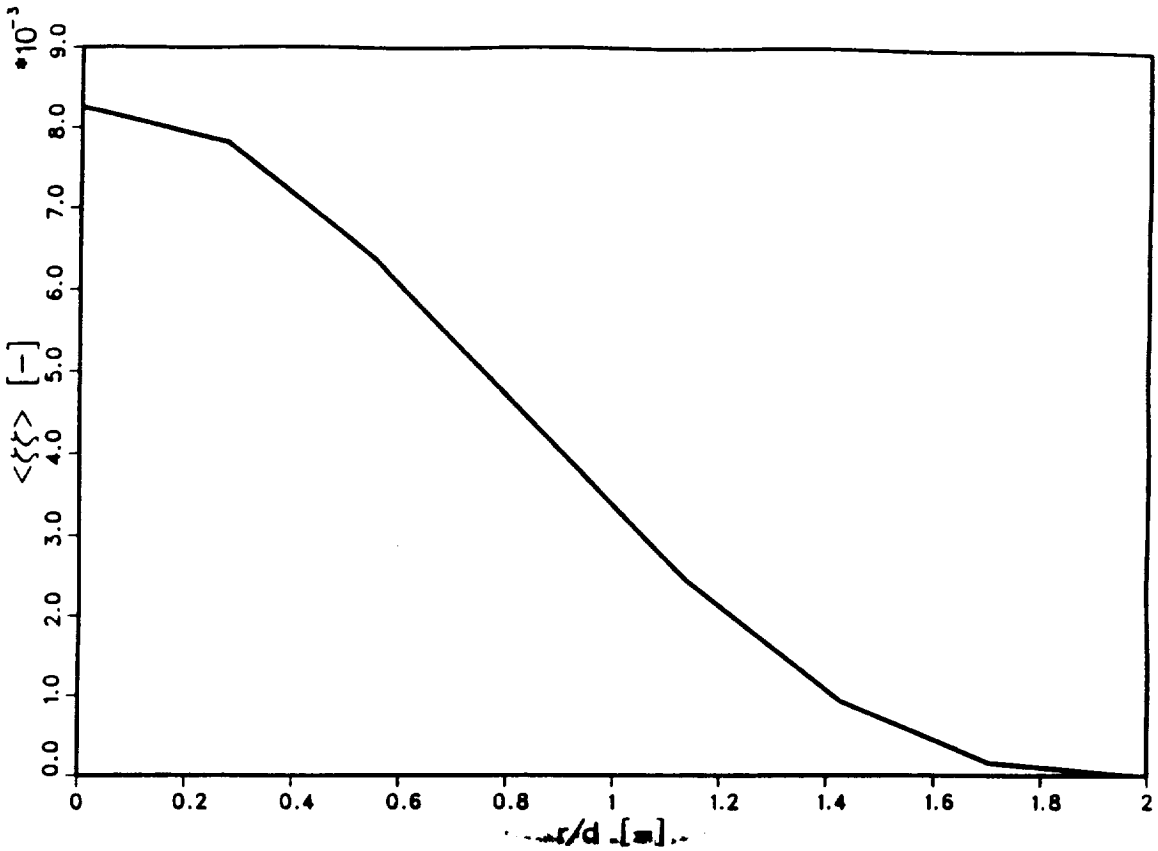

Fig. 27. Coaxial turbulent supersonic jet flame burning H_2 with air. Variance of mixture fraction at $x/D = 15.5$ for $c_{\rho 1} = 1.0$ and $c_{\rho 2} = 0.5$.

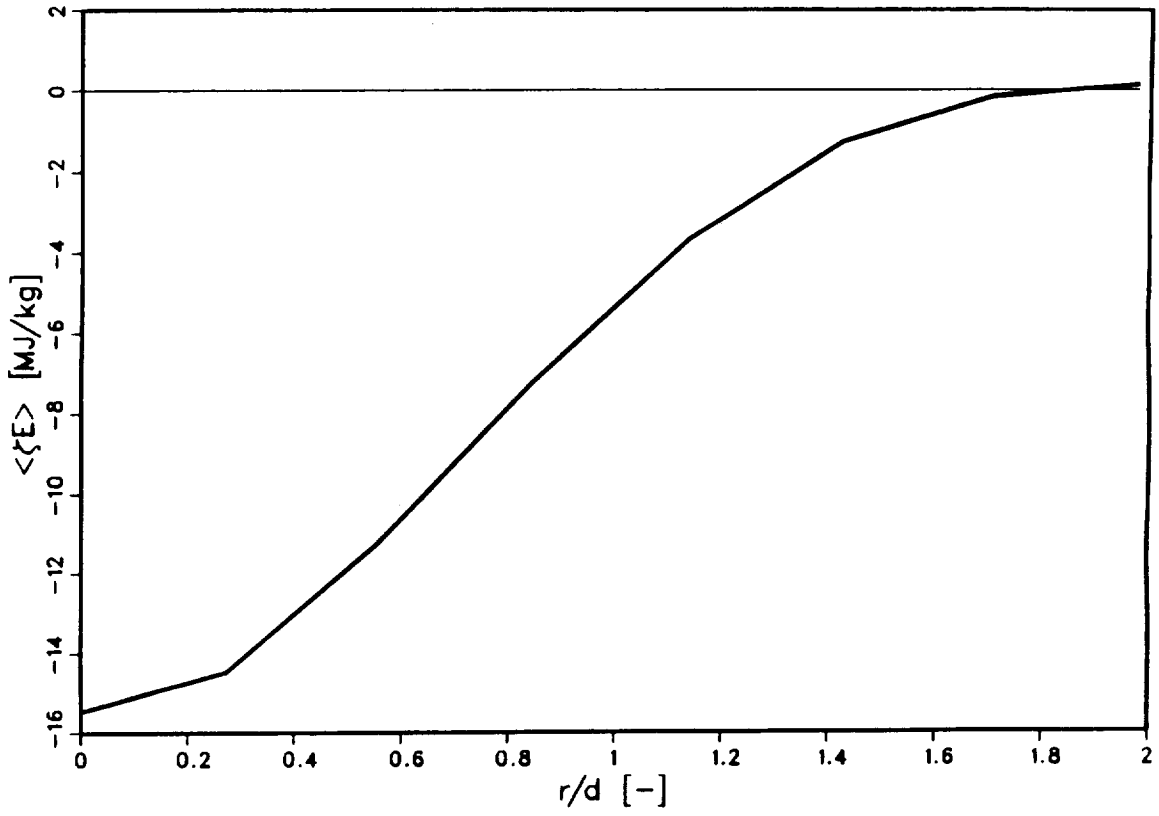

Fig. 28. Coaxial turbulent supersonic jet flame burning H_2 with air. Covariance of mixture fraction and internal energy at $x/D = 15.5$ for $c_{\rho 1} = 1.0$ and $c_{\rho 2} = 0.5$.

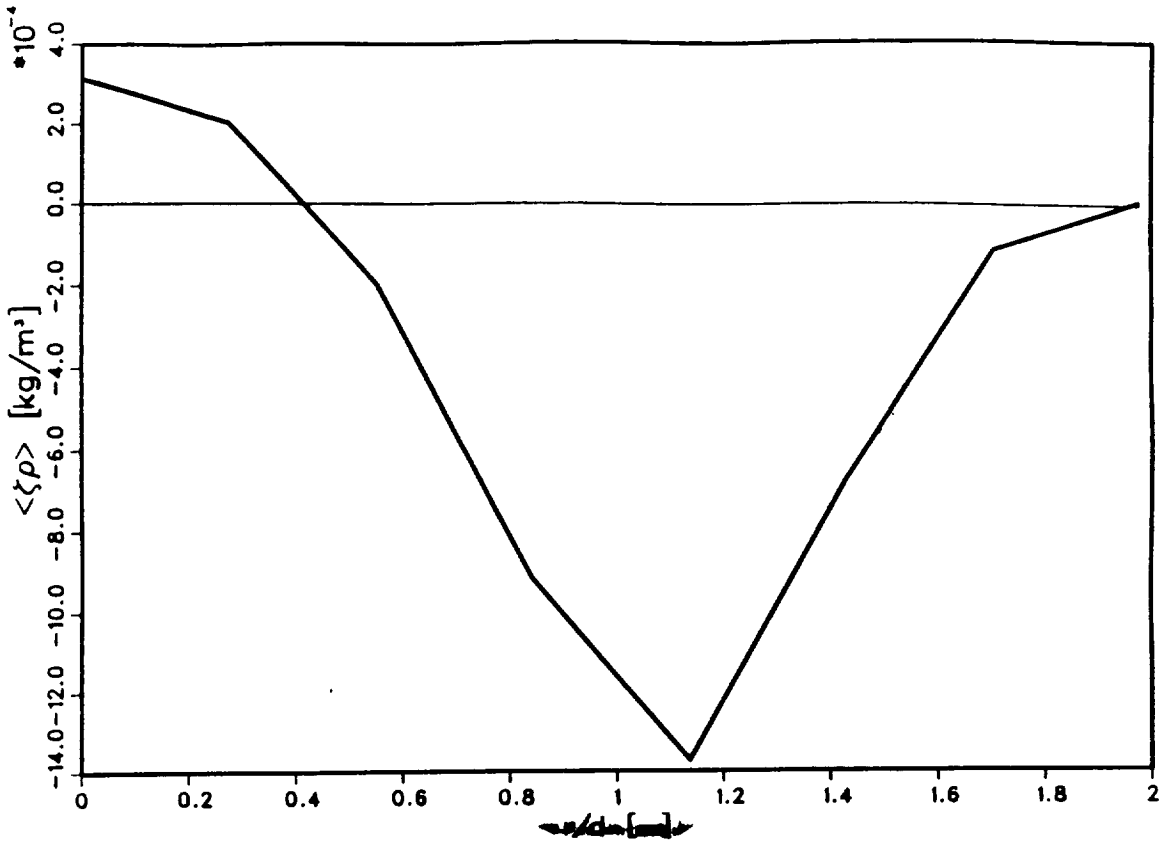

Fig. 29. Coaxial turbulent supersonic jet flame burning H_2 with air. Covariance of mixture fraction and density at $x/D = 15.5$ for $c_{\rho 1} = 1.0$ and $c_{\rho 2} = 0.5$.

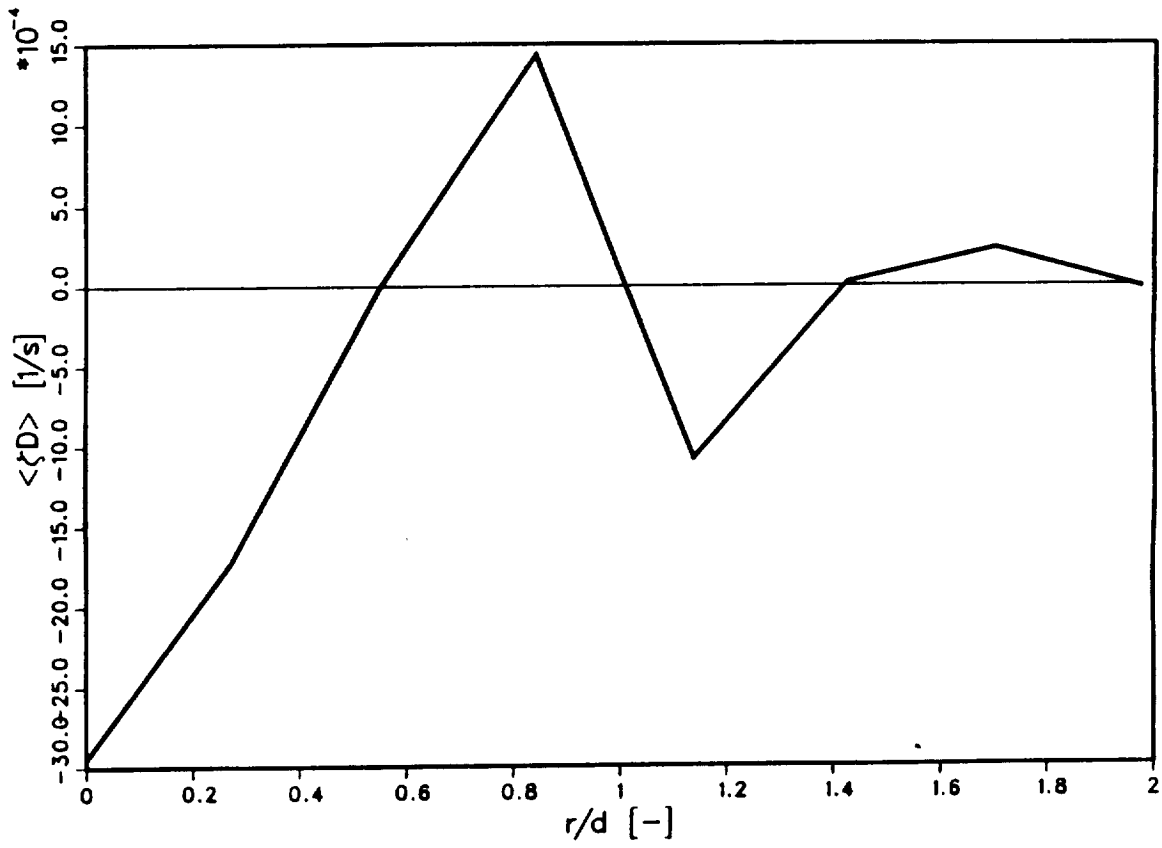

Fig. 30. Coaxial turbulent supersonic jet flame burning H_2 with air. Covariance of mixture fraction and relative rate of volume expansion at $x/D = 15.5$ for $c_{\rho 1} = 1.0$ and $c_{\rho 2} = 0.5$.

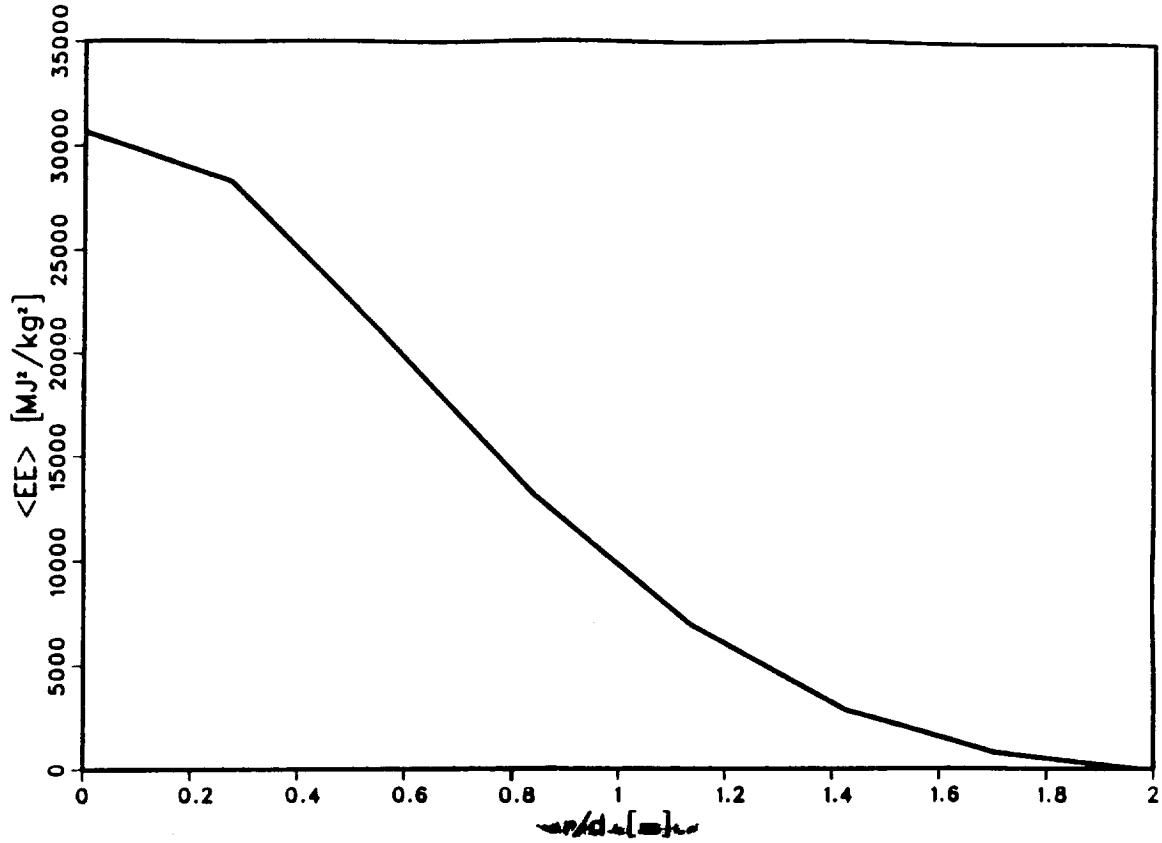

Fig. 31. Coaxial turbulent supersonic jet flame burning H_2 with air. Variance of internal energy at $x/D = 15.5$ for $c_{\rho 1} = 1.0$ and $c_{\rho 2} = 0.5$.

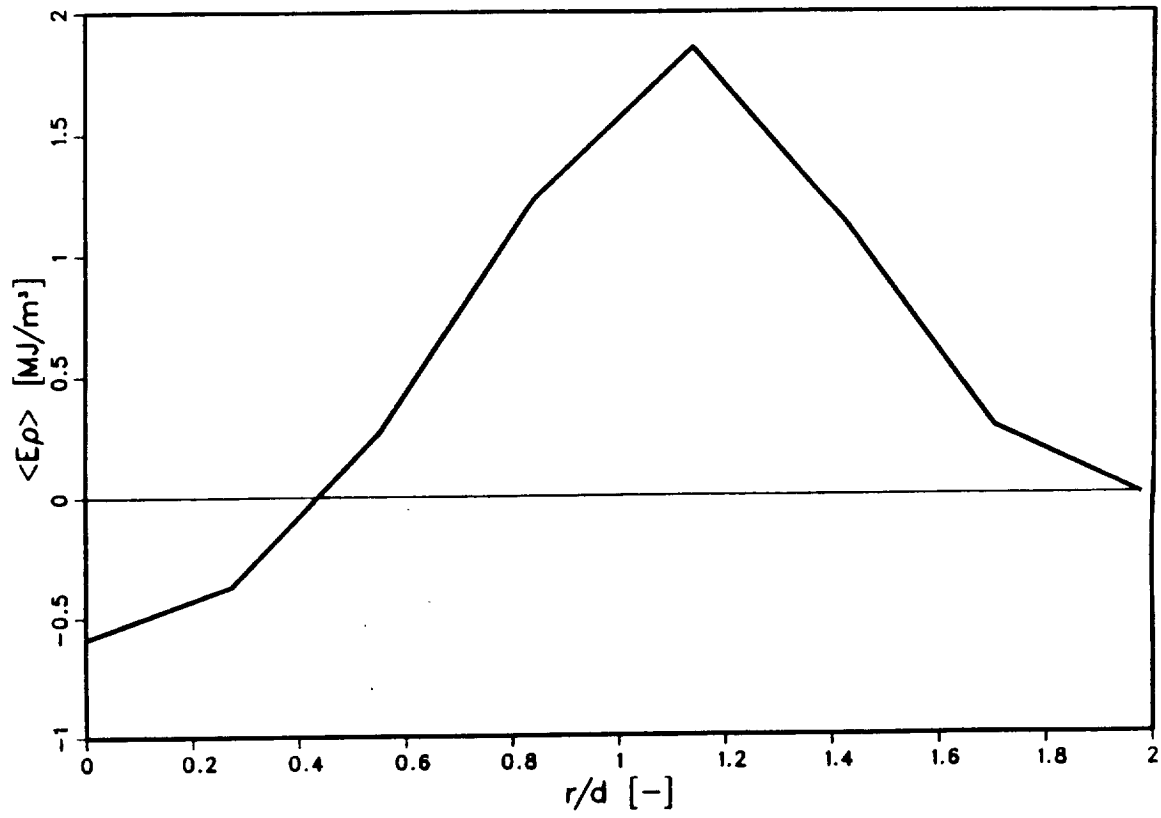

Fig. 32. Coaxial turbulent supersonic jet flame burning H_2 with air. Covariance of internal energy and density at $x/D = 15.5$ for $c_{\rho 1} = 1.0$ and $c_{\rho 2} = 0.5$.

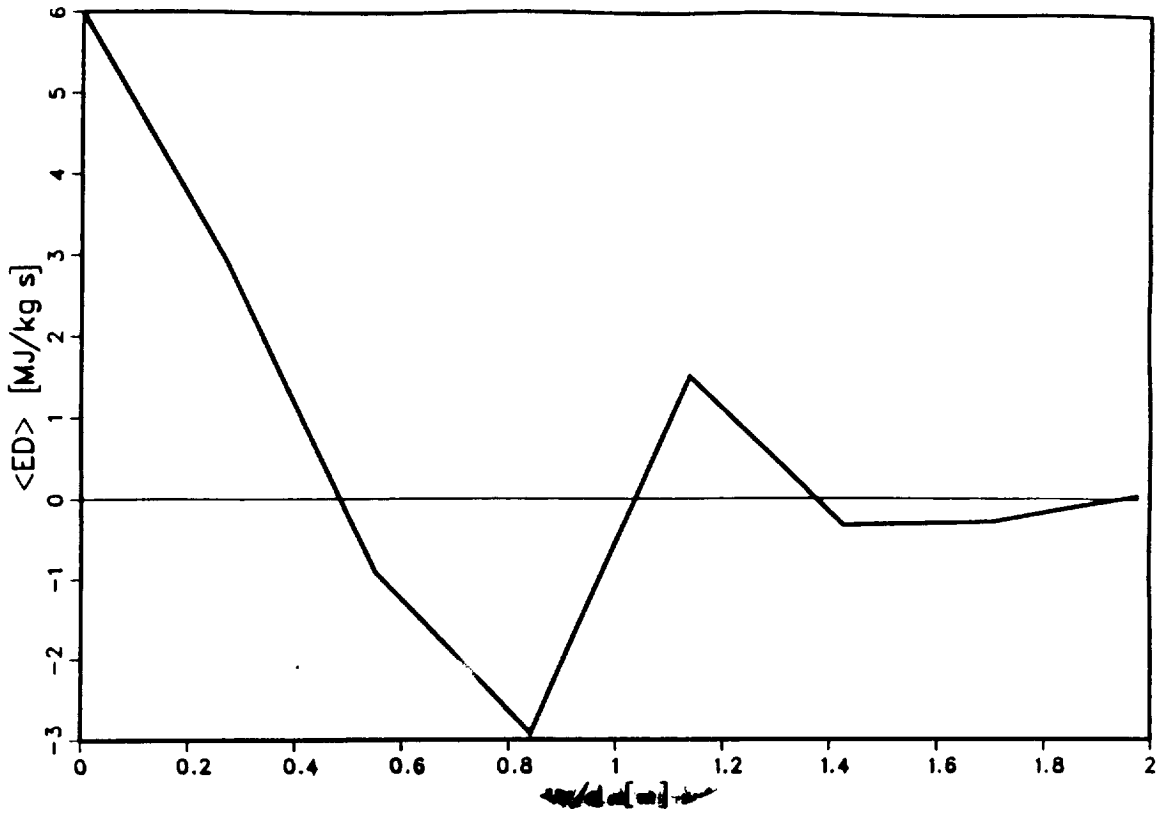

Fig. 33. Coaxial turbulent supersonic jet flame burning H_2 with air. Covariance of internal energy and relative rate of volume expansion at $x/D = 15.5$ for $c_{\rho 1} = 1.0$ and $c_{\rho 2} = 0.5$.

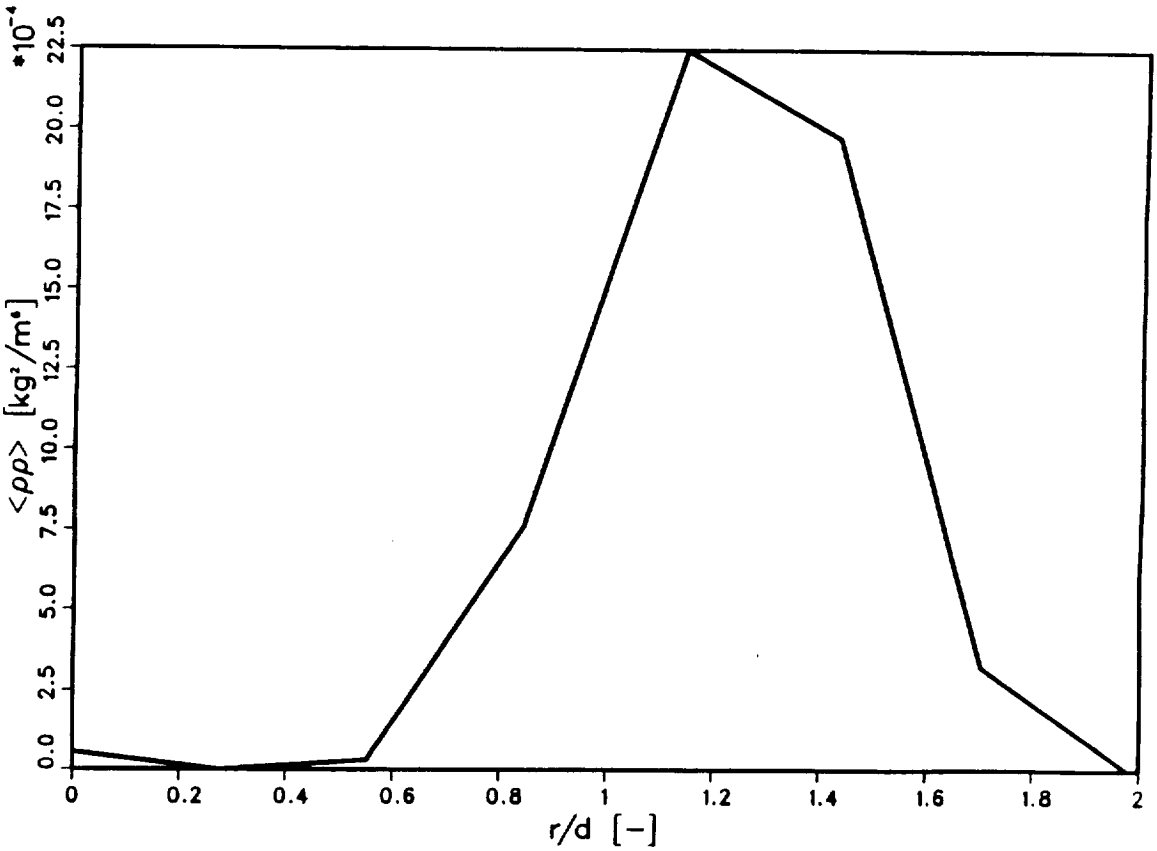

Fig. 34. Coaxial turbulent supersonic jet flame burning H_2 with air. Variance of density at $x/D = 15.5$ for $c_{\rho 1} = 1.0$ and $c_{\rho 2} = 0.5$.

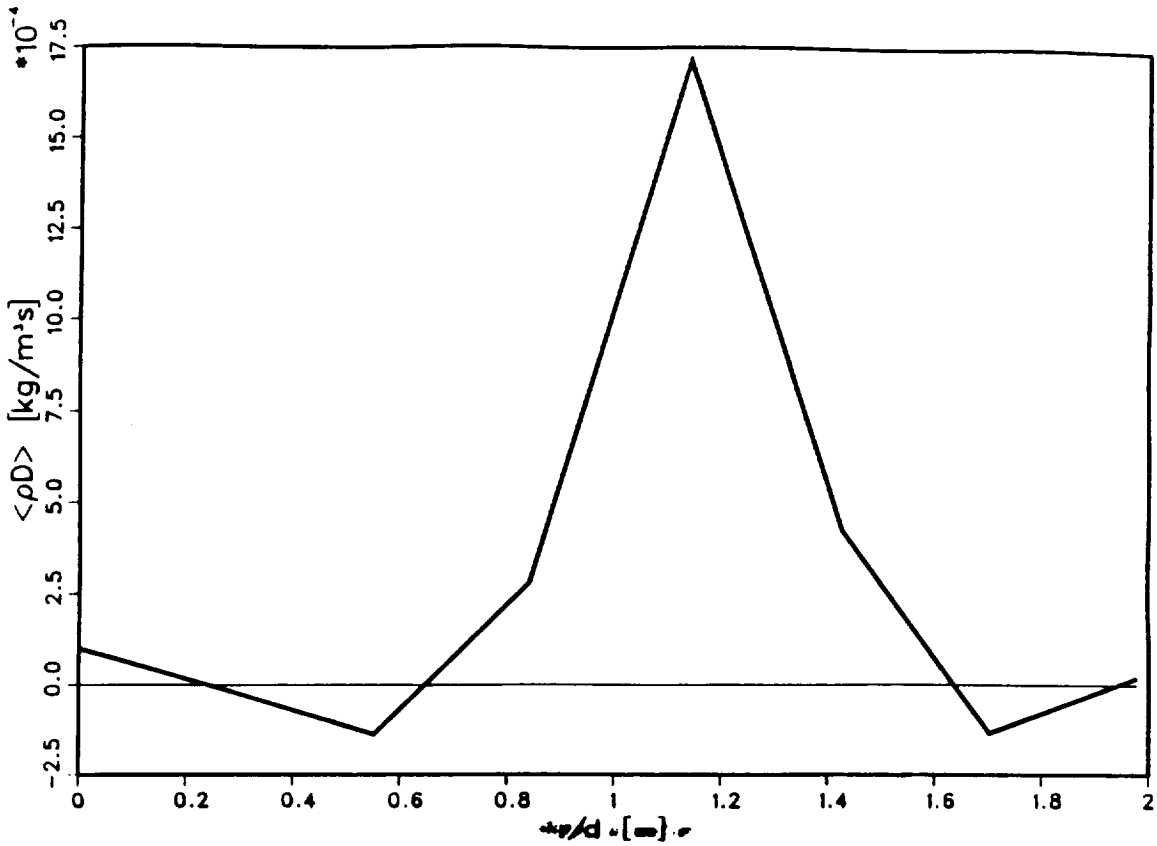

Fig. 35. Coaxial turbulent supersonic jet flame burning H_2 with air. Covariance of density and relative rate of volume expansion at $x/D = 15.5$ for $c_{\rho 1} = 1.0$ and $c_{\rho 2} = 0.5$.

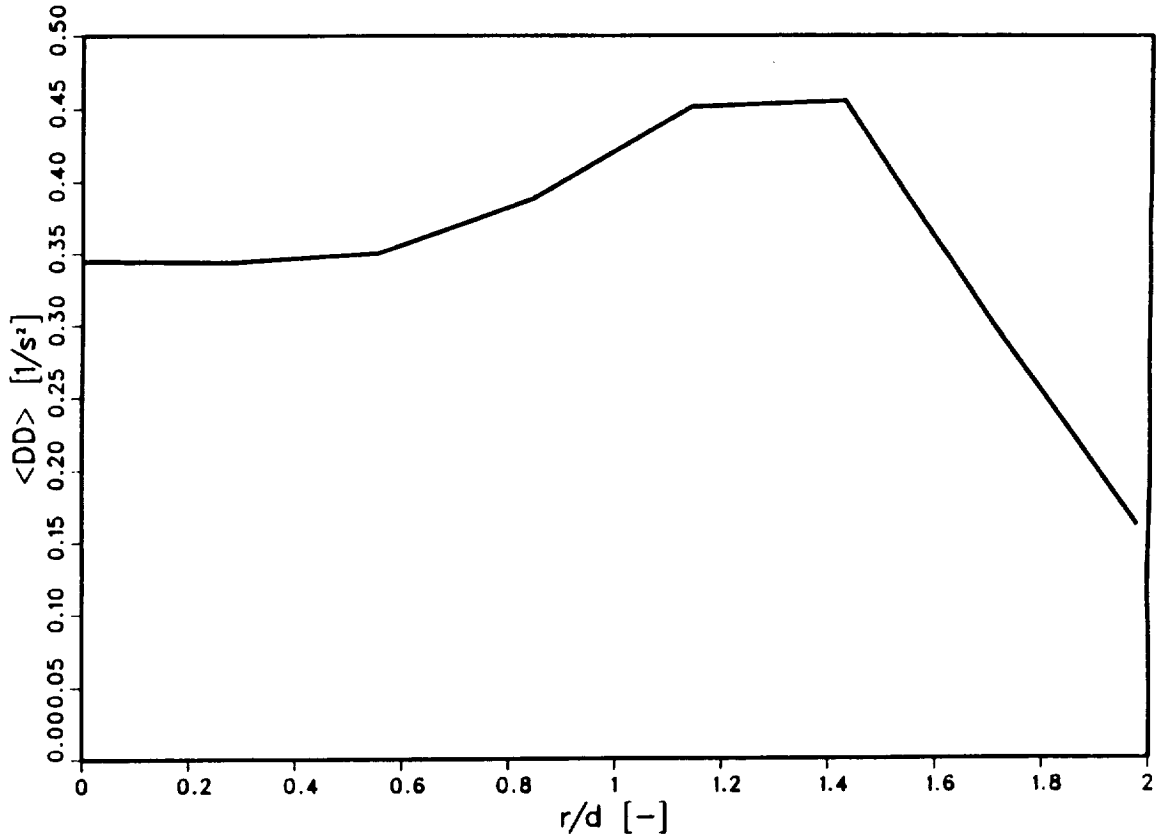

Fig. 36. Coaxial turbulent supersonic jet flame burning H_2 with air. Variance of relative rate of volume expansion at $x/D = 15.5$ for $c_{\rho 1} = 1.0$ and $c_{\rho 2} = 0.5$.

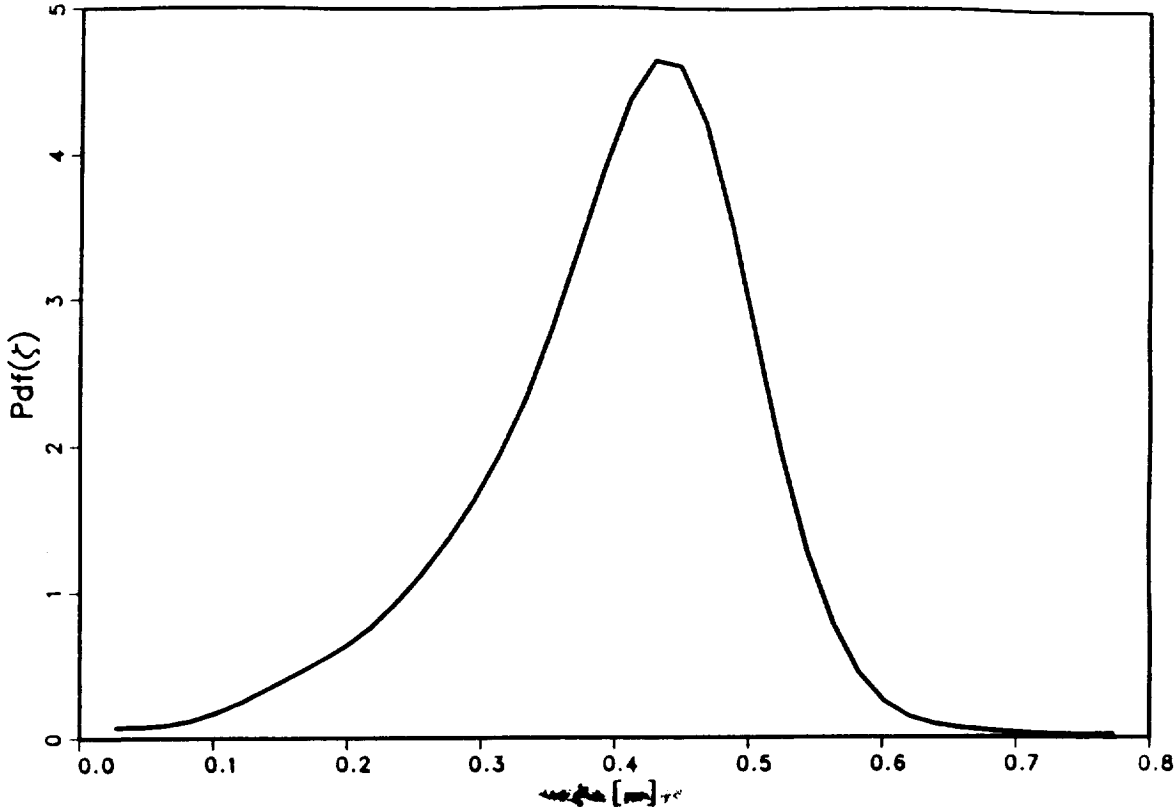

Fig. 37. Coaxial turbulent supersonic jet flame burning H_2 with air. Pdf of mixture fraction at $x/D = 15.5$ and $r/D = 0.27$ for $c_{\rho 1} = 1.0$ and $c_{\rho 2} = 0.5$.

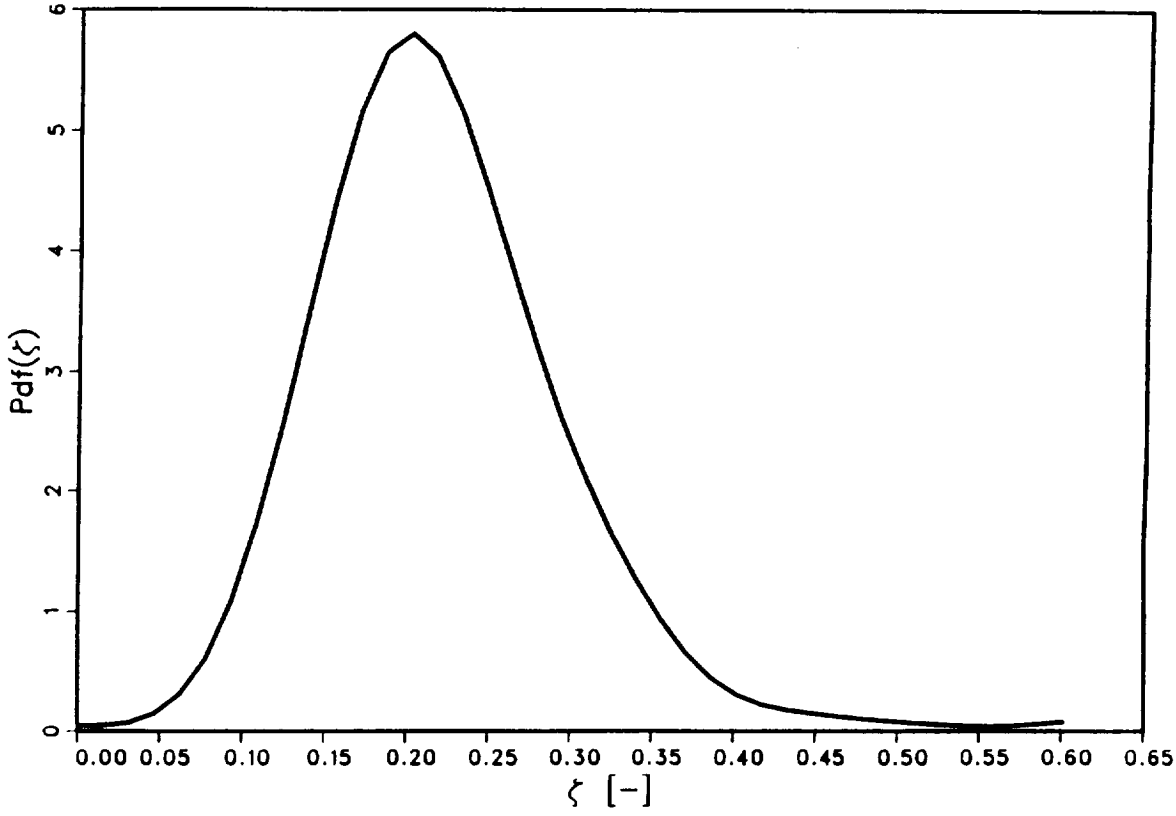

Fig. 38. Coaxial turbulent supersonic jet flame burning H_2 with air. Pdf of mixture fraction at $x/D = 15.5$ and $r/D = 0.55$ for $c_{\rho 1} = 1.0$ and $c_{\rho 2} = 0.5$.

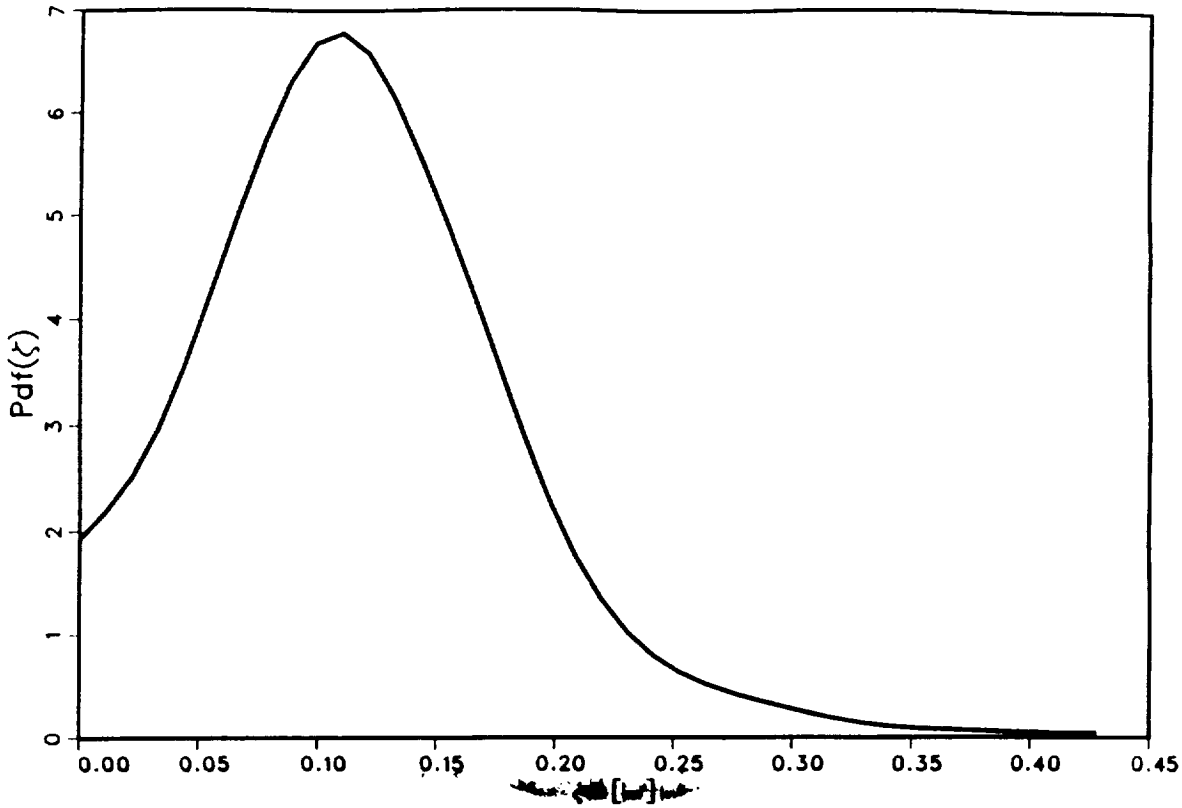

Fig. 39. Coaxial turbulent supersonic jet flame burning H_2 with air. Pdf of mixture fraction at $x/D = 15.5$ and $r/D = 0.84$ for $c_{\rho 1} = 1.0$ and $c_{\rho 2} = 0.5$.

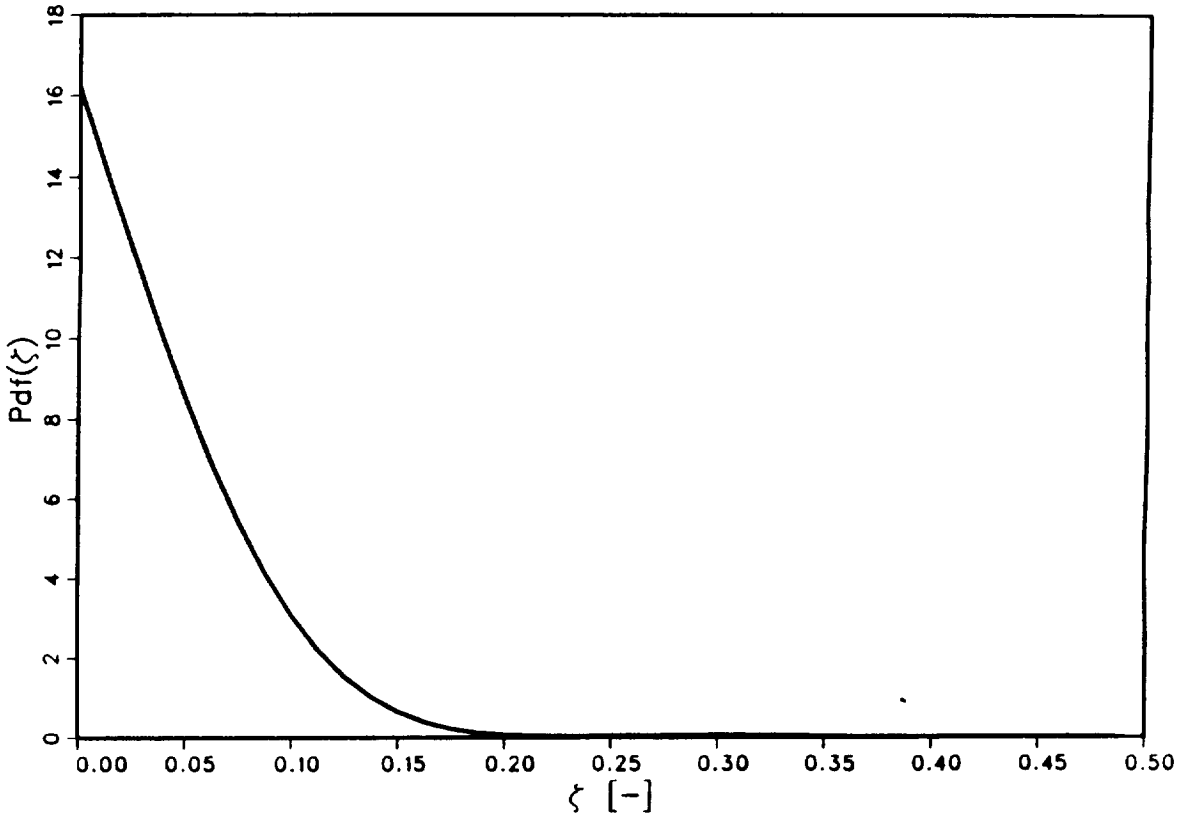

Fig. 40. Coaxial turbulent supersonic jet flame burning H_2 with air. Pdf of mixture fraction at $x/D = 15.5$ and $r/D = 1.14$ for $c_{\rho 1} = 1.0$ and $c_{\rho 2} = 0.5$.

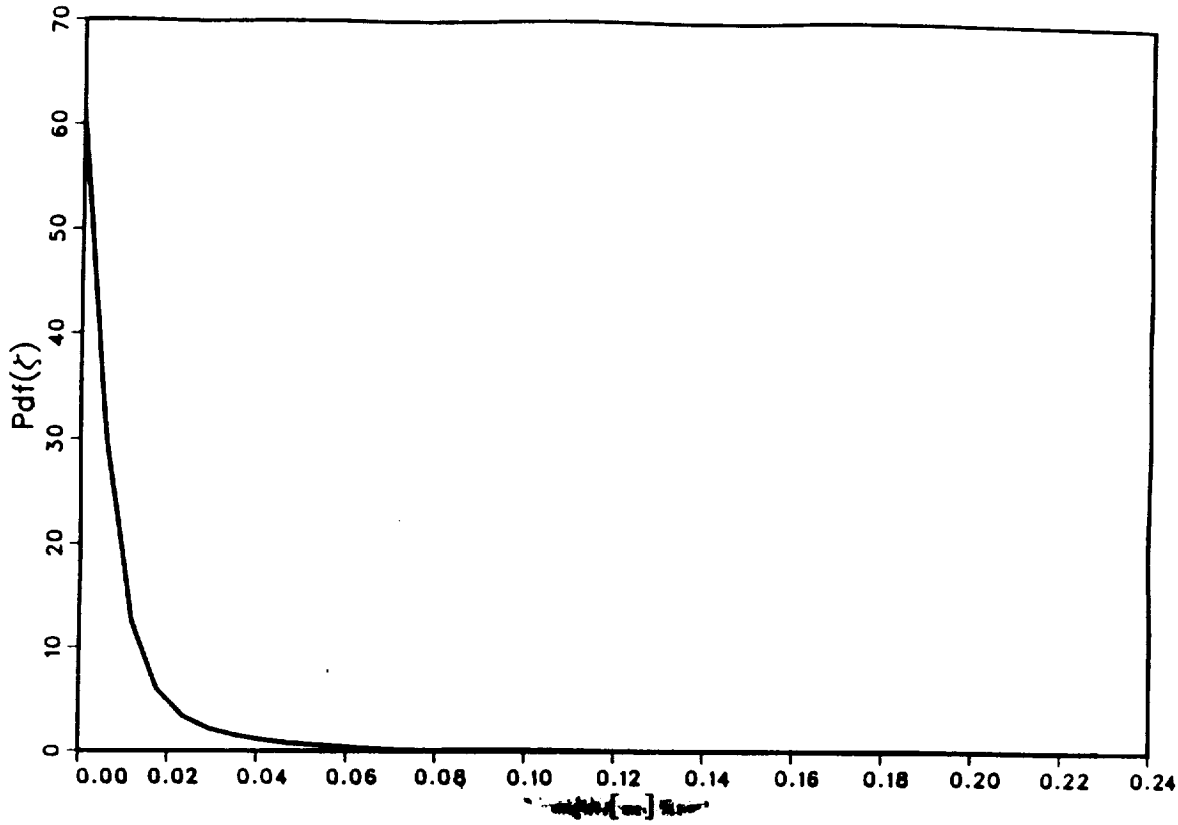

Fig. 41. Coaxial turbulent supersonic jet flame burning H_2 with air. Pdf of mixture fraction at $x/D = 15.5$ and $r/D = 1.42$ for $c_{\rho 1} = 1.0$ and $c_{\rho 2} = 0.5$.

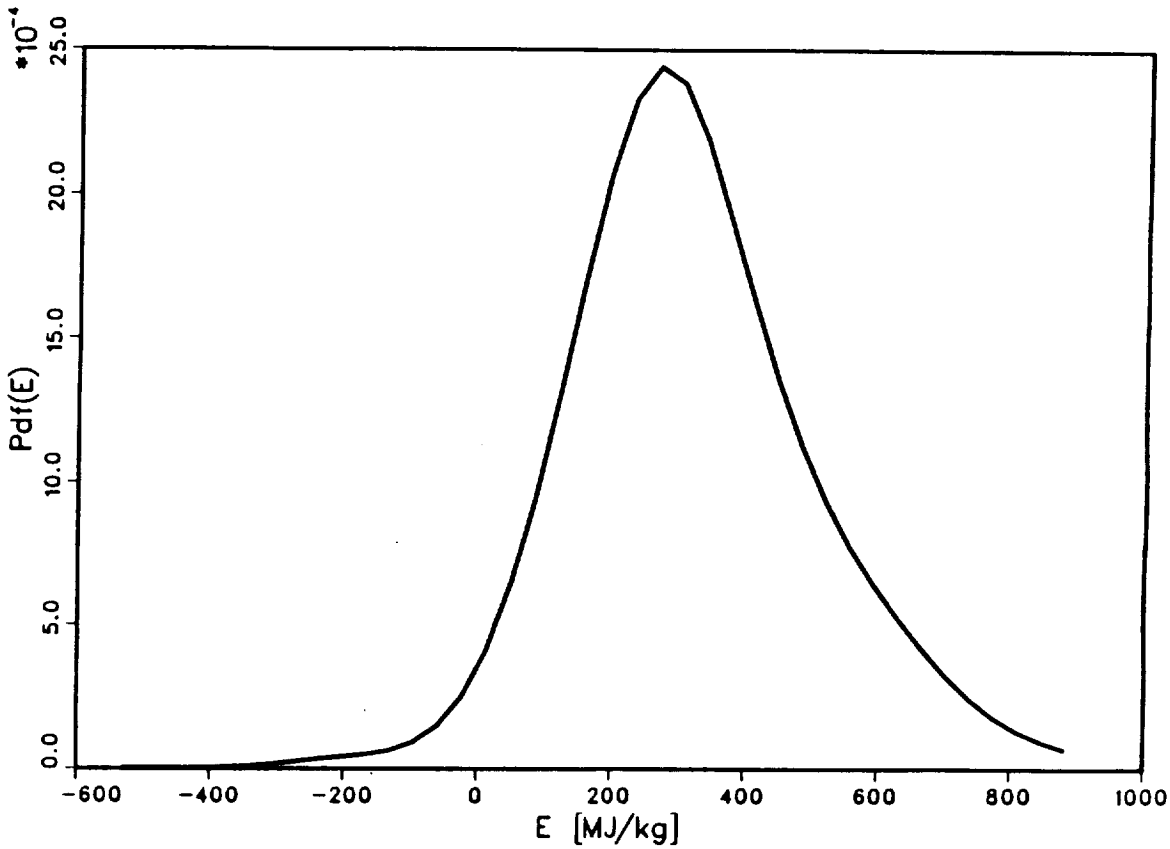

Fig. 42. Coaxial turbulent supersonic jet flame burning H_2 with air. Pdf of internal energy at $x/D = 15.5$ and $r/D = 0.27$ for $c_{\rho 1} = 1.0$ and $c_{\rho 2} = 0.5$.

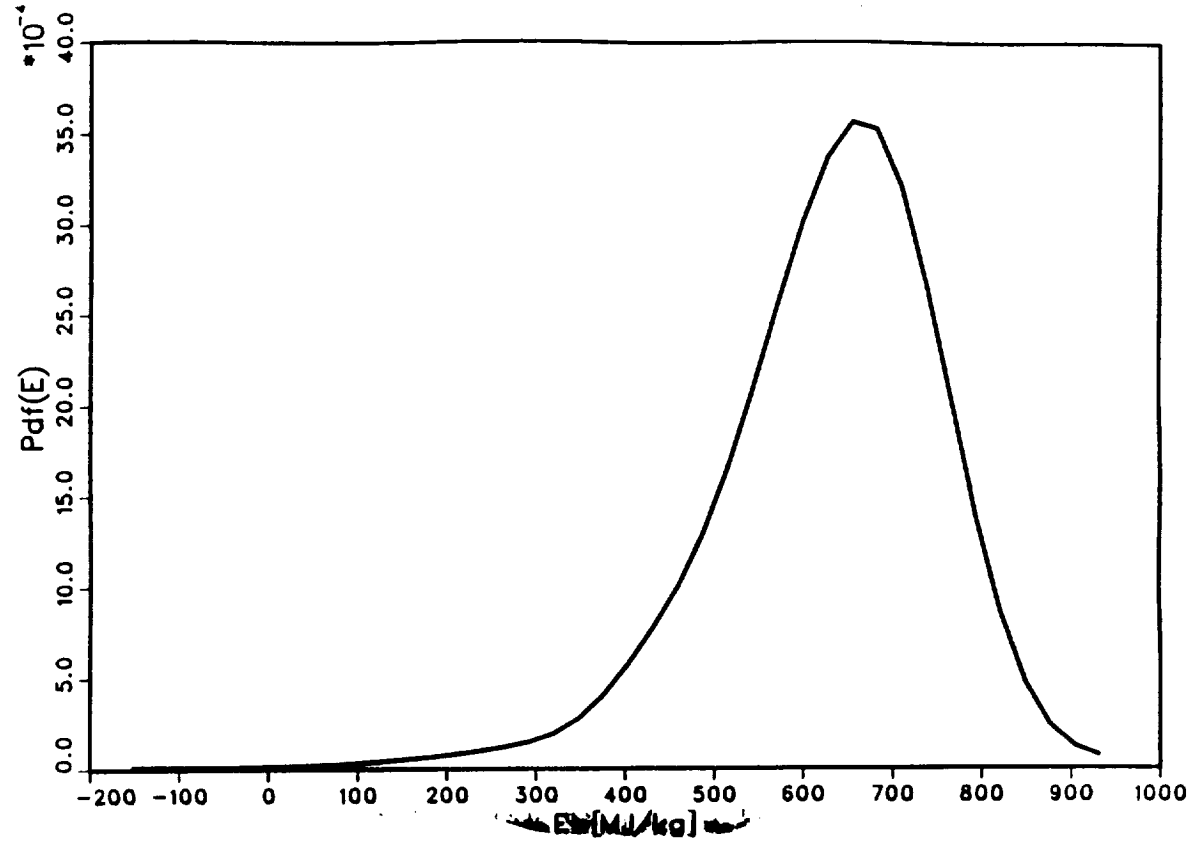

Fig. 43. Coaxial turbulent supersonic jet flame burning H_2 with air. Pdf of internal energy at $x/D = 15.5$ and $r/D = 0.55$ for $c_{\rho 1} = 1.0$ and $c_{\rho 2} = 0.5$.

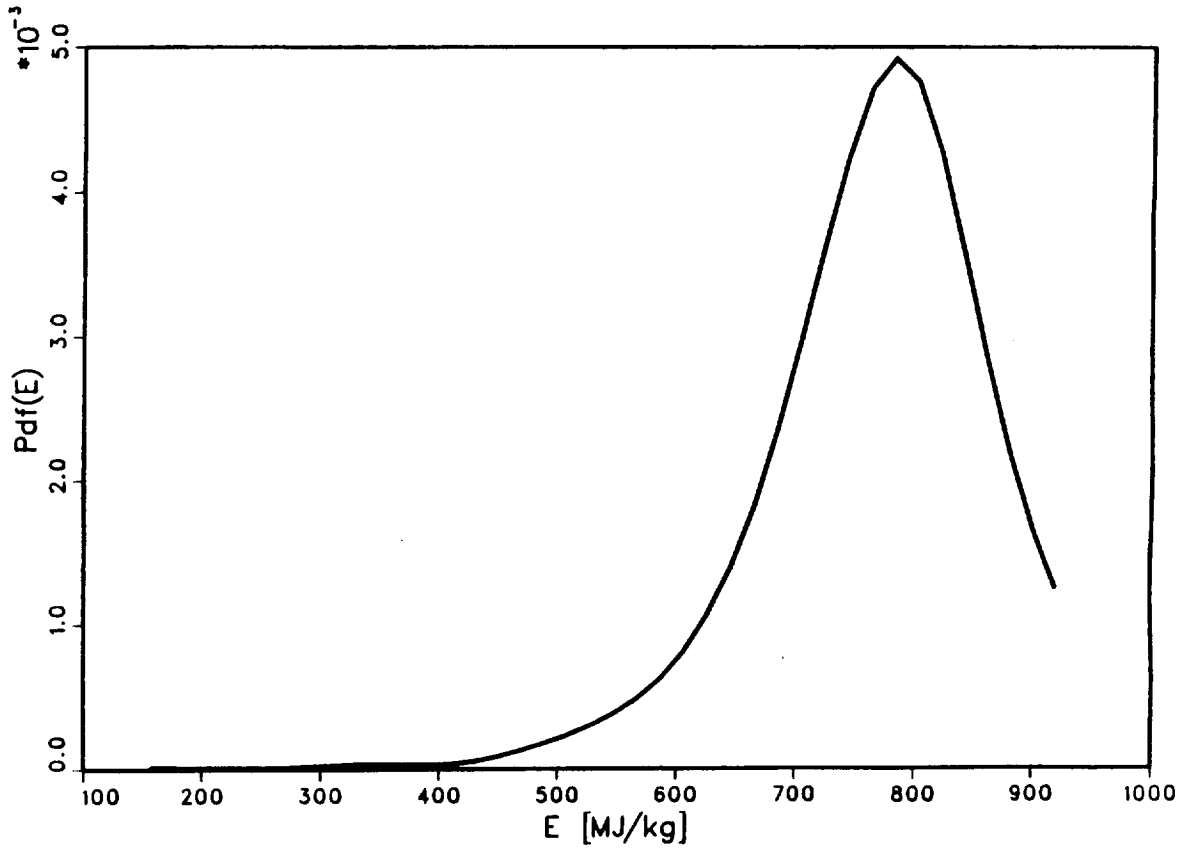

Fig. 44. Coaxial turbulent supersonic jet flame burning H_2 with air. Pdf of internal energy at $x/D = 15.5$ and $r/D = 0.84$ for $c_{\rho 1} = 1.0$ and $c_{\rho 2} = 0.5$.

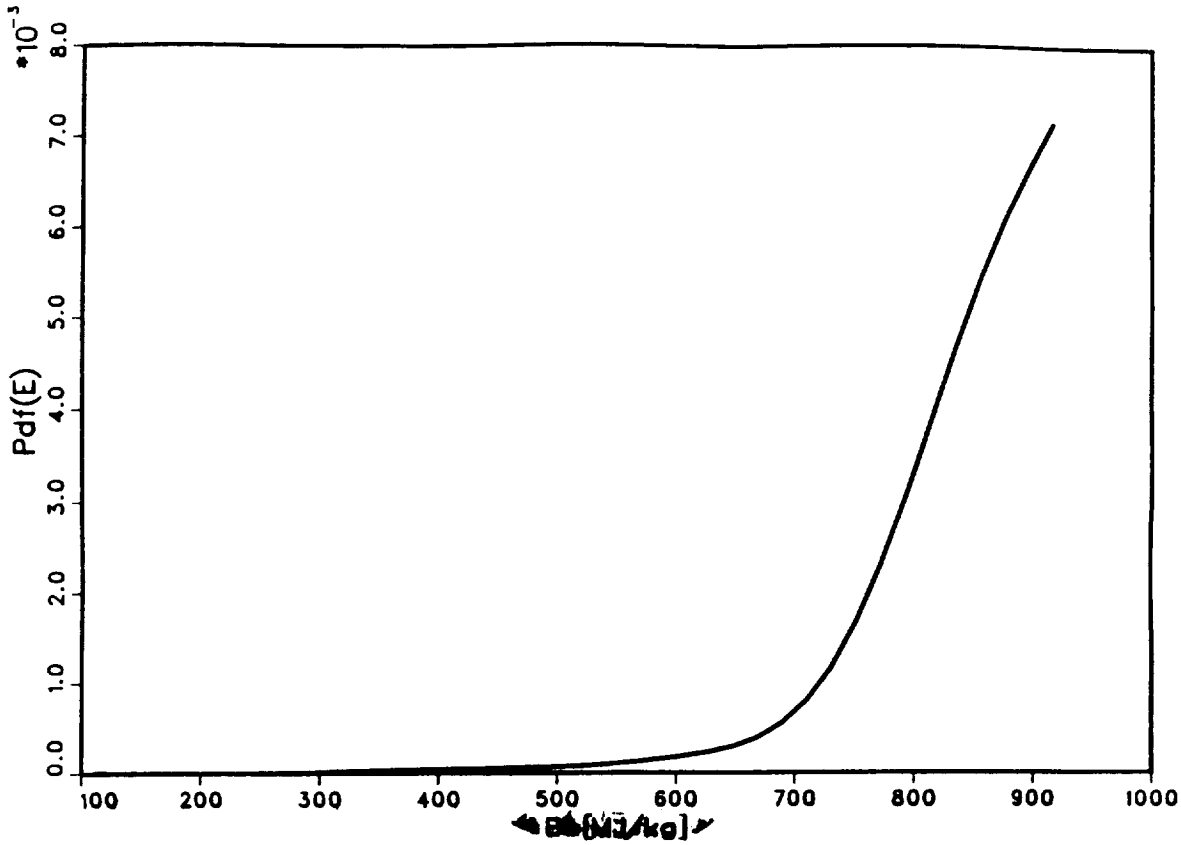

Fig. 45. Coaxial turbulent supersonic jet flame burning H_2 with air. Pdf of internal energy at $x/D = 15.5$ and $r/D = 1.14$ for $c_{\rho 1} = 1.0$ and $c_{\rho 2} = 0.5$.

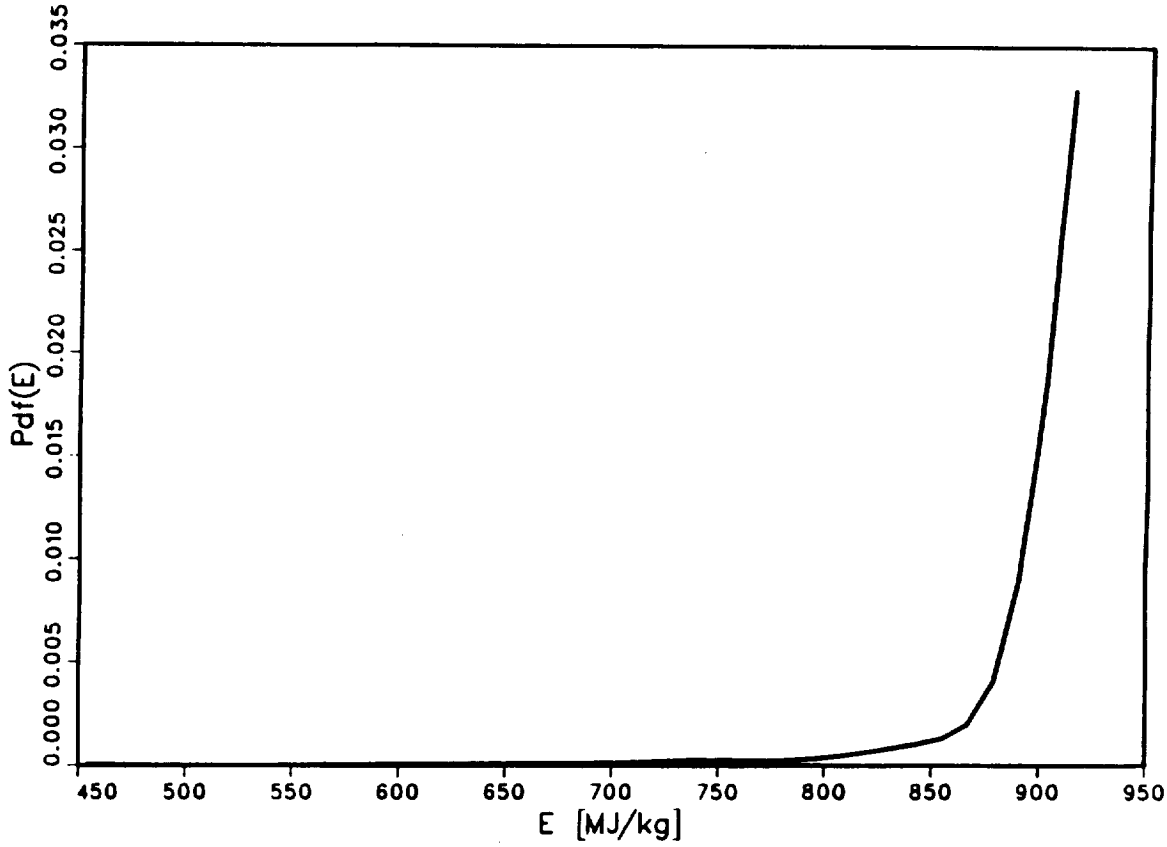

Fig. 46. Coaxial turbulent supersonic jet flame burning H_2 with air. Pdf of internal energy at $x/D = 15.5$ and $r/D = 1.42$ for $c_{\rho 1} = 1.0$ and $c_{\rho 2} = 0.5$.

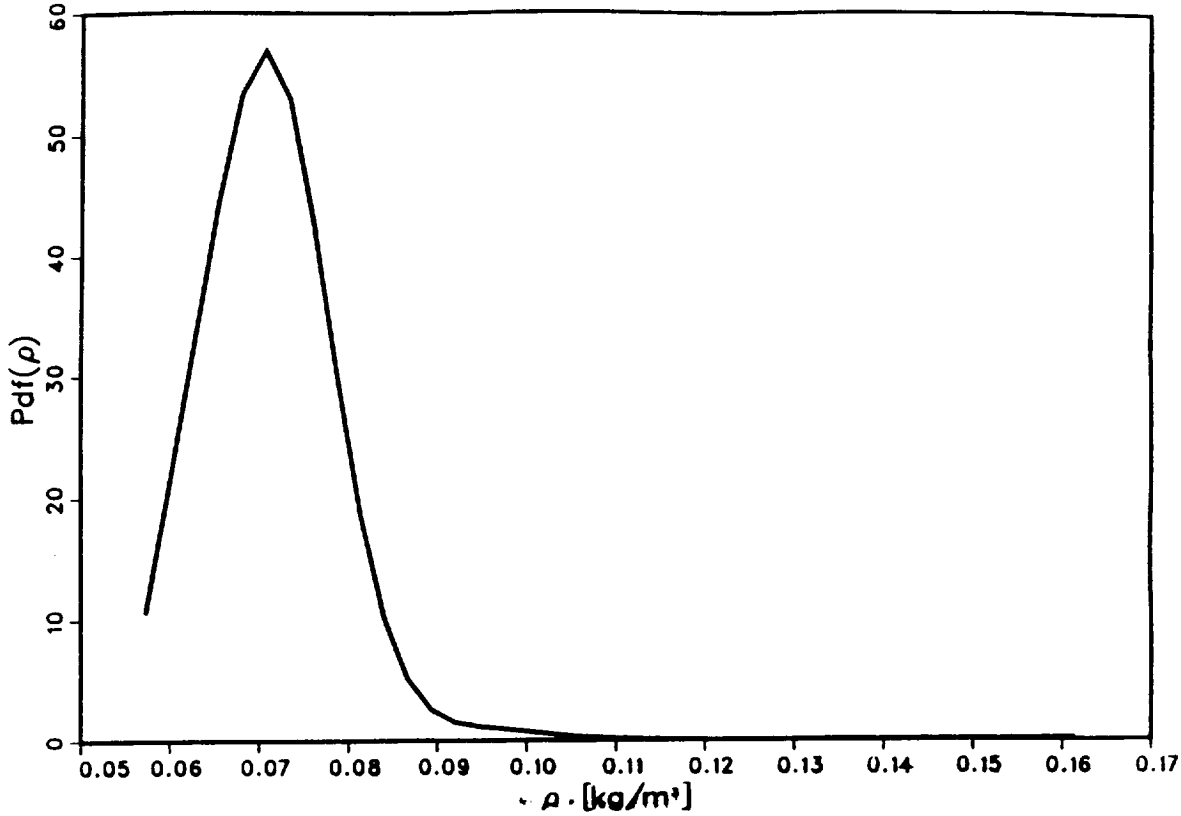

Fig. 47. Coaxial turbulent supersonic jet flame burning H_2 with air. Pdf of density at $x/D = 15.5$ and $r/D = 0.27$ for $c_{\rho 1} = 1.0$ and $c_{\rho 2} = 0.5$.

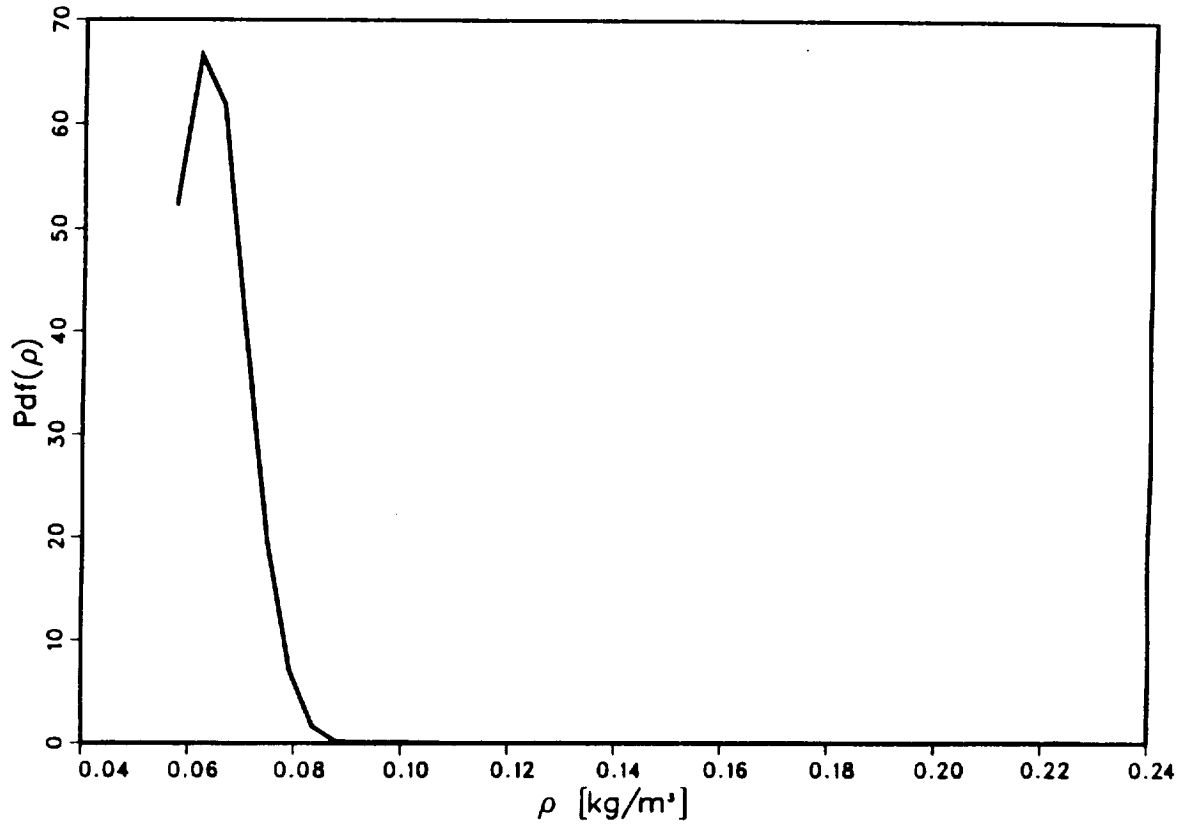

Fig. 48. Coaxial turbulent supersonic jet flame burning H_2 with air. Pdf of density at $x/D = 15.5$ and $r/D = 0.55$ for $c_{\rho 1} = 1.0$ and $c_{\rho 2} = 0.5$.

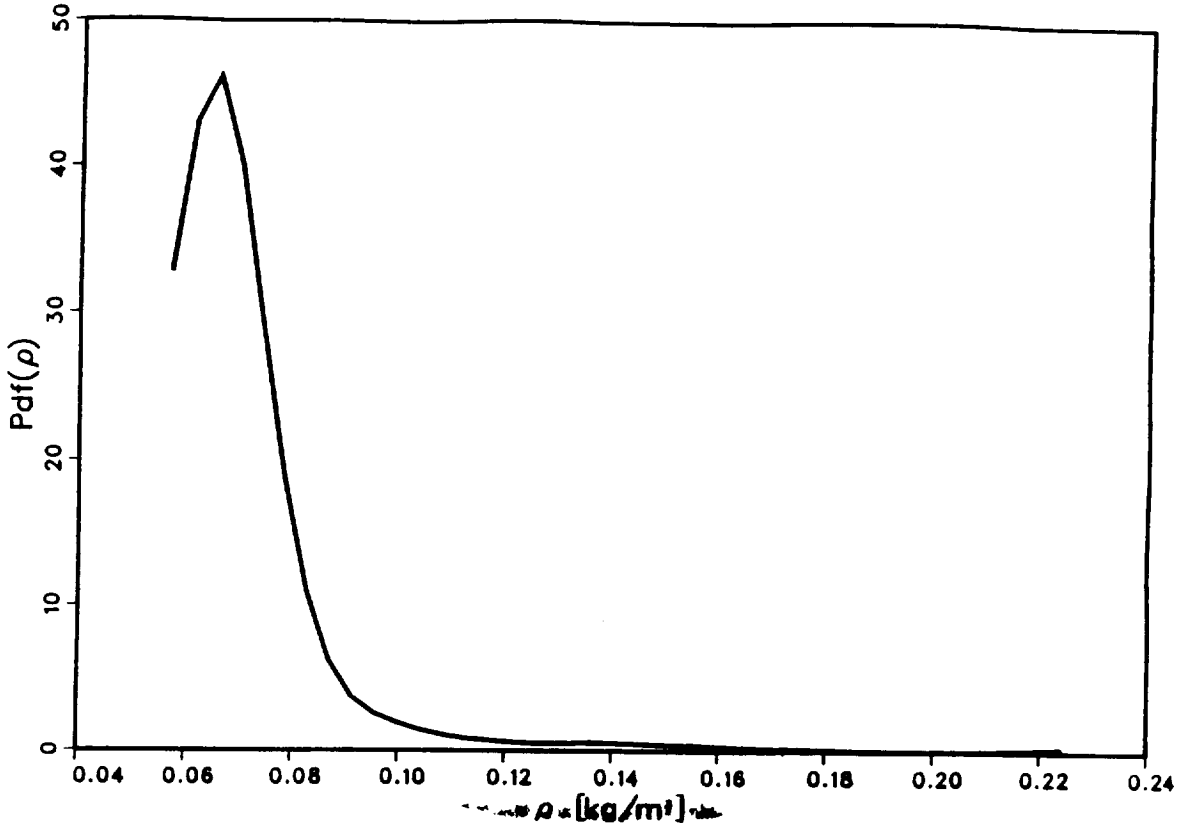

Fig. 49. Coaxial turbulent supersonic jet flame burning H_2 with air. Pdf of density at $x/D = 15.5$ and $r/D = 0.84$ for $c_{\rho 1} = 1.0$ and $c_{\rho 2} = 0.5$.

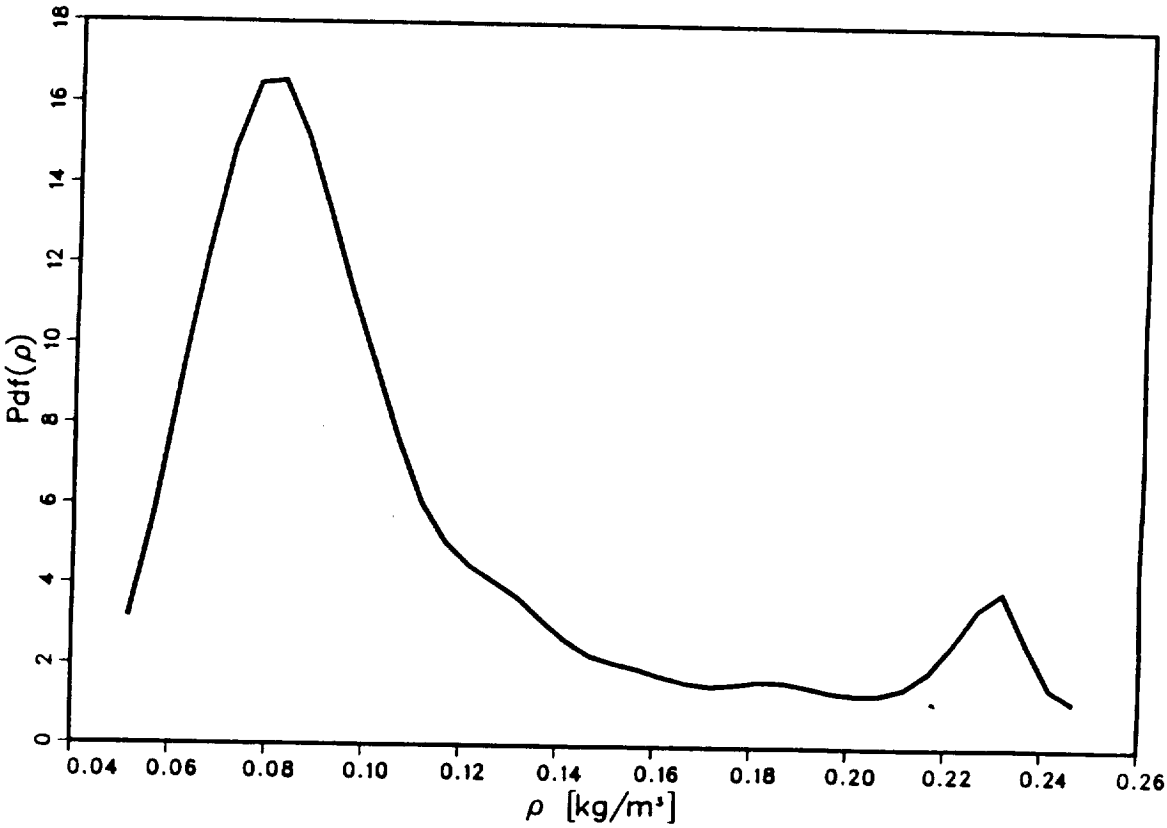

Fig. 50. Coaxial turbulent supersonic jet flame burning H_2 with air. Pdf of density at $x/D = 15.5$ and $r/D = 1.14$ for $c_{\rho 1} = 1.0$ and $c_{\rho 2} = 0.5$.

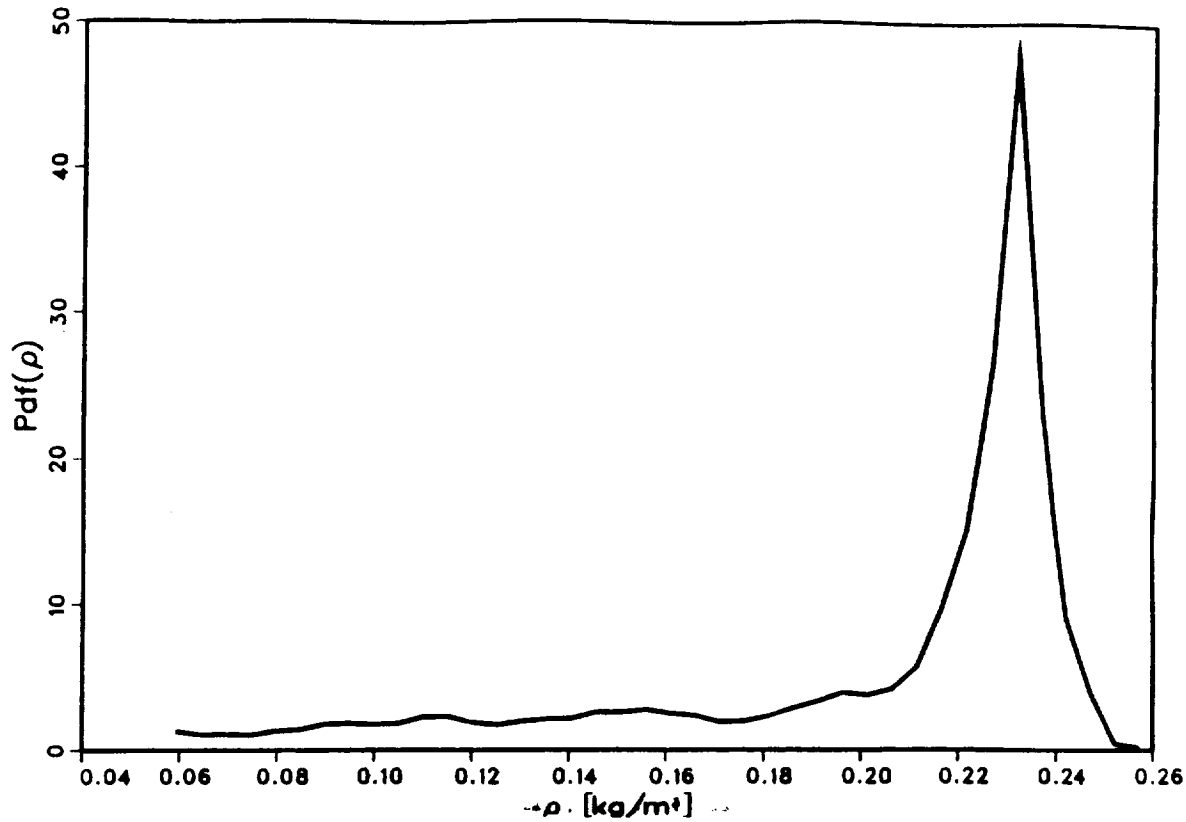

Fig. 51. Coaxial turbulent supersonic jet flame burning H_2 with air. Pdf of density at $x/D = 15.5$ and $r/D = 1.42$ for $c_{\rho 1} = 1.0$ and $c_{\rho 2} = 0.5$.

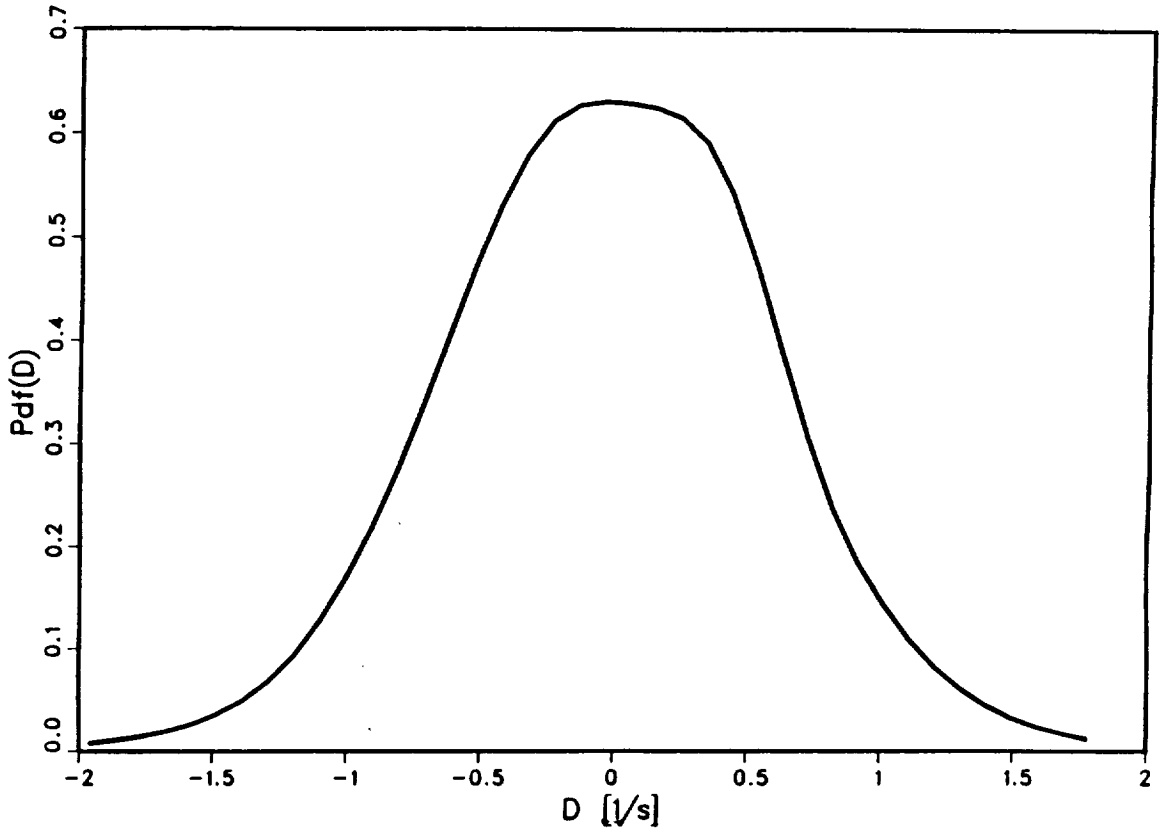

Fig. 52. Coaxial turbulent supersonic jet flame burning H_2 with air. Pdf of relative rate of volume expansion at $x/D = 15.5$ and $r/D = 0.27$ for $c_{\rho 1} = 1.0$ and $c_{\rho 2} = 0.5$.

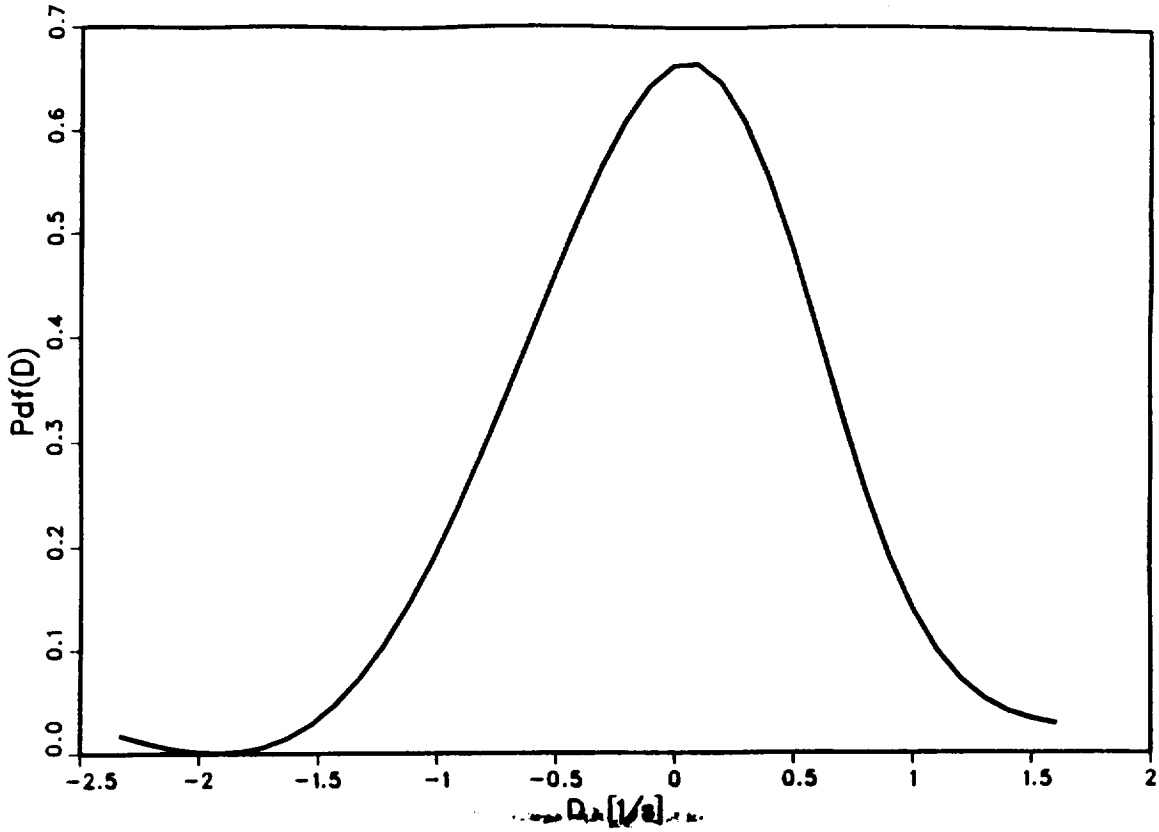

Fig. 53. Coaxial turbulent supersonic jet flame burning H_2 with air. Pdf of relative rate of volume expansion at $x/D = 15.5$ and $r/D = 0.55$ for $c_{\rho 1} = 1.0$ and $c_{\rho 2} = 0.5$.

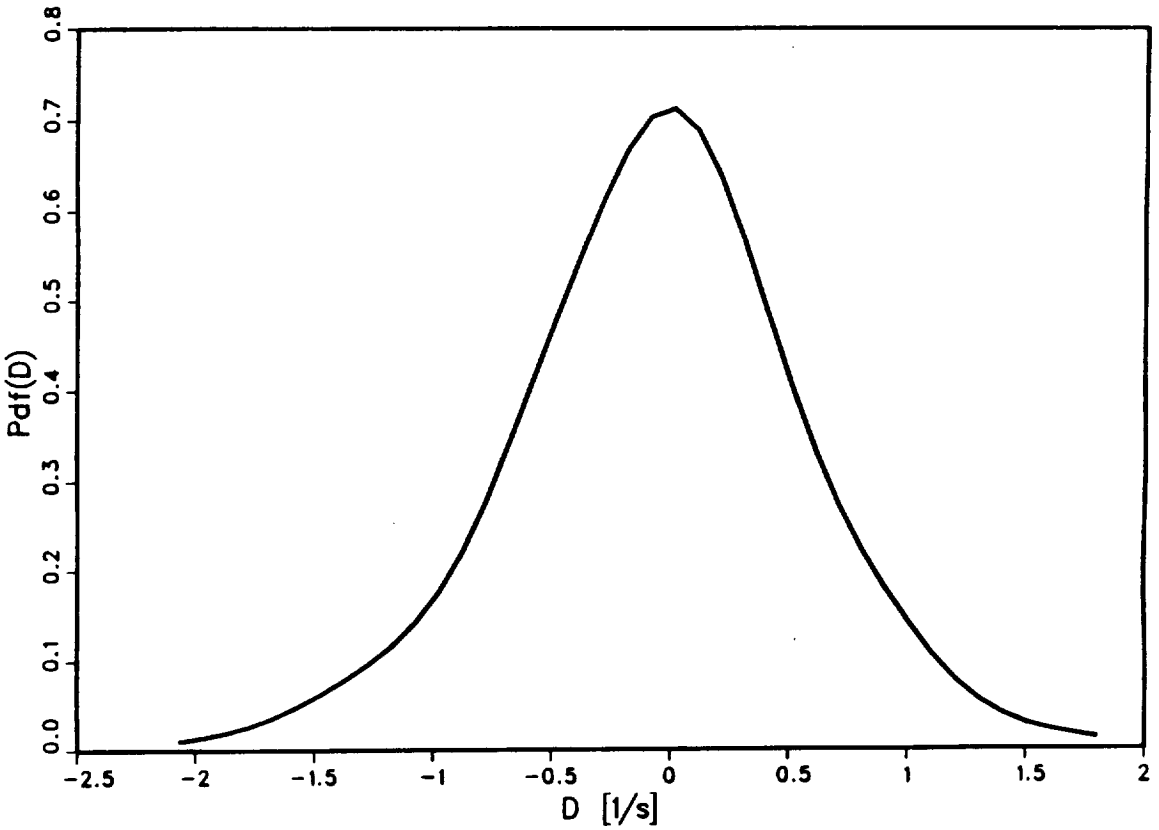

Fig. 54. Coaxial turbulent supersonic jet flame burning H_2 with air. Pdf of relative rate of volume expansion at $x/D = 15.5$ and $r/D = 0.84$ for $c_{\rho 1} = 1.0$ and $c_{\rho 2} = 0.5$.

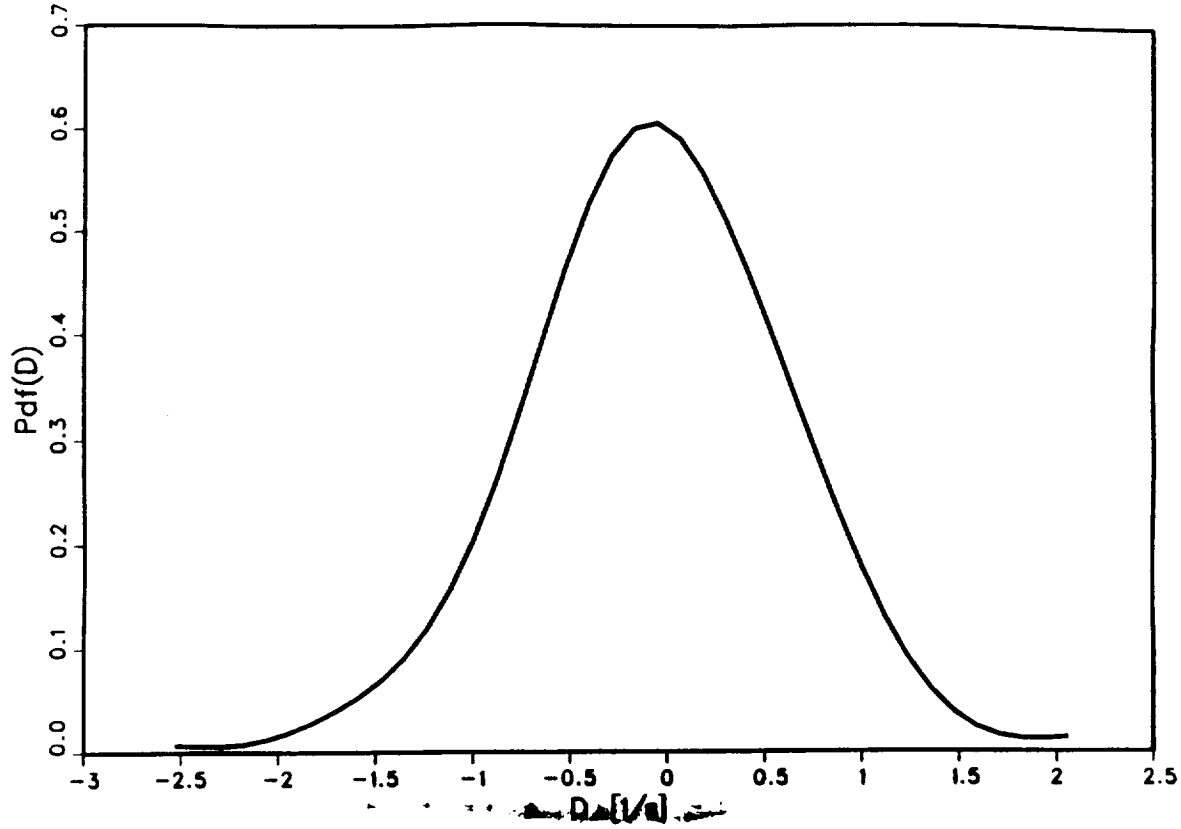

Fig. 55. Coaxial turbulent supersonic jet flame burning H_2 with air. Pdf of relative rate of volume expansion at $x/D = 15.5$ and $r/D = 1.14$ for $c_{\rho 1} = 1.0$ and $c_{\rho 2} = 0.5$.

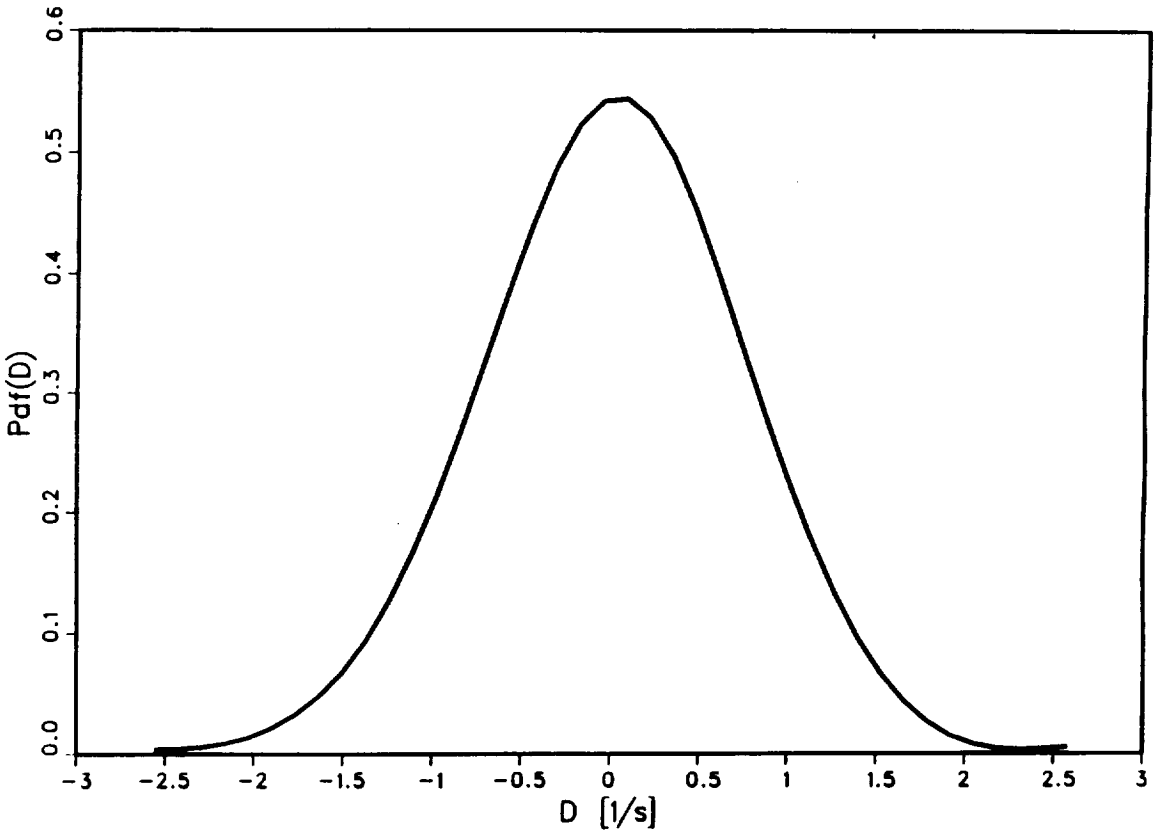

Fig. 56. Coaxial turbulent supersonic jet flame burning H_2 with air. Pdf of relative rate of volume expansion at $x/D = 15.5$ and $r/D = 1.42$ for $c_{\rho 1} = 1.0$ and $c_{\rho 2} = 0.5$.

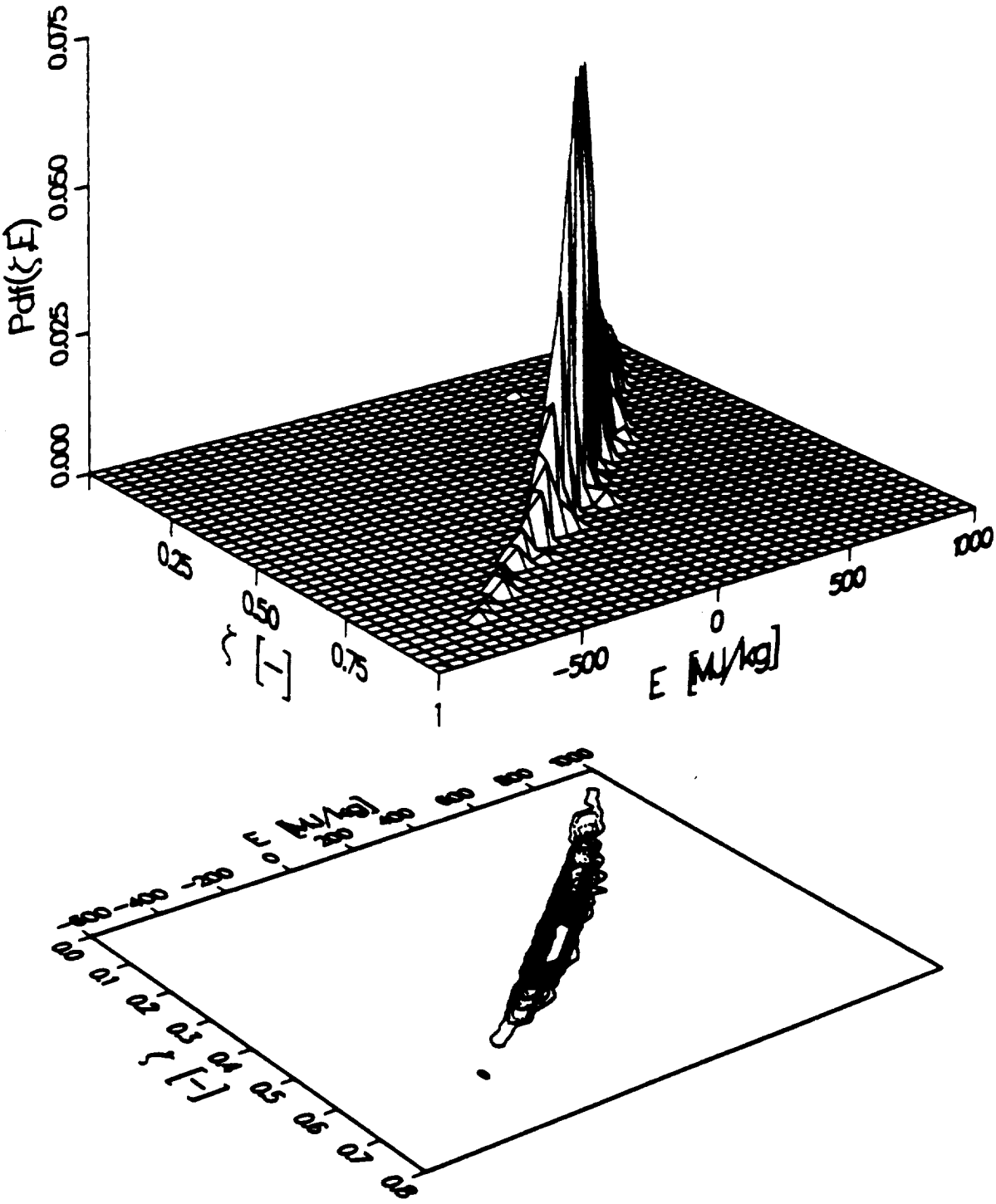

Fig. 57. Coaxial turbulent supersonic jet flame burning H_2 with air. Pdf of mixture fraction and internal energy at $x/D = 15.5$ and $r/D = 0.27$ for $c_{\rho 1} = 1.0$ and $c_{\rho 2} = 0.5$.

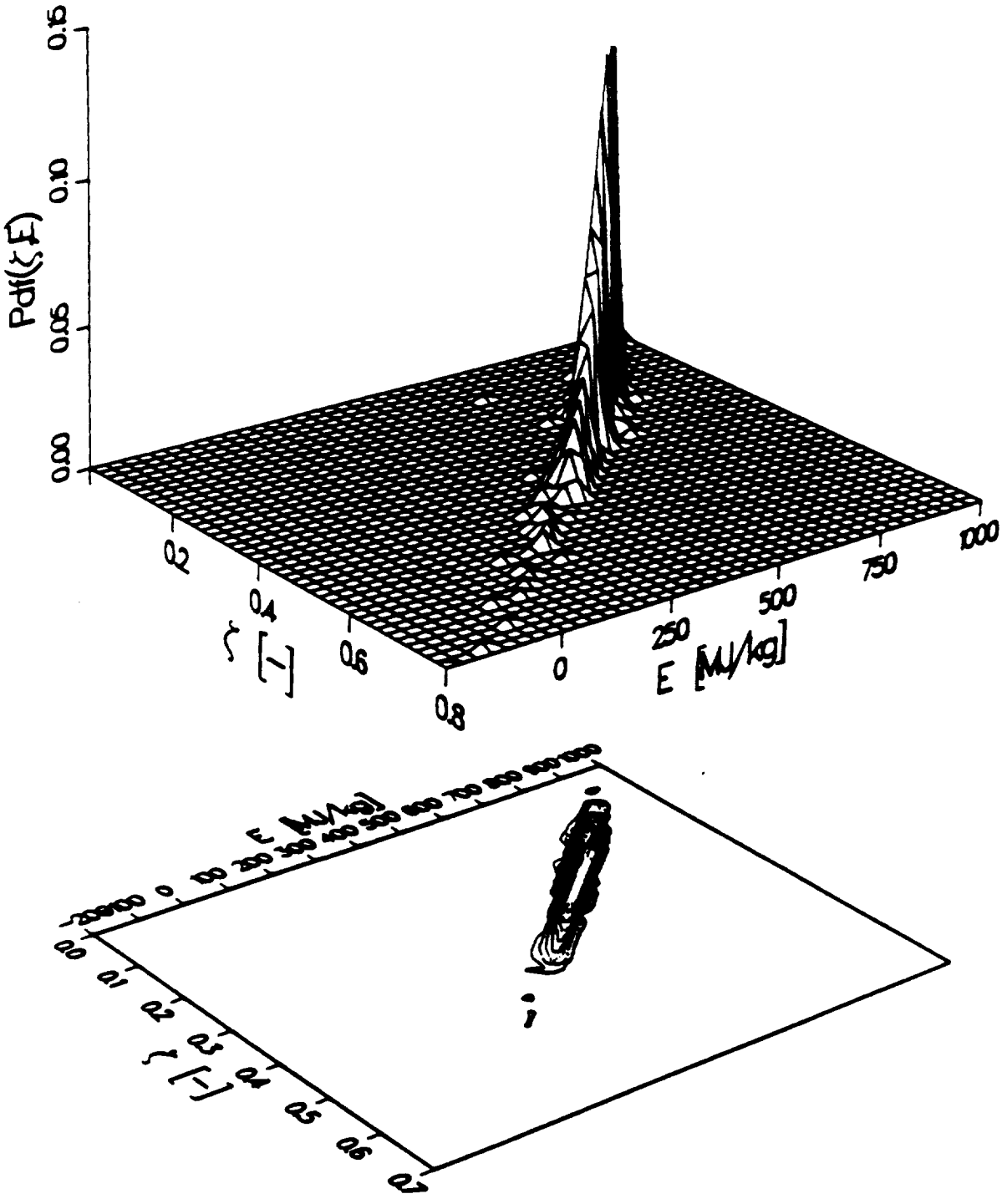

Fig. 58. Coaxial turbulent supersonic jet flame burning H_2 with air. Pdf of mixture fraction and internal energy at $x/D = 15.5$ and $r/D = 0.55$ for $c_{\rho 1} = 1.0$ and $c_{\rho 2} = 0.5$.

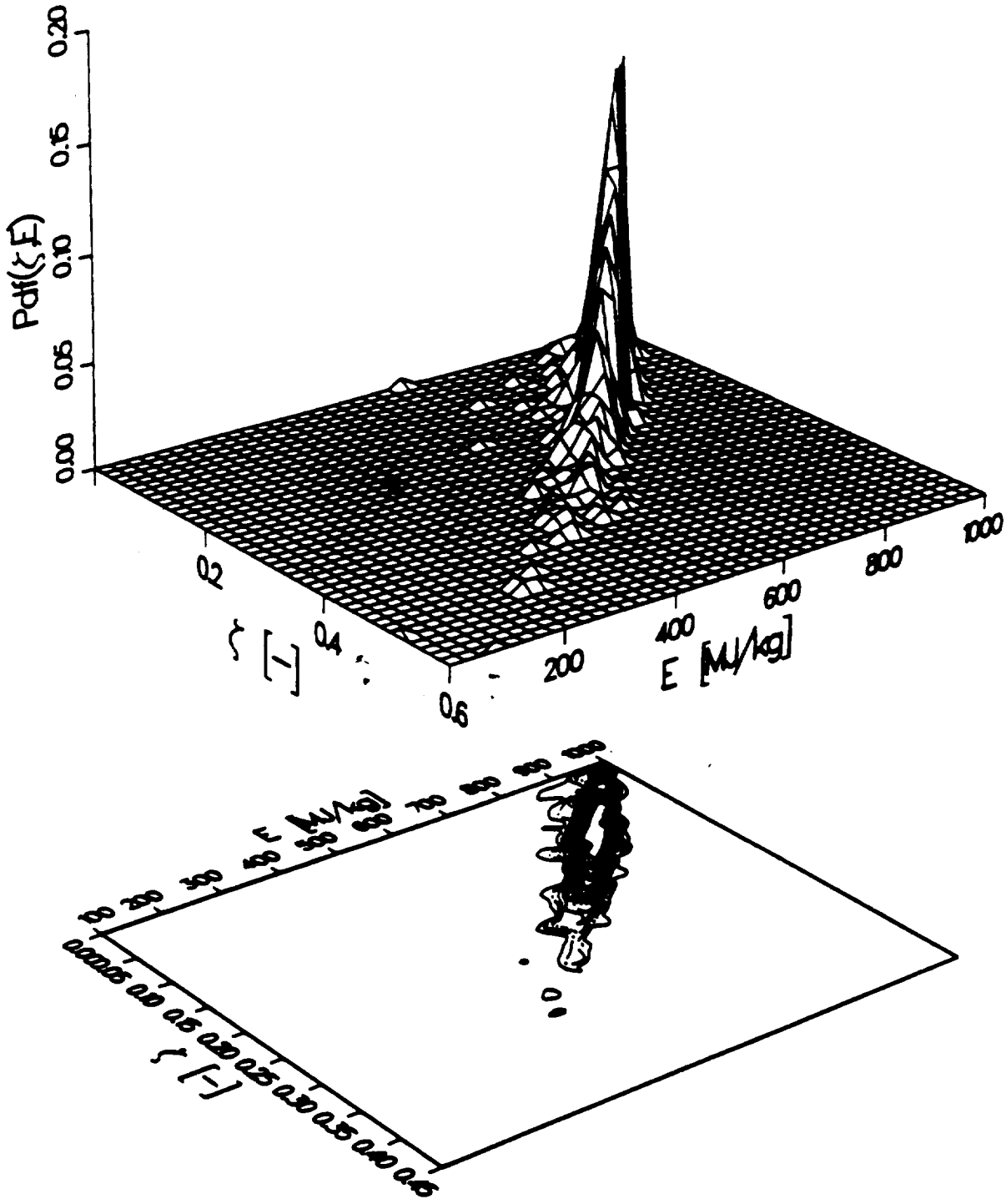

Fig. 59. Coaxial turbulent supersonic jet flame burning H_2 with air. Pdf of mixture fraction and internal energy at $x/D = 15.5$ and $r/D = 0.84$ for $c_{\rho 1} = 1.0$ and $c_{\rho 2} = 0.5$.

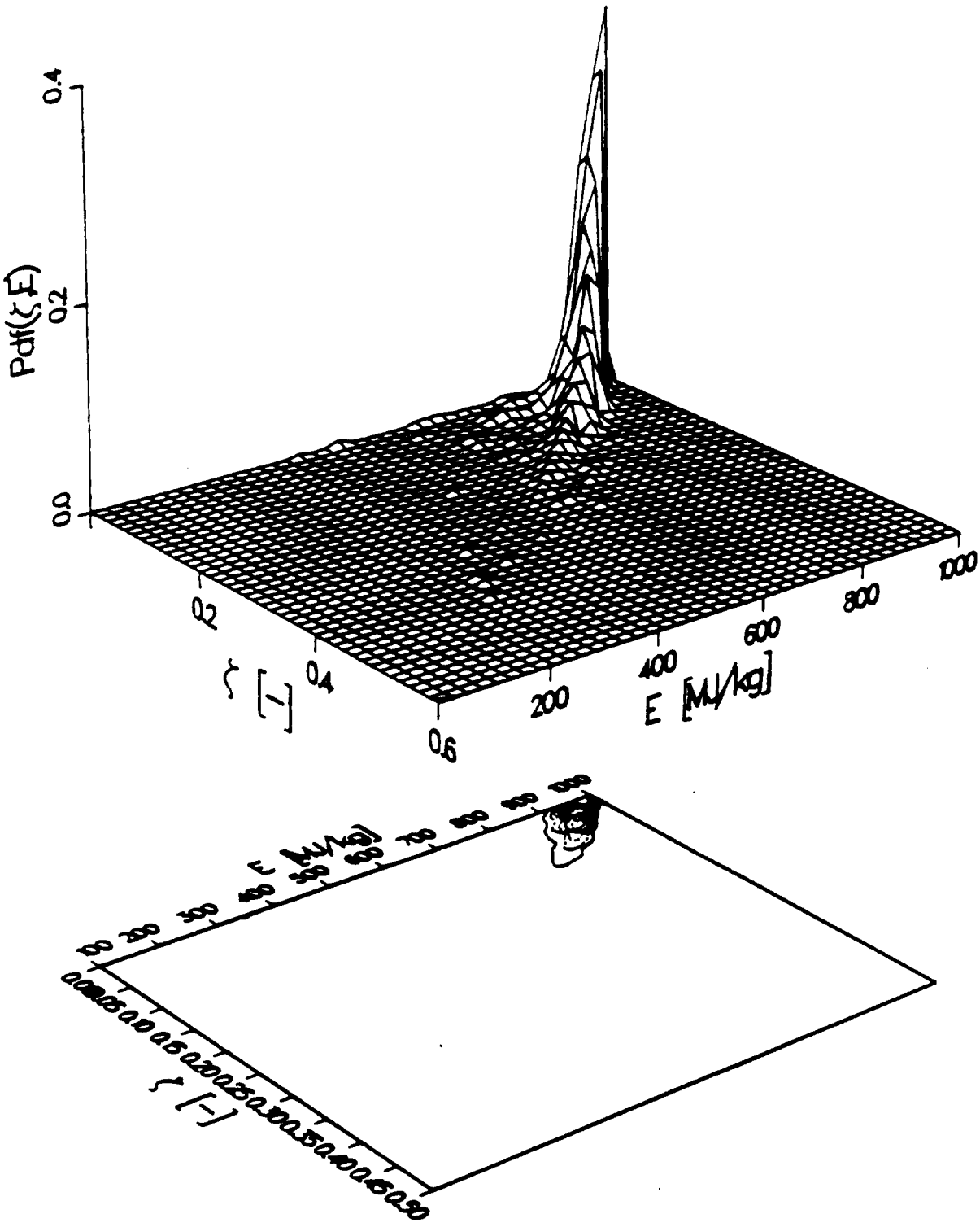

Fig. 60. Coaxial turbulent supersonic jet flame burning H_2 with air. Pdf of mixture fraction and internal energy at $x/D = 15.5$ and $r/D = 1.14$ for $c_{\rho 1} = 1.0$ and $c_{\rho 2} = 0.5$.

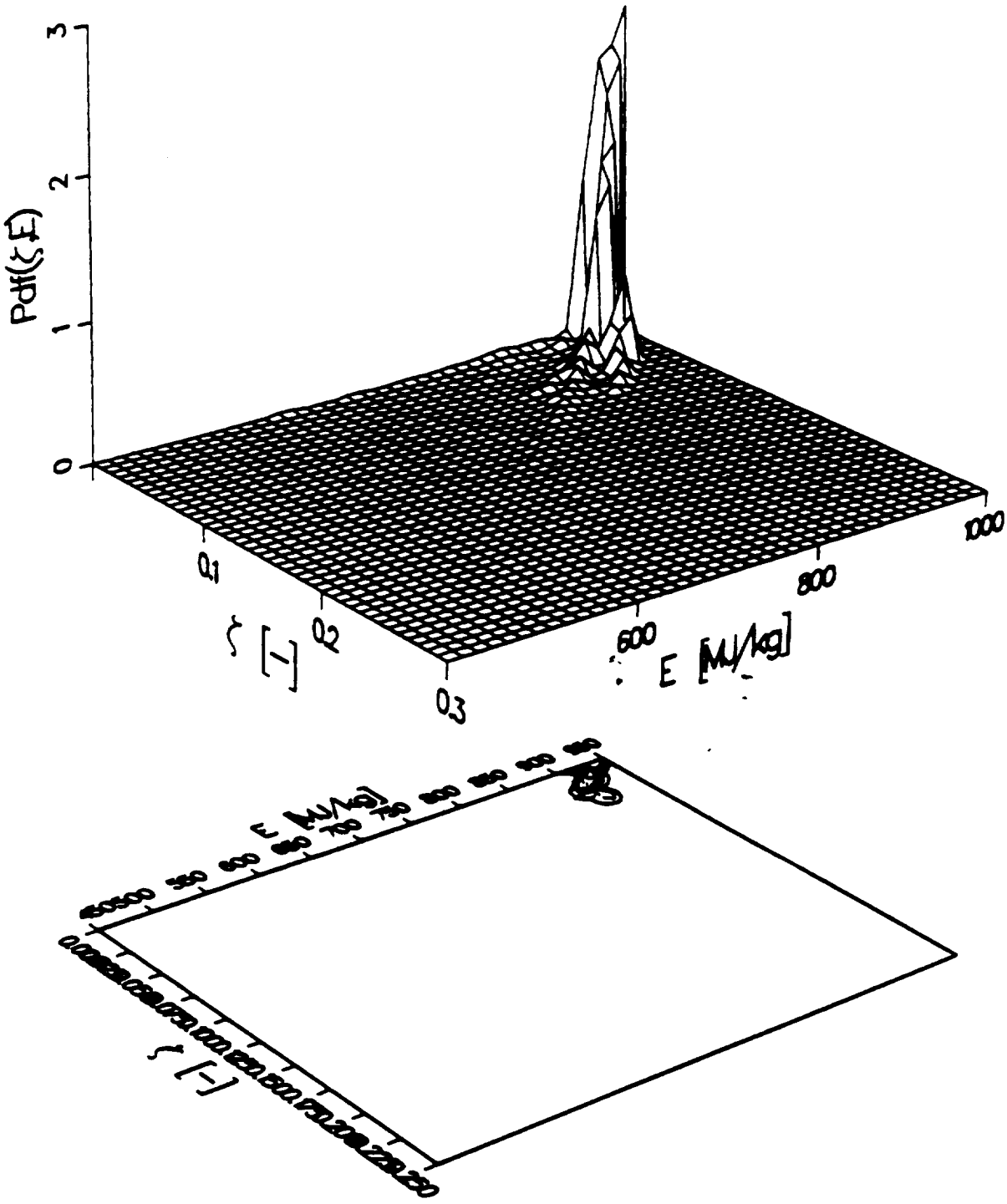

Fig. 61. Coaxial turbulent supersonic jet flame burning H_2 with air. Pdf of mixture fraction and internal energy at $x/D = 15.5$ and $r/D = 1.42$ for $c_{\rho 1} = 1.0$ and $c_{\rho 2} = 0.5$.

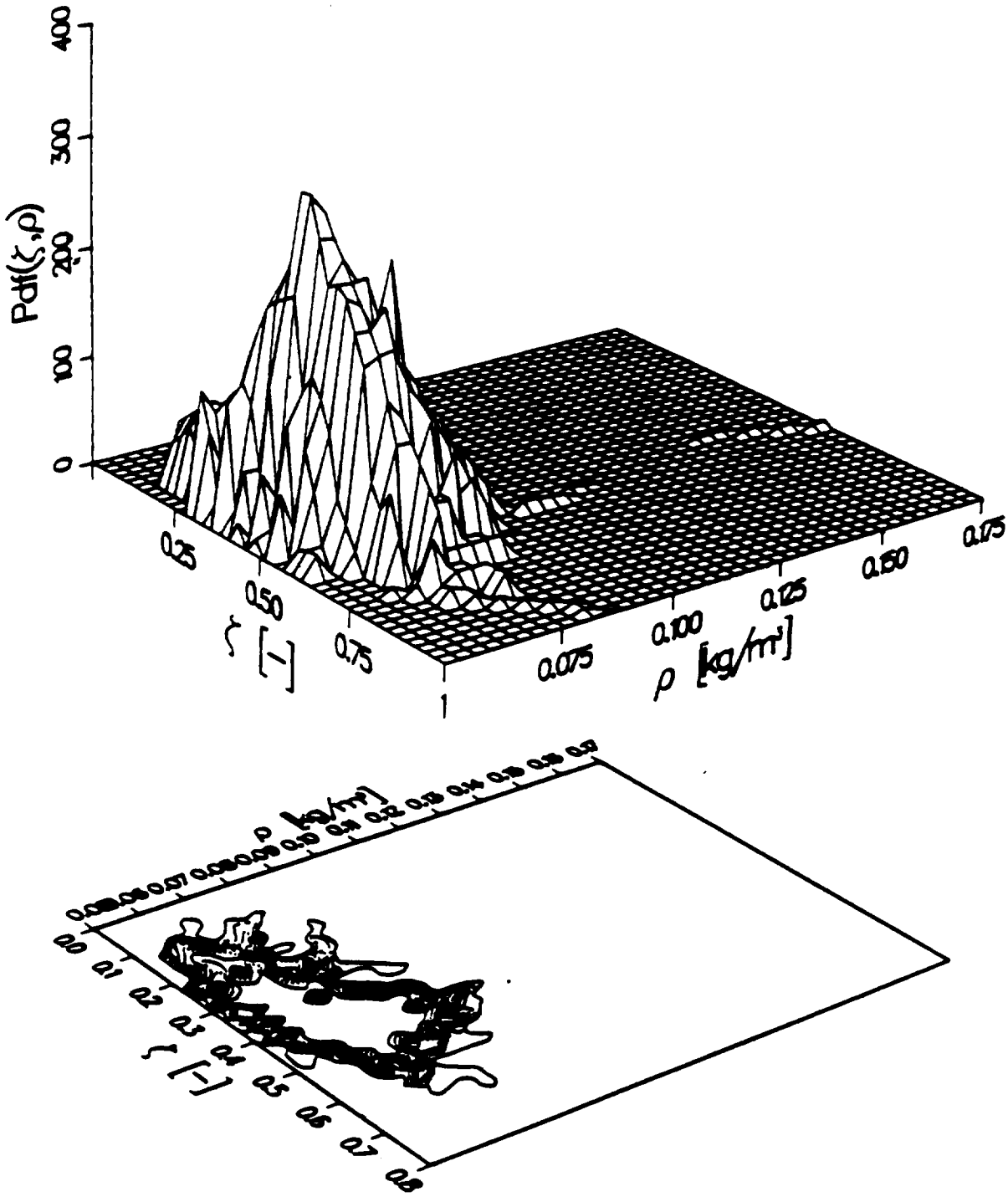

Fig. 62. Coaxial turbulent supersonic jet flame burning H_2 with air. Pdf of mixture fraction and density at $x/D = 15.5$ and $r/D = 0.27$ for $c_{\rho 1} = 1.0$ and $c_{\rho 2} = 0.5$.

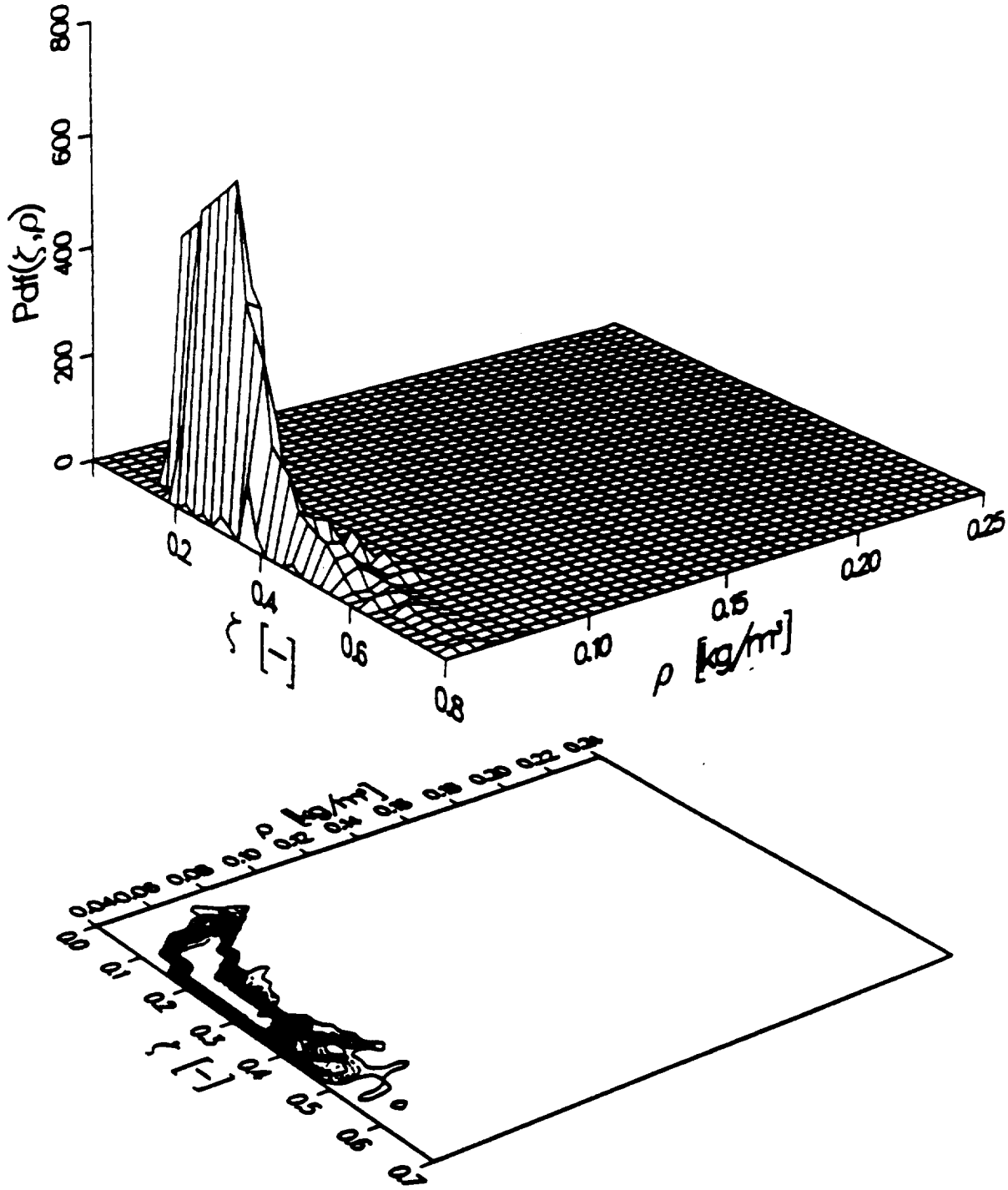

Fig. 63. Coaxial turbulent supersonic jet flame burning H_2 with air. Pdf of mixture fraction and density at $x/D = 15.5$ and $r/D = 0.55$ for $c_{\rho 1} = 1.0$ and $c_{\rho 2} = 0.5$.

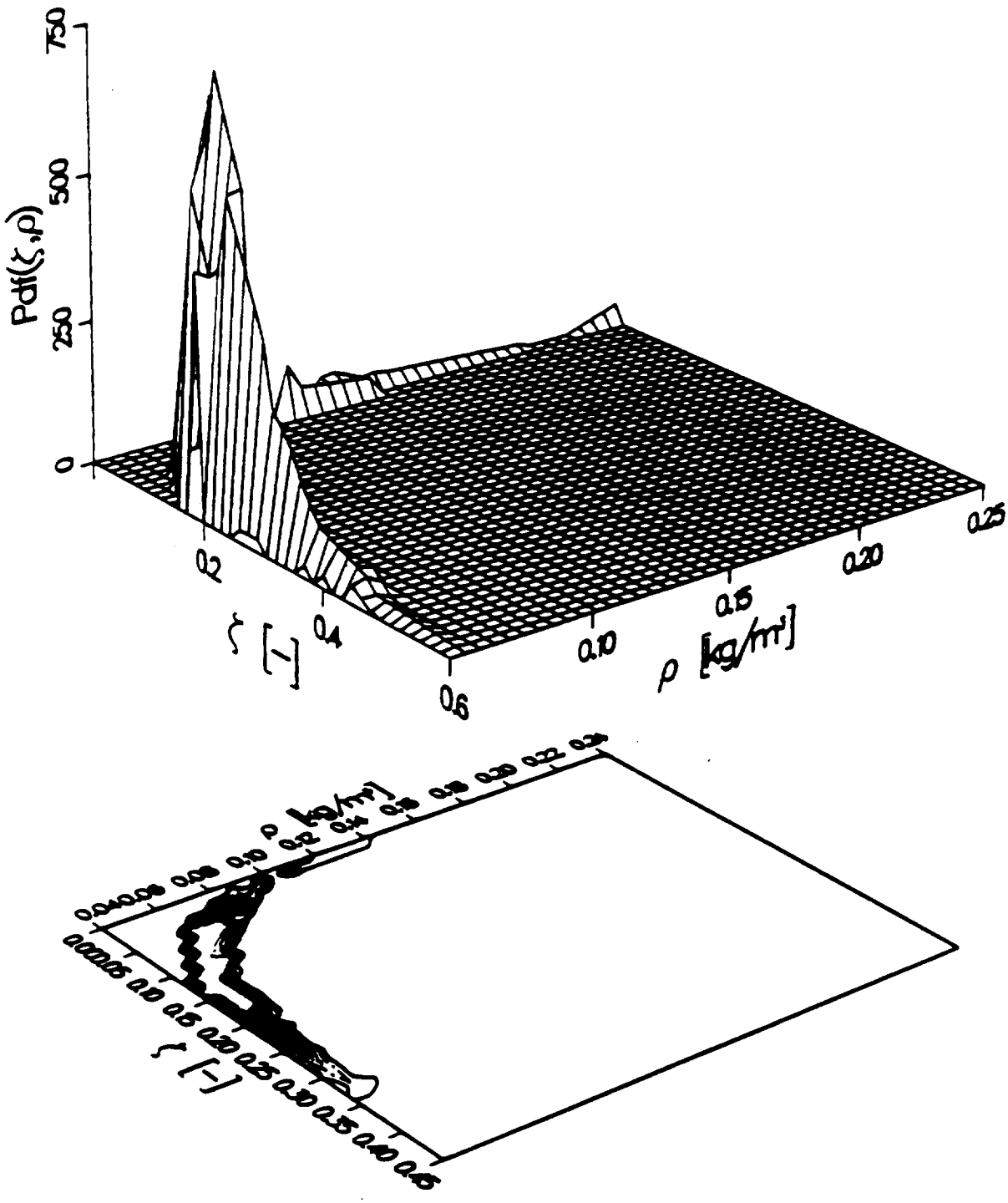

Fig. 64. Coaxial turbulent supersonic jet flame burning H_2 with air. Pdf of mixture fraction and density at $x/D = 15.5$ and $r/D = 0.84$ for $c_{\rho 1} = 1.0$ and $c_{\rho 2} = 0.5$.

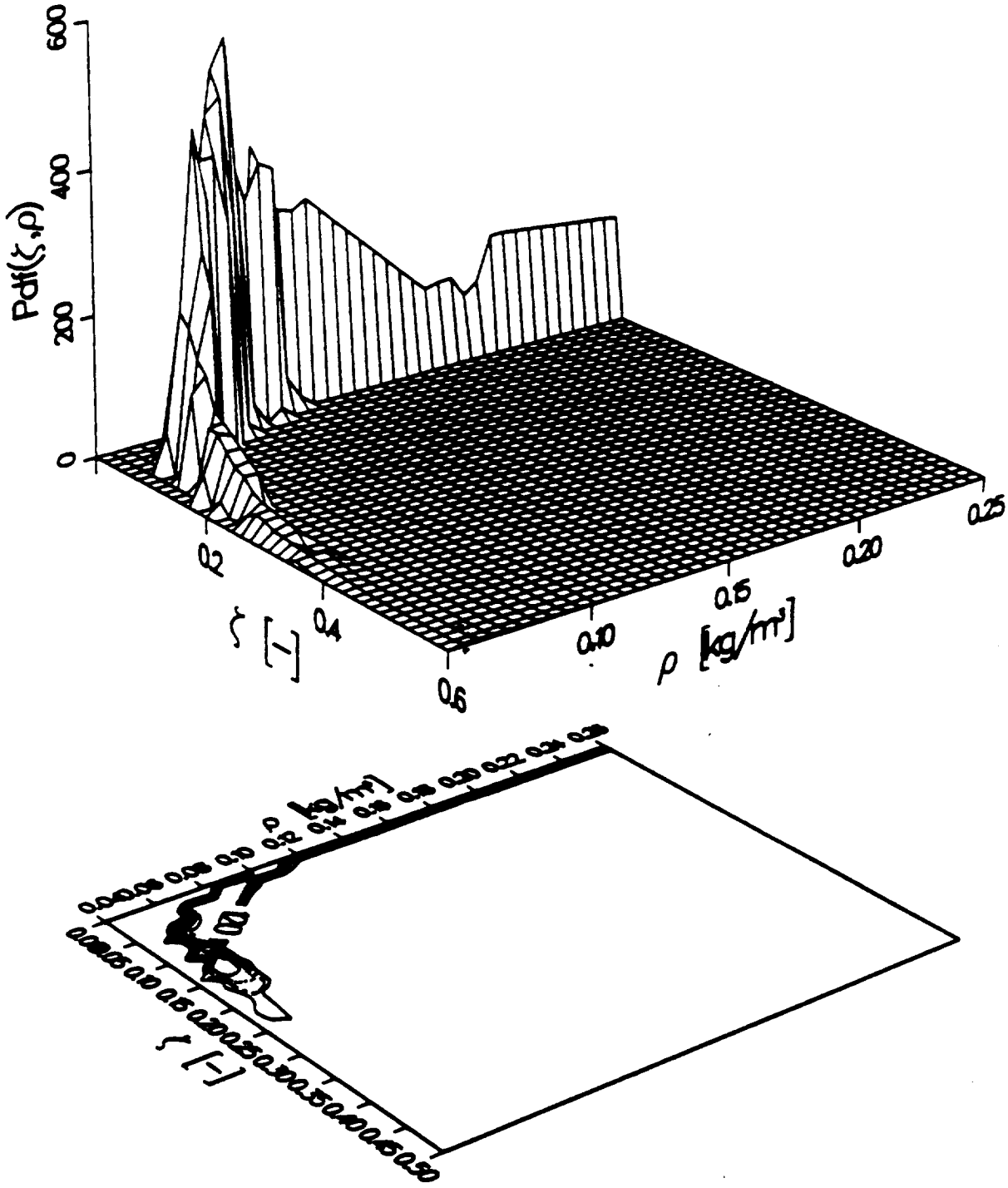

Fig. 65. Coaxial turbulent supersonic jet flame burning H_2 with air. Pdf of mixture fraction and density at $x/D = 15.5$ and $r/D = 1.14$ for $c_{\rho 1} = 1.0$ and $c_{\rho 2} = 0.5$.

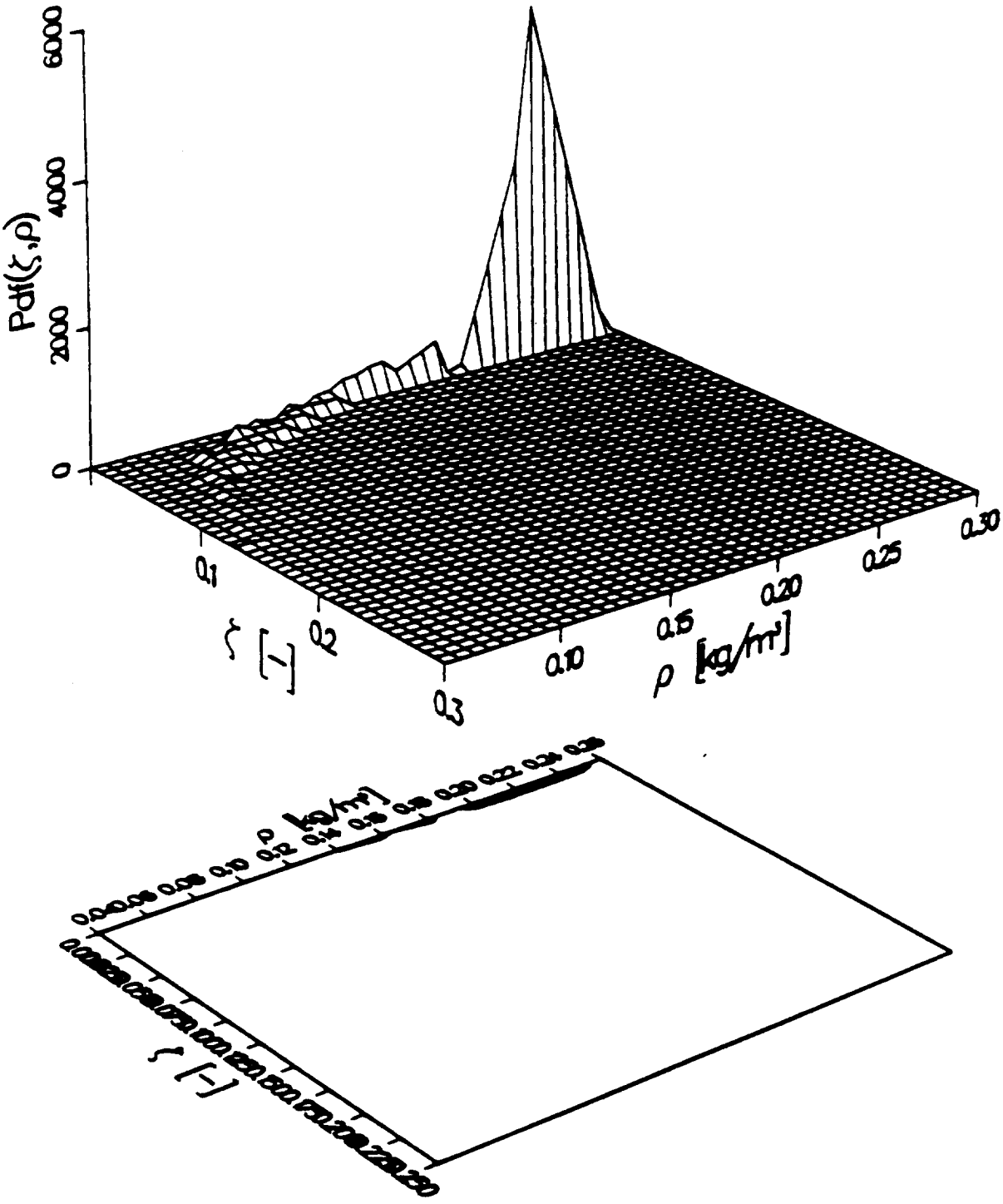

Fig. 66. Coaxial turbulent supersonic jet flame burning H_2 with air. Pdf of mixture fraction and density at $x/D = 15.5$ and $r/D = 1.42$ for $c_{\rho 1} = 1.0$ and $c_{\rho 2} = 0.5$.

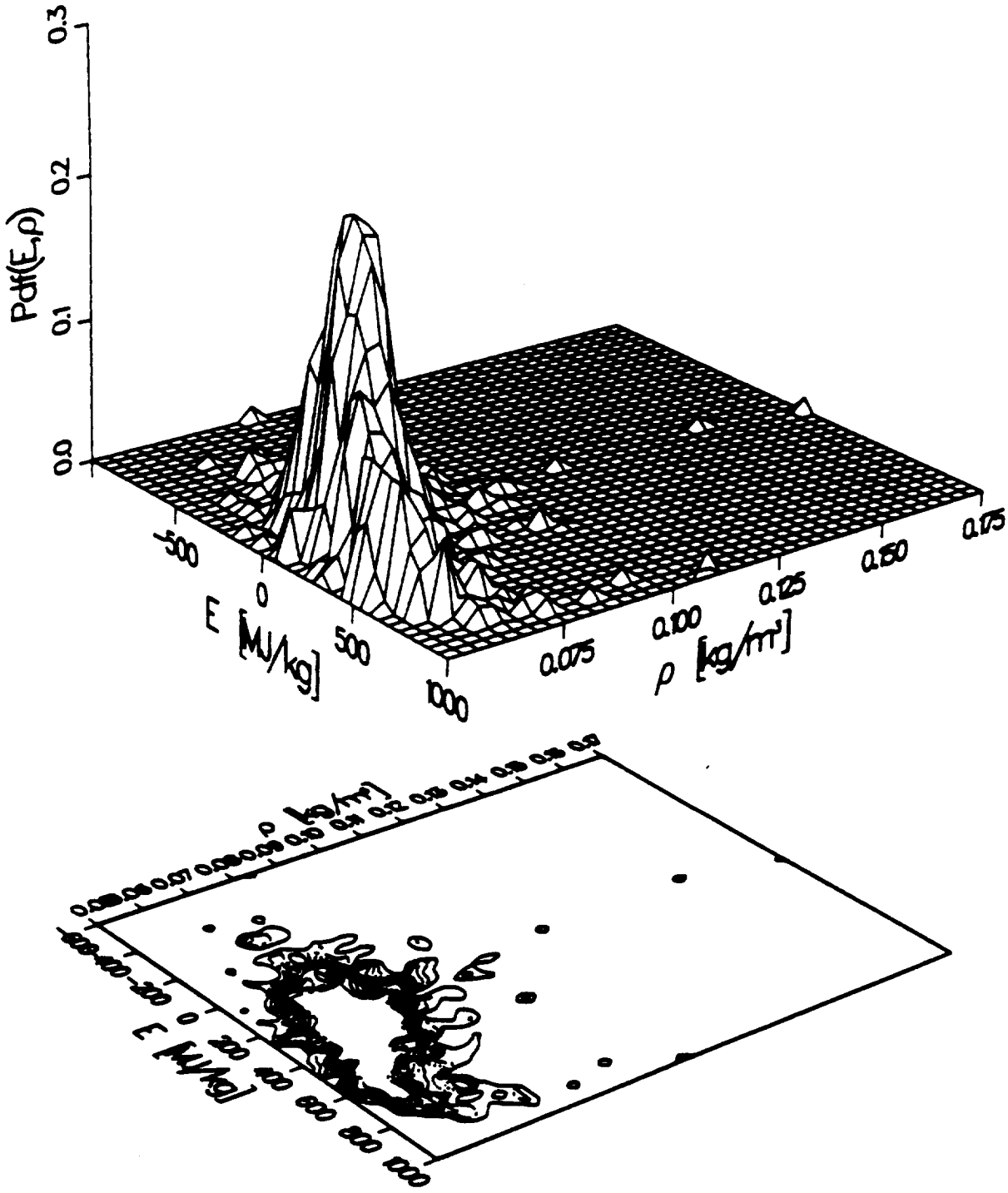

Fig. 67. Coaxial turbulent supersonic jet flame burning H_2 with air. Pdf of internal energy and density at $x/D = 15.5$ and $r/D = 0.27$ for $c_{\rho 1} = 1.0$ and $c_{\rho 2} = 0.5$.

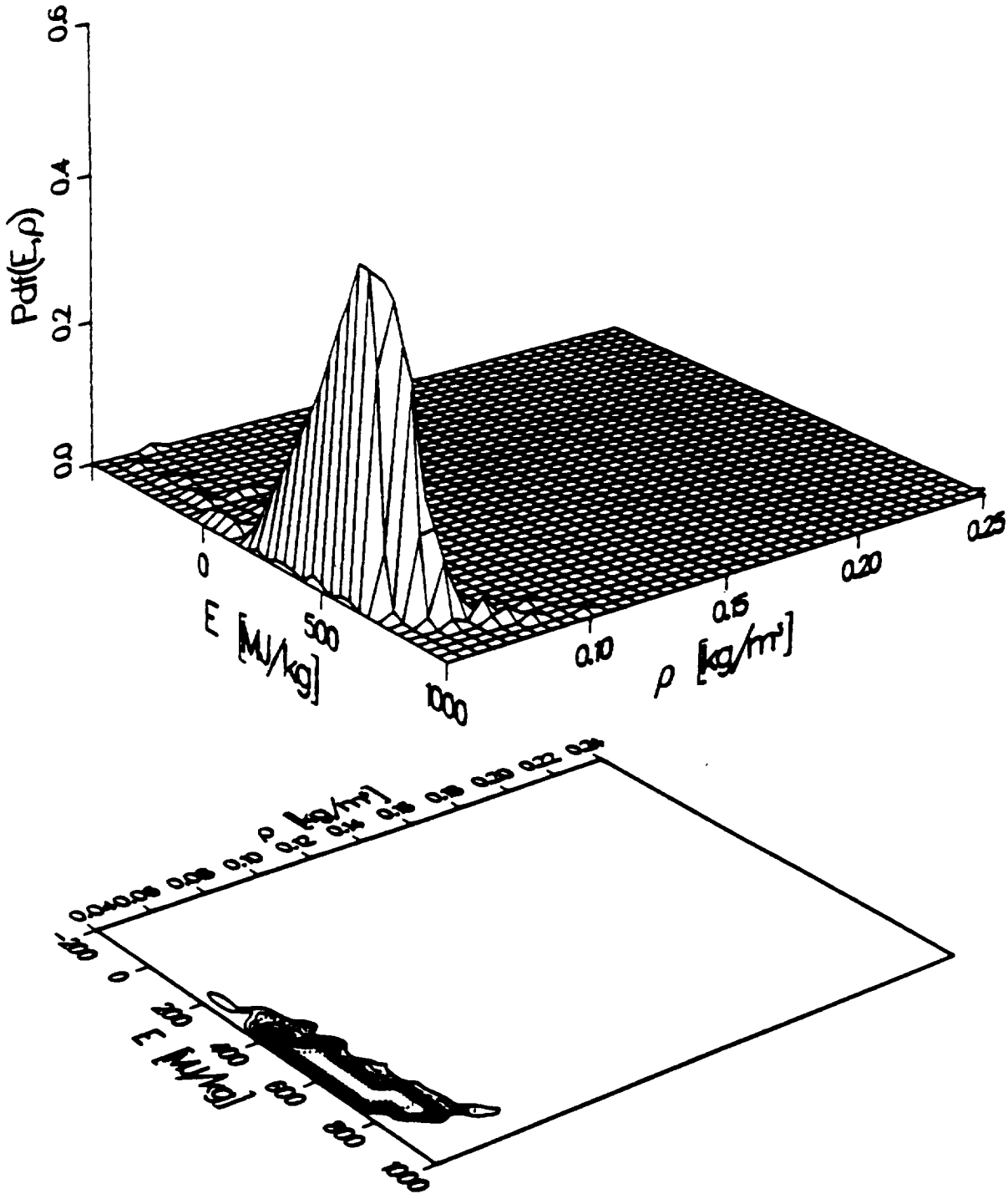

Fig. 68. Coaxial turbulent supersonic jet flame burning H_2 with air. Pdf of internal energy and density at $x/D = 15.5$ and $r/D = 0.55$ for $c_{\rho 1} = 1.0$ and $c_{\rho 2} = 0.5$.

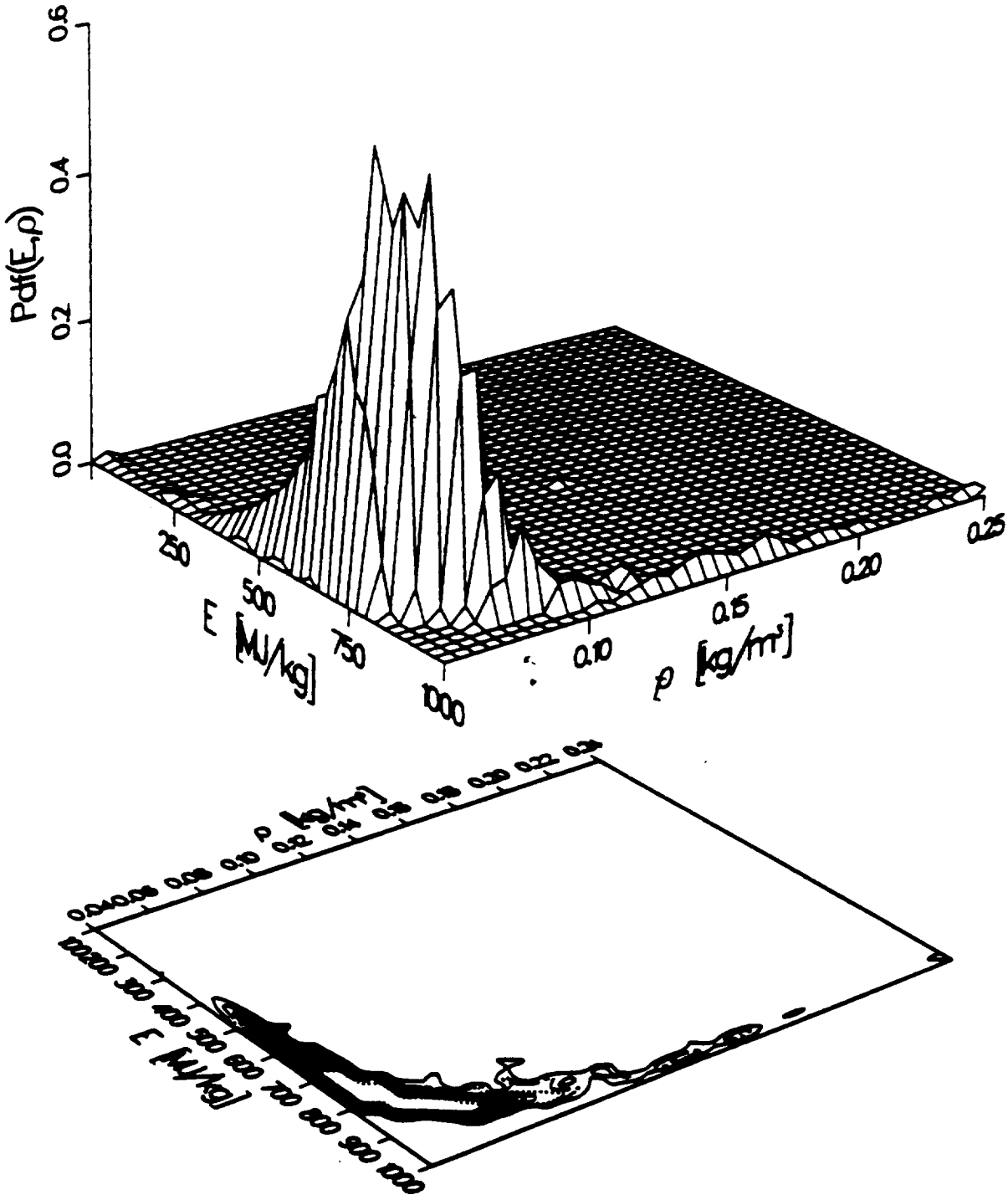

Fig. 69. Coaxial turbulent supersonic jet flame burning H_2 with air. Pdf of internal energy and density at $x/D = 15.5$ and $r/D = 0.84$ for $c_{\rho 1} = 1.0$ and $c_{\rho 2} = 0.5$.

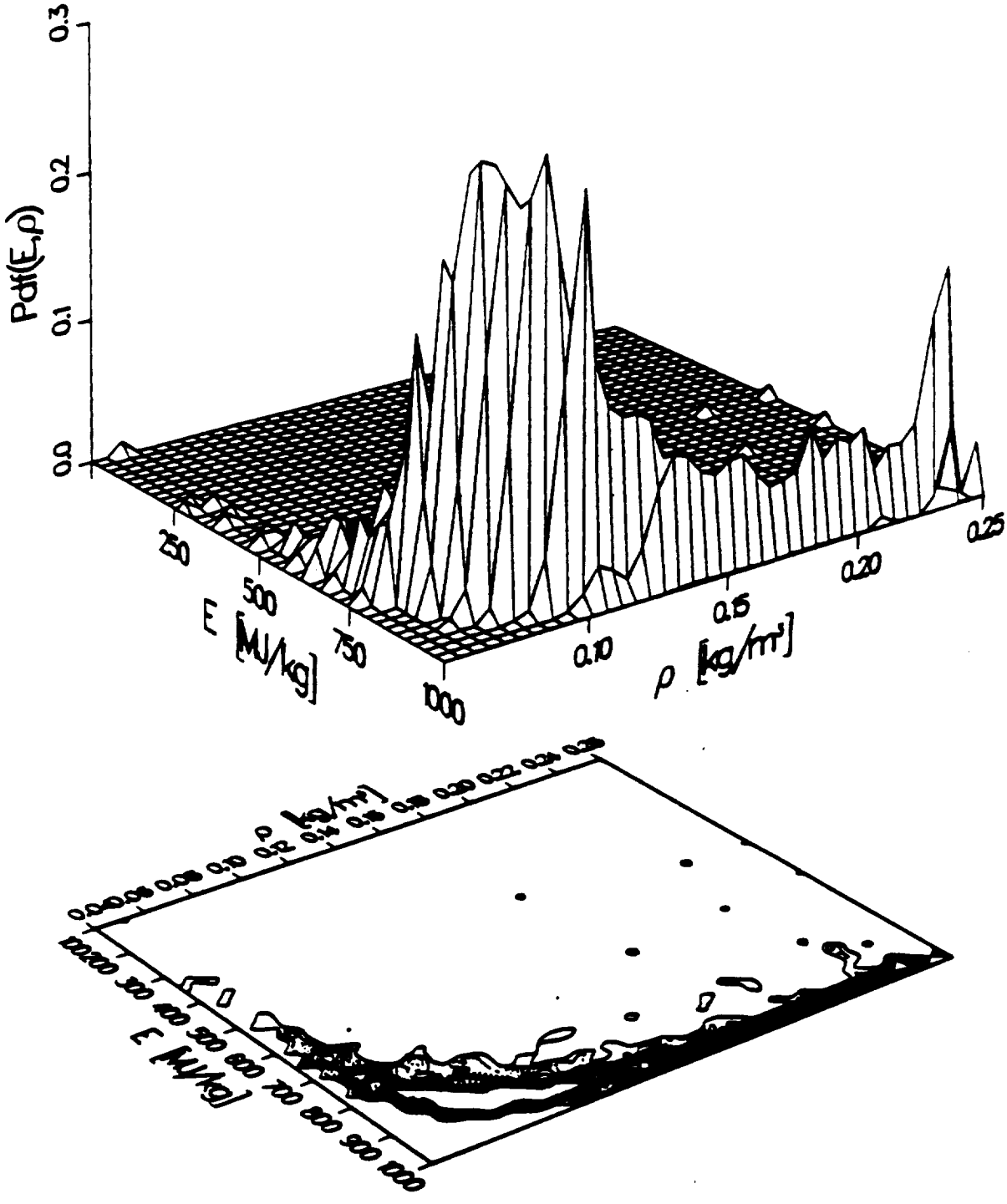

Fig. 70. Coaxial turbulent supersonic jet flame burning H_2 with air. Pdf of internal energy and density at $x/D = 15.5$ and $r/D = 1.14$ for $c_{\rho 1} = 1.0$ and $c_{\rho 2} = 0.5$.

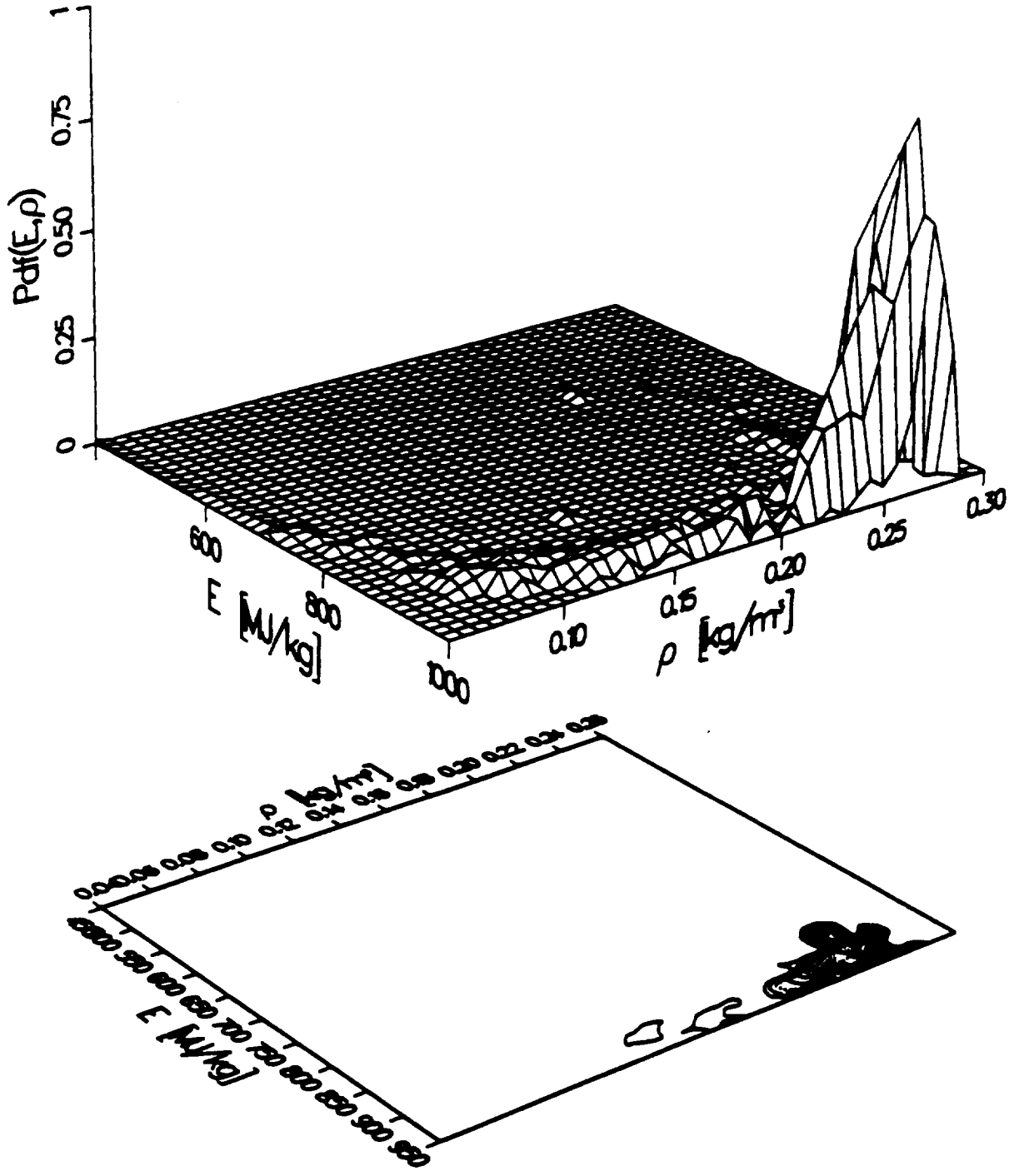

Fig. 71. Coaxial turbulent supersonic jet flame burning H_2 with air. Pdf of internal energy and density at $x/D = 15.5$ and $r/D = 1.42$ for $c_{\rho 1} = 1.0$ and $c_{\rho 2} = 0.5$.

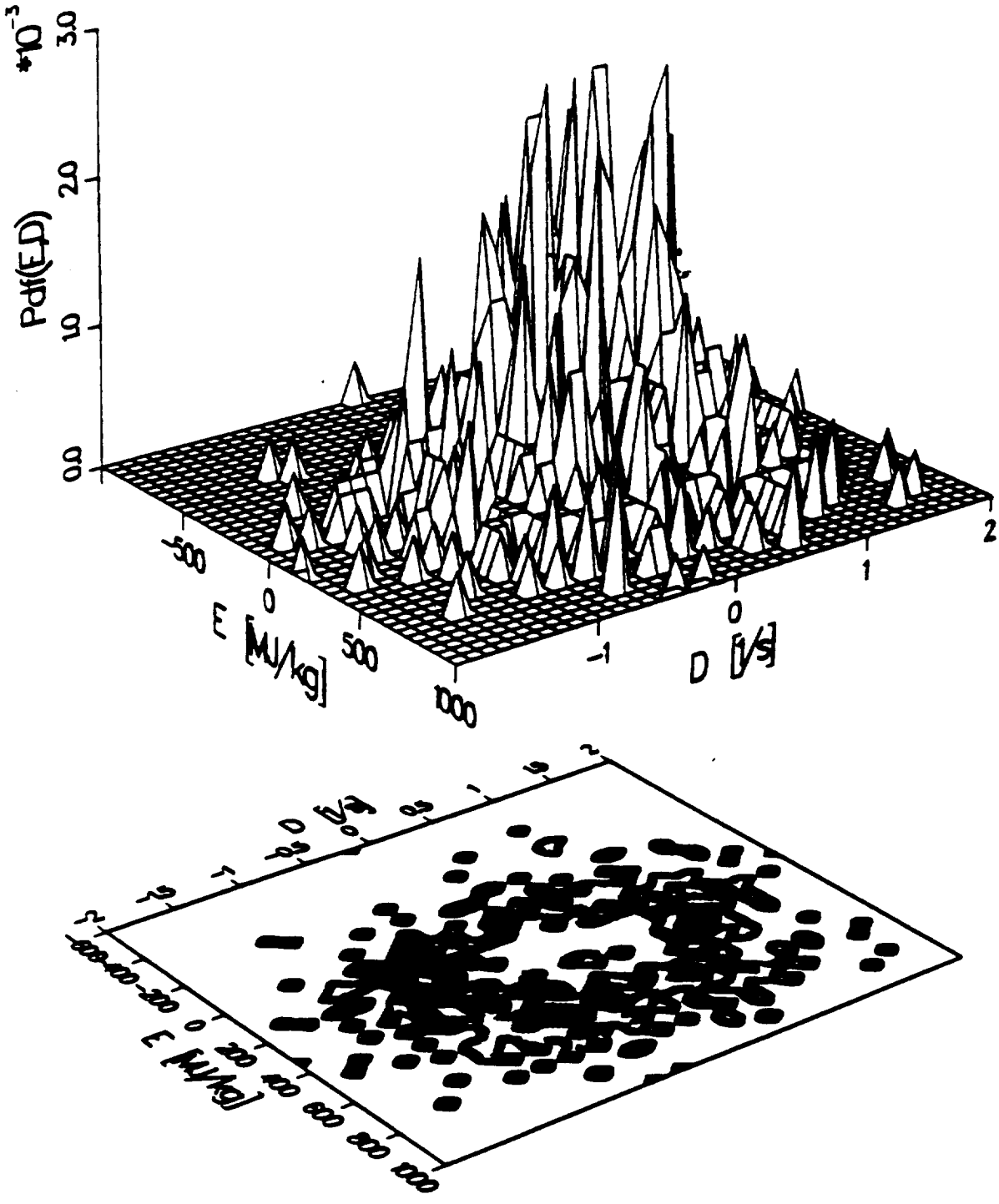

Fig. 72. Coaxial turbulent supersonic jet flame burning H_2 with air. Pdf of internal energy and relative rate of volume expansion at $x/D = 15.5$ and $r/D = 0.27$ for $c_{\rho 1} = 1.0$ and $c_{\rho 2} = 0.5$.

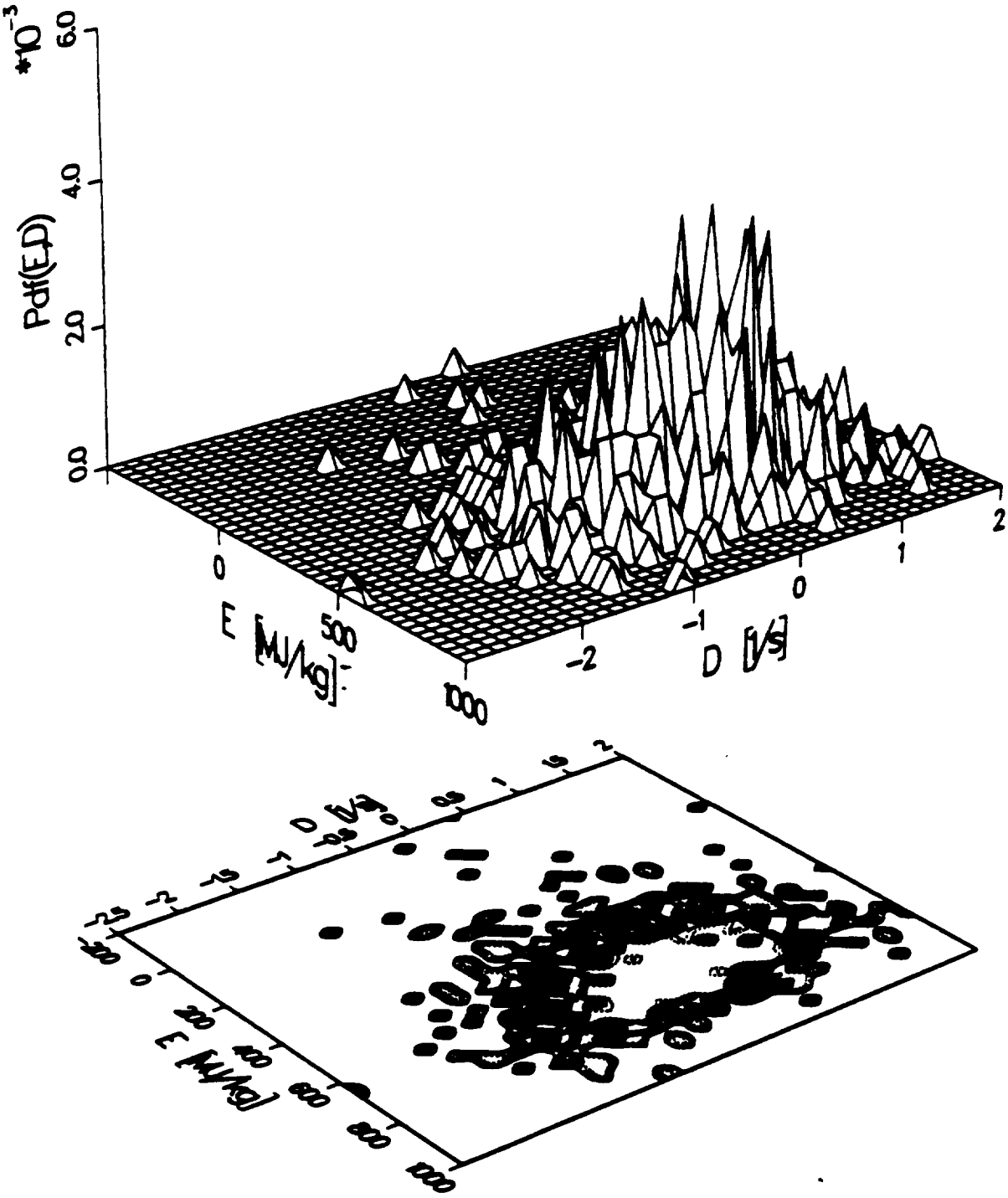

Fig. 73. Coaxial turbulent supersonic jet flame burning H_2 with air. Pdf of internal energy and relative rate of volume expansion at $x/D = 15.5$ and $r/D = 0.55$ for $c_{\rho 1} = 1.0$ and $c_{\rho 2} = 0.5$.

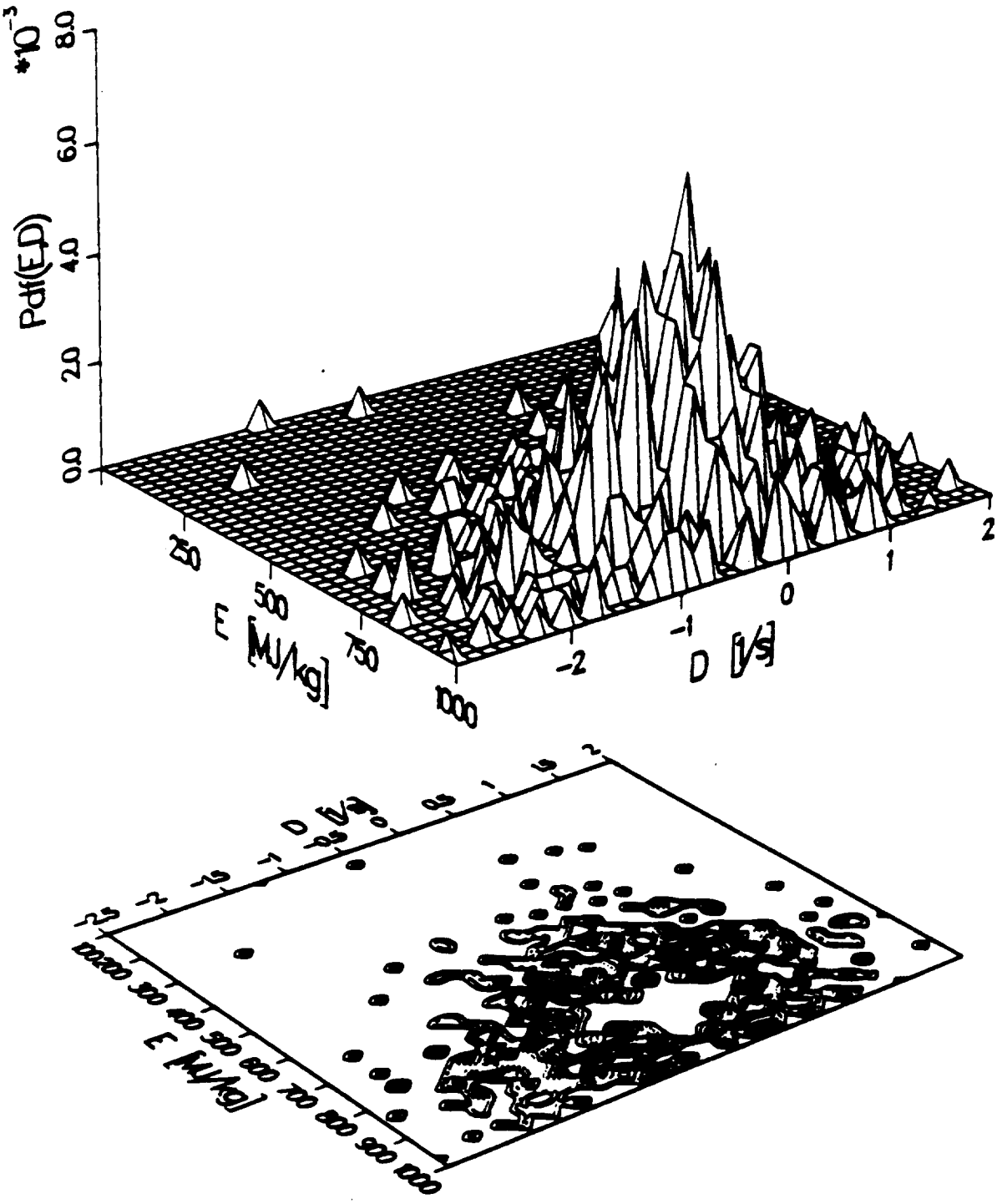

Fig. 74. Coaxial turbulent supersonic jet flame burning H_2 with air. Pdf of internal energy and relative rate of volume expansion at $x/D = 15.5$ and $r/D = 0.84$ for $c_{\rho 1} = 1.0$ and $c_{\rho 2} = 0.5$.

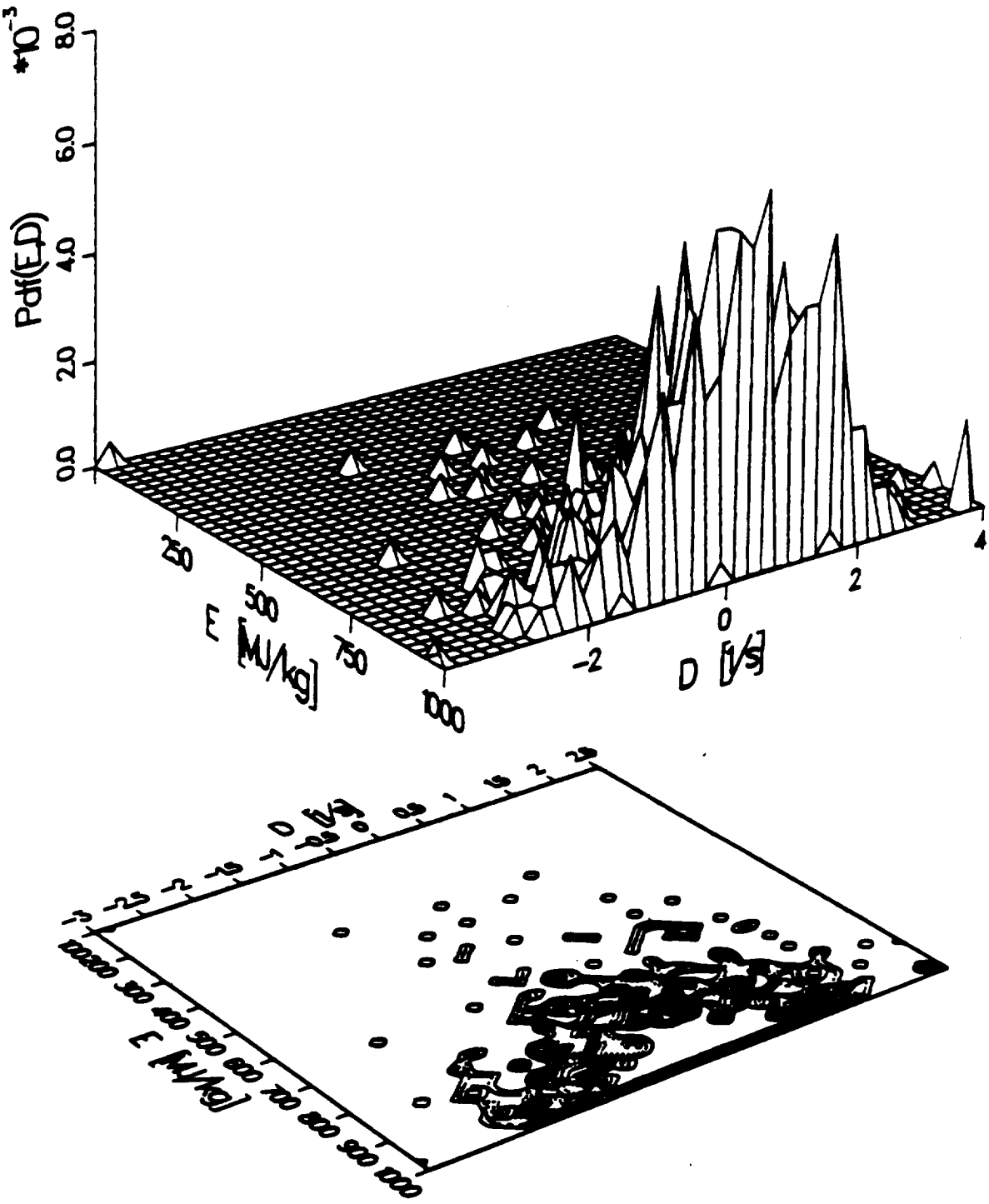

Fig. 75. Coaxial turbulent supersonic jet flame burning H_2 with air. Pdf of internal energy and relative rate of volume expansion at $x/D = 15.5$ and $r/D = 1.14$ for $c_{\rho 1} = 1.0$ and $c_{\rho 2} = 0.5$.

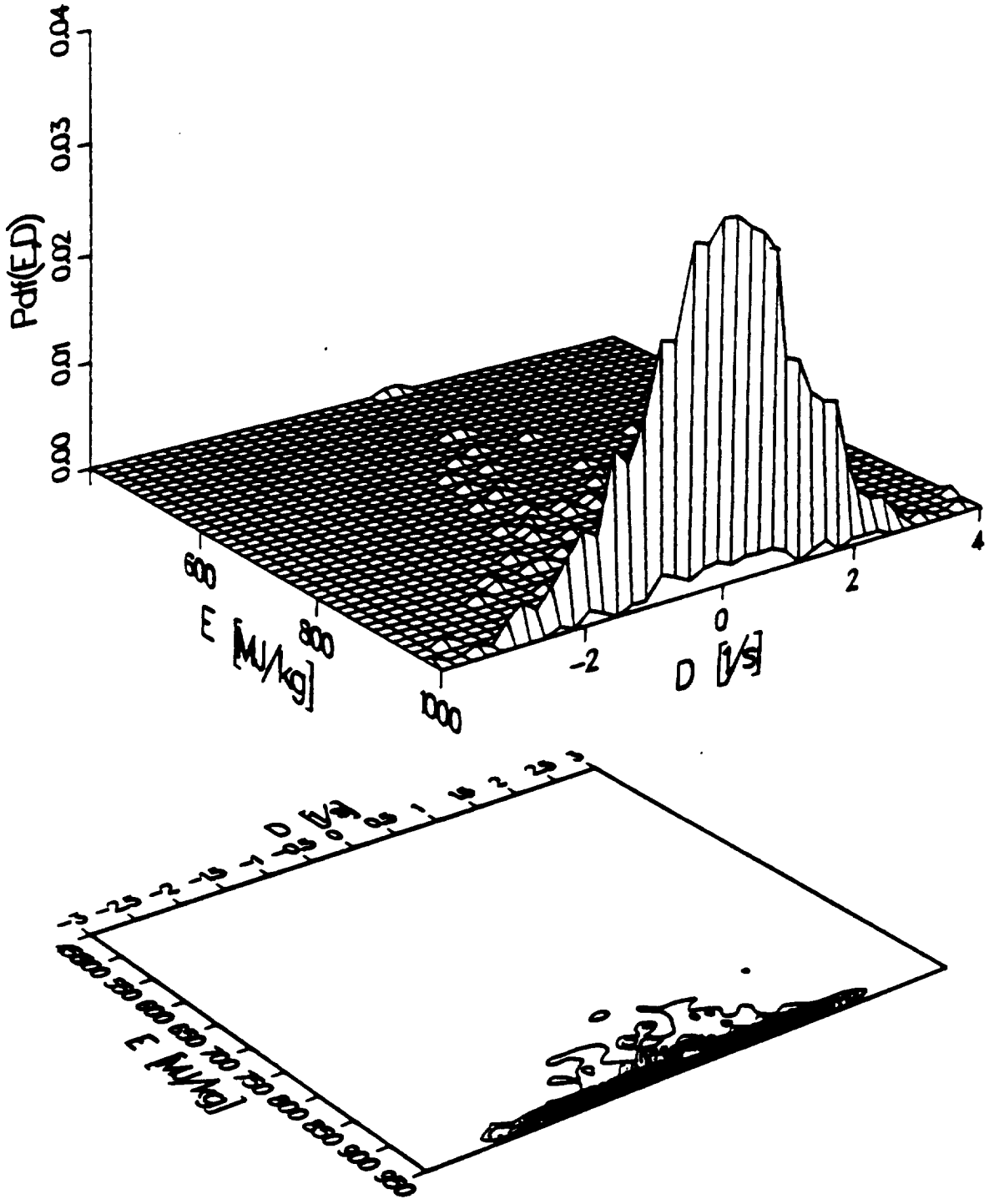

Fig. 76. Coaxial turbulent supersonic jet flame burning H_2 with air. Pdf of internal energy and relative rate of volume expansion at $x/D = 15.5$ and $r/D = 1.42$ for $c_{\rho 1} = 1.0$ and $c_{\rho 2} = 0.5$.

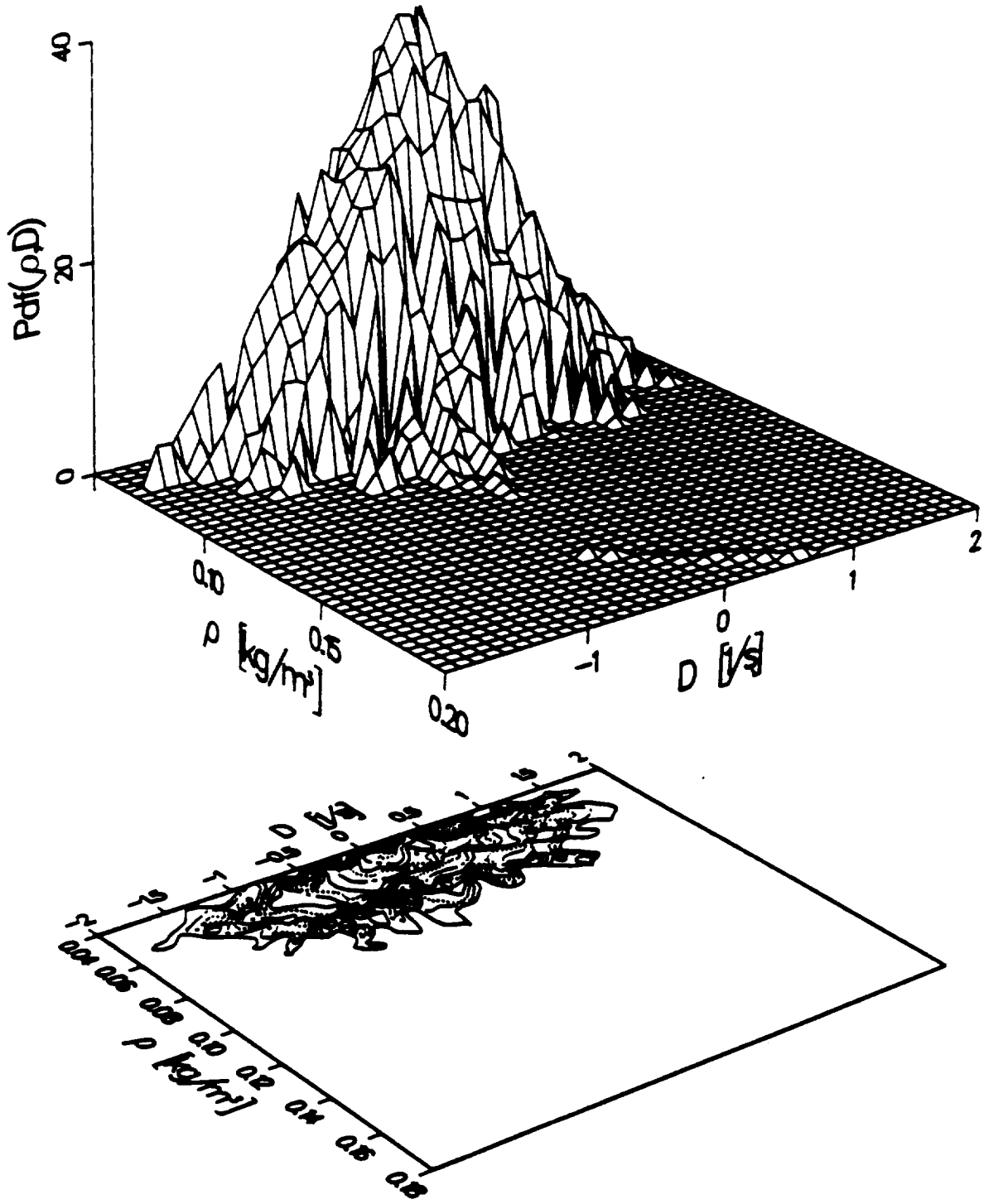

Fig. 77. Coaxial turbulent supersonic jet flame burning H_2 with air. Pdf of density and relative rate of volume expansion at $x/D = 15.5$ and $r/D = 0.27$ for $c_{\rho 1} = 1.0$ and $c_{\rho 2} = 0.5$.

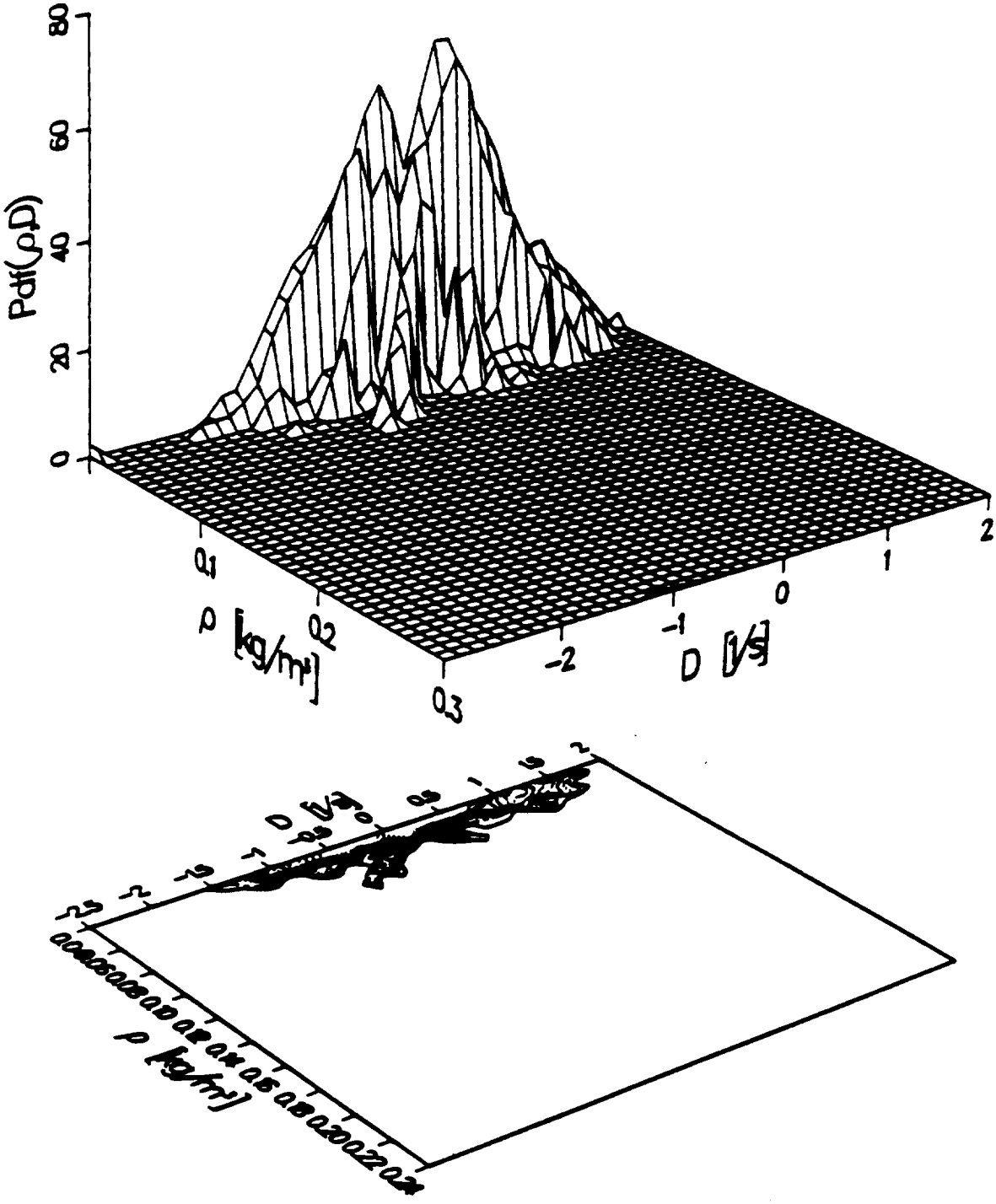

Fig. 78. Coaxial turbulent supersonic jet flame burning H_2 with air. Pdf of density and relative rate of volume expansion at $x/D = 15.5$ and $r/D = 0.55$ for $c_{\rho 1} = 1.0$ and $c_{\rho 2} = 0.5$.

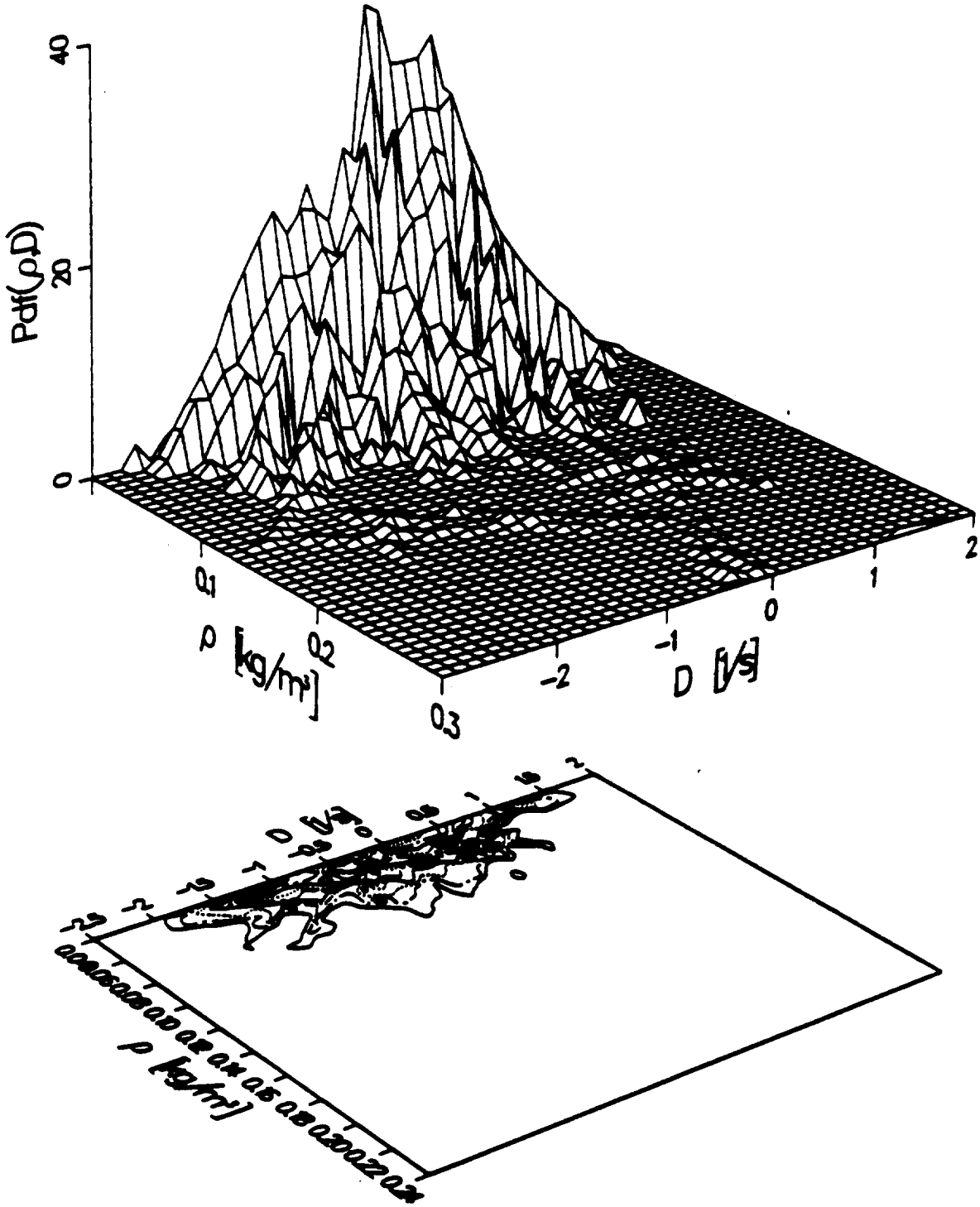

Fig. 79. Coaxial turbulent supersonic jet flame burning H_2 with air. Pdf of density and relative rate of volume expansion at $x/D = 15.5$ and $r/D = 0.84$ for $c_{\rho 1} = 1.0$ and $c_{\rho 2} = 0.5$.

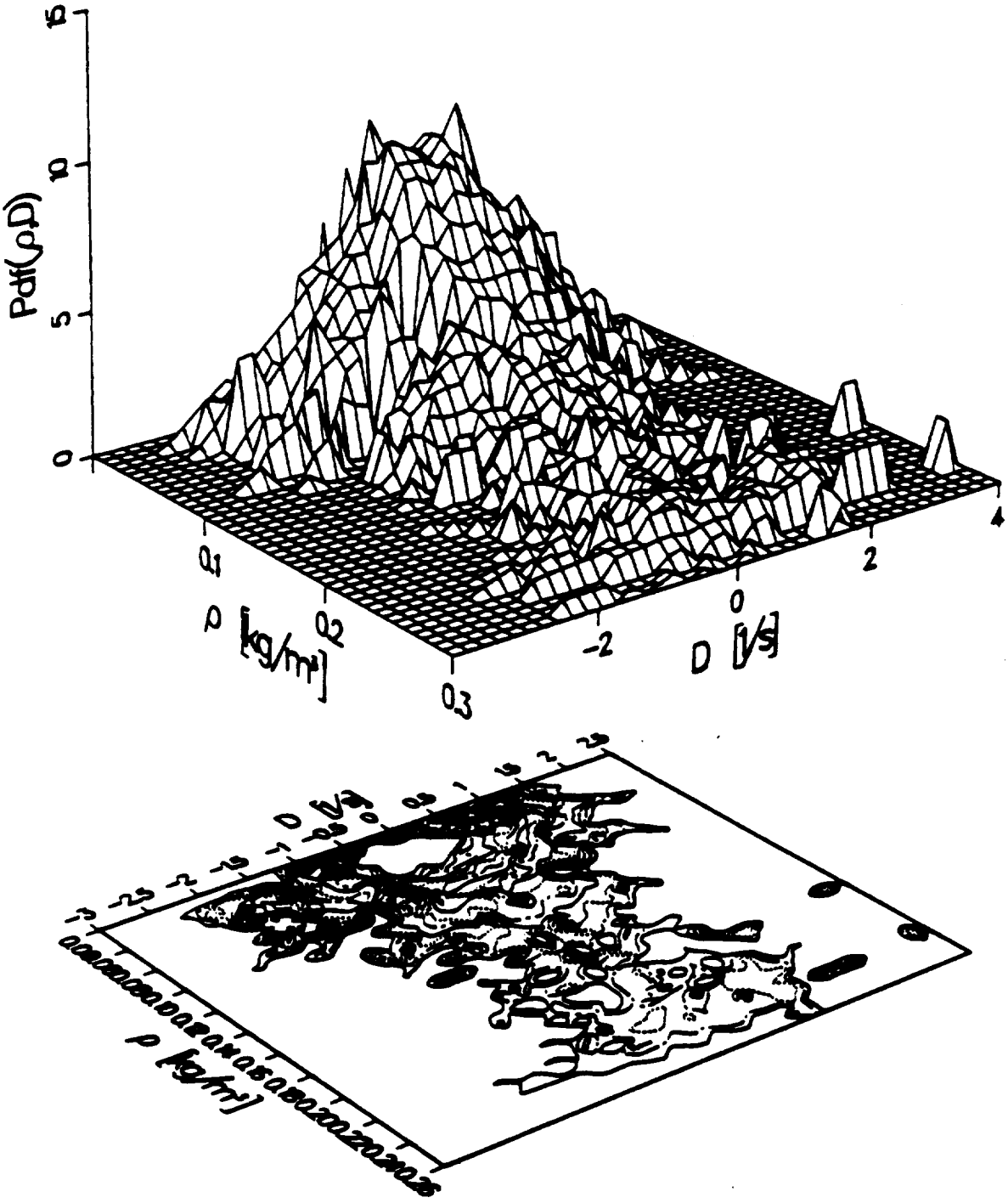

Fig. 80. Coaxial turbulent supersonic jet flame burning H_2 with air. Pdf of density and relative rate of volume expansion at $x/D = 15.5$ and $r/D = 1.14$ for $c_{\rho 1} = 1.0$ and $c_{\rho 2} = 0.5$.

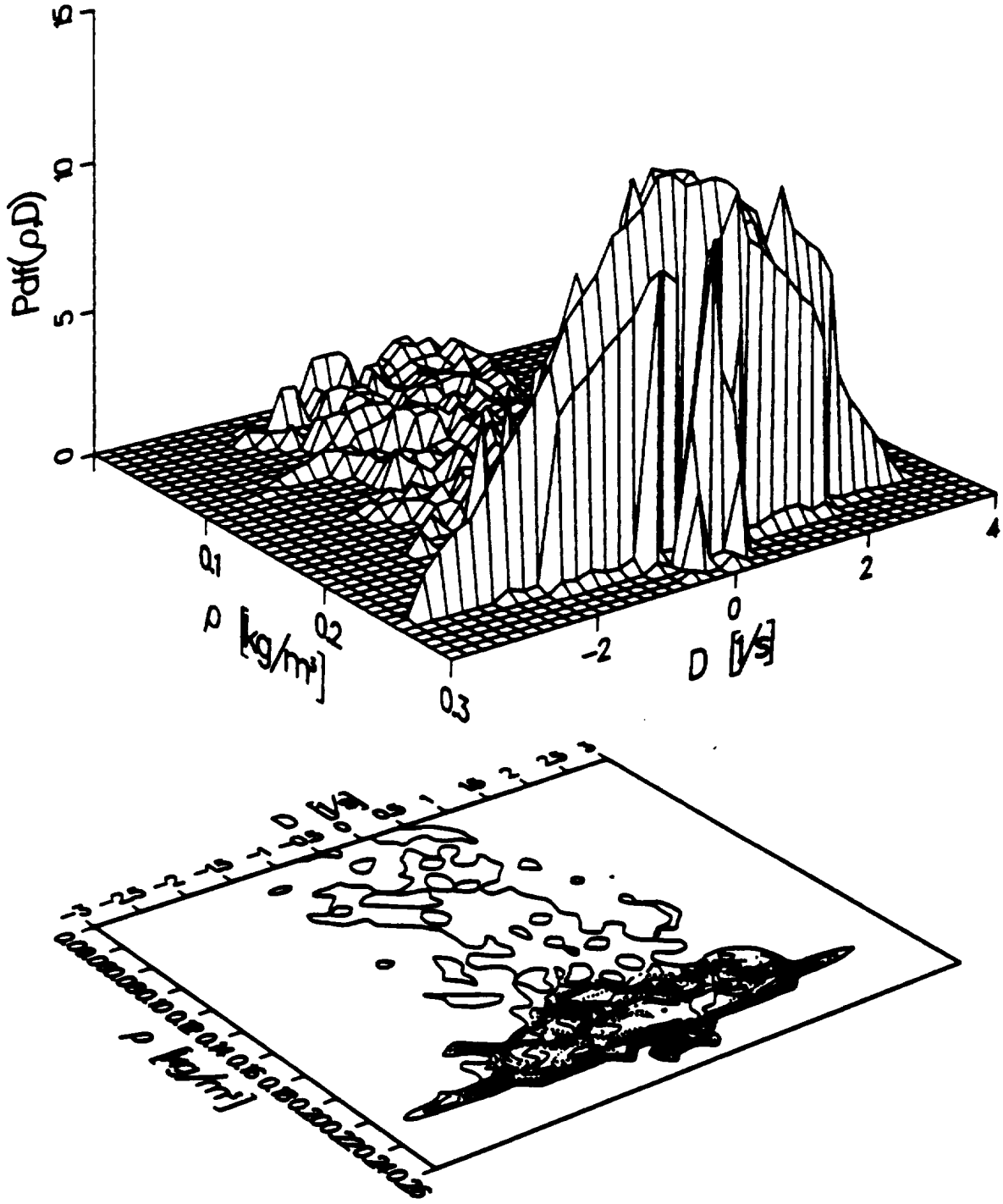

Fig. 81. Coaxial turbulent supersonic jet flame burning H_2 with air. Pdf of density and relative rate of volume expansion at $x/D = 15.5$ and $r/D = 1.42$ for $c_{\rho 1} = 1.0$ and $c_{\rho 2} = 0.5$.